Dissertation zur Erlangung des Doktorgrades

der Fakultät für Chemie und Pharmazie

der Ludwig-Maximilians-Universität München

T cell-dependent lysis of CD19-positive leukemia cells mediated by single-chain triplebodies with dual-targeting

Claudia Christina Roskopf

aus

Köln, Deutschland

2017

Erklärung

Diese Dissertation wurde im Sinne von § 7 der Promotionsordnung vom 28. November 2011 von Herrn Prof. Dr. Karl-Peter Hopfner betreut.

Eidesstattliche Versicherung

Diese Dissertation wurde eigenständig und ohne unerlaubte Hilfe erarbeitet.

München, den 06. November 2017

Claudia Roskopf

Dissertation eingereicht am:	17.11.2017
1. Gutachter:	Prof. Dr. rer. nat. Karl-Peter Hopfner
2. Gutachter:	PD Dr. med. Sebastian Kobold
Mündliche Prüfung am:	05.03.2018

This thesis was prepared from August 2012 to July 2016 in the laboratories of Professor Dr. Karl-Peter Hopfner at the Gene Center of the Ludwig-Maximilians-Universität (LMU) München and of Professor Dr. Dr. Fuat S. Oduncu at the Medizinische Klinik und Poliklinik IV of the Klinikum der Universität München (KUM).

This is a cumulative thesis based on the following five publications:

1. Braciak TA, Wildenhain S, Roskopf CC, Schubert IA, Fey GH, Jacob U, Hopfner KP, Oduncu FS (2013). NK cells from an AML patient have recovered in remission and reached comparable cytolytic activity to that of a healthy monozygotic twin mediated by the single-chain triplebody SPM-2.
   Journal of Translational Medicine **11**: 289

2. Roskopf CC, Schiller CB, Braciak TA, Kobold S, Schubert IA, Fey GH, Hopfner KP, Oduncu FS (2014). T cell-recruiting triplebody 19-3-19 mediates serial lysis of malignant B-lymphoid cells by a single T cell.
   Oncotarget **5** (15): 6466 – 6483

3. Chatzopoulou E, Roskopf CC, Sekhavati F, Braciak TA, Oduncu FS, Fenn NC, Hopfner KP, Fey GH, Rädler JO (2016). Chip-based platform for dynamic analysis of NK cell cytolysis mediated by a triplebody.
   Analyst **141** (7): 2284-2295

4. Roskopf CC, Braciak TA, Fenn NC, Kobold S, Fey GH, Hopfner KP, Oduncu FS (2015). Dual-targeting triplebody 33-3-19 mediates selective lysis of biphenotypic $CD19^+$ $CD33^+$ leukemia cells.
   Oncotarget **7** (16): 22579 - 22589

5. Schiller CB, Braciak TA, Fenn NC, Seidel UJ, Roskopf CC, Wildenhain S, Honegger A, Schubert IA, Schele A, Lämmermann K, Fey GH, Jacob U, Lang P, Hopfner KP, Oduncu FS (2016). CD19-specific triplebody SPM-1 engages NK and $\gamma\delta$ T cells for rapid and efficient lysis of malignant B-lymphoid cells.
   Oncotarget **7** (50): 83392 - 83408

Further parts of this thesis have been submitted for publication:

1. Braciak TA, Roskopf CC, Wildenhain S, Fenn NC, Schiller CB, Schubert IA, Jacob U, Honegger A, Krupka C, Subklewe M, Spiekermann K, Hopfner KP, Fey GH, Aigner M, Krause S, Mackensen A, Oduncu FS (2017). Dual-targeting triplebody 33-16-123 (SPM-2) mediates effective redirected lysis of primary blasts from AML patients with a broad range of disease subtypes in combination with natural killer cells.
   Manuscript submitted to *Oncoimmunology* on February 20th 2018.

Parts of this thesis have been presented at international conferences:

1. Roskopf CC, Schiller CB, Braciak TA, Wildenhain S, Fenn N, Schubert IA, Jacob U, Fey GH, Hopfner KP, Oduncu FS. Efficient CD19-positive leukemia cell lysis mediated by a T cell-recruiting triplebody a[19-3-19].
   Poster presentation at the 1st Immunotherapy of Cancer Conference (ITOC-1): 12. – 14.03.2014 in Munich, Germany.
   Journal for Immunotherapy of Cancer 2014; **2** (suppl. 2): 1-34 (P28).

2. Roskopf CC, Schiller CB, Braciak TA, Kobold S, Schubert I, Fey GH, Hopfner KP, Oduncu FS. Efficient lysis of malignant B-lymphoid cells mediated by the T cell-recruiting triplebodies [19-3-19] and [33-3-19].
   Poster presentation at the 12th Cancer Immunotherapy Meeting (CIMT): 06. – 08.05.2014 in Mainz, Germany.
   CIMT 2014 Abstracts; 12th Annual Meeting, 6-8 May 2014: 160.

3. Roskopf CC, Schiller CB, Braciak TA, Kobold S, Schubert I, Fey GH, Hopfner KP, Oduncu FS. Bispecific and trispecific triplebodies 19-3-19 and 33-3-19 mediate the efficient and serial lysis of malignant B lymphoid cells.
   Poster presentation at the International Symposium ImmunoFest Munich 2014: 25./26.09.2014 in Munich, Germany.

4. Roskopf CC. Malignant B-lymphoid cell lysis is mediated efficiently by bi- and trispecific T cell-recruiting triplebodies [19-3-19] and [33-3-19].
   Oral presentation at the Annual Conference of the German, Swiss and Austrian Societies for Hematooncology 2014: 10.-14.10.2014 in Hamburg, Germany.
   Oncology Research and Treatment 2014; **37** (suppl.5): 1-332 (V745).

5. Roskopf CC, Braciak TA, Fenn N, Kobold S, Jacob U, Fey GH, Hopfner KP, Oduncu FS. Selective lysis of biphenotypic leukemia cells is mediated by dual-targeting triplebody 33-3-19 treatment.
   Poster presentation at the 2nd Immunotherapy of Cancer Conference (ITOC-2): 25.-27.03.2015 in Munich, Germany.
   European Journal of Cancer 2015; **51** (suppl. 1): S9.

6. Roskopf CC, Braciak TA, Fenn N, Kobold S, Jacob U, Fey GH, Hopfner KP, Oduncu FS. Selective biphenotypic leukemia cell lysis is mediated by dual-targeting triplebody 33-3-19.
   Poster presentation at the 13th Cancer Immunotherapy Meeting (CIMT): 11.-13.05.2015 in Mainz, Germany.
   13th CIMT Annual Meeting; Abstracts, May 11-13, 2015: 274.

7. Roskopf CC. Triplebody 33-3-19 eliminates biphenotypic (CD19 plus CD33) leukemia cells selectively.
   Oral presentation at the Annual Conference of the German, Swiss and Austrian Societies for Hematooncology 2015: 09.-13.10.2015 in Basel, Switzerland.
   Oncology Research and Treatment 2015; **38** (suppl. 5): 1-288 (V133).

8. Roskopf CC, Braciak TA, Fenn N, Kobold S, Fey GH, Hopfner KP, Oduncu FS. Improving selective lysis of leukemia cells via dual-targeting antibody derivatives.
   Poster presentation at the 3rd Immunotherapy of Cancer Conference (ITOC-3): 21.-23.03.2016 in Munich, Germany.
   European Journal of Cancer 2016; **55** (suppl. 1): S13.

Abstract

Targeted tumor therapy with multispecific antibody formats bears great potential to improve the efficacy of cancer immunotherapy: The simultaneous interaction of antibody derivatives with immune effector cells and multiple tumor-associated antigens is expected to increase cancer cell selectivity, to block cancer cell survival mechanisms and to hamper immune escape. For this purpose a large number of bi- and multispecific molecular platforms have been developed including the single-chain triplebody format. Triplebodies are composed of three antibody-derived single-chain variable fragments interconnected by flexible glycine-serine peptide linkers. They are used for re-targeting of cytotoxic immune effector cells towards cancer cells, which are bound bivalently by the triplebody.

In the present work the triplebody-mediated engagement of T cells for the lysis of B lymphoid leukemia cells was established. A prototype with specificity for B lymphoid differentiation antigen CD19 and T cell trigger antigen CD3-epsilon – triplebody 19-3-19 – was shown to activate T lymphocytes at picomolar concentrations and to engage them for the efficient, serial lysis of target antigen-positive cancer cells. The triplebody 19-3-19 also induced T cell proliferation, which can lead to the partial regeneration of a patient's immune effector cell pool. In these capacities the triplebody 19-3-19 was comparable to the bispecific T cell engager (BiTE®) blinatumomab, which is approved for the treatment of relapsed or refractory acute precursor B lymphoid leukemia in the USA and in the European Union since late 2014/2015. Furthermore, it was shown with the trispecific triplebody 33-3-19 that dual targeting of CD19 and myeloid surface marker CD33 on biphenotypic leukemia blasts results in selective lysis of these target cells. The CD19 and CD33 double-positive blasts were 145-fold more sensitive to treatment with the triplebody 33-3-19 than CD19 single-positive cells. Parts of the author's work also contributed to the functional characterization of two previously developed NK cell-recruiting triplebodies – SPM-1 (19-16-19) and SPM-2 (33-16-123) – which are candidates for clinical development.

The results of this thesis project have established the triplebody format as a molecular platform, which can be employed for the recruitment of any cytotoxic effector cell population as required in a particular therapeutic setting. Furthermore, the improved target cell selectivity that was achieved *in vitro* with the dual-targeting triplebody 33-3-19 adds weight to the concept of improved therapeutic efficacy of multispecific antibodies.

Zusammenfassung

Die gezielte Behandlung von Patienten mit multispezifischen Antikörperformaten kann die Effizienz der Krebs-Immuntherapie verbessern: Die simultane Interaktion von Antikörperderivaten mit Immuneffektor-Zellen und mehreren Tumor-assoziierten Antigenen soll die Selektivität dieser Wirkstoffe für Krebszellen erhöhen, Überlebensmechanismen der Krebszellen blockieren und verhindern, dass Krebszellen der Elimination durch das Immunsystem entgehen. Zu diesem Zweck wurde bereits eine große Zahl an bi- und multispezifischen molekularen Plattformen entwickelt, die auch das Single-chain Triplebody-Format mit einschließt. Triplebodies bestehen aus drei einkettigen variablen Fragmenten, die von Antikörpern abgeleitet sind. Diese sind durch flexible Glycin-Serin Peptid-Linker miteinander verknüpft. Triplebodies werden dazu eingesetzt, zytotoxische Immuneffektorzellen gegen Krebszellen zu richten, welche bivalent von dem Triplebody gebunden werden.

In der vorliegenden Arbeit wurde die Rekrutierung von T Zellen mithilfe von Triplebodies zur Lyse von B lymphatischen Leukämiezellen etabliert. An einem Prototypen mit Spezifität für das B Zell Differenzierungs-Antigen CD19 und das T Zell-Trigger Antigen CD3-epsilon – Triplebody 19-3-19 – wurde gezeigt, dass T Lymphozyten schon bei picomolaren Konzentrationen aktiviert und zur effizienten seriellen Lyse von Antigen-positiven Krebszellen eingesetzt werden können. Außerdem induzierte der Triplebody 19-3-19 die T Zell-Proliferation. Diese Eigenschaft kann zu einer partiellen Regeneration der Immuneffektorzellen eines Patienten führen. Hierbei war der Triplebody 19-3-19 vergleichbar mit dem bispezifischen T Zell-Engager (BiTE®) Blinatumomab, der in der Europäischen Union und den USA für die Behandlung von rezidivierter oder refraktärer akuter Vorläufer B lymphatischer Leukämie zugelassen ist. Darüber hinaus wurde für den trispezifischen Triplebody 33-3-19 gezeigt, dass das duale Targeting von CD19 und dem myeloiden Oberflächen-Antigen CD33 auf biphänotypischen Leukämie-Blasten zur erhöhten selektiven Lyse dieser Zielzellen führt. Die CD19-CD33 doppelt-positiven Blasten waren gegenüber der Behandlung mit Triplebody 33-3-19 145-fach sensitiver als CD19 einfach-positive Zellen. Teile der Arbeit der Autorin haben des Weiteren zu der funktionellen Charakterisierung von den bereits entwickelten NK Zell-rekrutierender Triplebodies SPM-1 (19-16-19) und SPM-2 (33-16-123) beigetragen, welche Kandidaten für die klinische Entwicklung sind.

Die Ergebnisse dieses Promotionsprojektes etablieren das Triplebodyformat als eine molekulare Plattform, welche für die Rekrutierung jeder zytotoxischen Effektorzell-Population genutzt werden

kann, die für eine bestimmte Anwendung erforderlich ist. Des Weiteren betont die erhöhte Selektivität für Zielzellen, die mit dem dual-targeting Triplebody 33-3-19 *in vitro* erreicht wurde, das Konzept der verbesserten therapeutischen Effektivität durch multispezifische Antikörper.

Table of Contents

Abstract **1**

Zusammenfassung **3**

Abbreviations **7**

1 Introduction **9**

1.1 Aim of the experimental studies **9**

1.2 Acute Leukemias **9**

1.2.1 Pathogenesis and clinical presentation 10

1.2.2 Acute myeloid leukemia 10

1.2.3 Acute leukemia of ambiguous lineage 12

1.2.4 Precursor lymphoid neoplasms 14

1.3 Cancer stem cells and clonal evolution in acute leukemia **16**

1.3.1 AML initiating cells 17

1.3.2 ALL initiating cells 18

1.4 Immunotherapy of cancer **19**

1.4.1 Therapy with monoclonal antibodies and antibody derivatives 21

1.4.2 BiTE® and CAR-T 27

1.4.3 Single-chain triplebodies 29

1.5 Target antigens for immunotherapy in hematologic malignancies **31**

1.5.1 B lymphoid marker CD19 31

1.5.2 Myeloid marker CD33 33

1.5.3 CD123, the alpha-chain of the interleukin-3 receptor 35

1.6 Cell-mediated cytotoxicity and the immunological synapse **37**

2 Results **41**

2.1 NK cells from an AML patient have recovered in remission and reached comparable cytolytic activity to that of a healthy monozygotic twin mediated by the single-chain triplebody SPM-2 **41**

2.1.1 Summary 41

2.1.2 Contribution 42

2.2 T cell-recruiting triplebody 19-3-19 mediates serial lysis of malignant B lymphoid cells by a single T cell **59**

2.2.1 Summary 59

2.2.2 Contribution 60

2.3 Chip-based platform for dynamic analysis of NK cell cytolysis mediated by a triplebody 81
2.3.1 Summary 81
2.3.2 Contribution 82
2.4 Dual-targeting triplebody 33-3-19 mediates selective lysis of biphenotypic CD19$^+$ CD33$^+$ leukemia cells 97
2.4.1 Summary 97
2.4.2 Contribution 98
2.5 CD19-specific triplebody SPM-1 engages NK and γδ T cells for rapid and efficient lysis of malignant B lymphoid cells 113
2.5.1 Summary 113
2.5.2 Contribution 114
3 Discussion 133
3.1 Efficient T cell recruitment with single-chain triplebodies 133
3.2 Selective lysis of biphenotypic blasts by dual-targeting of CD19 and CD33 136
3.3 NK cells as immune effector cell population to combat MRD in AML patients 137
3.4 Engagement of γδ T cells by the CD16 binding moiety of SPM-1 139
3.5 Difference in γδ T cell and NK cell response kinetics between mAbs and triplebodies 139
3.6 Perspective 140
References 143
Figures 163
Tables 165
Acknowledgements 167
Appendix A: Sequence Data 169

Abbreviations

6xHis	hexa-histidine-tag
ADC	antibody-drug-conjugate
ADCC	antibody-dependent cellular cytotoxicity
ADCP	antibody-dependent cellular phagocytosis
ALL	acute lymphoid/lymphocytic leukemia
AML	acute myeloid/myelocytic leukemia
APC	antigen-presenting cell
APL	acute promyelocytic leukemia
AUL	acute undifferentiated leukemia
βc	beta common chain
BCR	B cell receptor
BCR-ABL-1	breakpoint cluster region – Abelson murine leukemia viral oncogene homolog 1
BiTE	bispecific T cell engager
c	cellular
C_L/C_{H1-3}	constant regions of Ig light or heavy chains
CAR	chimeric antigen receptor
CD	cluster of differentiation
CDC	complement-dependent cytotoxicity
CDR	complementarity-determining region
CFC	colony-forming cell
CLL	chronic lymphoid/lymphocytic leukemia
CML	chronic myeloid/myelocytic leukemia
CNS	central nervous system
CRS	cytokine release syndrome
CSC	cancer stem cell
CT	cancer/testis
CTL	cytotoxic T lymphocyte
DART	dual-affinity receptor re-targeting
DC	dendritic cell
DFS	disease-free survival
DOI	digital object identifier
dp	double-positive
EMA	European Medicines Agency
E : T	effector-to-target cell ratio
FAB	French-American-British
Fab	antigen-binding fragment
Fc	fragment crystallizable
FcR	Fc-receptor
FDA	U.S. Food and Drug Administration
FLT3	Fms-like-tyrosine-kinase-3
GO	gemtuzumab ozogamicin
GvHD	graft-versus-host disease
GvL	graft-versus-leukemia effect
HLA-DR	human leukocyte antigen – antigen D-related
HMG	high mobility group
HSC	hematopoietic stem cell
HSCT	hematopoietic stem cell transplantation
IDO	indoleamine-2,3-dioxygenase
Ig	immunoglobulin
Igκ	secretion leader sequence from the murine Igκ L chain
IL	interleukin
inv	inversion
ITAM	immunoreceptor tyrosine-based activating motif
ITD	internal tandem duplication
ITIM	immunoreceptor tyrosine-based inhibitory motif
K_D	equilibrium dissociation constant
LAK	lymphokine activated killer cells
LDH	lactate dehydrogenase
LIC	leukemia-initiating cell
LSC	leukemia stem cell
mAb	monoclonal antibody
MAPK	mitogen-activated protein kinase
MDR	multi-drug resistance
MDS	myelodysplastic syndrome
MDSC	myeloid-derived suppressor cell
MHC	major histocompatibility protein
MPAL	mixed phenotype acute leukemia
MPD	myeloproliferative disease
MLL	mixed lineage leukemia
MM	multiple myeloma
MNC	mononuclear cells
MRD	minimal (measurable) residual disease
NCR	natural cytotoxicity receptor

NHL	non-Hodgkin's lymphoma
Ni-NTA	nickel-nitrilotriacetic acid
NK	natural killer
NOS	not otherwise specified
NPM1	Nucleophosmin-1
NSCLC	non-small cell lung cancer
OS	overall survival
PBMC	peripheral blood mononuclear cells
PI	propidium iodide
PI3K	phosphoinositide 3-kinase
RDL	redirected lysis
SCC	single-cell cytometry
scFv	single-chain variable fragment
scTb	single-chain triplebody
SH2	Src-homology 2 domain
Siglec	sialic acid-binding immunoglobulin-like lectins
SMAC	supramolecular activation complex
sp	single-positive
t	translocation
TAA	tumor-associated antigen
TAM	tumor-associated macrophage
TCR	T cell receptor
TIL	tumor-infiltrating lymphocytes
TKI	tyrosine kinase inhibitor
TLR	Toll-like receptor
T_{reg}	regulatory T cell
TSA	tumor-specific antigen
V_L/V_H	V regions of Ig light or heavy chains
WHO	World Health Organization

1 Introduction

1.1 Aim of the experimental studies

New strategies to improve the effectiveness and specificity of cancer immunotherapy are currently under development. One such approach is the re-targeting of immune effector cells with multispecific antibodies for the rapid and selective elimination of cancer cells by cellular cytotoxicity. It was the aim of the present study to develop T cell-engaging trispecific antibody derivatives in the molecular format of single-chain triplebodies (triplebodies, scTb). Triplebodies that are capable of NK cell-recruitment already existed, but whether these antibody derivatives were also capable of T cell-engagement had never been tested prior to this work.

T cell-engaging triplebodies for the cytolysis of CD19-positive acute leukemia blasts, in particular for the selective lysis of blasts with aberrant antigen co-expression of CD19 and CD33, were developed. This co-expression is associated with specific genetic abnormalities and confers a poor prognosis.[1,2] Initially, the experimental procedures for the production, purification and functional analysis of T cell-engaging triplebodies were established at the example of the CD19- and CD3ε–specific prototype triplebody 19-3-19 (Roskopf *et al*. Oncotarget 2014 [references to own publications indicated with journal]). Subsequently, the dual-targeting capacity of triplebodies was implemented: The triplebody 33-3-19 with specificity for CD33, CD19 and CD3ε was designed with the aim of achieving not only efficient, but also selective cytolysis of CD19 and CD33 double-positive leukemia cells, while avoiding the lysis of healthy bystander cells. One aim of the present study was to establish reliable experimental methods for the *in vitro* analysis of the selectivity of lysis by dual-targeting triplebodies (Roskopf *et al*. Oncotarget 2016). The final aim of the present work was to contribute to the pre-clinical development of NK cell-engaging triplebodies SPM-1 (Schiller *et al*. Oncotarget 2016) and SPM-2 (Braciak *et al*. J Exp Med 2013 and Chatzopoulou *et al*. Analyst 2016).

1.2 Acute Leukemias

Cancer results from abnormal cells that grow beyond their usual tissue boundaries and that are capable of invading adjoining parts of the body and metastasizing to distant organs.[3] The types of cancer that arise from the hematopoietic system are as diverse as the cell types, which comprise this tissue: Lymphoid and myeloid cells at different developmental stages and in different compartments of the body (i. e. bone marrow or extramedullary sites) can undergo malignant transformation and

cause disease. Blood cancer thus includes multiple entities such as Hodgkin's disease and Non-Hodgkin lymphomas (NHL), multiple myeloma (MM), myelodysplastic and myeloproliferative diseases (MDS and MPS) as well as chronic and acute forms of leukemia.[3-5]

In Germany, the cumulative incidence of hematologic malignancies among cancer patients is approximately 6 to 7% in both females and males. Leukemia is diagnosed, when more than 20% of the nucleated cells in a diagnostic peripheral blood or bone marrow sample are blasts and affects half of the patients with hematologic neoplasias.[5] In Germany, 12,640 adults with an average age of approximately 70 years were diagnosed with leukemia in 2012. Chronic lymphocytic leukemia (CLL) struck a third of these patients. Another quarter was diagnosed with acute myeloid leukemia (AML).[4] In children under the age of 15, leukemias especially acute lymphocytic leukemias (ALL) are by far the most common form of cancer and account for 33% of all malignancies (ALL: 26%; AML: 4%; others: 3%).[4]

1.2.1 Pathogenesis and clinical presentation

Acute leukemias are distinguished into AML and related precursor neoplasms, acute leukemia of ambiguous lineage and precursor lymphoid neoplasms of the B and T lymphoid lineages.[5] They arise in the bone marrow upon malignant transformation of hematopoietic progenitor cells, which deregulates differentiation, proliferation and apoptosis and can confer stem cell-like properties.[6] The leukemia blasts populate the bone marrow, displace healthy hematopoietic cells and thereby hamper normal hematopoiesis. Eventually the cancer cells emigrate, enter the peripheral blood and invade extramedullary sites such as the central nervous system (CNS), lymphoid organs, the lung and bones.[7,8] In the majority of patients the obstruction of normal hematopoiesis results in anemia, thrombocytopenia and granulocytopenia. Accordingly, acute leukemia patients present with abnormal blood test values, since the numbers of leukocytes, thrombocytes and erythrocytes are affected. The pancytopenia gives rise to some of the typical symptoms including fatigue, paleness, tachycardia, fever, frequent infections and bleeding symptoms such as petechia, epistaxis and ecchymosis.[7,8] The involvement of distant organs may then produce various additional symptoms and abnormal diagnostic parameters.[7,8]

1.2.2 Acute myeloid leukemia

Diverse innate immune effectors from the granulocytic lineage (neutrophils, eosinophils and basophils), monocytic/macrophage, erythroid, megakaryocytic and mast cell lineages comprise the myeloid cells.[5] Accordingly, acute myeloid leukemia (AML) is a highly heterogeneous disease. The

distinct morphologic characteristics of AML blasts were employed by the French-American-British (FAB) cooperative group for the classification of this type of leukemia into eleven subtypes (M0 - M7) (Table 1).[7] However, the individual entities of AML can also be defined by precise molecular alterations and not only by the healthy counterparts of the neoplastic cells alone.[9] The identification of specific genetic aberrations, which are the most prominent prognostic factors for this type of cancer, thus led to the introduction of a new classification scheme by the World Health Organization (WHO) in 2008. It is based on criteria that comprise morphologic, cytochemical, immunophenotypic, genetic and clinical features. Resultantly, AML is subdivided into AML with recurrent genetic abnormalities, AML with myelodysplasia-related changes, therapy-related myeloid neoplasms and AML, not otherwise specified (NOS) (Table 1).[5]

Table 1: Currently used classification systems of Acute Myeloid Leukemia (AML).

French-American-British (FAB) Classification (1976/85)		**WHO Classification (2008)**
AML-M0	Undifferentiated acute myeloblastic leukemia	AML with recurrent genetic abnormalities
AML-M1	Acute myeloid leukemia with minimal maturation	with t(8;21)(q22;q22), RUNX1-RUNX1T1
AML-M2	Acute myeloid leukemia with maturation	with inv(16)(p13.1q22) or t(16;16)(p13.1;q22), CBFB-MYH11
AML-M3	Acute promyelocytic leukemia (APL)	with t(15;17)(q22;q12), PML-RARA (APL)
AML-M3v	Atypical APL with microgranula	with t(9;11)(p22;q23), MLLT3-MLL
AML-M4	Acute myelomonocytic leukemia	with t(6;9)(p23;q34), DEK-NUP214
AML-M4Eo	Acute myelomonocytic leukemia with eosinophilia	with inv(3)(q21q26.2) or t(3;3)(q21;q26.2), RPN1-EVI1
AML-M5a/b	Acute monocytic leukemia	with t(1;21)(p13;q13), RBN15-MKL1 (megakaryoblastic)
AML-M6	Acute erythroid leukemia	(AML with mutated NPM1)
AML-M7	Acute megakaryocytic leukemia	(AML with mutated CEBPA)
		AML with myelodysplasia-related changes
		Therapy-related myeloid neoplasms
		AML, not otherwise specified (NOS)

AML is an aggressive disease and fatal within a short period of time, when untreated. The conventional treatment approach upon diagnosis is chemotherapy, which is subdivided into two phases: induction and consolidation. During the induction phase the absolute tumor load is reduced by 3 to 4 logs from a total of 10^{12} to 10^{8} or 10^{9} leukemic blasts. During consolidation the residual leukemia cells are eliminated in order to prevent relapse.[7] Currently, intense chemotherapeutic regimens employ pyrimidine analogues (i. e. Cytarabin/Ara-C), cytostatic antibiotics (i. e. dauno-rubicin) and topoisomerase inhibitors (i. e. Etoposide) among others.[7,10] Hematopoietic stem cell transplantation (HSCT) is indicated for younger patients with high risk AML (i. e. aberrations of chromosome 3, 5 and/or 7, complex karyotype, involvement of the *mll*-gene) and with relapsed and/or refractory disease.[6,7]

While the majority of patients (more than 80%) initially respond to chemotherapy and achieve complete remission, there is a high rate (50 to 60%) of relapse and the long-term survival rate is only 30 to 40%.[7] The leukemia cell clone that is responsible for relapse is frequently refractory to the chemotherapeutic agents that were used during first line therapy. Furthermore, a large number of patients cannot cope with intense chemotherapy regimens or remain minimal (measurable) residual disease (MRD)-positive post induction. This especially concerns the elderly, who often display unfavorable genetic aberrations and a poor general condition of health. These patients have a very poor prognosis and urgently require new treatment options.[6,7,11] As an alternative to chemotherapy and the treatment-related mortality-prone HSCT, immunotherapeutic approaches have been developed for the treatment of AML. The myeloid differentiation antigen CD33 (see chapter 1.5.2) and the alpha-chain of the IL-3 receptor, i. e. CD123 (see chapter1.5.3), are the most prominent targets at present.[12] Thus far the only approved immunotherapeutic agent was the anti-CD33 antibody-drug-conjugate (ADC) gemtuzumab ozogamicin (Mylotarg®), which was, however, voluntarily withdrawn by Pfizer in 2010 due to the lack of additional benefit but occurrence of hepatic toxicity.[13,14] Nevertheless, the ADC was recently reapproved at a lower dose and for a limited patient population.[15] The development of an anti-CD33 antibody, i. e. Lintuzumab, was discontinued in 2010.[16,17] Since then the development of a bispecific T cell engager (BiTE®), which is also directed against CD33, and of T cells with CD33 or CD123-targeting chimeric antigen receptors (CAR-T) have been the most promising immunotherapeutic approaches in AML.[18-20]

1.2.3 Acute leukemia of ambiguous lineage

Very rarely the blast population of an acute leukemia patient cannot be assigned to a specific hematopoietic lineage, either because of the lack of differentiation markers or because of the simultaneous expression of differentiation markers from multiple hematopoietic lineages. The WHO grouped these types of leukemias, which affect approximately 3 to 5% of all acute leukemia patients, together into the new class of “acute leukemia of ambiguous lineage”.[5,21,22] This new class comprises acute undifferentiated leukemias (AUL), which do not display differentiation antigens but often express early progenitor markers (i. e. CD34, HLA-DR, CD38 and TdT), acute bilineage leukemias, which present with two blast populations of different hematopoietic lineages, and finally mixed phenotype acute leukemias (MPAL).[5,21-23]

The diagnosis of MPAL is based exclusively on immunophenotypic characteristics of the blast population (Table 2) and can only be applied, if all other types of acute leukemia have been excluded. This concerns acute leukemias with recurrent genetic abnormalities that often display aberrant

antigen expression in particular.[5,21,22] There appears to be a high incidence (approximately 83 to 87%) of cytogenetic abnormalities among MPAL patients.[23,24] Some of these are also recurrent including the translocation t(9;22) (q34;q11.2) (Philadelphia chromosome), which produces the BCR-ABL-1 fusion protein, and rearrangements of the mixed lineage leukemia gene (*mll*; t(v;11q23)), which frequently occur in infants younger than 10 months.[5,21-23,25] Rubnitz and colleagues reported that the gene expression profiles of blasts from eight out of thirteen MPAL patients were clearly different from those of ALL or AML blasts, thereby highlighting the distinct nature of MPAL.[24]

Table 2: Requirements for assigning more than one lineage to a single blast population in mixed phenotype acute leukemia according to the WHO 2008 classification.

Criteria for the diagnosis of mixed phenotype acute leukemia (MPAL)	
Myeloid lineage	
	Myeloperoxidase
or	Monocytic differentiation (at least 2 of the following: nonspecific esterase, CD11c, CD14, CD64, lysozyme)
T lineage	
	Cytoplasmic CD3
or	Surface CD3
B lineage (multiple antigens required)	
	Strong CD19 with at least 1 of the following strongly expressed: CD79a, cytoplasmic CD22, CD10
or	Weak CD19 with at least 2 of the following: CD79a, cytoplasmic CD22, CD10

In clinical practice, MPAL is subdivided into B-myeloid, T-myeloid, B/T or trilineage leukemia based on the immunophenotype of the blast population.[21,23,24,26,27] The relative frequencies of these subgroups vary in different studies, but the B-myeloid phenotype appears to be the most common (approximately 54%), followed by the T-myeloid (approximately 37%) and the very rare B/T (approximately 5%) and trilineage (approximately 3%) cases.[21,24-27] Lineage infidelity in MPAL raises a serious problem for clinicians, because the classical treatment protocols cannot be applied with confidence. HSCT is not a reliable curative option for MPAL patients either, but it can be beneficial, if patients display an incomplete molecular response, in Philadelphia chromosome-positive MPAL and in infants.[24,26,28,29] Prospective clinical studies to establish a consensus regarding the therapy regimen for MPAL patients have not been performed to date due to the rarity of this disease. Even retrospective analyses of this patient population are complicated, because of the discord regarding the diagnostic criteria for MPAL prior to the new WHO classification in 2008.[21,22] However, the clinical outcome of adult MPAL patients appears to be generally worse than that of adult ALL and AML patients. Among children it is worse than that of pediatric ALL patients.[24,30] Thus this particular subgroup of acute leukemia patients requires new therapy approaches. At this, the aberrant co-expression of myeloid, B and/or T lymphoid antigens turns MPAL blasts into a particularly

interesting cancer cell population for selective immunotherapeutic targeting with multispecific antibodies.

1.2.4 Precursor lymphoid neoplasms

Both lymphoid lineages, i. e. T and B lymphocytes, can give rise to precursor lymphoid neoplasms upon malignant transformation of early lymphoid progenitor cells.[5,8] The present work focuses on precursor B lymphoid neoplasms. A classification system by the FAB cooperative group from 1976 was based on cytologic criteria (Table 3), however, it had few clinical implications with regard to disease progression, prognosis or treatment strategy.[8] As new diagnostic techniques became available, immunophenotypic criteria such as CD10 positivity/negativity and cytogenetic features (i. e. rearrangement status of immunoglobulin (Ig) heavy and light chain genes) were taken into consideration for the further sub-classification of precursor B lymphoid neoplasms into pro-B, common-B, pre-B, and mature B-ALL. This system is still used today (Table 3).[8] Advances in genetic profiling in the past two decades additionally led to the introduction of a new WHO classification scheme of ALL in 2008 that puts strong emphasis on prognostically valuable recurrent genetic abnormalities (Table 3).[5,8]

Table 3: Classification systems used for B precursor lymphoid neoplasms.

FAB Classification (1976)			**WHO Classification (2008)**
L1	Small blasts with homogeneous nuclear chromatin, no or small nucleoli and scanty cytoplasm		B lymphoblastic leukemia/lymphoma, not otherwise specified (NOS)
L2	Large, heterogeneous cells with variable nuclear chromatin, one or more nucleoli and a variable amount of cytoplasm		B lymphoblastic leukemia/lymphoma with recurrent genetic abnormalities
L3	Large, homogeneous cells with fine, stippled chromatin, prominent nucleoli and basophilic cytoplasm; prominent cytoplasmic vacuolation		with t(9;22)(q34;q11.2), BCR-ABL 1
			with t(v;11q23), MLL rearranged
			with t(12;21)(p13;q22), TEL-AML1 (ETV6-RUNX1)
Immunophenotypic Classification (EGIL 1995)			with hyperdiploidy
	Immunophenotype	Morphology	with hypodiploidy
All B-ALL	HLA-DR$^+$; TdT$^+$; CD19$^+$, CD22$^+$ and/or CD79a$^+$		with t(5;14)(q31;q32), IL3-IGH
Pro-B-ALL	No additional differentiation markers	L1 or L2	with t(1;19)(q23;p13.3), TCF3-PBX1
Common B-ALL	CD10$^+$	L1 or L2	
Pre-B-ALL	CD10$^\pm$; cyIg$^+$	L1 or L2	
Mature B-ALL	CD10$^\pm$; sIg$^+$	L3	

Half a century ago the diagnosis of ALL was equivalent to a death sentence, but due to carefully developed intensive and risk-adapted chemotherapy regimens with multiple cytostatic agents more

than 80% of ALL patients can nowadays be cured from their disease.[31] Chemotherapy of ALL consists of three phases: During the induction phase the blast number in the bone marrow is reduced to less than 5% of nucleated cells using the ALL-specific agent asparaginase, mitosis inhibitors (i. e. vincristine), prednisone and anthracycline derivatives (i. e. daunorubicin). During consolidation a further reduction of blast numbers is achieved and the development of drug resistance prevented by applying new combinations of these or alternative cytostatic agents or high dose chemotherapy. Finally, during the maintenance phase, 6-mercaptopurine and methotrexate are employed for up to two and a half years to prevent relapse.[8] To relieve and/or prevent CNS-affliction, which occurs in approximately 7% of ALL patients, methotrexate can also be given intrathecally or the patients undergo radiation therapy for local tumor control.[8,31] Furthermore, supportive therapy is provided to relieve bleeding symptoms, to reduce the risk of infection and to speed up hematologic reconstitution.[8] This therapeutic strategy has resulted in 15-year survival rates as high as 89% among pediatric ALL patients.[4,32] In adults, however, ALL is still difficult to treat, because unfavorable biologic features such as the Philadelphia chromosome are frequent and heavy chemotherapy regimens are poorly tolerated.[8,32,33] Furthermore, there are still numerous cases of high risk leukemia patients as well as those with refractory and/or relapsed B-ALL that succumb to their disease.[30,32,34] For these patients a further intensification of chemotherapy is impractical due to treatment-related toxicity, morbidity and mortality. Furthermore, long-term survivors have an increased risk to develop secondary neoplasias (presently 4% in 25 years) and the rate of secondary relapses is greater than 50%.[4,31,35] Thus, there is an urgent need to develop new, more selective forms of therapy to cure high risk and elderly patients and to prevent the development of therapy-related malignancies.

Aside from specific tyrosine kinase inhibitors such as the BCR-ABL-1 inhibitor imatinib, immunotherapeutic approaches are the focus of drug development in B-ALL.[8,36] The B cell differentiation antigens CD19 (see chapter 1.5.1), CD20, CD22 and HLA-DR were identified as the most promising targets for antibody therapy of B cell neoplasias and the first approved immunotherapeutic agent, anti-CD20 antibody rituximab, is applied successfully to treat B cell lymphomas.[1,37,38] However, monoclonal antibodies (mAb) directed against CD19 in precursor B lymphoid neoplasms, whose blasts are characterized by dim CD20 but strong CD19 expression, failed to display therapeutic efficacy.[38-40] Other antibody derivatives, T cell-recruiting agents and modified T cells have been developed to combat relapsed and/or refractory B-ALL.[36] One CD19-targeting immunotherapeutic agent, the BiTE® blinatumomab, was approved by the FDA and EMA in late 2014 and 2015, respectively.[41,42] The adoptive transfer of CD19-specific CAR-Ts is also a highly efficient treatment option and the first CD19 CAR-T Kymriah™ (tisagenlecleucel by Novartis Pharmaceuticals Corp.) was approved in the United States in August 2017.[20,43,44] However, both of

these immunotherapeutic strategies have serious drawbacks (see chapter 1.4.2), and thus further developments of next generation immunotherapeutics are desirable.

1.3 Cancer stem cells and clonal evolution in acute leukemia

Within any leukemia cell population there is a significant level of inter- and intraclonal genetic and epigenetic heterogeneity. As a result thereof and due to microenvironmental influences clonal subpopulations have different functional properties, for example with regard to differentiation, proliferation potential and drug sensitivity.[45-49] To explain the rise of clonal heterogeneity, several models have been proposed, two of which are of particular relevance in acute leukemia (see Figure 1): (1) According to the cancer stem cell (CSC) model, self-renewing, immature tumor cells, which are capable of asymmetric cell division, give rise to more differentiated clonal progeny and maintain the tumor tissue in a manner similar to the development and maintenance of normal tissues. CSCs are at the apex of a malignant clonal hierarchy[48-51] and acute myeloid leukemia behaves largely in accordance with this model.[48,52-54] Quiescence, drug insensitivity and other stem cell properties enable leukemia stem cells (LSC) to survive therapy and cause relapse. Therefore, the targeted elimination of LSC is paramount, especially because relapse propagating clones are often more aggressive than the diagnostic ones and are therefore more difficult to combat.[49,51] (2) Acute lymphocytic leukemia, however, is described more accurately by the second model, i. e. clonal evolution[45,46,55,56], which suggests that genetic alterations accumulate in malignantly transformed cells and can provide leukemia initiating potential to different coexisting subclones. In a Darwinian fashion, interclonal competition and environmental bottlenecks lead to the development of a nonlinear, branched clonal architecture.[45,46] Properties, which are usually attributed to stem cells such as self-renewal and chemoresistance, arise spontaneously and are selected, because they provide survival advantages.[47] Unlike the CSC model, the clonal evolution model does not propose a fixed leukemia initiating clonal subpopulation that can be targeted to prevent disease recurrence. Instead these properties may be gained by any subclone, which results in a transient stem cell phenotype.

Evidence for each of these models has been provided in acute leukemia and it is likely that they are not mutually exclusive, but that clonal heterogeneity emerges due to a combination of both plus additional phenomena such as pre-leukemic stem cells, tumor cell plasticity and interconvertibility. It has for example been proposed that clonal evolution may take place within the CSC compartment.[46] Other authors suggest that CSC initiate the disease, but that the entire cancer cell population acquires beneficial stem cell properties throughout disease progression and thus the CSC model

becomes obsolete at advanced disease stages.[47,48] Finally, cancer cells may move fluidly into and out of stem cell states, which has been described in solid tumors.[50,57] The elimination of CSC may thus be essential to cure patients, but continues to be a difficult goal because they are a highly complex moving target.[47-49] Nonetheless efforts to develop CSC-targeting therapies are underway and for some cancers, including AML, targetable stem cell markers have been described.

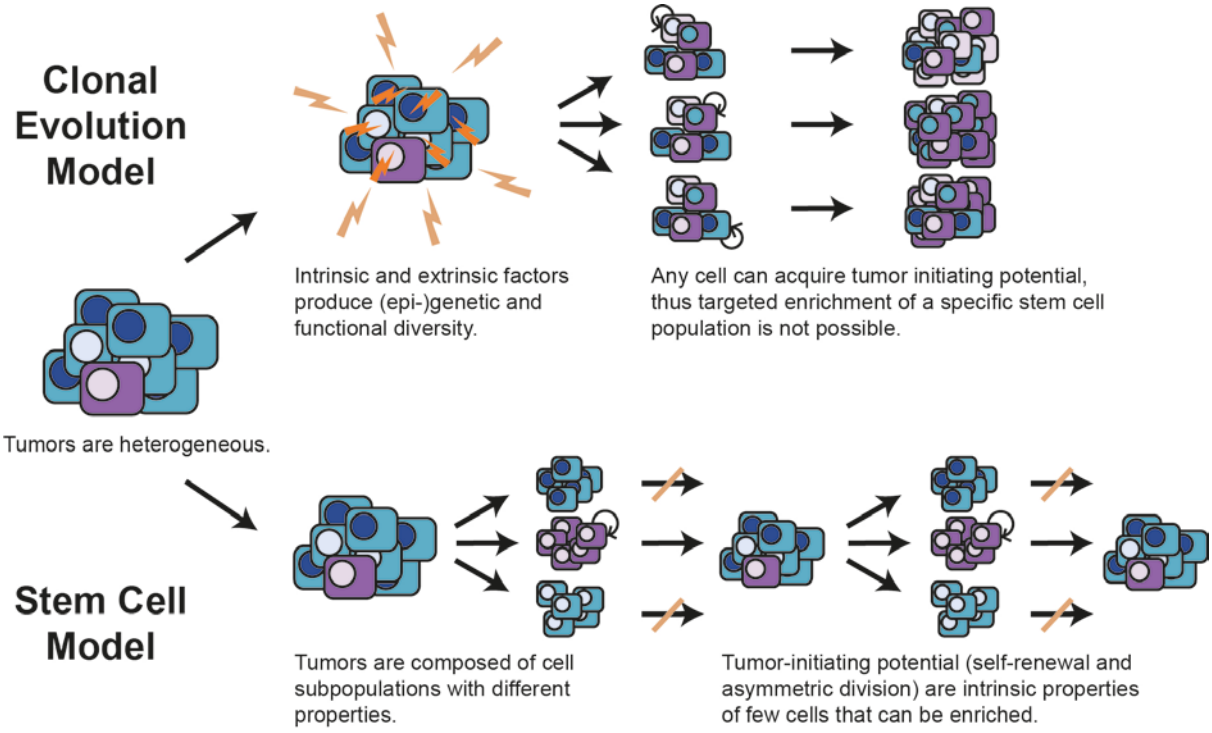

Figure 1: Models of tumor heterogeneity. Tumors are composed of phenotypically and functionally heterogeneous cells. There are two theories as to how this heterogeneity arises, which are particularly relevant in acute leukemia. The clonal evolution model and the cancer stem cell model [based on John E. Dick, 2008][48]

1.3.1 AML initiating cells

In the 1990s the group of John Dick identified a leukemia initiating subpopulation within the lineage negative (Lin^-) $CD34^+$ $CD38^{-/low}$ cell compartment of AML patients based on its serial transplantability in NOD/SCID mice. While the majority of leukemia blasts was post-mitotic, this subpopulation, which reflected the immunophenotype of healthy hematopoietic stem cells (HSC), self-renewed and repopulated the tumor tissue. It was found at a (highly variable) frequency of approximately 1 in 10^6 leukemia blasts.[58,59] This discovery started a period of intense research into the nature of leukemia initiating cells (LIC) and into potential therapeutic targets in order to eliminate this persistent cell population. In 2000, Jordan and colleagues demonstrated that the interleukin-3 receptor alpha chain (IL-3Rα/CD123; see chapter 1.5.3), but not its hetero-dimerization partner CD131, was more strongly expressed on $CD34^+$ $CD38^{-/low}$ LIC compared to normal hematopoietic stem cells (HSC), though

signaling through the IL-3R was not active.[60] Vergez *et al*. later found that a percentage of $CD34^+ CD38^{-/low} CD123^+$ cells greater than 1% at diagnosis already correlated with a poor disease-free and overall survival in a retrospective study.[61] Thus CD123 is one of the most promising surface antigens for targeted elimination of AML LIC. In line with these observations, monoclonal antibody (mAb) 7G3 directed against CD123 prevented engraftment of AML LIC in NOD/SCID mice.[62] However, the antigen is also expressed on healthy hematopoietic progenitors to a lower extent. To prevent "on-target off-tumor" effects that hamper or destroy normal hematopoiesis, immunotherapeutic approaches targeting CD123 need to be developed very carefully.[63] Further potential surface antigen targets that are preferentially expressed by $CD34^+ CD38^{-/low}$ LIC rather than normal HSC include CLL1, CD25, CD32, CD33 (Siglec-3), CD44 (hyaluronan), CD47, CD96, CD157 and TIM3.[64-66] In addition to targetable surface markers, other LIC-specific characteristics such as their metabolic and epigenetic properties and their interactions with the microenvironment are also investigated to identify new potential therapy targets.[65,67] This has become necessary since more sensitive detection methods for LIC have proven that LIC are also present in the $CD34^+ CD38^+$ and even in the $CD34^-$ compartment. These experiments include functional repopulation tests in NOD/SCID/$\beta 2m^{null}$ or NOD/SCID/IL2Rγ^{null} (NSG) mice as well as using intra-femoral instead of tail vein injection of leukemia cells.[67-69] Thus AML LIC display phenotypic diversity between patients and even within the blast population of an individual patient and may not always be eliminated entirely by therapeutic approaches targeting surface molecules.[67] Moreover, pre-leukemic stem cells as well as LIC can undergo clonal evolution in response to therapy, which may shift their immunophenotype.[67,68,70] To prevent this, it has been proposed that LIC-directed therapy should already be included at early treatment stages and that suitable read-outs for the efficacy of LIC-directed therapies are disease-free (DFS) and overall survival (OS) rather than response rate and complete remission.[52,67]

1.3.2 ALL initiating cells

After it had been ascertained that AML initiating cells reside mostly in the $Lin^- CD34^+ CD38^{/low}$ cell compartment, similar attempts to discover LIC in B-ALL were undertaken. However, a distinct immunophenotype could not be identified.[46] B-ALL initiating potential was detected in $CD34^+ CD38^{-/low} CD19^+$ leukemia blasts[71,72], in $CD34^+ CD38^+ CD19^+$ and $CD34^+ CD38^{-/low} CD19^+$ (even though the $CD34^+ CD38^+ CD19^+$ predominantly reproduced themselves)[73] and in $CD34^+$ CD19, $CD34^+ CD19^+$ and $CD34^- CD19^+$ cell compartments.[74,75] As few as $2*10^3$ $CD34^+ CD19^-$ blasts sufficed to produce leukemia in up to four serial recipient NOD/SCID mice.[75] In *mll*-rearranged B-ALL the co-expression of the myeloid antigen CD33 was not indicative of leukemia-initiating potential either.[74] It was, however, confirmed in these studies that the $CD34^+ CD38^- CD19^-$ ($CD33^-$)

compartment is enriched for healthy HSC, which can regenerate normal hematopoiesis.[73,74] These results highlight that neither CD34, nor CD38 or CD19 are robust markers for potential B-ALL LIC and contest the existence of a distinct LIC compartment in B-ALL. Numerous studies on evolutionary relationships of B-ALL subclones[46,56,76] and of monozygotic twins one or both of whom develop leukemia[71,77-79] rather indicate that the existence of pre-leukemic subclones and ongoing clonal evolution that leads to the acquisition or retention of stem cell properties play a more important role in B-ALL. Nevertheless B-ALL clones displaying "stemness" need to be eradicated to prevent relapse and refractoriness.

1.4 Immunotherapy of cancer

Because chemo- and radiotherapy of cancer are not specific but rather aggressive systemic treatment approaches, they have two serious drawbacks: systemic toxicity, including secondary neoplasias, and the development of long-term resistance.[80] Moreover, cancer cells with a low proliferation rate and an intrinsic drug insensitivity such as LIC frequently survive systemic therapy aimed at rapidly proliferating cells and can subsequently cause relapsed disease that is refractory to the original treatment.[49] In contrast to chemo- and radiotherapy, immunotherapy is a more specific approach that does not only aim at eliminating cancer cells directly. Instead the immune system is enabled to specifically detect and kill cancer cells.[81] The human immune system has a natural cancer suppressive function, especially via NK cell surveillance[82], and is intact in most cancer patients except at advanced stages.[81,83] Thus it can be harvested for therapy. Targeted immunotherapy is highly selective, which does not only allow the potential elimination of specific cell (sub-)populations such as LIC, but also decreases toxic side effects on non-target tissues and reduces dosage requirements compared to systemically active substances.[84] In all forms of acute leukemia, however, the displaced leukocyte populations and inhibition of normal hematopoiesis weaken the immune system significantly.[7,8] Targeted immunotherapeutic approaches against acute leukemia thus need to overcome this additional hurdle.

The first systematic application of cancer immunotherapy was described in the late 19th century by William B. Coley. He observed tumor regression in sarcoma patients after the injection of soluble bacterial toxins.[85,86] Coley's results are attributed to the (re-)activation of the sarcoma patients' immune system (including tumor-infiltrating lymphocytes (TIL)) in response to the feigned bacterial infection.[86] In line with this explanation, the engagement of autologous cytotoxic T lymphocytes (CTL) and NK cells as immune effectors is considered to be a particularly promising therapeutic approach due to the high cytotoxic potential of these leukocytes.[87]

A successful adaptive immune response against cancer is raised, when three prerequisites are fulfilled: First, tumor antigen-specific lymphocytes need to be present that can recognize cancer cells, but would not cause severe autoimmunity upon activation. Second, these lymphocytes need to be activated by professional antigen-presenting cells (APC) and need to expand. And third, they need to infiltrate the tumor tissue, overcome local immunosuppression and kill the cancer cells.[88]

Unfortunately, general immune activation by Coley's toxin or other adjuvants, cytokines and growth factors or via immune activators such as TLR agonists and unmethylated CpG is rarely able to induce tumor regression by itself.[89] One of the reasons is the dependence of such approaches on the intrinsic immunogenicity of the underlying malignancy: Some cancer entities are more immunogenic than others, because they display tumor-specific antigens (TSA). Among these are neoplasias with high mutational frequencies, which can result in the generation of neo-antigens (e. g. malignant melanoma and NSCLC).[90] Other immunogenic cancer entities express cancer/testis (CT) antigens (e. g. NY-ESO1, MAGE1/3) or are caused by oncogenic viruses and thus display viral antigens (e. g. HPV in cervical cancer), which can be recognized by the adaptive immune system.[89] Patients suffering from immunogenic cancer entities naturally develop TILs that can be recruited upon immune stimulation or expanded *ex vivo* and adoptively transferred in order to reject the tumor.[81] Another approach in such cases is cancer vaccination via peptide-, DNA/RNA- or dendritic cell (DC)-based vaccines.[91,92] However, within such cancer entities there is a high level of heterogeneity with regard to their immunogenicity. As a result only modest therapeutic benefits were achieved with general immune stimulation and vaccination approaches in the past.[81]

Aside from the lack of immunogenicity, two other important mechanisms prevent immunologic eradication of established tumors that have escaped immune surveillance by NK cells: The first one is immunoediting, which refers to the progressive loss of immunogenic surface markers under selective pressure mediated by T cells.[82] The second one is immunosuppression.

Cancer cells achieve immunosuppression by multiple mechanisms: (1) They downregulate MHC class I molecules. (2) They hijack immune checkpoints, which prevent autoimmunity in healthy subjects, by upregulating immunosuppressive surface markers (e.g. CTLA4, PD-L1). (3) They secrete immunosuppressive molecules (e.g. anti-inflammatory cytokines, IDO). (4) They recruit immunosuppressive cells (i. e. myeloid-derived suppressor cells (MDSC), tumor-associated macrophages (TAM) and regulatory T cells (T_{reg})). (5) And finally, most cancers promote hypoxia.[88]

Immunosuppression has to be overcome to enable an effective anti-cancer immune response. This is the goal of immune checkpoint blockade, which is commonly referred to as "releasing the break"[80]:

Anti-tumor immunity is enhanced upon blocking immune checkpoints, for example the inhibitory CD80/CD86 ligand cytotoxic T lymphocyte antigen-4 (CTLA4)[93], with monoclonal antibodies[94,95], which was discovered by the group of James Allison. The blockade of immune inhibiting interactions such as CTLA4 and CD80/CD86 or PD-L1/-L2 and PD-1 (also innate immune checkpoint: SIRPα and CD47) by monoclonal antibodies[96-100] is an effective new method for oncologists to fight cancer and leads to long-term remission in a significant proportion of patients with different immunogenic malignancies including malignant melanoma[100,101] and NSCLC.[102] Recently, checkpoint blockade has also become an experimental treatment for acute leukemia[103-105] since leukemia blasts upregulate immunosuppressive surface markers upon treatment.[105-107]

However, in many less immunogenic tumor entities the cancer cells resemble "self" too closely to raise a natural immune response that may be "released" by checkpoint blockade.[90] In the absence of TSAs, tumor-associated antigens (TAA), such as tissue-specific differentiation markers (including CD19 and CD33), have therefore been in the focus of developing targeted immunotherapeutic approaches. The induction of adaptive immunity via APC is circumvented and an effective immune response is raised by applying TAA-specific immune effector cell-engaging agents. These can be in the form of therapeutic monoclonal antibodies (mAb) and antibody derivatives (see chapter 1.4.1) or in the form of cellular therapeutics modified with tumor-specific receptors (see chapter 1.4.2).

The impressive therapeutic results that have been achieved with immune checkpoint blockade and other novel targeted therapies that are described in the following chapters have strongly increased the applicability and value of immunotherapy in the past two decades. This led to the recognition of immunotherapy by the journal "Science" as "breakthrough of the year - 2013".[108,109]

1.4.1 Therapy with monoclonal antibodies and antibody derivatives

The history of antibody therapy begins in the late 19th century, when Emil A. von Behring and Kitasato Shibasaburo discovered active blood serum components for the treatment of tetanus and diphtheria.[110] Their discovery resulted in the establishment of passive vaccination with anti-sera, which they developed together with Paul Ehrlich, and thus in the first therapeutic application of antibodies. Paul Ehrlich later proposed two concepts that had a significant impact on antibody therapy: The "side chain theory" (1891)[111], which suggests that selective structure-based receptor-ligand interactions, for example between antibodies and antigens, result in specific pharmacological activities, and the "magic bullet" concept (1908)[112], which states that disease-specific drug substances that spare healthy tissues are required for cure. In his time, Paul Ehrlich referred to small chemical compounds for the treatment of infections such as syphilis and tuberculosis as "magic

bullets", but the concept soon became a guiding general principle in modern pharmacology. Nowadays, the most selective drug substances are specific tyrosine kinase inhibitors (TKI) and monoclonal antibodies or derivatives thereof.

Antibodies, which are also referred to as immunoglobulins (Ig), are antigen-recognition molecules that are produced by terminally differentiated B lymphocytes, i. e. plasma cells. Each plasma cell produces an antibody of a single specificity.[113] In human beings there are five classes (or isotypes) of antibodies, which can be distinguished based on their constant regions: IgM (membrane-bound immunoglobulin or B cell receptor (BCR)), IgD, IgG, IgA and IgE. The most abundant isotype is the secreted immunoglobulin G (IgG) format, which is also most frequently used for therapeutic applications and can be further subdivided into four subclasses with different Fc-receptor (FcR) affinities, i. e. IgG1, IgG2a/b, IgG3 and IgG4.[114,115] The typical structure of an antibody is depicted in Figure 2.

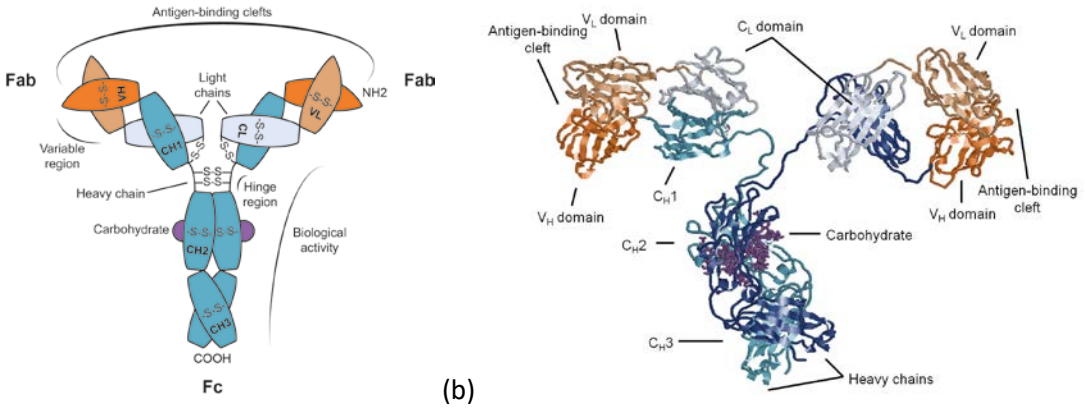

Figure 2: Schematic representation of IgG domains and 3D structure of IgG based on x-ray crystallography studies. (a) IgG is composed of 2 heavy and 2 light chains. V domains (V_L/V_H) at the N-terminal end of the polypeptide chains, which form the antigen-binding clefts, are followed by one (C_L) or three (C_{H1-3}) constant domains, respectively. Each domain has one internal disulfide bond. The two heavy chains are linked via two cystines in the highly flexible hinge region. The light and heavy chains are also connected via a disulfide bond between the C_L and C_{H1} domains. The C_{H2} and C_{H3} domains form the fragment crystallizable (Fc), while the V domains plus the C_L and C_{H1} domains in the two identical arms with antigen binding activity form the antigen-binding fragments (Fab). (b) Three-dimensional structure of mouse IgG2a antibody Mab231 based on x-ray diffraction data (blue shades: constant domains; orange shades: variable domains). The distinct barrel-shaped structure that is constructed from two β sheets in each Ig domain is clearly discernible. The junction between the V domains and the C_L/C_{H1} domains (elbow region) confers additional flexibility [adapted from Harris *et al.*, 1997].[116]

IgGs are roughly Y-shaped and have a molecular mass of approximately 150 kDa. Two of the three equal-sized arms of an IgG are responsible for antigen-binding (antigen-binding fragments (Fab)) via the variable or V region, while the third arm (fragment crystallizable (Fc)) binds to effector molecules or cells via the constant or C region. IgG are composed of two identical heavy chains (approximately 50 kDa) with 4 domains each that are linked via two disulfide bonds in a highly flexible hinge region, and of two identical light chains (approximately 25 kDa) with 2 domains that are each paired with one heavy chain and covalently bound to it via a single disulfide bond. All domains of the heavy and

light chains are constructed from anti-parallel β–strands that form two β–sheets with an intra-domain cystine to form a barrel-shaped structure (i. e. β–barrel). This is known as the immunoglobulin fold and is the hallmark of members of the immunoglobulin superfamily of proteins. Each of the variable domains at the N-terminal ends of the light and heavy chains (V_L/V_H domain) possesses three unique hypervariable loops, which combine into the complementarity-determining regions (CDR) that are responsible for binding the antigenic determinants known as epitopes.[117] While the CDR determine antigen-specificity, the surrounding, less variable framework regions are species-specific and may thus be immunogenic, when transferred from one species to another. The constant domains of the light and heavy chains (C_L/C_{H1-3} domains) are slightly smaller than the V_L/V_H domains, because they lack the hypervariable loops.[114,115]

Immunoglobulins have several effector functions (Figure 3): Upon binding to soluble ligands or cell surface receptors they can activate or silence signaling pathways and neutralize pathogens by coating (i. e. opsonizing) them. Moreover, the glycosylated Fc-fragment of antibodies can interact with several components of the innate immune system and thus provoke complement-dependent cytotoxicity (CDC), antibody-dependent cellular cytotoxicity (ADCC) and antibody-dependent cellular phagocytosis (ADCP). The Fc-mediated effector functions have proven to be of particular value in cancer immunotherapy and the cross-presentation of tumor antigens to T cells by DCs or macrophages that have phagocytosed antibody-coated cancer cells can even induce an adaptive anti-tumor immune response (Figure 3).[118]

Modern antibody technology, which allows the careful design, engineering and large scale production of therapeutic mAb with a predefined antigen-specificity, has been carefully developed over many decades. One of the most important milestones was the introduction of hybridoma technology, i. e. the fusion (and thus immortalization) of plasma cells with myeloma cells, by Köhler and Milstein in the 1970s.[119,120] This technology allowed the production of monoclonal antibodies with a single specificity for the first time. Initially, the majority of mAb was generated by immunizing rodents, which was of limited therapeutic use: Patients treated with mAb that originated from different species often developed immune responses (i. e. autologous antibodies) against the foreign framework regions of the therapeutic antibodies and thus became not just severely ill, but also resistant to therapy.[121-123]

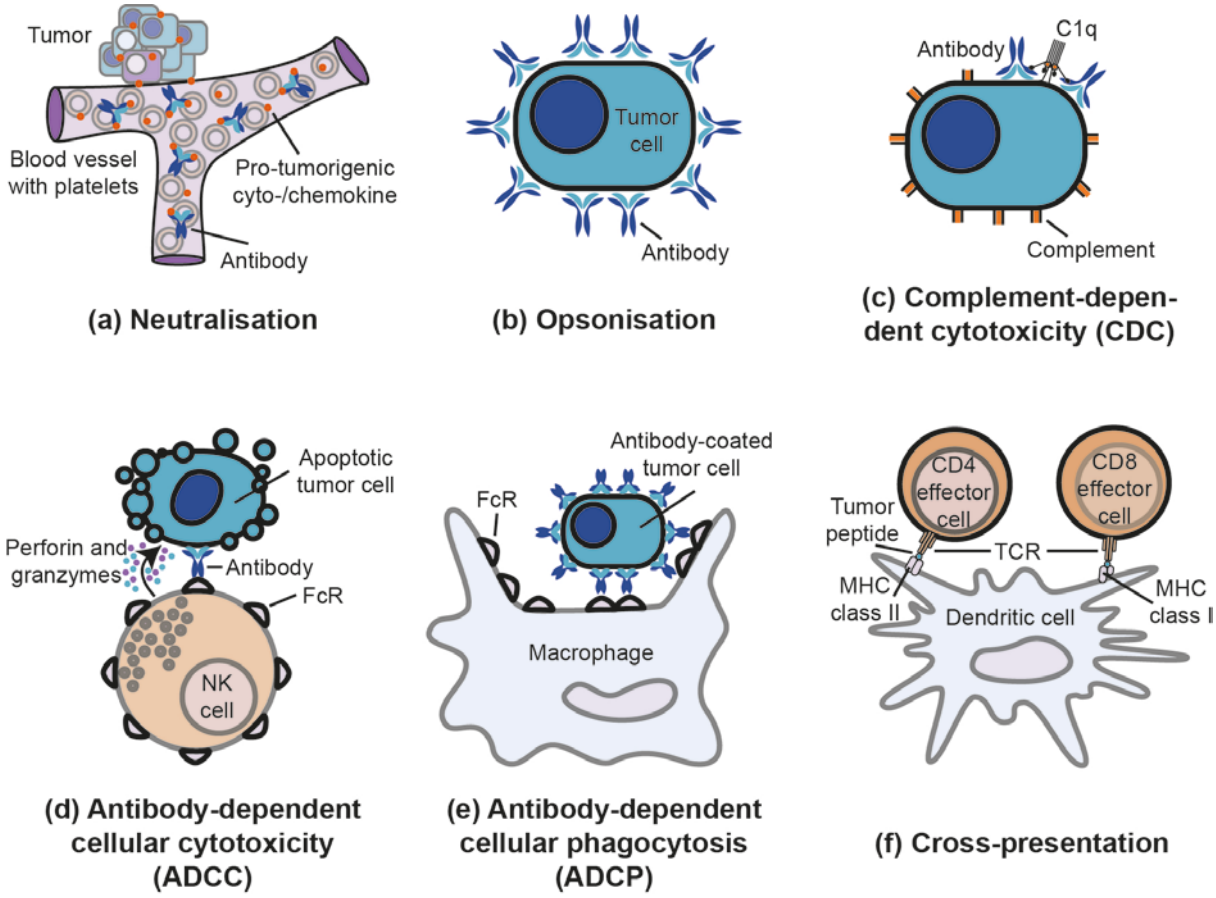

Figure 3: Anti-tumor mechanisms mediated by IgGs. (a) IgGs bind to pro-tumorigenic chemokines and cytokines and thereby neutralize them. (b) Antibodies opsonize (i.e. coat) the tumor cell and block pro-tumorigenic receptors and/or interactions with the tumor microenvironment. (c) Tumor-specific antibodies recruit complement to the tumor cell surface, thereby labeling the cell for destruction. (d) Antibody-dependent cellular cytotoxicity (ADCC) is initiated by the recognition of IgG-coated tumors by FcR, which are expressed on immune effector cells such as NK cells, macrophages and neutrophils. These interactions lead to ADCC and tumor cell apoptosis through the delivery of perforin and granzymes. (e) The IgG-coated apoptotic tumor cells can bind FcR on phagocytes and initiate Fc-dependent phagocytosis, leading to the lysosomal degradation of the tumor cell. (f) Peptides derived from lysosomal degradation of tumor cells can be loaded onto MHC class II molecules, leading to the activation of $CD4^+$ T helper cells. In addition to $CD4^+$ T cell activation, DCs can cross-present tumor antigen-derived peptides and prime cytotoxic $CD8^+$ T cells [based on Weiner *et al*., 2010].[118]

Moreover, the interaction between antibodies from foreign species and other components of the human immune system such as complement or Fc-receptor (FcR)-bearing leukocytes was poor.[123] Thus therapeutic antibodies needed to become more "human". With the advent of recombinant DNA technology this goal became achievable[124]: The first approach towards more human, less immunogenic mAb was the development of chimeric antibodies, which were composed of human immunoglobulin constant regions and murine variable domains with defined specificity.[125,126] While such chimeras displayed considerably less immunogenicity than murine antibodies, an even higher degree of immunotolerance of therapeutic mAb was achieved by CDR-grafting.[127] This technique developed by Jones *et al*. (1985) generated mAb that were 85 to 90% human, i. e. "humanized", by grafting the hypervariable loops and adjacent framework residues from the V_L and V_H domains of

antigen-specific murine antibodies onto human immunoglobulin frameworks. Today, fully human antibodies can also be generated by means of phage libraries and transgenic mice.[128]

Recombinant DNA technology not only enabled humanization of mAb, it also allowed the transfer of immunoglobulin-production from hybridoma cell lines to highly efficient and stable eukaryotic expression systems such as Chinese Hamster Ovary (CHO) cells.[129] Thereby the large scale production of therapeutic antibodies became feasible. Moreover, the effector functions of mAb can be tuned by modern technologies such as Fc-[130] and glycoengineering.[131,132]

As a result of these developments, therapeutic monoclonal antibodies have emerged as a fast growing and valuable biopharmaceutical branch. The murine anti-CD3 antibody muronomab was the first therapeutic mAb to receive approval by the FDA in 1985 for the prevention of graft-versus-host disease (GvHD) upon organ transplantation.[133,134] A few years later, in 1994, the first humanized antibody for the treatment of cancer was approved, i. e. the anti-CD20 antibody rituximab (MabThera®).[135] Since the early 1990s, four to nine therapeutic mAb received marketing authorization in Europe and the USA annually, with a record of nine approvals in 2015.[136,137] 47 antibodies were available on the market in November 2014 and the global sales revenue of antibodies had already reached $75 billion by 2013.[136] These numbers continue to rise rapidly as more than 60 therapeutic antibodies are commercially available in 2017 and 52 mAb for cancer and non-cancer indications (20 and 32 mAb, respectively) have entered late stage clinical trials.[137]

Furthermore, a number of antibody-derived agents, including antibody-drug-conjugates (ADC), radioimmunoconjugates, immunocytokines and bispecifics, have been developed and begin to enter the biopharmaceutical market. These major classes of antibody derivatives are reviewed by Christian Hess and colleagues (2014)[84] in detail and combine the target specificity of full-length antibodies or antigen-binding antibody fragments with additional therapeutic functions to overcome some of the limitations of the classical IgG-format. In the context of acute leukemia, the first ADC that received regulatory approval is of particular interest: the CD33-specific agent gemtuzumab ozogamicin (GO; Mylotarg®). GO is a humanized IgM antibody that is conjugated to the bacterial cell toxin calicheamicin via a composite hydrazine/disulfide linker. It achieved promising responses in 30% of AML patients in clinical trials. However, at a dose of 9 mg/m^2 the patients experienced dose-limiting hepatotoxicity. In post-approval trials, the balance between clinical benefit and toxicity tipped towards the latter leading to the voluntary withdrawal of GO by Pfizer in 2010.[13,14] However, the agent was recently (September 1st 2017) re-approved at lower concentrations, with a different dosing schedule and for a different patient population with newly diagnosed AML.[15] Next-generation ADC with more stable linkers and conjugated drugs that are only activated upon internalization are

being developed, three of which were approved as of August 2017.[137] Aside from ADC, bi- and multispecific antibodies or antibody-derived agents that simultaneously target one or more TAA and recruit immune effector cells, in particular CTL,[138,139] in an FcR-independent manner have shown promise for the treatment of acute leukemias.[42,140-142]

The first bispecific full-length IgG that engaged T cells was the TriomAb® catumaxomab (Removab®), which consisted of half a murine IgG2a antibody with specificity for EpCAM paired with half a rat IgG2b antibody with specificity for CD3 (Figure 4, left panel). Catumaxomab efficiently induced ADCC and ADCP and also engaged CTL for the lysis of EpCAM-positive cancer cells in malignant ascites. However, the marketing authorization for catumaxomab from 2009 was withdrawn upon request of Neovii Biotech GmbH in 2017.[84] Other companies developed alternative technologies for the generation of bispecific full-length antibodies (Figure 4, left panel) that have various advantages with regard to production or therapeutic properties and are currently investigated in clinical trials. These bispecifics are mostly intended for the treatment of solid tumors.[84]

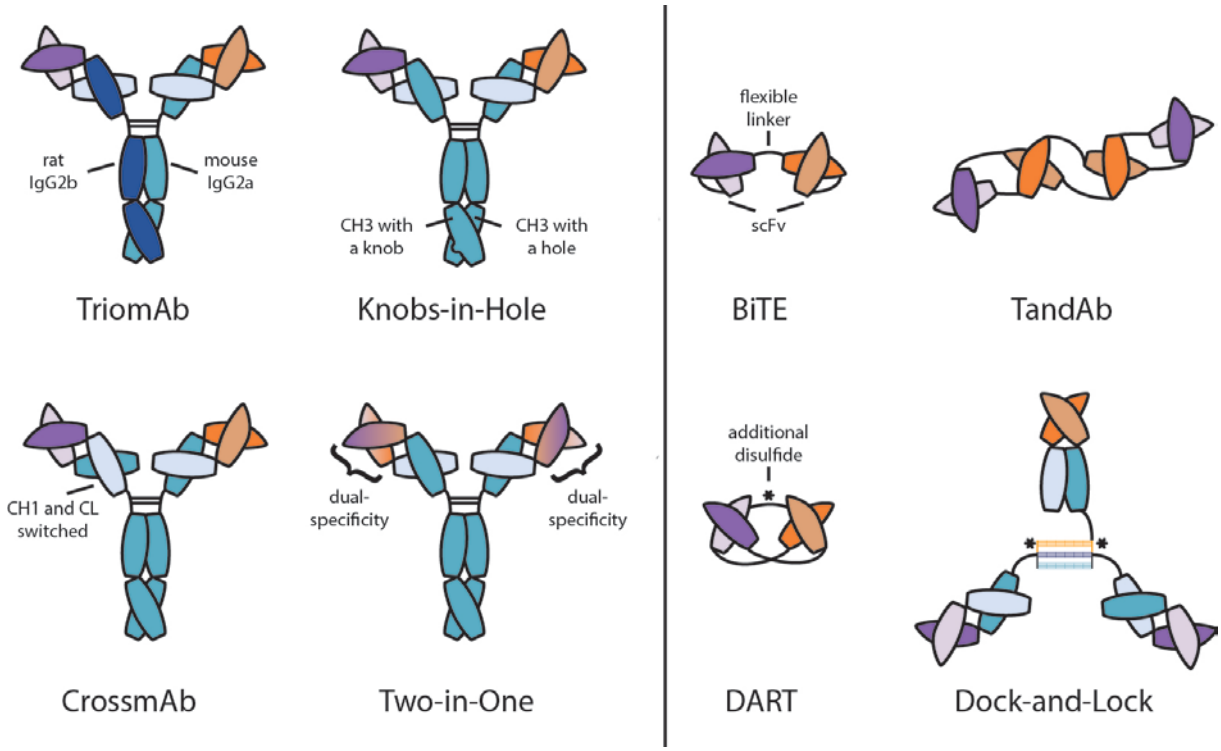

Figure 4: Schematic representation of bispecific antibody and antibody-derived formats that are investigated in clinical trials. Left panel: Bispecific full-length IgGs. Right panel: Bispecific antibody fragments [based on Hess *et al.*, 2013].[84]

Instead of employing full-length IgG, antibody-fragments can also be used for the generation of multispecifcs. In particular so-called single-chain variable fragments (scFv), which are constructed by connecting the V_H and V_L domains with a flexible linker and represent the smallest antigen-binding unit of an antibody.[143] Numerous multispecifics based on antibody-fragments target hematologic

malignancies and have already entered the clinic. The molecular formats include BiTE® (Amgen Inc., formerly Micromet) and DART® (dual-affinity retargeting scaffold by MacroGenics Inc.), which each have two antigen-binding domains, TandAbs (Affimed GmbH) with four binding moieties, and the Dock-and-Lock™ or DNL™ platform (Immunomedics, Inc.), which can generate multivalent antibody derivatives with multiple specificities (Figure 4, right panel).[84] The majority of these bispecific antibody fragments engage immune effector cells for the elimination of cancer cells via a scFv-domain that is specific for a trigger antigen of the effector cell such as CD3 or TCR on T cells[141,144,145], CD16 (FcγRIII) on NK cells and macrophages[146], CD64 (FcγRI) on macrophages[147] or CD89 (FcαRI) on neutrophil granulocytes.[148] The smaller size of bispecific antibody fragments compared to full-length IgG comes with the advantage of penetrating tumor tissues more easily (though it also results in rapid blood clearance).[149-151] Furthermore, they do not compete with other serum IgG for FcR and are therefore highly efficient activators of their engaged immune effector cells. Finally, they are not subject to an Fc-mediated antibody sink and can therefore be applied in lower dosages than bispecific full-length mAbs.[87,152-154] Multivalent binding of more than one TAA on the cancer cell by multispecific agents can also enable the distinction of a malignant cell (sub-)population from its healthy counterpart, for example in biphenotypic leukemia (see chapter 1.2.3). Moreover, immune escape by the targeted tumor cells is hampered, because antigen double-negative cancer cell clones are less likely to arise than single-negative ones.[139,155]

1.4.2 BiTE® and CAR-T

With its approval by the FDA and EMA for the treatment of relapsed/refractory B-ALL in late 2014 and 2015, respectively, the CD19/CD3-epsilon (CD3ε)-specific BiTE® blinatumomab (Blincyto®, formerly MT103) became the first-in-class bispecific antibody fragment for therapeutic use in patients. A CD19/CD3ε-bispecific scFv (bsscFv) and thus the molecular BiTE format was first described by the group of P. Kufer at the Ludwig-Maximilians-Universität in Munich.[156] The preclinical[157-161] and clinical[162-176] development of this agent, i. e. blinatumomab (name derived from "B-lineage-specific anti-tumor mouse monoclonal antibody"), and other BiTE® was subsequently continued in the newly founded company Micromet AG, which was bought by Amgen GmbH in 2012.

BiTE® are constructed from two scFv that are covalently linked by $(Gly_4Ser)_n$ linkers. The CD3ε–specific domain is common to all BiTE®, but the TAA-specific domain varies depending on the indication (for example anti-CD19[156-176], -CD33[18,106], -EpCAM[177-181], -CEA[182,183], or -EGFR[184]). The CD3ε–domain has a lower affinity for its antigenic target than the TAA-specific domain ($K_{D,CD3\varepsilon} = 10^{-7}$ M vs. $K_{D,\ TAA} = 10^{-9}$ M), therefore the target cells are preferentially coated by BiTE®, whereas the

T cells retain their mobility and can serially eliminate several coated cancer cells.[160] The MHC : peptide-independent, but target cell-specific connection that BiTE® facilitate between effector T cells and cancer cells results in T cell activation by cross-linking, the production of an efficient cytolytic synapse (see chapter 1.6), as well as cytokine production (IFN-γ, TNF-α, IL-2, IL-6 and IL-10) and T cell proliferation.[157-160] In contrast to full-length antibodies for the treatment of hematologic malignancies such as rituximab, which are effective at nanomolar concentrations, Blinatumomab displayed EC_{50}-values in the high femto-/low picomolar range *in vitro*.[157] In patients this translated into effective therapeutic concentrations of 15 µg/m^2/day (at less than 45 kg body weight) or 28 µg/day (at more than 45 kg body weight). However, due to its low molecular weight of approximately 60 kDa, the BiTE® is rapidly cleared from the blood by the kidneys and thus has to be administered as a continuous intravenous infusion in 4 week cycles.[42,185]

The novel mechanism of action of blinatumomab, i. e. the redirection of CTL, can be accompanied by several immune-related adverse events that need to be carefully monitored. Aside from general flu-like symptoms due to the induced inflammatory reaction, blinatumomab can cause serious adverse events including cytokine-release syndrome (CRS)[174,185-187], a condition that led to multi-organ failure in six healthy volunteers upon treatment with the CD28-superagonist TGN1412 in 2006[188], and CNS-related events[174,185,189], which may be the result of activated T cells crossing the blood-brain-barrier to eliminate malignant CD19$^+$ CNS infiltrates.[185] Because of the risk to induce CRS, blinatumomab administration is staggered (from 5 to 15 µg/m^2/day or 9 to 28 µg/day) during the first cycle and is not indicated in patients with a high tumor burden. Moreover, toxicity management with corticosteroids and anti-IL-6 mAb is available for patients, who develop CRS.[176,190] Similarly, blinatumomab-induced neurotoxic events in B-ALL patients with CNS involvement are managed by discontinuation of therapy with the possibility for reintroduction at a lower dose and with concomitant anticonvulsant treatment.[176,185] Another phenomenon resulting from blinatumomab treatment is the emergence of CD19-negative ALL relapse clones in some patients as in the case of any other targeted therapy.[191-195]

The next most advanced BiTE®, which entered its first clinical trial (NCT02520427) in August 2015, is AMG 330, a CD33-specific BiTE® for the treatment of relapsed/refractory AML.[42,196] Preclinical data indicated a very high efficacy of the agent in combination with allogeneic as well as residual autologous T cells *in vitro* and *in vivo*. Moreover, AMG 330 can potentially be applied to more than 99% of AML patients with CD33$^{+/dim}$ blasts.[18,19] In addition, the efficiency of AMG 330 might even be enhanced by checkpoint blockade of the PD-1/PD-L1 axis.[106]

Chimeric antigen receptor-modified T cells (CAR-T) represent an alternative, highly effective strategy for the engagement of cytotoxic T lymphocytes to eliminate cancer cells[20,197]: The widely used second generation CARs, which have entered the clinic, are artificial activating receptors for T cells that are constructed from several domains: (1) an extracellular scFv for TAA-recognition, (2) a transmembrane domain, (3) a costimulatory domain derived from TCR-coreceptors such as CD28, 4-1BB or OX40, and (4) the intracellular signaling domain of the CD3ζ-chain.[198] To introduce CAR-T into cancer patients, autologous T lymphocytes are isolated and modified with a TAA-specific CAR by retro- or lentiviral transduction or non-viral technologies such as the transposon-transposase or CRISPR-Cas systems. Subsequently the CAR-T are expanded *ex vivo* and reinfused into the patient where they eliminate target antigen-positive cells in a TCR-independent manner.[20,198]

CAR-T display an even higher level of sensitivity for target antigen-positive cells than BiTE®[199] and can generate immunologic memory.[20,200] This results in a high efficacy on the one hand, but on the other hand in more pronounced immune-related adverse events (in particular CRS) and prolonged depletion of target antigen-positive healthy cells ("on-target off-tumor"-toxicity).[190,198] Therefore the applicability of CAR-T is currently limited to TAA expressed by cancer cells and non-essential tissues only.[20,198] Consequently, the CD19-specific CAR-T for the treatment of relapsed/refractory B-ALL[201-204] are the most successful ones to date, since prolonged lymphodepletion of B cells can be compensated by regular infusions of immunoglobulins.[204,205] The first CD19-targeting CAR-T, i. e. tisagenlecleucel (Kymriah™ by Novartis) received marketing approval on August 30th 2017.[44] CD33- and CD123-specific CAR-T for the treatment of myeloid malignancies are also investigated in preclinical[206,207] and clinical settings (NCT01864902 and NCT03126864 for CD33 CAR-T; NCT03114670, NCT02623582, NCT02159495 and NCT03190278 for CD123 CAR-T). However, two ongoing phase I trials with allogeneic CD123-specific CAR-T (UCART123) by Cellectis Inc. with the ClinicalTrials.gov identifiers NCT03190278 and NCT03203369 were put on hold by the FDA in late August after one patient died following grade five CRS.[208] It also remains to be determined whether the treated patients can survive prolonged myeloablation and depletion of CD33-/CD123-positive progenitors. To tackle some of these problems, a new generation of CAR is under development that incorporates suicide genes[198] or depends on the combinatorial recognition of more than one antigen[209,210], but none of these have entered the clinic yet.

1.4.3 Single-chain triplebodies

The antibody-derived single-chain triplebody format (scTb), which carries three scFv-domains in tandem, was developed by the research group of Prof. Fey at the University of Erlangen-Nuremberg.

The molecular design was first published by Kellner *et al*. in 2008[211], who developed a triplebody with specificity for lymphoid differentiation marker CD19 and the activating FcγRIII (CD16) expressed by NK cells, macrophages and neutrophil granulocytes. ScTb carry two binding moieties for tumor antigens and one binding moiety for a trigger antigen to engage immune effector cells for the redirected lysis (RDL) of cancer cells. Thus they are capable of monospecific bivalent as well as bispecific bivalent binding of the targeted cancer cell. This "dual-targeting" capacity is one of the distinguishing features of the triplebody format and may allow selective binding and elimination of double-positive cancer cells rather than single-positive cells, as has been shown *in vitro* for a triplebody with specificity for CD19 and HLA-DR.[212,213] The three scFv are connected by flexible $(Gly_4Ser)_4$ linkers in a single polypeptide chain, can be easily exchanged by standard cloning techniques and can carry different tags (Figure 5). This simplifies their production and purification considerably in comparison to other multispecific antibody fragments.[211,212,214,215]

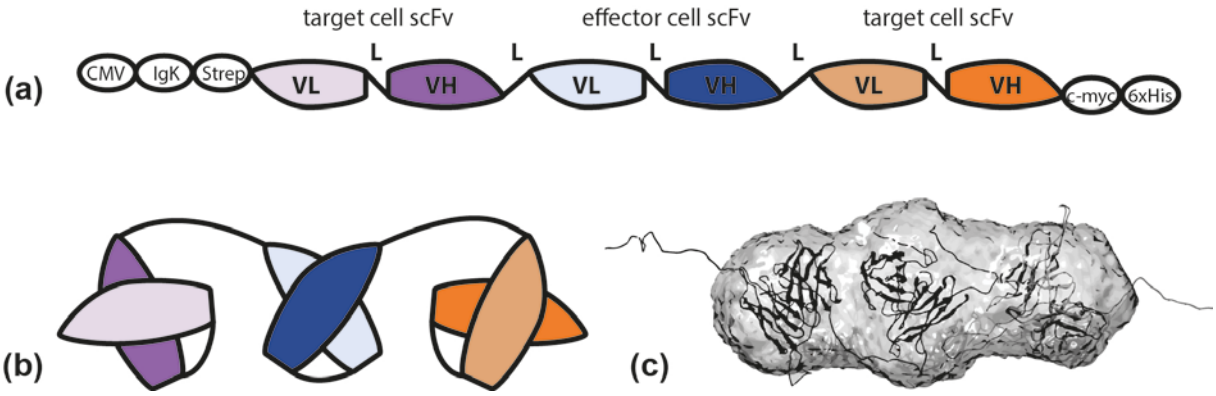

Figure 5: Domain arrangement and putative 3D shape of a single-chain triplebody based on small angle x-ray scattering (SAXS) data. (a) Block-structure of the gene cassette for a scTb is shown [based on Kellner *et al.*, 2008].[211] (b) Schematic representation of a scTb. (c) An overlay of the shape of triplebody [19x16x19] predicted from SAXS data [Nadja C. Fenn, unpublished] and the three-dimensional structure of 3 scFv based on x-ray crystallography is shown. The two distal scFv have a putative spread of 20 nm [adapted from Georg H. Fey, 8th Fabisch-Symposium, March 21st 2012].

The molecular weight of scTb ranges between 80 and 90 kDa, which results in a plasma half-life of four hours in mice[211], because the molecules are not immediately removed by renal clearance. The avidity that results from bivalent target cell binding by scTb is not as pronounced as that of antibodies, however, they still display cytotoxic efficacy at very low concentrations in the picomolar range.[211,212,214,215] Thus far, NK cell-recruiting triplebodies with monospecific bivalent targeting of CD19[211] and bispecific bivalent targeting of CD19 and HLA-DR[212,213], of CD19 and CD33[215], and of CD33 and CD123[214] have been described for the potential treatment of different forms of leukemia. Whether other immune effector cells can also be recruited by scTb has yet to be determined. Moreover, the question whether target antigen combinations other than CD19 and HLA-DR can lead

to selective lysis *in vitro* and *in vivo* is of interest for therapeutic applications. If so, and provided that the large scale production of highly pure protein is possible, then the single-chain triplebody format may be a suitable platform for a wide variety of effective and highly selective targeted immunotherapeutics.

1.5 Target antigens for immunotherapy in hematologic malignancies

Many antigens are specific for the hematopoietic system and not expressed by other tissues, which makes them suitable for targeted immunotherapy of hematopoietic malignancies. However, in the present work lymphoid differentiation marker CD19, myeloid differentiation marker CD33 and the interleukin-3 receptor alpha-chain (CD123) were chosen as TAA, because they are therapeutically validated targets and when combined, they may serve to distinguish particularly relevant malignant cell subpopulations. Their structure and biology is described in detail in the following paragraphs.

1.5.1 B lymphoid marker CD19

The B lymphoid marker CD19 (formerly B4 antigen) is a 95 kDa (556 amino acids) type I transmembrane-glycoprotein from the immunoglobulin (Ig)-superfamily that augments B cell signaling via both B cell receptor (BCR)-dependent and -independent mechanisms.[216,217] The *cd19* gene is encoded on the short arm of chromosome 16 (gene locus 16p11.2) and is highly expressed during different maturation stages of healthy B cells, i. e. from the time of initial immunoglobulin heavy chain gene rearrangement to the terminal differentiation into plasma cells.[217,218] CD19 expression is absent from virtually all cells in the body other than B cells and follicular dendritic cells, but is homogenous and high in the majority of precursor B lymphoid blasts. Therefore it is ideally suited for targeted immunotherapy in B cell malignancies.[217-219]

The CD19 protein is comprised of an extracellular region with two C2-type Ig-like domains, a single transmembrane region and a highly conserved cytoplasmic tail (see Figure 6). It does not display significant homology to any other proteins.[216-218] The signaling functions of CD19 are exerted via differential phosphorylation of specific tyrosine residues in its cytoplasmic region, especially via residues Y391, Y482 and Y513.[216,220,221] At the B cell surface, CD19 is present in a co-receptor complex with the BCR together with CD21/CD35, CD225 and CD81.[216,217,222,223] While CD21 is involved in complement-modified antigen recognition, the tetraspanin membrane protein CD81 serves as a chaperone.[216,223]

Upon triggering of the pre-BCR complex by cell autonomous aggregation or of the mature BCR by ligand binding, the tyrosine residues in the cytoplasmic tail of CD19 are sequentially phosphorylated by membrane kinases LYN and SYK. The CD19 co-receptor complex then translocates into lipid rafts and serves as interaction partner for signaling proteins with Src-homology 2 (SH2) domains such as PI3K, LYN, FYN, VAV, GRB2 and PLCγ2. By activating multiple signaling cascades, the CD19 co-receptor complex enhances (pre-)BCR signaling and facilitates clonal proliferation, IgL gene recombination and further differentiation events.[216,220,221] BCR-independent signaling via the CD19 co-receptor complex is for example induced by binding of complement component C3d via CD21. Thereby it links innate with adaptive immunity.[216,217,222] While the interaction of the CD19 co-receptor complex with different interaction partners usually promotes B cell growth and differentiation, direct ligand-binding of CD19-L – a 54 kDa high mobility group (HMG)-box protein – to the extracellular domain of CD19 led to the disruption of CD19-signaling and rapid apoptotic cell death.[217,224] This mechanism might also play a role in the efficacy of anti-CD19 therapeutics.[217]

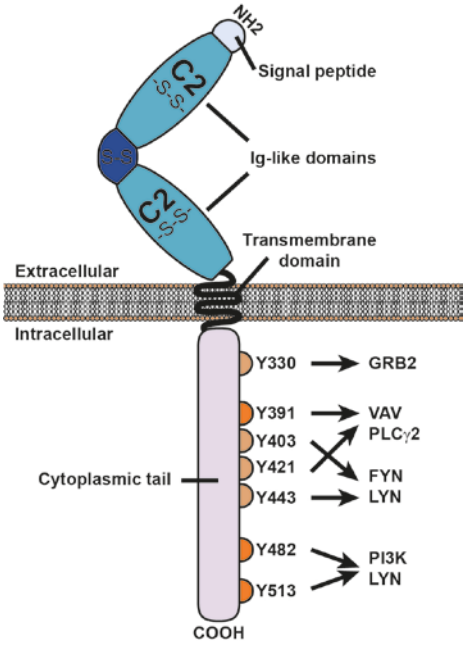

Figure 6: Schematic representation of the molecular structure of CD19. The extracellular region of CD19 with its two C2-type Ig-like domains forms a co-receptor complex together with CD21/CD35, CD225 and CD81. Signaling through CD19 can either be triggered upon cell autonomous aggregation or upon ligand-binding to the mature BCR. This results in sequential phosphorylation of the indicated tyrosine residues in the cytoplasmic tail of CD19 and subsequent activation of multiple signaling cascades that induce B cell proliferation and differentiation [based on Wang *et al.*, 2012 and Carter *et al.*, 2002].[216,220]

During malignant transformation of precursor B lymphocytes, a positive feedback loop between CD19 and cellular (c)-MYC appears to play a role in addition to its pro-proliferative function: CD19-mediated activation of the RAS/ERK2 pathway via GRB2 or of the PI3K/PKB/GSK3β signaling cascade leads to the phosphorylation and stabilization of c-MYC and thus of important downstream effectors

(e. g. cell cycle regulator Cyclin D2). C-MYC in turn promotes CD19 overexpression and phosphorylation.[217,225] During advanced stages of B cell malignancies, however, the contribution of CD19-signaling to cell proliferation appears to become dispensable, which may partially explain the rise of CD19-negative escape mutants under CD19-targeted immunotherapy.[217]

The homogenous and high surface expression of CD19 that is restricted to healthy and malignant B cells, its easy accessibility and its internalization and potentially pro-apoptotic function upon direct ligand binding have prompted the development of multiple and diverse targeted immunotherapeutic approaches.[216,217,219] After the initial limited success with conventional anti-CD19 monoclonal antibodies, new strategies using multispecific antibody derivatives, antibody-drug-conjugates, Fc-engineered antibodies and CAR-Ts have produced more promising results[219] and may be improved even further by rational design.

1.5.2 Myeloid marker CD33

The CD33 (alternatively Siglec-3) differentiation antigen (gene locus 11q13.1) is a type I transmembrane-glycoprotein that is expressed by myeloid cells from early to late stages of development.[226,227] The 67 kDa protein (364 amino acids) is a member of the Ig-superfamily, more particularly of the sialic acid-binding immunoglobulin-like lectins (Siglecs), which are involved in mediating cell-cell interactions and modulating intracellular signaling.[227,228] Each member of the Siglec family specifically recognizes a sialylated glycan.[228] CD33 is one of nine CD33-related Siglecs expressed by human immune cells and it functions as a negative regulator of cell proliferation and differentiation.[228]

The protein carries two disulfide-linked Ig-like folds of the V- and C2-set in its extracellular region, has a single transmembrane region and a cytoplasmic tail with a membrane-proximal immunoreceptor tyrosine-based inhibitory motif (ITIM) and a membrane-distal ITIM-like motif (see Figure 7).[227,228] An alternative splice variant of CD33, i. e. CD33m, lacks the extracellular V-set Ig-like domain and disulfide-bridges to the C2-set Ig-like domain. Since the V domain is immunodominant, CD33m is not recognized by the majority of early anti-CD33 antibodies.[227] Furthermore, a soluble CD33 protein has been detected in AML patients, however, its prognostic value and potential impact on CD33-targeted therapies are unknown.[227]

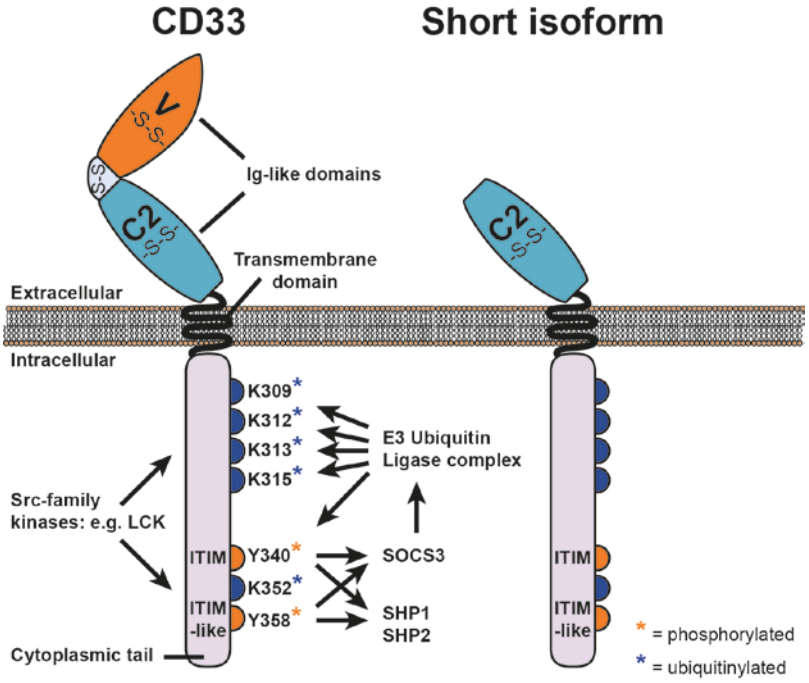

Figure 7: Schematic representation of the molecular structure of CD33. The extracellular region of CD33 is composed of two Ig-like domains of the V- and C2-set with intra-domain disulfide-links. CD33 recognizes specific sialylated glycans and thereby mediates cell-cell interactions. Intracellular signaling is modulated by CD33 upon phosphorylation of specific tyrosine residues within the ITIM and ITIM-like motifs in its cytoplasmic tail and upon ubiquitination [based on Laszlo et al., 2012].[227]

Though CD33 has been implicated as a potential inhibitory receptor in multiple cellular processes including cellular activation, secretion of pro-inflammatory cytokines and proliferation, the signaling pathways that the myeloid antigen employs are poorly understood.[227,228] It is known, however, that phosphorylation of the ITIM and ITIM-like motif by Src-family kinases such as LCK leads to the recruitment of SH2-domain containing phosphatases SHP1 and SHP2. These phosphatases dephosphorylate CD33 and adjacent membrane receptors in a negative feedback loop and thereby, as well as by their downstream effectors, dampen tyrosine kinase signaling and cytokine secretion.[227-229] Alternatively, the competitive binding of suppressor of cytokine signaling-3 (SOCS3) to the phosphorylated ITIM-motif of CD33 results in the recruitment of the E3 ubiquitin ligase complex and proteasomal degradation of CD33.[227,228] Importantly, CD33 can also act as an endocytic receptor upon ligand-binding.[227,228] Under normal physiological conditions this is thought to help the clearance of sialylated antigens and may promote or inhibit antigen presentation.[227,228] Furthermore, CD33 ligand-binding and internalization affect cytokine secretion by monocytes.[227,230]

In AML, CD33 is present on the blast surface of the majority of patients. High CD33 expression is generally associated with inferior disease-free and overall survival.[227] Though the myeloid antigen displays strongly variable densities in the plasma membrane, it is an attractive target for

immunotherapy of AML and other myeloid neoplasias.[19,227] Furthermore, CD33 is expressed by at least a subset of leukemia stem cells, but is largely absent from healthy hematopoietic stem cells. [12,61,227]

The endocytic properties of CD33 have been carefully studied in order to exploit them for immunotherapy with unconjugated antibodies, ADCs such as gemtuzumab ozogamicin (Mylotarg™) and radiolabeled antibodies[227]: Bivalent binding and cross-linking of CD33 results in slow and limited internalization of the antigen and can inhibit proliferation and induce apoptosis.[227,228,231,232] The slow internalization kinetics, however, may have limited the therapeutic success of CD33-targeting agents in addition to shortcomings in their design.[227] New approaches with monoclonal antibodies engineered for enhanced ADCC, with improved ADCs, with bispecific T cell-engaging agents and with CAR-T are hoped to improve the success of CD33-based immunotherapy in AML.[227]

1.5.3 CD123, the alpha-chain of the interleukin-3 receptor

The interleukin-3 receptor is a type I cytokine receptor of the βc family, which also comprises the interleukin-5 and the GM-CSF receptors.[233,234] The heterodimeric complex is composed of a beta common chain (βc), which it shares with the other βc family members, and of a highly ligand-specific alpha-chain, the IL-3Rα or CD123 (see Figure 8). While CD123 by itself only has low affinity for IL-3 (K_D ~ 100 nM), a high-affinity complex with a K_D-value of 100 pM that can bind the cytokine at physiological concentrations is formed upon hetero-dimerization with the βc.[234,235] Upon ligand binding, higher order structures, i. e. dodecamers, are likely assembled – as is the case for the GM-CSF receptor.[236] The dodecamers would be composed of two hexamers containing a βc homodimer that is associated with two IL-3Rα chains and two IL-3 molecules in a head-to-head configuration.[236] The IL-3R complex transduces pro-proliferative, anti-apoptotic and multi-directional differentiation signals.[234,235]

Intracellular signaling of the IL-3R is mostly transduced via the beta common chain: Upon ligand binding and subsequent multimerization, the βc-associated JAK2 kinases are brought into close proximity, which enables βc transphosphorylation.[234,236] Intracellular signals are transmitted via two important pathways: (1) The kinases SHC, GRB2 and SOS are recruited to the phosphorylated βc. This leads to the activation of RAS, which in turn stimulates RAF signaling and thereby the activation of the MAPK pathway. As a result transcription factors c-FOS and c-JUN are upregulated and induce proliferation.[234,237] Additionally, MAPK-activated p38 and JNK/SAPK signaling induce the expression of BCL-2 family member MCL-1, which has anti-apoptotic functions.[234,237] (2) PI3K/AKT signaling is also

activated upon association of the PI3K subunit p85 with the phosphorylated Serine residue 585 of the IL-3R βc. p85 then recruits PKB/AKT. This signal transduction pathway also leads to the expression of MCL-1.[234,237] Furthermore, AKT can phosphorylate the IκB kinase, which phosphorylates IκB and initiates its proteasomal degradation. Resultantly, NFκB can translocate to the nucleus and induce the expression of BCL-2, BCL-X_L and A1, thereby enhancing cell survival.[234,237]

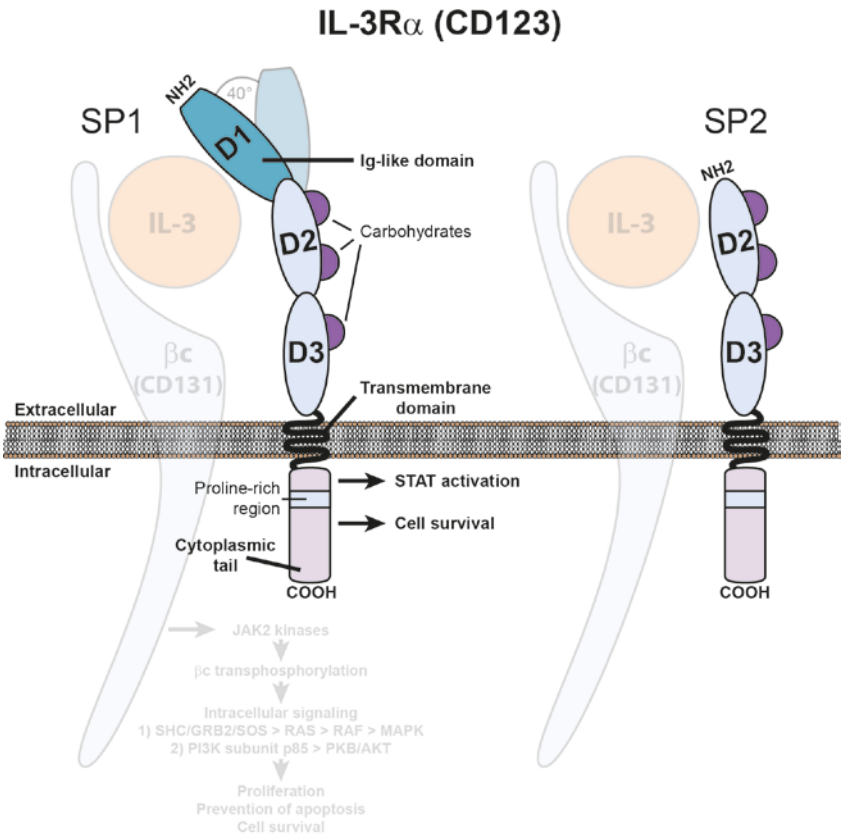

Figure 8: Schematic representation of the molecular structure of CD123, the alpha-chain of the IL-3 receptor. Two isoforms of CD123 exist with three (SP1) and two (SP2) extracellular domains, respectively. Both isoforms have a transmembrane domain and identical short cytoplasmic domains with a membrane-proximal proline-rich region. CD123 is involved in activation of the STAT signaling pathway and in cell survival. The N-terminal Ig-like D1 of the SP1 isoform of CD123 is flexible and can adopt an open and a closed conformation, whose biological function is unclear [based on Blalock et al., 1999].[237]

CD123 itself is a heavily glycosylated membrane protein with an apparent molecular weight of 75 kDa (378 amino acids) that is mostly expressed by hematopoietic cells, in particular by hematopoietic stem and progenitor cells, monocytes, megakaryocytes, B lymphocytes and plasmacytoid dendritic cells.[234,238] The gene encoding CD123 is composed of 12 exons and is located on the short arms of the x and y chromosomes, i. e. Xp22.3 and Yp11.3.[238] Abnormalities in IL-3R expression are frequently observed in AML and B-ALL and are associated with lower complete remission rates and a shorter overall survival.[234,238,239] Moreover, CD123 is a particularly interesting

target antigen for the immunotherapy of AML, because elevated expression levels of the IL-3Rα chain have been reported on the surface of AML stem cells (see chapter 1.3.1).[60,61,240,241]

Two isoforms of CD123 exist, which are composed of three (SP1) or two (SP2) extracellular domains, a transmembrane domain and a short cytoplasmic domain, which does not contribute to the stability of the ligand-receptor complex, but whose proline-rich membrane-proximal region is indispensable for downstream signaling events.[233,234,238] The extracellular domains D1, D2 and D3 adopt fibronectin type III-like folds and form the cytokine receptor module.[236] Via the immunoglobulin-like N-terminal D1 of the SP1 isoform, CD123 can adopt an open or a closed conformation. These two conformations differ by an angle of 40° and the open conformation is unique to the IL-3 receptor.[236] While the functional role of these two different conformations is not clear, they do offer two additional modes of action to CD123-targeting immunotherapeutic agents, which mediate cytotoxicity. These modes of action are the inhibition of multimerization and competitive binding with IL-3. Thereby CD123-targeting agents can block signaling and prevent IL-3-dependent proliferation.[236]

1.6 Cell-mediated cytotoxicity and the immunological synapse

Cytotoxic immune effector cells such as CTLs and NK cells induce caspase-dependent apoptosis in cancer cells by two mechanisms: (1) The injection of cytotoxic effector molecules into the target cell, and/or (2) the direct induction of apoptosis via binding of Fas ligand (FasL) on the immune effector cell surface to the Fas receptor (FAS) on the target cell surface.[114] For efficient cytolysis it is necessary that a cytolytic immunological synapse is formed at the contact site between effector and target cell.[242] This cytolytic synapse has a width of approximately 14 nm and is the focal point for the calcium-dependent release of lytic granules containing perforin, granzymes and granulysin by the cytotoxic effector cells.[114,242]

In CTLs the formation of a cytolytic synapse is initiated upon specific MHC:peptide recognition via the T cell receptor (TCR) complex, which results in prolonged cell-cell contacts.[243,244] In NK cells the balance between activating (i. e. NCRs, NKG2D, CD16) and inhibiting (i. e. inhibitory KIR) receptor signals during dynamic cell contacts is the determining factor, which can also be mediated by antibodies.[244] Upon target recognition, intracellular signaling events downstream of the activating immunoreceptors result in a massive and rapid reorganization of the actin and microtubule cytoskeletons as well as of adhesion molecules, signaling molecules and receptors in the plasma membrane into a supramolecular activation cluster (SMAC) with three concentrical zones.[242,244] In the central SMAC (cSMAC), microclusters of immunoreceptors and their associated signaling molecules are gathered. Here they are subject to the interaction with their respective activating or inhibitory

ligands on the one hand and to internalization and recycling on the other hand. The strength and quality of the ligand-immunoreceptor interaction in contrast to the recycling process determines whether apoptosis is efficiently induced.[242,243] The cSMAC is surrounded by a zone of tight adhesion, i. e. the peripheral SMAC (pSMAC). Adhesion is mediated by interactions between molecules such as LFA1 and ICAM1.[242,244] The pSMAC in turn is surrounded by a dense ring of actin filaments and microtubules (distal or dSMAC) that leave minimally sufficient clearances for lytic granule release.[242] The reorganization of the actin and microtubule cytoskeletons pulls the centrosomes of the immune effector cell towards the cytolytic synapse. In addition, some stacks of the Golgi apparatus and intracellular lytic granules are pulled towards the cytolytic synapse, which leads to a polarized secretion of cytotoxic effector molecules as well as cytokines such as IL-2, IL-4, IL-5 and IFN-γ into the synaptic cleft.[242] While centrosomes and Golgi apparatus are associated with the actin cytoskeleton and experience polarization towards the cytolytic synapse via actin polymerization, the lytic granules are transported to the SMAC by dyneins along the microtubules in a retrograde manner. Once they are in plasma membrane proximity, non-muscle myosin II mediates the contact between the lysosomes and F-actin and thus their final delivery to the minimal clearance sites within the dSMAC.[244,245] Here, they fuse with the plasma membrane and release their toxic load into the synaptic space. As a result, lysosomal membrane proteins including LAMP1 (CD107a) and LAMP2 are exposed at the cell surface.[242] By exerting physical force on the target cell membrane, components of the pSMAC and dSMAC zones also allow perforin to penetrate the target cell membrane more easily and thereby increase the efficiency of cytolysis.[246] Importantly, both CTL and NK cells are capable of serial lysis of several target cells. This is likely achieved by releasing only a fraction of the intracellular lytic granules into a single cytolytic synapse, by neosynthesis of cytotoxic effector molecules upon effector cell activation and possibly by the recycling and reuse of superfluous cytotoxic effector molecules from the synaptic space via endocytosis.[244]

Since one of the activating receptors in NK cells is FcγRIII (CD16), which is stimulated by IgG, it is not surprising that scTb with a CD16 binding moiety can efficiently induce NK cell activation and partake in cytolytic synapse formation. However, CTL do not require soluble ligands for activation. They interact with their target cells directly via the CD3 : TCR-complex and co-stimulatory as well as co-inhibitory receptors such as CD8 and PD-1. When stimulatory signals predominate, the T cell becomes active. However, the engagement of the CD3 : TCR-complex alone without co-stimulatory signals can lead to T cell anergy.[247] Therefore it was unknown whether CTL could be efficiently and specifically activated by antibody-derived agents with only a CD3- or TCR-specific binding moiety in the presence of target cells. However, the BiTE® have proven that a cytolytic T cell synapse can be

formed efficiently, even without a co-stimulus and when an additional molecule is included into the synapse. A similar mode of action remains to be shown with the larger scTb.

2 Results

2.1 NK cells from an AML patient have recovered in remission and reached comparable cytolytic activity to that of a healthy monozygotic twin mediated by the single-chain triplebody SPM-2

Todd A. Braciak*, Sarah Wildenhain*, Claudia C. Roskopf, Ingo A. Schubert, Georg H. Fey, Karl-Peter Hopfner & Fuat S. Oduncu

*: equal contribution

Journal of Translational Medicine 2013 November 16; **11** (1): 289

DOI: 10.1186/1479-5876-11-289

2.1.1 Summary

Immunotherapeutic agents that redirect the effector functions of a cancer patient's autologous leukocytes, such as the natural killer (NK) cell-recruiting triplebody SPM-2 (33-16-123), can only be effective, when the recruited leukocyte population is unimpaired. It has been reported, however, that the functional NK cell compartment in AML patients is greatly reduced. This can, for example, be due to low cell surface concentrations of activating natural cytotoxicity receptors (NCR) or to low cytokine production and release levels. In this publication, a case study is reported, in which the cytolytic activity of NK cells from an AML-M1 patient at first diagnosis and during remission was compared to the cytolytic activity of NK cells from her healthy monozygotic twin.

At diagnosis, the patient's NK cell compartment accounted for only 1.4% of the mononuclear cells and NK cell enrichment by negative selection was unsuccessful due to poor differentiation of the blast population. As a result, merely 4.3 ± 3% of the blasts were depleted in a redirected lysis assay against autologous AML blasts with SPM-2. Encouragingly, however, the percentage of NK cells in the peripheral blood of the AML patient during remission had been almost restored to the level detected in the twin's blood (6.3% vs. 7.7%, respectively). The cytolytic potential of the patient's NK cells during remission was comparable to that of the healthy monozygotic twin (% lysis of AML blasts: 37.2 ± 2% vs. 47.7 ± 7% and % lysis of Raji: 26 ± 4% vs. 25 ± 8%, respectively). Triplebody SPM-2 also mediated the reduction of the $CD34^+$ bulk AML blasts and even eliminated the $CD34^+ CD38^{-/low} CD123^+$ cells, which includes potential leukemia stem cells.

The patient displayed the same expression pattern and intensity of activating NCRs NKp30, NKp44 and NKp46 on her NK cells at diagnosis and during remission as the healthy monozygotic twin. Thus, differential expression was not a reason for a potential functional impairment. The release of TNF-α upon stimulation of the patient's NK cells with SPM-2 was slightly reduced compared to the twin's NK cells (1.1 and 4.7 pg/mL, respectively). However, this had no or a weak impact only on the cytolytic potential of SPM-2 together with the NK cells isolated in remission.

In conclusion, the NK cells from this particular AML patient were not functionally impaired, but only reduced in total numbers compared to a healthy monozygotic twin. Thus functional impairment would probably not prevent a therapeutic benefit from SPM-2 treatment in this patient or comparable cases. Furthermore, SPM-2 treatment is a promising strategy to eliminate residual leukemia stem cells via autologous NK cells during remission.

2.1.2 Contribution

I collected information on the patient and her healthy twin, handled their blood samples and isolated peripheral blood mononuclear cells. Additionally, I performed antibody-dependent cellular cytotoxicity (ADCC) assays using the monoclonal anti-CD20 antibody rituximab. Finally, I determined the expression patterns of the NK cell receptors NKp30, NKp44 and NKp46 on the NK cells of the patient at first diagnosis and in remission as well as on the NK cells of the healthy monozygotic twin.

JOURNAL OF TRANSLATIONAL MEDICINE

RESEARCH Open Access

NK cells from an AML patient have recovered in remission and reached comparable cytolytic activity to that of a healthy monozygotic twin mediated by the single-chain triplebody SPM-2

Todd A Braciak[1*†], Sarah Wildenhain[2†], Claudia C Roskopf[1], Ingo A Schubert[3], Georg H Fey[4], Uwe Jacob[2], Karl-Peter Hopfner[2] and Fuat S Oduncu[1]

Abstract

Background: The capacity of patient's Natural Killer cells (NKs) to be activated for cytolysis is an important prerequisite for the success of antibody-derived agents such as single-chain triplebodies (triplebodies) in cancer therapy. NKs recovered from AML patients at diagnosis are often found to be reduced in peripheral blood titers and cytolytic activity. Here, we had the unique opportunity to compare blood titers and cytolytic function of NKs from an AML patient with those of a healthy monozygotic twin. The sibling's NKs were compared with the patient's drawn either at diagnosis or in remission after chemotherapy. The cytolytic activities of NKs from these different sources for the patient's autologous AML blasts and other leukemic target cells in conjunction with triplebody SPM-2, targeting the surface antigens CD33 and CD123 on the AML cells, were compared.

Methods: Patient NKs drawn at diagnosis were compared to NKs drawn in remission after chemotherapy and a sibling's NKs, all prepared from PBMCs by immunomagnetic beads (MACS). Redirected lysis (RDL) assays using SPM-2 and antibody-dependent cellular cytotoxicity (ADCC) assays using the therapeutic antibody Rituximab™ were performed with the enriched NKs. In addition, MACS-sorted NKs were analyzed for NK cell activating receptors (NCRs) by flow cytometry, and the release of TNF-alpha and IFN-gamma from blood samples of both siblings after the addition of the triplebody were measured in ELISA-assays.

Results: Patient NKs isolated from peripheral blood drawn in remission produced comparable lysis as NKs from the healthy twin against the patient's autologous bone marrow (BM) blasts, mediated by SPM-2. The NCR receptor expression profiles on NKs from patient and twin were similar, but NK cell titers in peripheral blood were lower for samples drawn at diagnosis than in remission.

Conclusions: Peripheral blood NK titers and *ex vivo* cytolytic activities mediated by triplebody SPM-2 were comparable for cells drawn from an AML patient in remission and a healthy twin. If these results can be generalized, then NKs from AML patients in remission are sufficient in numbers and cytolytic activity to make triplebodies promising new agents for the treatment of AML.

Keywords: Single chain triplebody (triplebodies), Antibody-dependent cellular cytotoxicity (ADCC), Natural killer (NK) cells, Acute myeloid leukemia (AML), Cancer immunotherapy

* Correspondence: Todd.Braciak@med.uni-muenchen.de
†Equal contributors
[1]Division of Hematology and Oncology, Medizinische Klinik und Poliklinik IV, Klinikum der Universität München, Ziemssenstrasse 1, D-80336 Munich, Germany
Full list of author information is available at the end of the article

BioMed Central

© 2013 Braciak et al.; licensee BioMed Central Ltd. This is an open access article distributed under the terms of the Creative Commons Attribution License (http://creativecommons.org/licenses/by/2.0), which permits unrestricted use, distribution, and reproduction in any medium, provided the original work is properly cited.

Background

Interest in the development of antibodies and antibody-derived agents such as antibody-drug conjugates (ADCs) and bispecific agents for the treatment of acute myeloid leukemia (AML) has increased over the past years. A prototypical agent, gemtuzumab ozogamycin (GO; Mylotarg^{TM}), has been effective in the treatment of AML, but was withdrawn from the market because of side toxicities [1,2]. The problem causing this withdrawal was not related to the suitability of the myeloid surface antigen CD33 as a target, but rather to the chemical linker connecting the toxin component of this drug to the antibody carrier. CD33 remains a valuable and clinically validated target for the therapy of CD33-positive subtypes of AML with antibody-derived agents [3-5], and consequently, several major drug developers currently study new agents for the treatment of AML with specificity for CD33. One class of such agents relies on potent new toxins coupled with improved linkers to the antibody, such as the agent SGN-CD33a [6]. Another class recruits effector cells including NKs or T cells for the elimination of AML cells. This class includes the agent AMG-330 [7] recruiting T cells as effectors, as well as our team's single chain triplebodies 123-16-33 [8] and 33-16-33 [9], recruiting NKs. It further includes CD33-specific antibodies with Fc domains engineered for improved binding to Fc-receptors on effector cells. Also, antibodies specific for CD123, the alpha subunit of the receptor for Interleukin-3, an important growth and differentiation factor for early hematopoietic cells and the myeloid lineage, have produced promising results in preclinical studies [10]. Antibodies against CD123 have mediated cytolysis of AML cells and in particular of AML-Leukemia Stem Cells (AML-LSCs) [11,12].

Our team has developed a new class of antibody-derived fusion proteins called triplebodies, suited for the elimination of AML cells [8,9,13-17]. These agents carry two binding sites for surface antigens on the cancer cell and one for a trigger molecule on an effector cell. They can bind two different tumor antigens on the same target cell and through this mode of "dual targeting" address the cancer cell with enhanced selectivity [15,16,18]. In addition, they bind a trigger molecule on an effector cell, such as CD16 on NKs, and thereby activate the effector for cytolytic elimination of the cancer cell. Triplebody SPM-2 employed in the present study carries single chain Fv (scFv) antibody fragments specific for CD33 and CD123 on AML cells linked in a single polypeptide chain to an scFv module specific for CD16, the low affinity Fc gamma RIII receptor on NKs and macrophages and a few other cells of the hematopoietic system [8]. SPM-2 was designed for the elimination of both bulk AML cells and AML-LSCs, because both are double-positive for this pair of antigens.

LSCs from patients with most subtypes of AML however carry a higher combined cell surface density of this pair of antigens than bulk AML cells, normal hematopoietic cells, and healthy hematopoietic stem cells (HSCs) [3,11,19,20]. SPM-2 was therefore designed for a preferential elimination of AML-LSCs *in vivo*. It is still unknown whether this objective can be reached because the agent has still not been tested in humans. It is important to eliminate not only bulk AML cells, but also the LSCs, because the LSCs are believed to be the relevant subset within the population of minimal residual disease (MRD) cells, which are responsible for relapse and poor disease outcome [4,21-23]. New agents intended to induce a deeper remission and to prolong the time to relapse must therefore make a deliberate effort to target the MRD cells. Currently available chemotherapeutic agents achieving remission for many AML patients probably also act (at least in part) through the elimination of some LSCs. However, most often they do not achieve long-lasting complete remissions and have not been designed with the intent to specifically eliminate MRD cells but rather bulk AML cells. A well-defined immunophenotype of MRD cells is not available, which would lend itself as a specific address for the design of antibody-derived agents. However, in a retrospective clinical study the MRD cell compartment responsible for early relapse was tentatively equated with the $CD34^+$ $CD38^-$ $CD123^+$ subset of AML cells [24]. If these results can be confirmed by prospective studies, then triplebody SPM-2 could be especially promising for the therapeutic removal of AML-MRD cells. Its ability to reach this objective critically hinges upon the availability of sufficient numbers of active NKs in AML patients at the time of the intended use of the agent.

The compartment of functional NKs is often reduced in AML patients [25-29]. This impairment has been attributed to different causes, among them a down-regulated cell surface expression of the activating natural cytotoxicity receptors (NCRs) NKp30, NKp44 and NKp46 [25-27,29,30]. Low-level expression of NCRs (NCR^{dim}) on patient-derived NKs was correlated with poor prognosis in AML, as patients with NCR^{dim} NKs had significantly lower 5-year survival rates than matched patients with NCR^{bright} NKs [26]. Deficiencies in cytokine release have also been linked to an impairment of NK cell function in AML patients. The capacity of NKs to secrete IFN-gamma was highly impaired in AML patients and was correlated with suppressed immune responses against autologous leukemic cells [31-33]. Finally, in adult acute leukemia, impaired production of cytokines by NKs was associated with early relapse [34].

Triplebody SPM-2 was not designed as a frontline therapeutic for the initial debulking of AML blasts. This objective is reached in most cases by the initial chemotherapy. Rather, SPM-2 was designed to be used after chemotherapy when the blast titer is greatly reduced for most patients and when the titer of functional NKs is

expected to have at least partially recovered towards normal levels [28]. Therefore, here we studied the effectiveness of SPM-2 to mediate lysis of an AML patient's BM blasts as targets, in combination with autologous NKs drawn from peripheral blood at diagnosis and in remission. The analysis was performed in comparison with NKs isolated from the patient's healthy monozygotic twin. This exceptional situation provided us with a unique opportunity to compare the activity of the patient's NKs with NKs genetically as closely identical as possible from a healthy donor.

Here the patients NKs, drawn in remission, were restored to titers in the blood comparable to those of the healthy twin and were able to achieve effective lysis of autologous AML blasts in conjunction with SPM-2. Notably, they also achieved comparably effective lysis of an established lymphoma-derived target cell line mediated by the reference antibody Rituximab™, and had similar expression profiles of NCRs as the healthy sibling's cells. The present study provides a precedent case in support of our hypothesis that SPM-2, administered at appropriate stages in the course of a standard therapy for AML, will become useful as an adjuvant drug.

Methods

Expression in mammalian cells, purification and protein-chemical characterization of triplebody SPM-2

The DNA construct coding for SPM-2 was based on the published triplebody 123-16-33 [8] and was synthesized by a commercial provider (Eurofins/MWG-Operon, Ebersberg; Germany). The CD16-specific scFv was stabilized following published procedures [8,35] and humanized. Humanization of the CD123- and CD33-specific scFvs and the stabilization of the CD123-specific scFv followed similar procedures (S. Wildenhain, I. Schubert, A. Honegger et. al., unpublished data). The N- and C-terminal CD33- and CD123-specific scFvs were separated from the central CD16-specific scFv by (G_4S)x4 linkers. For expression purposes, human 293 F cells (DSMZ; German Collection of Microorganisms and Cell Lines; Braunschweig, Germany) were stably transfected with plasmid DNA using the 293fectin™ transfection reagent (Life Technologies, Darmstadt, Germany) according to the manufacturer's instructions in a total volume of 30 ml. The cells were then cultured under continuous selection with hygromycin C. The recombinant protein was captured from culture supernatants via its C-terminal hexahistidine tag by retention on a metal-ion affinity matrix and purified by anion- and cation-exchange chromatography. Concentrations of the purified protein were determined by spectrophotometry and calculated using the molar extinction coefficient derived from the amino acid sequence. The resulting final protein meets current regulatory standards and industry norms, and was named SPM-2 to indicate its status as a candidate for clinical development. Equilibrium binding constants (K_D) of each of the individual scFvs of SPM-2 were in the 20–30 nM range, and thus were similar to the values reported for the initial agent [8].

Preparation of primary cells from blood and bone marrow of human donors

Peripheral blood and bone marrow samples were drawn from subjects into EDTA solution after receiving informed consent. The project was approved by the Ethics Committee of the University of Munich Medical Center. Bone marrow mononuclear cells (BMMC) containing the leukemic blasts and Peripheral Blood Mononuclear Cells (PBMCs) were enriched by ficoll density centrifugation using the Lymphoflot reagent (Biotest, Dreieich, Germany) according to manufacturer's instructions. Isolated cells were then either suspended in RPMI medium (Life Technologies) containing 10% fetal bovine serum (FBS) with penicillin and streptomycin (PS) at 100 units/ml and 100 μg/ml, respectively, for immediate use, or stored frozen in a solution containing 90% FBS and 10% DMSO for future use. Cell viability was assessed by trypan blue exclusion.

Ex vivo expansion of MNCs from healthy donors in the presence of IL-2

PBMCs were expanded *ex vivo* in RPMI medium containing Interleukin-2 (IL-2) plus 5% human serum (Life Technologies) for 20 days as described [16,36], and were then frozen in aliquots for subsequent use. Prior to use in cytolysis experiments, the cells were thawed and cultured overnight in RPMI medium containing 5% human serum plus 50 units/ml and 50 μg/ml PS, respectively, but no additional IL-2.

Flow cytometric analysis

Flow cytometric analysis was performed with an Accuri C6 flow cytometer (BD Biosciences, Heidelberg, Germany). The CD3-, CD16-, and CD56-specific monoclonal antibodies (mAbs) used for the analysis of NK cell content in PBMC-preparations as well as isotype control mAbs were from Immunotech (Marseille, France), while the NKp30-, NKp44-, NKp46-specific and isotype control mAbs used for the analysis of NK cell receptors (NCRs) [37] on isolated NKs were from eBioscience (Frankfurt, Germany). Cell surface densities of CD33 and CD123 were measured using a calibrated cytofluorimetric assay as described [8,35]. For this purpose, a commercial kit of fluorescent beads with known numbers of fluorescent chromophores per bead (QIFIKIT®; DAKO; Hamburg, Germany) was employed, as well as fluorescent-labeled mAbs. This procedure allows the investigator to express the measured fluorescent intensity of mAbs bound to the surface of the patient's cells in terms of average number of antigen copies per cell [38].

Antibody Dependent Cellular Cytotoxicity (ADCC) and Redirected Lysis (RDL) assays using Calcein release

In this study we refer to cell-mediated cytolysis assays with whole antibodies as "ADCC" and to tests with antibody-derived agents such as triplebodies as "redirected lysis (RDL)" assays. Non-radioactive cytolysis assays based on the release of calcein from target cells pre-labeled with calcein AM (Life Technologies) were performed as described [16,39]. The cytolytic activity of NKs from various sources was calibrated in standard ADCC assays with the commercial CD20-mAb Rituximab^{TM} [39,40] as the mediator of lysis and lymphoma-derived Raji cells [41] as targets. This calibration allowed us to assess the cytolytic activity of NKs from various sources using a standard mAb and a commonly used target cell line, and thus to make our results comparable to the current benchmarks in the field. For the calibration reaction with Rituximab^{TM}, untouched NKs were first enriched by the MACS kit (Miltenyi kit; see above) from PBMC samples and then used at a constant effector-to-target (E : T) ratio of 2.5 : 1 against Raji targets. The same NKs were also used in redirected lysis experiments with the patient's autologous bone marrow AML blasts as targets in conjunction with SPM-2. Specific lysis was measured by quantitating the release of calcein from target cells using a fluorimeter/ELISA plate reader and expressed in relative light units (RLU) at 485/535 nm. Calcein release was measured at 3 and 4 hour time points for ADCC and RDL experiments, respectively. Specific cellular cytotoxicity was expressed as overall lysis minus the background of spontaneous lysis mediated by the NKs alone, in the absence of added antibody-reagents. Specific lysis was evaluated by the formula:

% specific lysis = 100 * (Experimental Release RLU – Background Release RLU)/(Maximal Release RLU – Background RLU).

Enrichment of human NK cells by preparative sorting with immunomagnetic beads

NKs were enriched by negative selection using a commercial NK cell isolation kit (Miltenyi Biotec MACS sorting kit, Bergisch Gladbach, Germany) according to manufacturer's instructions. The enriched cells are referred to as "untouched" NKs, because as a result of the negative selection, no residual mAb is bound to their surface and they have not been eluted from an affinity matrix with harsh reagents. Starting material were ficoll-hypaque purified PBMCs from blood samples of the donors. The enriched NKs were then either resuspended in RPMI medium containing 10% FBS with PS at 100 units/ml and 100 μg/ml, respectively, for use in ADCC and RDL assays, or placed in PBS solution containing 1% bovine serum albumin (BSA) for flow cytometric analysis.

Measurement of IFN-gamma and TNF-alpha release into peripheral blood samples by ELISA assays

Concentrations of human cytokines IFN-gamma and TNF-alpha were measured with ELISA kits (eBioscience) following manufacturer's instructions. Triplebody SPM-2 was added to peripheral blood samples at concentrations of 10, 1, or 0.1 nM , and the reaction mixtures were then cultured for 6 h at 37°C in 96 well round bottom Nunc plates in 200 ul volumes. Blood samples were frozen and stored at −20°C and were thawed only immediately before use in cytokine assays. In addition, cytokine release was studied with the same ELISA kits in supernatants from the 4 h RDL and 3 h ADCC assays, in which MACS-purified NKs had been used as effectors against autologous BM blasts as targets.

Statistics

All statistical analysis was performed by STATVIEW 4.5 programs from Abacus Concepts (Berkeley, CA) using Student's *t*-test for the final determination of significance ($p < 0.05$).

Results

SPM-2 mediates efficient lysis of BM leukemic blasts from a patient with FAB M1 AML in conjunction with effector cells from a healthy unrelated donor

To evaluate the ability of SPM-2 (Figure 1) to mediate lysis of blasts from a patient diagnosed with an AML FAB M1, RDL experiments were performed with isolated BMMCs obtained from the patient at diagnosis as targets. The BMMCs prepared in this manner contained 89.7% AML blasts, as determined by morphology and cytological criteria (Table 1). Five hundred million (5 x 10^8) MNCs were recovered from a 5 ml BM sample of this patient,

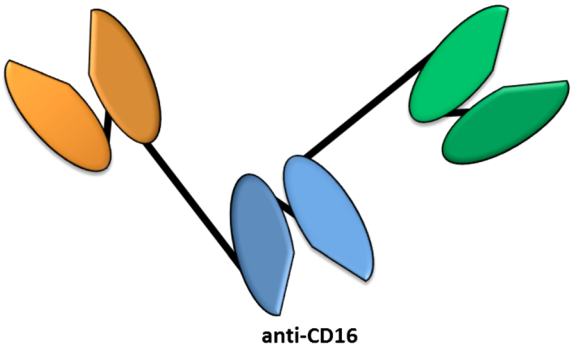

Figure 1 Structure of single chain triplebody SPM-2. ScFv domains (colored in the diagram) specific for CD33, CD16 and CD123, respectively, were connected by two (Gly_4Ser)x4 linkers (black lines) into a single polypeptide chain. The distal scFv domains specific for CD33 (orange) and CD123 (green), bind targets on the same AML blast while the central scFv domain (blue) binds CD16 on NK cells. Antigen binding sites are indicated by the triangular pockets.

Table 1 Data and immunophenotype of AML FAB-M1 patient BMMCs

Gender	Female		
Age:	21 years old		
Diagnosed with:	AML FAB-M1; AML without maturation according to WHO classification [42]		
Blast titer:	89.7% blast in the marrow at diagnosis		
Case history	One course of induction chemotherapy following HAM protocol high dose cytarabine with mitoxantrone [49]		
Current status:	Complete remission acheived by induction chemotherapy (HAM)		
Myeloid cells % (in blast gate)		Co-expression (cross-lineage) % (in blast gate)	
CD 34	89.6%	CD34/CD56	47.9%
CD 33	<19%	CD34/CD7	12.3%
CD 123	n.d. at diagnosis	CD34/HLA-DR	90.5%
CD 117	< 1%	CD34/CD7	12.3%
CD 38	89.9%		
cy MPO	41.7		

n.d. not determined.
Cy MPO cytoplasmic myeloperoxidase; flourescent marker enzyme for the myeloid lineage.

drawn at diagnosis, and some aliquots were cryopreserved for further analysis.

Among the isolated BMMCs, 89.6% expressed detectable levels of CD34, consistent with the diagnosis of a FAB M1 AML. The FAB M1 AML subtype commonly displays very immature blasts and a high percentage of CD34-positive cells. It is called "AML without maturation" in the WHO classification [42] and often leads to low white blood cell counts. At diagnosis less than 1% of the BMMCs expressed cell surface CD33, leading to the initial diagnosis of a "CD33-negative AML". Expression data for CD123 at diagnosis are not available. Subsequent cytofluorimetric analysis gated on the BMMC population (consisting of approx. 90% AML blasts) performed under more sensitive conditions (calibrated cytofluorimetry; Figure 2A) revealed a mean expression of 130 and 230 copies per cell of CD33 and CD123, respectively, in this population of cells. These are very low levels, considering that blasts from other AML subtypes can commonly carry up to several thousand and sometimes several ten-thousand copies per cell of these antigens [8,43,44].

This patient's AML blasts were lysed efficiently by SPM-2 in combination with MNCs expanded *ex vivo* for 20 days with IL-2 from a healthy unrelated donor used as a source of effectors (Figure 2B). Net lysis of the targets by the effector cells alone was 15 ± 11%, net lysis in the presence of a saturating (10 nM) dose of SPM-2 plus effectors was 80 ± 20% (Figure 2B). Thus, specific lysis induced by the triplebody was approximately 65%. This is a surprisingly high value for a 4 h assay, considering the low surface density of both target antigens.

The majority of AML-LSCs are contained in the CD34-positive subset of bone marrow cells [11,45]. Therefore we analyzed, whether SPM-2 was capable of mediating lysis of this subset, as a first step towards answering the key question, whether SPM-2 can mediate lysis of AML-LSCs. As a result, in a 4 h RDL-reaction using isolated AML BMMCs as targets and *ex vivo* expanded MNCs from an unrelated donor as effectors, SPM-2 mediated a significant reduction of the CD34-expressing subset to 15%, down from 89.6% at the start of the reaction (Figure 2C, right panel). Exposure to the MNC effectors alone reduced the CD34-positive blasts down to only 62% (Figure 2C, left panel). Thus, the net effect of treatment with SPM-2 was a specific depletion of the CD34-bearing cells by 47%.

Beyond the CD34-positive compartment, the majority of AML-LSCs are typically found in the $CD34^{pos}$ $CD38^{neg}$ subset, although some LSCs are also present in other cellular subsets [19]. Moreover, the AML MRD cells relevant for relapsed disease have been reported to be predominantly contained in the $CD34^{pos}$ $CD38^{neg}$ $CD123^{pos}$ compartment [24]. Therefore, in an attempt to determine, whether SPM-2 was capable of eliminating AML-MRD cells in a narrower cellular subset beyond the broader $CD34^{pos}$ compartment, we analyzed whether SPM-2 also affected the $CD34^{pos}$ $CD38^{neg}$ $CD123^{pos}$ subset within the AML BMMC sample in combination with IL-2 expanded effector cells from a healthy donor. The experiment was performed using a similar 4-color flow cytometric analysis as reported by others [24].

As an initial result, obtained with limited numbers of cells, depletion of the $CD34^{pos}$ $CD38^{neg}$ $CD123^{pos}$ subset was observed following treatment with SPM-2 plus allogeneic effectors in comparison to treatment with MNCs alone (data not shown). For this patient, the $CD34^{pos}$ $CD38^{neg}$ cells represented approximately 1.4% of the total BMMCs. This value falls into the typical range reported for this subset

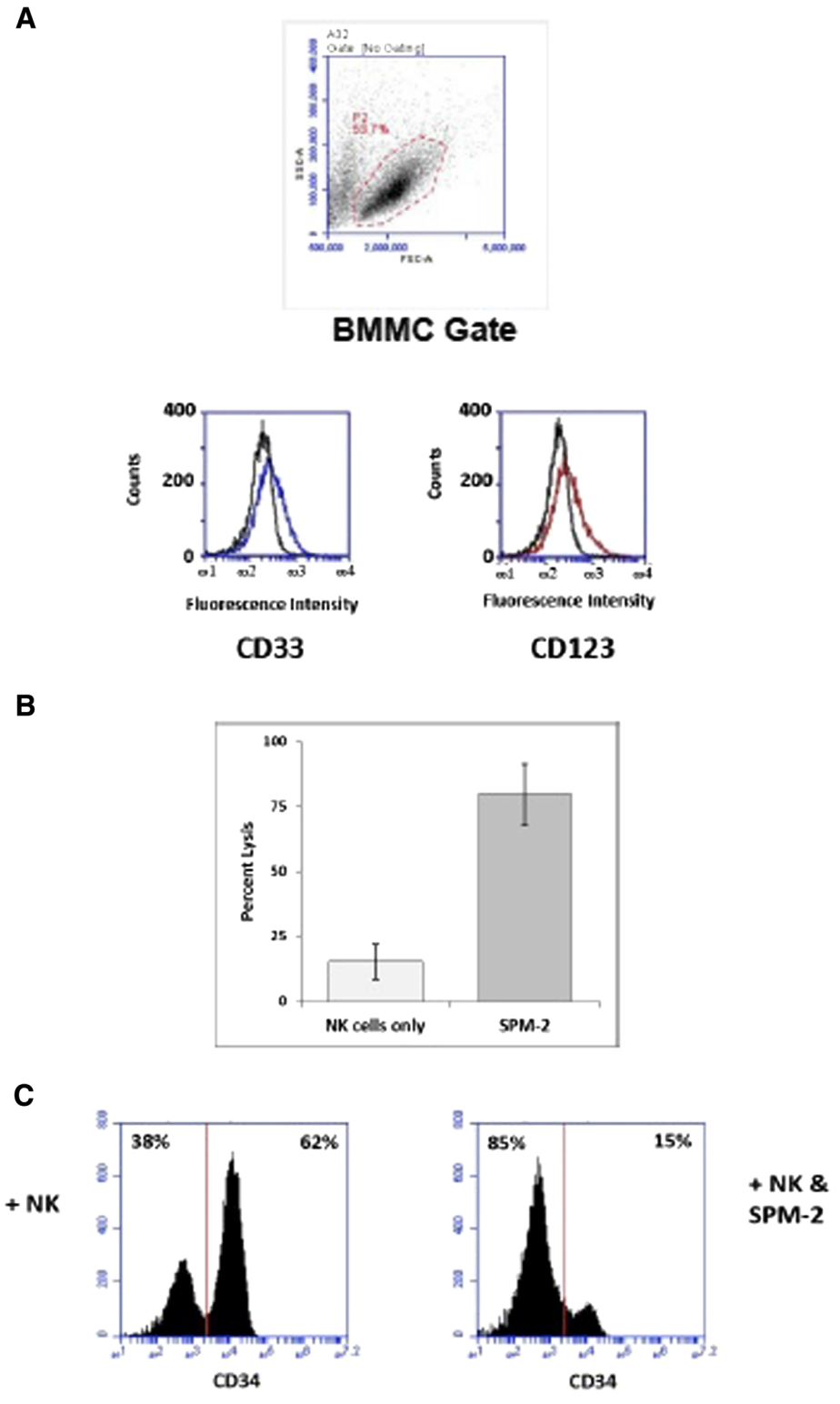

Figure 2 (See legend on next page.)

(See figure on previous page.)
Figure 2 BM blasts from an FAB M1 AML patient are lysed efficiently in a RDL reaction by effectors from an unrelated donor, mediated by SPM-2. (A) Patient isolated BMMC were stained with fluorescent antibodies specific for CD33 and CD123, respectively, in comparison to isotype controls. P2: gate used for analysis of live BMMCs allowing their discrimination from dead cells. Mean fluorescence Intensities measured for each antigen were converted to antigen densities by calibrating fluorescence intensities with the QuiFi kit (Methods). **(B)** MNCs from an unrelated healthy donor, expanded *ex vivo* in the presence of IL-2 (Methods), were used as effectors at an MNC : target (E:T) ratio of 10 : 1 in a 4 h RDL assay. This corresponds to an E:T ratio of NK cells : targets of 2.5 : 1, because NK cells were 25% of all cells in this expanded MNC population. Targets were BMMCs from the AML patient obtained at diagnosis, pre-labeled with calcein AM. SPM-2 was added at 10 nM concentration (right bar). The control reaction was allowed to proceed without added agents (left bar; NKs alone). Cellular lysis was measured by calcein release and plotted as fraction (%) of maximum release. Error bars: arithmetic means over 3 separate experiments (n = 3). **(C)** Flow cytometric analysis after an RDL reaction. Patient's BMMCs were treated with effector cells and SPM-2 in a 4 h RDL experiment as in panel A. At the end of the reaction, cells were stained with a fluorescent-labeled CD34-specific mAb and analyzed by FACS. Numbers of $CD34^{pos}$ cells are plotted against the intensity of CD34-specific fluorescence. Left panel: after reaction with effectors alone; right panel: after reaction with effectors plus SPM-2. Numbers in upper right corner: percent of $CD34^{pos}$ cells surviving at the end of the reaction.

by other authors [24]. Taken together, this set of data provides a first indication in favor of our contention that SPM-2 is capable of eliminating cellular subsets enriched in AML-LSCs and MRD cells through the recruitment of activated NKs. While this result is consistent with the claim that SPM-2 can eliminate LSCs, definitive proof requires further and more stringent analysis than we were able to perform here due to the scarcity of this BMMC sample.

Cytolytic activity of patient's NKs drawn at diagnosis and in remission compared with NKs from a healthy monozygotic twin

Next, we wished to determine whether SPM-2 was capable of mediating lysis of the patient's AML blasts by autologous NKs. For this patient, we had the rare opportunity to obtain NKs from peripheral blood both at diagnosis and in remission after completion of the induction chemotherapy, and to compare their titers and cytolytic activities to NKs isolated from a healthy monozygotic twin.

As a result, MACS-purified NKs drawn from the sibling and the patient in remission showed similar cytolytic activity mediated by SPM-2 towards the patient's AML blasts (Figure 3A, red). Mean specific lysis obtained with NKs from the sibling was 47 ± 7% versus 37 ± 2% for NKs from the patient in remission. These values are arithmetic means over 3 independent experiments (n = 3). By contrast, the cytolytic activity of the NKs drawn from the patient at diagnosis was significantly lower. With equal numbers of effector cells used as an input for each reaction, only 4.3 ± 2.6% specific lysis was observed with a saturating dose of SPM-2 (10 nM; Figure 3A, left bar).

Finally, we wished to determine whether these comparable activities of the patient's and sibling's NKs were only observed with the patient's AML blasts as targets, or whether this was an intrinsic property of these NKs, also observed for other targets. Therefore, a benchmark ADCC experiment was performed with CD20-positive Raji lymphoma-derived cells as targets (Figure 3B, blue), the commercial CD20 antibody Rituximab™ as the therapeutic agent, and with immunomagnetically purified NKs as effectors. As a result, comparable lytic activity was found again for NKs from the patient in remission and the twin (Figure 3B). Here, NKs from the patient in remission produced 26 ± 4% specific lysis using a standard dose of Rituximab™ compared to 25 ± 8% for the sibling's NKs. NKs from the patient at diagnosis also produced lower specific lysis in this assay (4 ± 2%).

Taken together, these results indicate that the peripheral blood NKs from the patient in remission are comparable in cytolytic activity to those of the healthy twin in response to SPM-2. One needs to bear in mind, however, that this patient was younger than the average AML patient at diagnosis and that response to therapy is usually better for younger patients.

Titers of AML blasts and NK cells in peripheral blood at diagnosis and in remission

To look for explanations for the apparent deficiency in cytolytic activity of the NKs from the patient at diagnosis, frequencies of NKs and leukemic blasts in the various PBMC samples were assessed by flow cytometry (Figure 4). Plots of side scatter (SSC) vs. fluorescence intensity of cells stained with a FITC-labeled CD45 mAb revealed a well-defined population of $CD45\text{-}FITC^{dim}$ x SSC^{low} cells (P1 in Figure 4A). These cells have been identified as AML blasts by other authors [24,46]. Among the patient's PBMCs drawn at diagnosis, this subset was abundant (58%; Figure 4A, left panel), while it accounted for only about 1% of all PBMCs from the patient in remission and the healthy twin (Figure 4A, central and right panels).

NKs were identified in cytofluorimetric studies as $CD16^{pos}CD56^{pos}$ cells (Figure 4B). Only 1% of the patient's PBMCs at diagnosis fell into this gate (Figure 4B, left panel), whereas 6.3 and 7.7% of all PBMCs had this phenotype for the patient in remission and the healthy sibling (Figure 4B, central and right panels). This finding supports our initial expectation that for an AML patient in remission the NK cell compartment should be restored to almost normal levels. It also is the most likely explanation for the results shown in Figure 3, where we observed that NKs from the

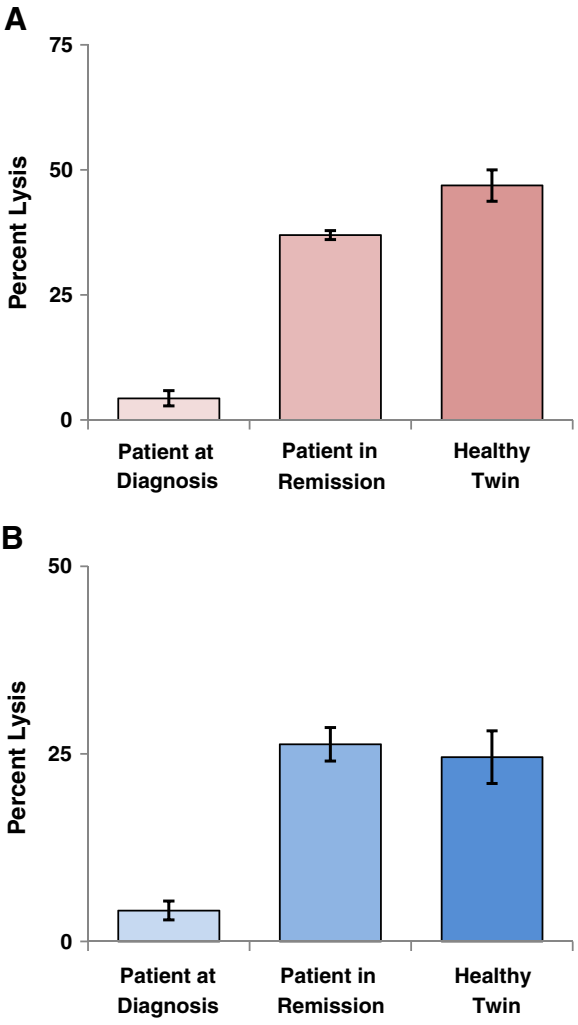

Figure 3 NK cells from PBMCs of the patient in remission and the healthy twin have comparable cytolytic activity. (A) MACS sorted NKs isolated from PBMCs of the patient drawn at diagnosis (left bar), in remission (central bar) and from the healthy twin (right bar) were used in RDL assays against calcein labeled BMMCs from the patient at diagnosis as targets (red). 4 h RDL reactions were run at an E : T ratio of 2.5 : 1 and incubated with a 10 nM dose of SPM-2 versus NKs alone as control. Error bars: arithmetic means over 3 separate experiments (n = 3). **(B)** The same NK effector populations as in panel **A** were also used in 3 h ADCC reactions at the same E : T ratios. Target cells were calcein labeled Raji cells ($CD20^{pos}$). Reactions mediated by 10 μg/ml (approx. 70 nM) of the commercial CD20-antibody Rituximab™ (blue). Error bars: arithmetic means over 3 separate experiments (n = 3).

patient at diagnosis had lower cytolytic activity in ADCC and RDL assays than the corresponding cells from the patient in remission and her healthy twin. These data suggest that the deficiency in cytolytic function observed at diagnosis most likely was due to reduced NK cell titers.

Interestingly, a high percentage of $CD56^{bright}$ $CD16^{low}$ cells were found in PBMCs of the patient at diagnosis (Figure 4B, left panel, upper left quadrant). This population has previously been reported by other authors to be increased in AML patients and has been described as a characteristic NK cell subset with elevated production of cytokines [30]. This result is consistent with the diagnosis of this patient showing an unusually high percentage of $CD34^{pos}CD56^{pos}$ cross-lineage cells amongst the AML blasts (47.9% of blasts; Table 1).

Enrichment of NK cells by MACS sorting and titers of T cells in PBMCs

After preparative enrichment by MACS sorting, $CD56^{bright}CD16^{bright}$ NKs accounted still for only 1.4% of total cells in the sample from the patient at diagnosis (Figure 5A, left). This poor enrichment probably reflects the high content of AML blasts with very immature, early progenitor phenotype, devoid of lineage markers, in the PBMC sample taken at diagnosis. Therefore, negative sorting using antibodies specific for lineage markers did not remove these cells. In contrast, the MACS-enriched $CD56^{bright}CD16^{bright}$ NKs accounted for approx. 77% of all cells in the corresponding samples from the patient in remission and the healthy twin used in the RDL and ADCC assays (Figure 5A; central and right panels). These observations are consistent with previously reported decreased frequencies of NKs in the blood of AML patients [30].

Finally, an approximate 10-fold reduction of the T cell compartment was also observed comparing PBMCs from this patient drawn at diagnosis with those obtained in remission and those from the healthy twin (Figure 5B). Only 6.9% of the patient's PBMCs drawn at diagnosis were $CD56^{neg}CD3^{pos}$ T cells, compared with 65.2% and 78.7%, respectively, for the cells from the patient in remission and the healthy twin. This finding indicates that in the remission stage after the initial chemotherapy, not only NKs are restored but also the T cell compartment recovered to approximately normal levels.

Expression levels of natural cytotoxicity receptors (NCRs) in PBMC samples

As impaired cytolytic activity of NKs from AML patients had been proposed to be caused by reduced expression of NCRs [25,26], expression of NKp30, NKp44 and NKp46 on enriched NKs was studied (Figure 6). No significant difference in the expression patterns was observed between MACS enriched NKs from the patient in remission versus the healthy sibling (Figure 6A). The corresponding analysis for NKs from the patient at diagnosis was rendered more difficult by the fact that NKs were of low abundance in the MACS-enriched sample at this time. This analysis was therefore refined by further gating for $CD16^{pos}$ cells and then analyzing the NCRs on this gated population of NKs. In this manner, an essentially unchanged NCR expression profile

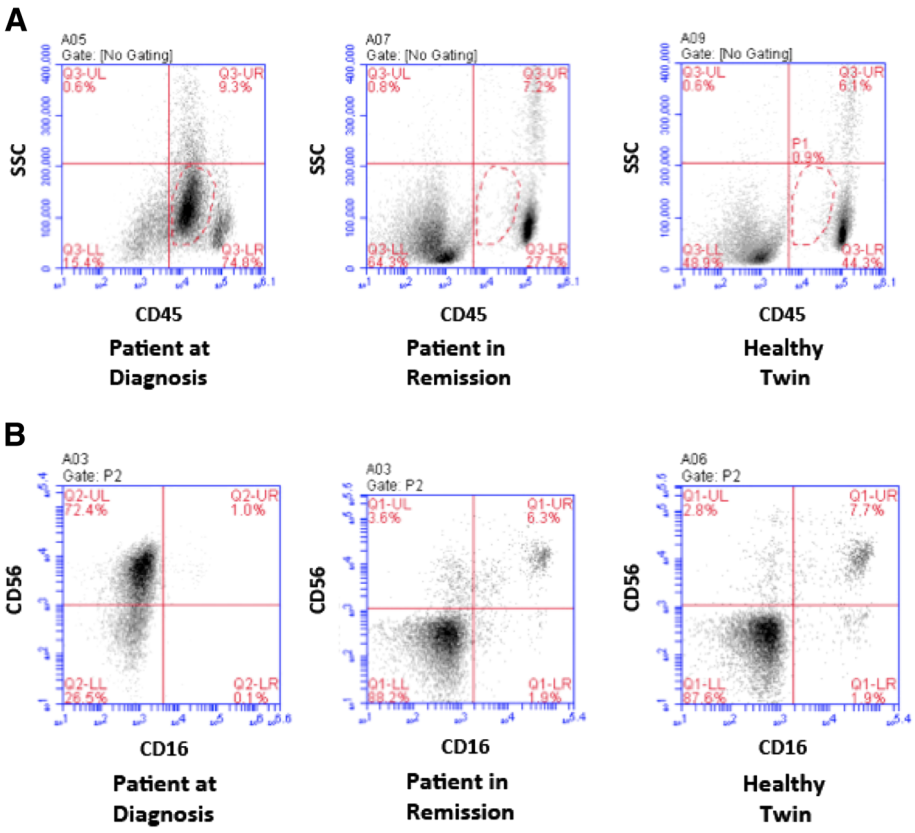

Figure 4 Analysis of AML blasts and NKs within PBMCs from the different donor samples. (A) Blast content among PBMCs from the patient at diagnosis and in remission (left and central panels) or from the healthy twin (right) is shown. PBMCs were stained with a FITC-labeled CD45 mAb and analyzed against side scatter (SSC) by flow cytometry. $CD45^{dim}$ x SSC^{LOW} cells have been defined as AML blasts [24]. Dashed line: P1 gate (blasts). Numbers in the corners of quadrants: fraction of total cells falling into this quadrant. **(B)** Analysis of NK cell content. PBMCs form the same sources as in A were stained with FITC-labeled CD16 and PE-labeled CD56 mAbs. NKs were defined as $CD16^{pos}CD56^{pos}$ cells (upper right quadrant). The population in the upper left corner in the left panel is the unusual population of $CD56^{bright}CD16^{neg}$ cells, previously reported in AML samples [30] as an NK subset that exclusively produces cytokines.

was found for these gated NKs (Figure 6B). The gating strategy used for this analysis of the PBMC sample drawn at diagnosis is shown in Figure 6C. From these combined observations, we conclude that for this particular patient the NCR expression profiles remained unchanged and that changes in the levels of NCRs are unlikely to be the cause of the impaired cytolytic functions recorded here.

Whole blood samples from the AML-patient and the healthy sibling show different levels of cytokine release after addition of SPM-2

Reduced cytokine (IFN-gamma) release by NKs from AML patients had been reported to be correlated with suppressed immune responses against autologous leukemic cells [32,33,45]. Therefore, we tested whether differences in cytokine release were detectable after addition of SPM-2 either to whole blood samples from the patient drawn at diagnosis or those from the patient in remission and the twin. Determinations of IFN-gamma release by ELISA produced no signal above the detection threshold (4 pg/ml). However, TNF-alpha was detected in the corresponding samples after addition of SPM-2 (Figure 7A). Following incubation for 6 h with a saturating dose of SPM-2 (10 nM), 4.7 ± 0.1 pg/ml of TNF-alpha were detected in blood from the healthy sibling versus only 1.1 ± 0.1 pg/ml in the patient's sample drawn in remission (Figure 7A). Thus, whole blood cells from the patient in remission showed a reduced release of TNF-alpha in response to the addition of SPM-2, compared to cells from the healthy sibling. This differential cytokine response does not appear to have affected the cytolytic activity mediated by SPM-2, as these two sources of NKs did not show major differences in our RDL and ADCC assays with autologous and allogeneic leukemic cells as targets.

To investigate, whether cytokine release during cytolytic reactions with MACS-purified NKs from these different sources was similarly independent of target antigen and the type of target cell line, we analyzed the cytokine

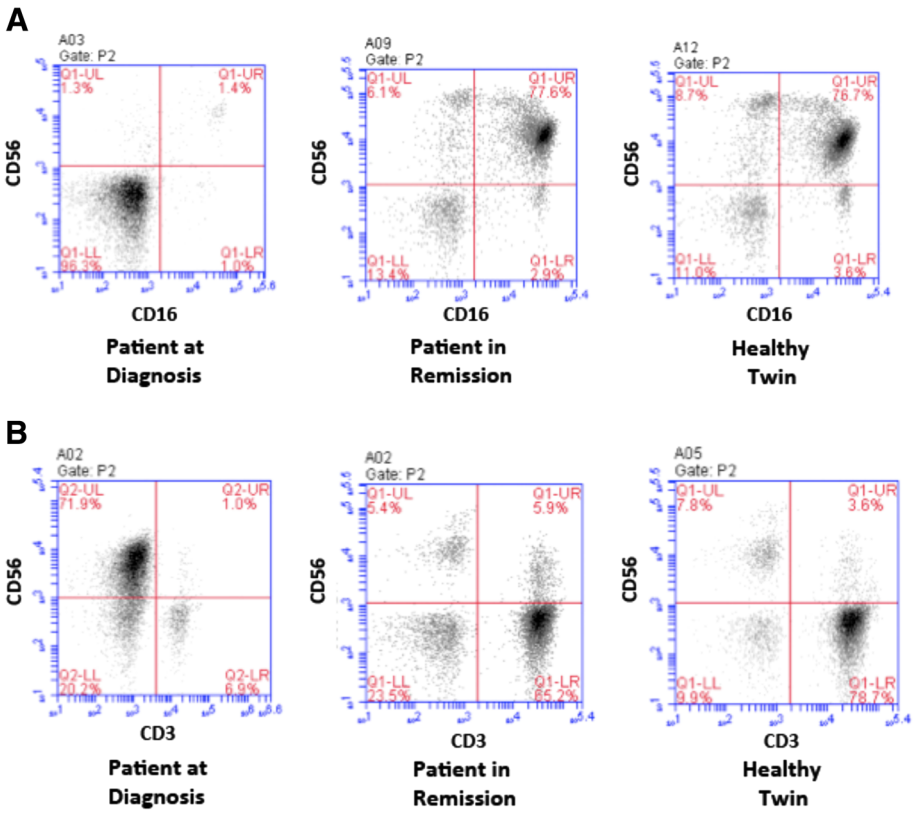

Figure 5 Analysis of MACS sorted NKs and T cells within PBMCs isolated from the different donor samples. (A) The $CD16^{POS}CD56^{POS}$ NK cells enriched by immunomagnetic beads (MACS; Methods) are shown in the upper right quadrant. Events in the lower left quadrant in the sample from the patient at diagnosis are considered to be very immature blasts devoid of lineage markers as discussed in the text. **(B)** $CD3^{POS}$ $CD56^{neg}$ cells (lower right quadrant): T cells.

release occurring during the ADCC and RDL reactions, by assaying the supernatants of these reactions in our ELISA assay (Figure 7B and C). TNF-alpha production was reduced for the reaction with NKs from the patient in remission relative to the healthy sibling but even more so with NKs from the patient at diagnosis. This result was observed for the supernatants from both the ADCC and RDL assays. IFN-gamma release was undetectable. These results are consistent with previous reports indicating that NKs from AML patients are attenuated in their release of cytokines [27,29].

Discussion

The most important result of this study is that it helped to dispel concerns raised by critics about the use of triplebodies for the treatment of AML, because they rely on NK cells as effectors. The main argument was that too few NK cells were present in an AML patient for triplebodies to be effective. The critics held that it would be preferable to recruit T cells rather than NK cells as effectors, because T cells were present in greater numbers, because they have higher intrinsic cytolytic activity, are capable of serial lysis of several target cells in a consecutive manner, and can be stimulated to proliferate as a result of exposure to the agent. We cannot address all of these points here in detail, and some of our arguments regarding the relative merits of recruiting NK cells vs. T cells have been reviewed elsewhere [17]. Suffice it to state that NKs are also capable of serial lysis and that their numbers can be increased in patients after treatment with antibody-derived agents recruiting NKs as effectors [28,47]. Therefore, after clinical administration of agents related to SPM-2 such as the tandem diabody AFM-13 specific for CD30 and CD16, NKs can expand in human recipients *in vivo*, and sufficient numbers can become available for therapeutic effects, even for malignancies such as Hodgkin Lymphoma that include semi-solid tumor masses [47]. Our results presented above (Figure 5B) suggest that for the patient of the present study, CD3-positive T cells were also greatly reduced in peripheral blood at diagnosis and only recovered together with other leukocytes in the remission phase. Finally, it is not known how many T cells and how many NKs are needed for an effective therapy with such agents. The absolute numbers of NK cells in

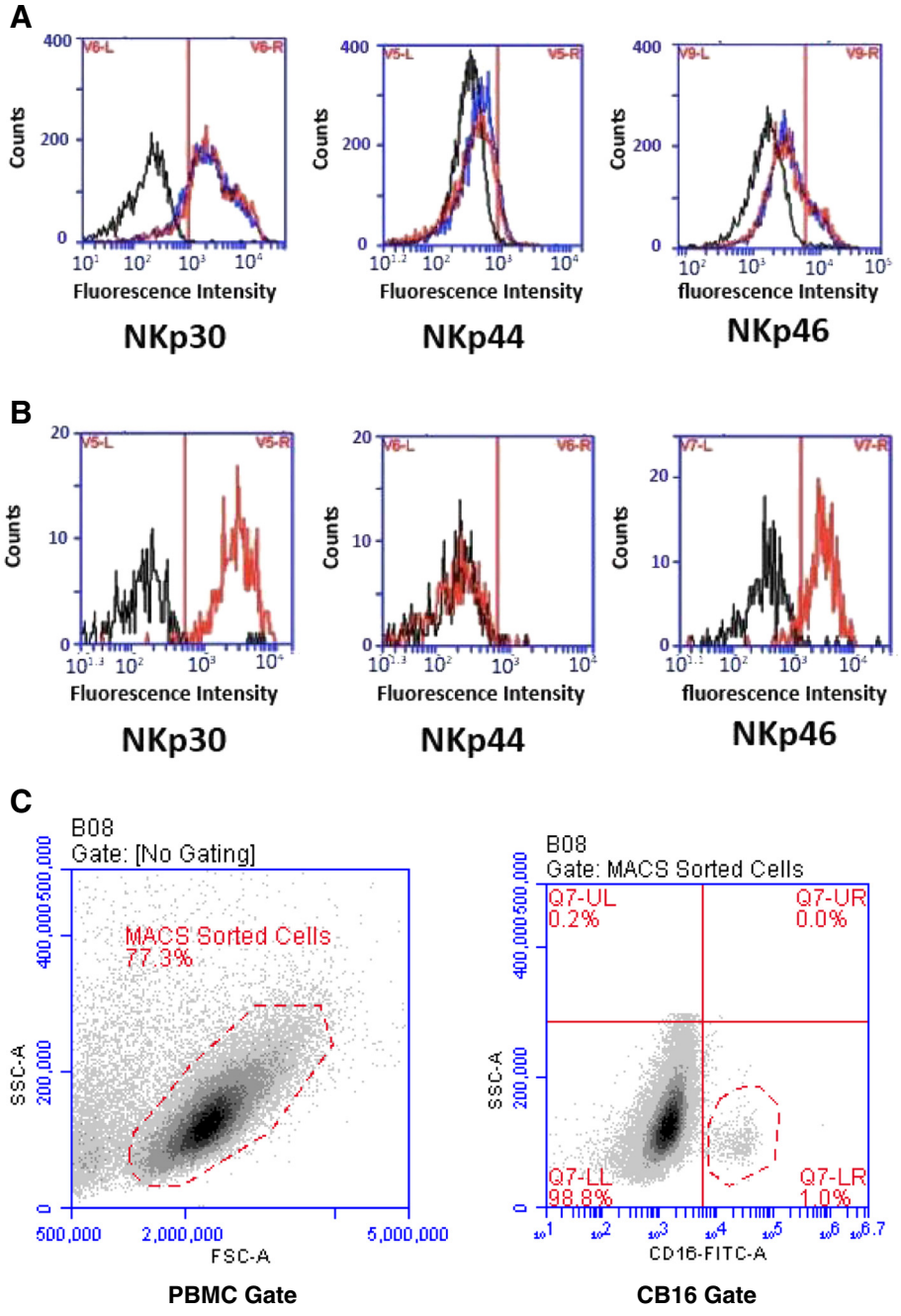

Figure 6 Unaltered expression patterns of the NCRs NKp30, NKp44 and NKp46 on enriched NKs from the patient at diagnosis, in remission and the healthy twin. (A) Expression pattern of NCRs on enriched NKs from the patient in remission (red) and the healthy twin (blue) compared with cells stained with an isotype control mAb (black). **(B)** To analyze NCR expression on enriched NKs from the patient at diagnosis, an additional sorting step for CD16 positive cells was performed to focus the analysis on the small subpopulation of NKs. NKs from the patient at diagnosis (red) are compared with cells stained with an isotype control mAb (black). **(C)** Gates chosen to generate data shown in panels **A)** and **B)**. Left: gate chosen to identify MACS-sorted cells (negative selection for NK cells). Right: additional gate used for identification of the CD16 pos subset (lower right quadrant) of the MACS sorted cells from the patient sample obtained at diagnosis (Methods).

remission (Figure 4B) may be lower than those of T cells, although absolute numbers have not been determined, but even lower numbers of NKs may be sufficient for therapeutic success.

In the present study, the patient's NK cells were greatly reduced in relative abundance. At diagnosis their frequency was at least 6–7 fold reduced compared to the two reference samples obtained from the patient in

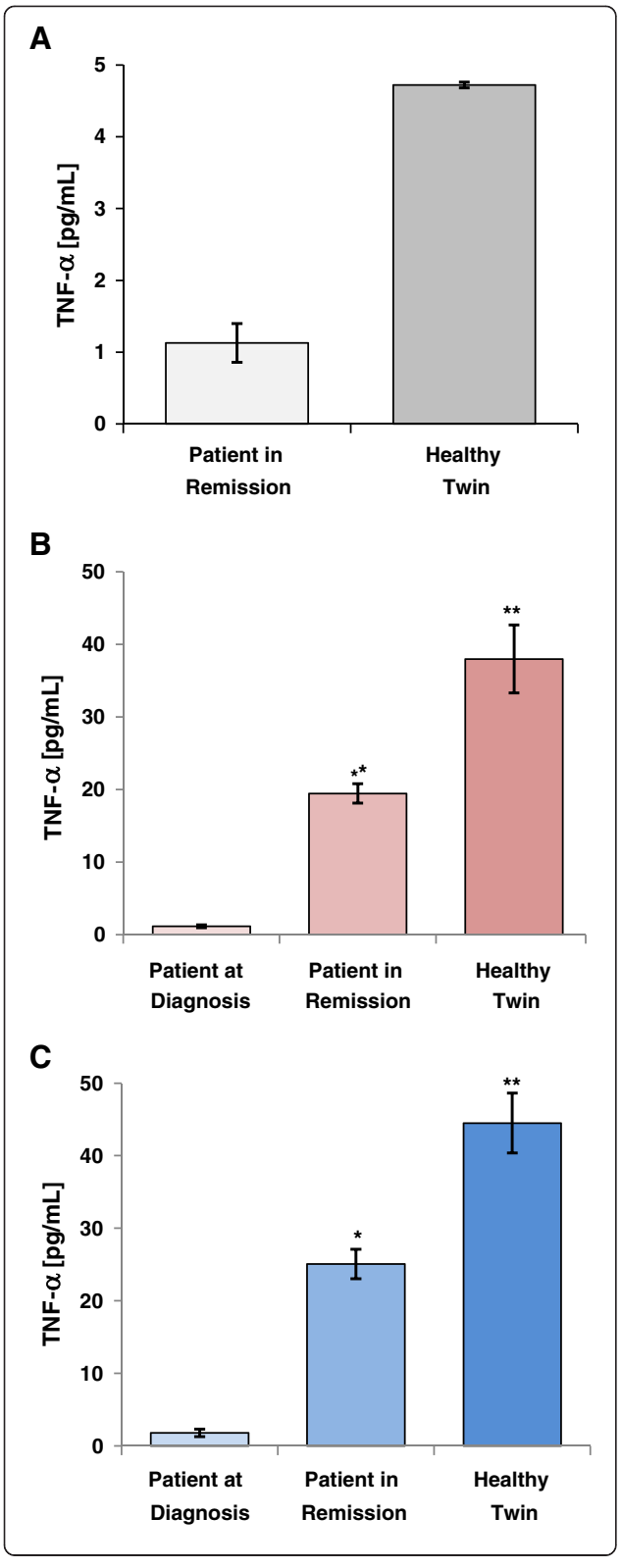

Figure 7 Secretion of TNF-alpha from whole blood or from supernatants of cytolysis reactions after treatment with SPM-2. **(A)** Release of TNF-alpha into whole EDTA treated blood from the patient in remission versus the healthy twin after addition of SPM-2. 200 μl samples of EDTA-blood were incubated for 6 h at 37°C with a 10 nM dose of SPM-2. Secretion of TNF-alpha was measured with a commercial ELISA kit (Methods). **(B)** Supernatants from a 4 h RDL assay using 10 nM dose of SPM-2 and the patient's autologous BMMCs drawn at diagnosis as targets (red). Effector cells were MACs enriched NKs isolated from PBMCs taken from the patient at diagnosis (left), in remission (center), or from the healthy sibling (right). Secreted TNF-alpha was measured as in panel **A**. Plotted data are the arithmetic means over 6 independent experiments (n = 6). Error bars represent the standard error of the mean (SEM). Statistical significance was reached with p = .002 (*) and .004 (**) for the differences between cells from the healthy twin and the patient in remission versus at diagnosis, respectively. **(C)** Supernatants from a 3 h ADCC assay using 10 μg/ml dose of Rituximab and Raji leukemia cells as targets were assayed for TNF-alpha secretion using the same NK effector populations as for panel **A** (blue). Plotted data are mean values over six independent experiments (n = 6). Statistical significance was reached with p = .0001 (*) and .0003 (**), for the differences between healthy twin and patient in remission versus at diagnosis, respectively.

remission and the healthy twin. In the remission sample, normal numbers of NKs with typical cytolytic activity were found. This observation is important for us because SPM-2 was not designed to debulk the mass of leukemic blasts as a frontline agent. Instead, it was designed to act as an adjuvant to further reduce the MRD pool after an initial induction chemotherapy and thus to achieve deeper and longer-lasting remissions.

In this context, the observation that not only the total population of AML blasts from this patient was efficiently lysed by SPM-2 together with MNC effectors (Figure 2B), but that the $CD34^{pos}$ subset was also specifically reduced (Figure 2C), is encouraging. This finding opens the possibility that the AML-LSCs contained within the CD34 compartment were also affected by this treatment. If this were true more generally beyond this single patient, then this would be a welcome result, because AML-LSCs are reported to have increased resistance to treatment with standard chemotherapeutic agents [19,48]. AML-LSCs are typically contained in the $CD34^{pos}$ compartment, and if the LSCs of this patient were similarly sensitive towards cytolysis mediated by SPM-2 in conjunction with NKs as the overall population of $CD34^{pos}$ cells, then this would suggest, that SPM-2 may become a useful new agent for the removal of LSCs. However, these extrapolations are made with due caution, because the AML-LSCs may only account for a minor subset of all $CD34^{pos}$ blasts in this patient and therefore may have escaped lysis in our experiments.

We were further encouraged by our preliminary finding reported here that SPM-2 mediated specific lysis of the $CD34^{pos}CD38^{neg}$ $CD123^{pos}$ subset contained within the

patient AML blasts, which presumably more narrowly confines the relevant MRD cells than the broader $CD34^{pos}$ compartment. Admittedly, this was only a single initial experiment and further confirmation is needed. Yet, the results obtained so far suggest that SPM-2 in conjunction with functional NKs was capable of effectively eliminating the $CD34^{pos}CD38^{neg}$ $CD123^{pos}$ subset, reported by others [24] to include the MRD cells.

No major changes were observed here in the expression profiles of NCRs on NKs between the samples from the patient at diagnosis and in remission, and both profiles were similar to those observed for the healthy sibling. This result was somewhat surprising, because it had been reported by others that differences in NCR expression profiles could be a major cause for impaired functional activity of NKs from AML patients [25-27,29]. One possible explanation for our result is that the expression profile of this particular patient is unique and differs from those of the majority of patients reported elsewhere. Another possible explanation is that in the cases published by others, NCR expression levels were generally compared between NKs from AML patients and those from unrelated healthy donors. This comparison may be less informative than the more rigorous comparison reported here, because it is not excluded that patients in the published studies expressed lower intrinsic NCR levels than the average healthy donor, and that this reduced expression may even have been a cofactor predisposing them to the development of the disease.

Conclusions

Titers of peripheral blood NKs from a FAB M1 AML patient had recovered to normal levels in remission after induction chemotherapy, and these cells showed normal functional activity in cytolytic assays mediated by the therapeutic triplebody SPM-2. Comparable cytolytic activity of NKs from the patient in remission and a healthy twin were observed both for the patients autologous leukemic blasts as targets, and in benchmark experiments with the standard antibody Rituximab™ against Raji lymphoma cells as targets. The functional impairment of this patient's NKs obtained at diagnosis probably is not caused by an altered expression pattern of the NCRs, NKp30, NKp40 and NKp46, as suggested in the literature. Expression profiles of these receptors were unaltered in our case. The major cause for a functional impairment of the patients NK cell response at diagnosis appears to be the result of a reduced NK cell titer. Overall, our results indicate that a useful time point to administer SPM-2 for the treatment of AML patients will be the remission phase after induction chemotherapy when blast titers are reduced and titers and functional activity of normal leukocytes have recovered.

Abbreviations

ADCC: Antibody-dependent cellular cytotoxicity; AML: Acute myeloid leukemia; ELISA: Enzyme-linked immunosorbent assay; FAB: French american british classification of AML; FITC: Fluorescein isothiocyanate; HAM: High-dose cytarabine with mitoxantrone, a standard therapy modality for the treatment of AML [49]; IFN-Gamma: Interferon gamma; MNC: Mononuclear cells; PBMC: Peripheral blood mononuclear cells; RDL: Redirected lysis; TNF-alpha: Tumor necrosis factor alpha; WHO-classification: World Health Organization classification of AML from 2008, as published in 2009 [42].

Competing interest

The authors declare that they have no competing interests. UJ and GHF are employees of SpectraMab, Munich, Germany.

Authors' contributions

TAB participated in the design of the study, performed experiments, analyzed data and helped write the manuscript. SW participated in the design of the study, performed experiments, analyzed data and helped in editing the manuscript. CCR performed experiments, analyzed data and helped in editing the manuscript. IAS contributed to SPM-2 design and performed functional studies. KPH and GHF participated in the design of the study, secured extramural funding and helped in editing the manuscript. FSO managed and coordinated the process of gathering patients, patient material and patient data, helped to secure funding, to plan the study design and to edit the manuscript. All authors read and approved the final manuscript.

Acknowledgements

We thank K. Lämmermann, A. Schele and B. Schnabel for technical assistance and Drs. B. Emmerich, BM Peterlin and M. Subklewe for scientific advice. The study was funded by support from the M4 excellence award (to KPH, GHF and FO) from the Bavarian Government and by the association "Chimney Sweeps Help Children with Cancer" (Kaminkehrer Helfen Krebskranken Kindern e.V.) to FO and GHF.

Author details

[1]Division of Hematology and Oncology, Medizinische Klinik und Poliklinik IV, Klinikum der Universität München, Ziemssenstrasse 1, D-80336 Munich, Germany. [2]Department of Biochemistry and Gene Center, Ludwig-Maximilians-University, Munich, Germany. [3]Department of Biology, University of Erlangen-Nuremberg, Erlangen, Germany. [4]SpectraMab GmbH, Munich, Germany.

Received: 13 July 2013 Accepted: 14 November 2013
Published: 16 November 2013

References

1. Rowe JM, Lowenberg B: **Gemtuzumab ozogamicin in acute myeloid leukemia: a remarkable saga about an active drug.** *Blood* 2013, **121:**4838–4841.
2. **Press release: FDA (US government).** 2010. June 21, 2010. http://www.fda.gov/NewsEvents/Newsroom/PressAnnouncements/ucm216448.htm.
3. Hauswirth AW, Florian S, Printz D, Sotlar K, Krauth MT, Fritsch G, Schernthaner GH, Wacheck V, Selzer E, Sperr WR, Valent P: **Expression of the target receptor CD33 in CD34+/CD38-/CD123+ AML stem cells.** *Eur J Clin Invest* 2007, **37:**73–82.
4. Valent P: **Targeting of leukemia-initiating cells to develop curative drug therapies: straightforward but nontrivial concept.** *Curr Cancer Drug Targets* 2010, **11:**56–71.
5. Walter RB, Appelbaum FR, Estey EH, Bernstein ID: **Acute myeloid leukemia stem cells and CD33-targeted immunotherapy.** *Blood* 2012, **119:**6198–6208.
6. Kung Sutherland MS, Walter RB, Jeffrey SC, Burke PJ, Yu C, Kostner H, Stone I, Ryan MC, Sussman D, Lyon RP, Zeng W, Harrington KH, Klussman K, Westendorf L, Meyer D, Bernstein ID, Senter PD, Benjamin DR, Drachman JG: **SGN-CD33A: a novel CD33-targeting antibody-drug conjugate utilizing a pyrrolobenzodiazepine dimer is active in models of drug-resistant AML.** *Blood* 2013(J. A. McEarchern). Jun 14. [Epub ahead of print].
7. Aigner M, Feulner J, Schaffer S, Kischel R, Kufer P, Schneider K, Henn A, Rattel B, Friedrich M, Baeuerle PA, Mackensen A, Krause SW: **T lymphocytes can be effectively recruited for ex vivo and in vivo lysis of AML blasts by a novel CD33/CD3-bispecific BiTE antibody construct.** *Leukemia* 2013, **27**(5):1107–1115.

8. Kugler M, Stein C, Kellner C, Mentz K, Saul D, Schwenkert M, Schubert I, Singer H, Oduncu F, Stockmeyer B, Mackensen A, Fey GH: **A recombinant trispecific single-chain Fv derivative directed against CD123 and CD33 mediates effective elimination of acute myeloid leukaemia cells by dual targeting.** *Br J Haematol* 2010, **150:**574–586.
9. Singer H, Kellner C, Lanig H, Aigner M, Stockmeyer B, Oduncu F, Schwemmlein M, Stein C, Mentz K, Mackensen A, Fey GH: **Effective elimination of acute myeloid leukemic cells by recombinant bispecific antibody derivatives directed against CD33 and CD16.** *J Immunother* 2010, **33:**599–608.
10. Busfield SJ, Biondo M, Wong M, Ramshaw HS, Lee EM, Martin K, Ghosh S, Braley H, Tomasetig V, Panousis C, Vairo G, Roberts AW, He SZ, Sprigg N, Thomas D, DeWitte M, Lock RB, Lopez AF, Nash A: **CSL362: a monoclonal antibody to human interleukin-3 receptor CD123, optimized for NK cell-mediated cytotoxicity of AML stem cells.** *ASH* 2012:3598. Abstract.
11. Jin L, Lee EM, Ramshaw HS, Busfield SJ, Peoppl AG, Wilkinson L, Guthridge MA, Thomas D, Barry EF, Boyd A, Gearing DP, Vairo G, Lopez AF, Dick JE, Lock RB: **Monoclonal antibody-mediated targeting of CD123, IL-3 receptor alpha chain, eliminates human acute myeloid leukemic stem cells.** *Cell Stem Cell* 2009, **5:**31–42.
12. Roberts AW, He S, Ritchie D, Hertzberg MS, Kerridge I, Durrant ST, Kennedy G, Lewis ID, Marlton P, McLacian AJ: **A phase I study of anti-CD123 monoclonal antibody (mAb) CSL360 targeting leukemia stem cells (LSC) in AML.** *J. Clin Oncol* 2010, **28**(15 Suppl):Abstract e13012.
13. Kellner C, Bruenke J, Stieglmaier J, Schwemmlein M, Schwenkert M, Singer H, Mentz K, Peipp M, Lang P, Oduncu F, Stockmeyer B, Fey GH: **A novel CD19-directed recombinant bispecific antibody derivative with enhanced immune effector functions for human leukemic cells.** *J Immunother* 2008, **31:**871–884.
14. Schubert I, Kellner C, Stein C, Kugler M, Schwenkert M, Saul D, Mentz K, Singer H, Stockmeyer B, Hillen W, Mackensen A, Fey GH: **A single-chain triplebody with specificity for CD19 and CD33 mediates effective lysis of mixed lineage leukemia cells by dual targeting.** *MAbs* 2011, **3:**21–30.
15. Schubert I, Kellner C, Stein C, Kugler M, Schwenkert M, Saul D, Stockmeyer B, Berens C, Oduncu FS, Mackensen A, Fey GH: **A recombinant triplebody with specificity for CD19 and HLA-DR mediates preferential binding to antigen double-positive cells by dual-targeting.** *MAbs* 2012, **4:**45–56.
16. Schubert I, Saul D, Nowecki S, Mackensen A, Fey GH, Oduncu F: **A dual-targeting triplebody mediates preferential redirected lysis of antigen double-positive over single-positive leukemic cells.** *MAbs* 2013, **6** [Epub ahead of print].
17. Stein C, Schubert I, Fey GH: **Natural killer (NK)- and T-cell engaging antibody-derived therapeutics.** *Antibodies* 2012, **1:**88–123.
18. Schubert I, Stein C, Fey GH: **Dual-targeting for the elimination of cancer cells with increased selectivity.** *Antibodies* 2012, **1:**2–18.
19. Jordan CT: **Targeting myeloid leukemia stem cells.** *Sci Transl Med* 2010, **2:**21–31.
20. Jordan CT, Upchurch D, Szilvassy SJ, Guzman ML, Howard DS, Pettigrew AL, Meyerrose T, Rossi R, Grimes B, Rizzieri DA, Luger SM, Phillips GL: **The interleukin-3 receptor alpha chain is a unique marker for human acute myelogenous leukemia stem cells.** *Leukemia* 2000, **14:**1777–1784.
21. Dick JE: **Stem cell concepts renew cancer research.** *Blood* 2008, **112:**4793.
22. Jordan CT: **Targeting the most critical cells: approaching leukemia therapy as a problem in stem cell biology.** *Nat Clin Pract Oncol* 2005, **2:**224–225.
23. Wertheim GB, Bagg A: **Minimal residual disease testing to predict relapse following transplant for AML and high-grade myelodysplastic syndromes.** *Expert Rev Mol Diagn* 2011, **11:**361–366.
24. Vergez F, Green AS, Tamburini J, Sarry JE, Gaillard B, Cornillet-Lefebvre P, Pannetier M, Neyret A, Chapuis N, Ifrah N, Dreyfus F, Manenti S, Demur C, Delabesse E, Lacombe C, Mayeux P, Bouscary D, Recher C, Bardet V: **High levels of CD34 + CD38low/-CD123+ blasts are predictive of an adverse outcome in acute myeloid leukemia: a Groupe Ouest-Est des Leucemies Aigues et Maladies du Sang (GOELAMS) study.** *Haematologica* 2011, **96:**1792–1798.
25. Costello RT, Sivori S, Marcenaro E, Lafage-Pochitaloff M, Mozziconacci MJ, Reviron D, Gastaut JA, Pende D, Olive D, Moretta A: **Defective expression and function of natural killer cell-triggering receptors in patients with acute myeloid leukemia.** *Blood* 2002, **99:**3661–3667.
26. Fauriat C, Just-Landi S, Mallet F, Arnoulet C, Sainty D, Olive D, Costello RT: **Deficient expression of NCR in NK cells from acute myeloid leukemia: Evolution during leukemia treatment and impact of leukemia cells in NCRdull phenotype induction.** *Blood* 2007, **109:**323–330.
27. Lion E, Willemen Y, Berneman ZN, Van Tendeloo VF, Smits EL: **Natural killer cell immune escape in acute myeloid leukemia.** *Leukemia* 2012, **26:**2019–2026.
28. Olive D, Anfossi N, Andre P, Rey J, Orlanducci F, Breso V, Peri V, Prebet T, Charbonnier A, Perrot E, Romagne F, Vey N: **Long lasting alteration of natural killer cells post-chemotherapy in elderly patients with acute myeloid leukemia (AML).** *ASH* 2009. Abstract 1653.
29. Sanchez CJ, Le Treut T, Boehrer A, Knoblauch B, Imbert J, Olive D, Costello RT: **Natural killer cells and malignant haemopathies: a model for the interaction of cancer with innate immunity.** *Cancer Immunol Immunother* 2011, **60:**1–13.
30. Szczepanski MJ, Szajnik M, Welsh A, Foon KA, Whiteside TL, Boyiadzis M: **Interleukin-15 enhances natural killer cell cytotoxicity in patients with acute myeloid leukemia by upregulating the activating NK cell receptors.** *Cancer Immunol Immunother* 2010, **59:**73–79.
31. Baessler T, Charton JE, Schmiedel BJ, Grunebach F, Krusch M, Wacker A, Rammensee HG, Salih HR: **CD137 ligand mediates opposite effects in human and mouse NK cells and impairs NK-cell reactivity against human acute myeloid leukemia cells.** *Blood* 2010, **115:**3058–3069.
32. Baessler T, Krusch M, Schmiedel BJ, Kloss M, Baltz KM, Wacker A, Schmetzer HM, Salih HR: **Glucocorticoid-induced tumor necrosis factor receptor-related protein ligand subverts immunosurveillance of acute myeloid leukemia in humans.** *Cancer Res* 2009, **69:**1037–1045.
33. Coles SJ, Wang EC, Man S, Hills RK, Burnett AK, Tonks A, Darley RL: **CD200 expression suppresses natural killer cell function and directly inhibits patient anti-tumor response in acute myeloid leukemia.** *Leukemia* 2011, **25:**792–799.
34. Tajima F, Kawatani T, Endo A, Kawasaki H: **Natural killer cell activity and cytokine production as prognostic factors in adult acute leukemia.** *Leukemia* 1996, **10:**478–482.
35. Bruenke J, Barbin K, Kunert S, Lang P, Pfeiffer M, Stieglmaier K, Niethammer D, Stockmeyer B, Peipp M, Repp R, Valerius T, Fey GH: **Effective lysis of lymphoma cells with a stabilised bispecific single-chain Fv antibody against CD19 and FcgammaRIII (CD16).** *Br J Haematol* 2005, **130:**218–228.
36. Alici E, Sutlu T, Bjorkstrand B, Gilljam M, Stellan B, Nahi H, Quezada HC, Gahrton G, Ljunggren HG, Dilber MS: **Autologous antitumor activity by NK cells expanded from myeloma patients using GMP-compliant components.** *Blood* 2008, **111:**3155–3162.
37. Lanier LL: **NK cell recognition.** *Annu Rev Immunol* 2005, **23:**225–274.
38. Olejniczak SH, Stewart CC, Donohue K, Czuczman MS: **A quantitative exploration of surface antigen expression in common B-cell malignancies using flow cytometry.** *Immunol Invest* 2006, **35:**93–114.
39. Leidi M, Gotti E, Bologna L, Miranda E, Rimoldi M, Sica A, Roncalli M, Palumbo GA, Introna M, Golay J: **M2 macrophages phagocytose rituximab-opsonized leukemic targets more efficiently than m1 cells in vitro.** *J Immunol* 2009, **182:**4415–4422.
40. Weiner GJ: **Rituximab: mechanism of action.** *Semin Hematol* 2010, **47:**115–123.
41. Epstein MA, Achong BG, Barr YM, Zajac B, Henle G, Henle W: **Morphological and virological investigations on cultured Burkitt tumor lymphoblasts (strain Raji).** *J Natl Cancer Inst* 1966, **37:**547–559.
42. Vardiman JW: **The World Health Organization (WHO) classification of tumors of the hematopoietic and lymphoid tissues: an overview with emphasis on the myeloid neoplasms.** *Chem Biol Interact* 2009, **184:**16–20.
43. Du X, Ho M, Pastan I: **New immunotoxins targeting CD123, a stem cell antigen on acute myeloid leukemia cells.** *J Immunother* 2007, **30:**607–613.
44. Stein C, Kellner C, Kugler M, Reiff N, Mentz K, Schwenkert M, Stockmeyer B, Mackensen A, Fey GH: **Novel conjugates of single-chain Fv antibody fragments specific for stem cell antigen CD123 mediate potent death of acute myeloid leukaemia cells.** *Br J Haematol* 2010, **148:**879–889.
45. Bonnet D, Dick JE: **Human acute myeloid leukemia is organized as a hierarchy that originates from a primitive hematopoietic cell.** *Nat Med* 1997, **3:**730–737.
46. Carey JL, McCoy JP, Keren DF: *Flow Cytometry in Clinical Diagnosis.* 4th edition. Chicago: ASCP Press; 2007.
47. Reiners KS, Kessler J, Sauer M, Rothe A, Hansen HP, Reusch U, Hucke C, Kohl U, Durkop H, Engert A, von Strandmann EP: **Rescue of impaired NK cell activity in hodgkin lymphoma with bispecific antibodies in vitro and in patients.** *Mol Ther* 2013, **21:**895–903.
48. Dick JE, Lapidot T: **Biology of normal and acute myeloid leukemia stem cells.** *Int J Hematol* 2005, **82:**389–396.

49. Buchner T, Hiddemann W, Wormann B, Loffler H, Gassmann W, Haferlach T, Fonatsch C, Haase D, Schoch C, Hossfeld D, Lengfelder E, Aul C, Heyll A, Maschmeyer G, Ludwig WD, Sauerland MC, Heinecke A: **Double induction strategy for acute myeloid leukemia: the effect of high-dose cytarabine with mitoxantrone instead of standard-dose cytarabine with daunorubicin and 6-thioguanine: a randomized trial by the German AML Cooperative Group.** *Blood* 1999, **93:**4116–4124.

doi:10.1186/1479-5876-11-289
Cite this article as: Braciak *et al.*: NK cells from an AML patient have recovered in remission and reached comparable cytolytic activity to that of a healthy monozygotic twin mediated by the single-chain triple-body SPM-2. *Journal of Translational Medicine* 2013 **11**:289.

Submit your next manuscript to BioMed Central and take full advantage of:

- **Convenient online submission**
- **Thorough peer review**
- **No space constraints or color figure charges**
- **Immediate publication on acceptance**
- **Inclusion in PubMed, CAS, Scopus and Google Scholar**
- **Research which is freely available for redistribution**

Submit your manuscript at
www.biomedcentral.com/submit

BioMed Central

2.2 T cell-recruiting triplebody 19-3-19 mediates serial lysis of malignant B lymphoid cells by a single T cell

Claudia C. Roskopf, Christian B. Schiller, Todd A. Braciak, Sebastian Kobold, Ingo A. Schubert, Georg H. Fey, Karl-Peter Hopfner & Fuat S. Oduncu

Oncotarget 2014 July 23; **5** (15): 6466-6483
DOI: 10.18632/oncotarget.2238

2.2.1 Summary

T lymphocytes are one of the most effective cytotoxic immune effector cell populations and are thus very well suited for the depletion of cancer cells. Prior to this study, single-chain triplebodies had been successfully employed to recruit NK cells for tumor cell lysis, but it had not been tested whether the triplebody format is suitable for T cell engagement as well. Therefore a prototype triplebody with monospecific bivalent targeting of the B lymphoid TAA CD19, i. e. 19-3-19, was constructed and described in this publication. 19-3-19 recruits T cells via a central CD3-epsilon-specific binding moiety that is derived from the monoclonal antibody clone OKT3. The use of CD3-epsilon as trigger antigen on CTLs had previously been validated, for example in the BiTE®-format.

Triplebody 19-3-19 as well as control triplebody Her2-3-Her2 and bispecific monovalent control proteins Her2-3 and 19-3 were produced and tested for biological activity in this study. All constructs displayed specific binding. The CD3-epsilon equilibrium dissociation constant (K_D) of 19-3-19 was determined to be 53.3 ± 19 nM, which was higher than the K_D-value of 19-3 (34.7 ± 14 nM) and suggested dependence on the molecular context of the scFv. Furthermore, the overall avidity of 19-3-19 for CD19 was twice as high as that of 19-3. This implied simultaneous binding of the two CD19 binding moieties as well as an additive rather than a synergistic combination of the affinities of the individual scFv. 19-3-19 also mediated the specific lysis of several $CD19^+$ cell lines, which represented different types of B cell malignancies. The EC_{50}-values were in the low picomolar range (5.5 to 189.6 pM) and comparable to those that were achieved with the bispecific control molecule 19-3. Since 19-3-19 also led to the lysis of 69 ± 13% SEM cells at an effector-to-target cell (E : T) ratio of 1 : 10, it was concluded that the triplebody induced serial lysis of several CD19-positive target cells by a single T cell. 19-3-19 mediated the activation of non-stimulated T cells in cytolysis assays as evidenced by the increase in cell surface levels of activation markers CD69 and CD25. T cell activation by 19-3-19 was dependent on the presence of CD19-bearing target cells. The subset of $CD3^+$ $CD45RO^+$ T cells, which was defined as the memory T cell population, proliferated. Maximum target cell depletion of 94.2% to 99.6% was achieved after 48 hours.

In combination with allogeneic pre-stimulated mononuclear cells (40% NK cells and 60% T cells), 19-3-19 also led to the efficient depletion of primary target cells from patients with different hematopoietic malignancies. The response to 19-3-19 treatment was compared to that towards the standard-of-care treatment with monoclonal anti-CD20 antibody rituximab (MabThera®). The extent of the treatment response generally coincided with the copy number of CD19 or CD20 on the cancer cell surface of the patient samples. Here, EC_{50}-values for 19-3-19 were 30- to 925-fold lower than those for rituximab. Further, in an autologous setting within an NHL patient sample, 19-3-19 led to the depletion of lymphoma cells and the notable 7-fold expansion of the entire T cell population.

At the example of 19-3-19 this study has thus proven that the triplebody format is suitable for the engagement of T lymphocytes as immune effectors in cancer therapy in an MHC:peptide-independent manner. Thus triplebodies may be a universal platform that is suited for the engagement of any desirable immune effector cell population with the added advantage of a longer plasma half-life than BiTE® and the potential for bivalent bispecific (i. e. dual) targeting.

2.2.2 Contribution

I designed, purified and characterized triplebody 19-3-19 and control molecules, performed binding studies and investigated the cytolytic potential of the molecules in combination with allogeneic pre-stimulated effector T cells against cell line targets and primary patient target cells. Additionally, I investigated the activation of resting T cell subsets from healthy donors and patients with B cell malignancies upon treatment with 19-3-19 in cytolysis assays. I am also the author of the manuscript, which was edited by Prof. Fey and reviewed by all co-authors.

T cell-recruiting triplebody 19-3-19 mediates serial lysis of malignant B-lymphoid cells by a single T cell

Claudia C. Roskopf[1], Christian B. Schiller[2], Todd A. Braciak[1], Sebastian Kobold[3], Ingo A. Schubert[4], Georg H. Fey[4], Karl-Peter Hopfner[2], Fuat S. Oduncu[1]

[1] Klinikum der Universität München, Medizinische Klinik und Poliklinik IV, Haematology/Oncology, Munich, Germany

[2] Ludwig-Maximilians-Universität München, Department of Biochemistry/Gene Center, Munich, Germany

[3] Klinikum der Universität München, Medizinische Klinik und Poliklinik IV, Division of Clinical Pharmacology, Munich, Germany

[4] Friedrich-Alexander-Universität Erlangen-Nürnberg, Department of Biology, Erlangen, Germany

Correspondence to:
Claudia C. Roskopf, **e-mail:** Claudia.Roskopf@med.uni-muenchen.de

Key Words: immunotherapy, triplebody, cytolytic T cells, antibody-dependent cellular cytotoxicity, leukemia

Received: June 06, 2014 ***Accepted:*** July 15, 2014 ***Published:*** July 23, 2014

ABSTRACT

Triplebody 19-3-19, an antibody-derived protein, carries three single chain fragment variable domains in tandem in a single polypeptide chain. 19-3-19 binds CD19-bearing lymphoid cells via its two distal domains and primary T cells via its CD3-targeting central domain in an antigen-specific manner. Here, malignant B-lymphoid cell lines and primary cells from patients with B cell malignancies were used as targets in cytotoxicity tests with pre-stimulated allogeneic T cells as effectors. 19-3-19 mediated up to 95 % specific lysis of CD19-positive tumor cells and, at picomolar EC_{50} doses, had similar cytolytic potency as the clinically successful agent Blinatumomab™. 19-3-19 activated resting T cells from healthy unrelated donors and mediated specific lysis of both autologous and allogeneic CD19-positive cells. 19-3-19 led to the elimination of 70 % of CD19-positive target cells even with resting T cells as effectors at an effector-to-target cell ratio of 1 : 10. The molecule is therefore capable of mediating serial lysis of target cells by a single T cell. These results highlight that central domains capable of engaging different immune effectors can be incorporated into the triplebody format to provide more individualized therapy tailored to a patient's specific immune status.

BACKGROUND

Therapeutic antibodies such as MabThera®, Herceptin® and Avastin® are potent and successful tools in the fight against cancer.[1] Recombinant proteins derived from conventional antibodies have been designed to increase tumor cell selectivity and deeper penetration into tumor tissues, and to exploit the patients' innate defense mechanisms against their disease. [2, 3] Several of the new antibody-derived agents - including immunoligands[4-6], diabodies, bispecific (bs) scFvs[7, 8], single chain triplebodies[9-12] and, most recently, a modular targeting system[13] - are based on single chain variable fragment (scFv) building blocks and lack an Fc region. While maintaining target specificity, the scFv-based agents are expected to reach deeper tissue penetration due to their reduced molecular mass. [14, 15] The lack of an Fc region is also thought to reduce undesired side effects, which are caused by binding to Fc receptors that are exposed on cells other than the desired cytolytic effectors.[2, 3]

Despite the lack of an Fc region, scFv-based agents have effective mechanisms of action. The anti-Her2/anti-Her3 bsscFv MM-111[16], for example, relies on simultaneous blockage of two different growth factor receptors and the cooperative inhibition of essential growth-promoting and anti-apoptotic downstream signals. Other mechanisms of action include the induction of apoptosis via surface receptors such as FasR (CD95)[17] and target-specific delivery of a toxin or radioisotope cargo by internalization (receptor-mediated endocytosis). Another option is the engagement of autologous effector

cells, such as natural killer (NK)-cells and cytotoxic T lymphocytes (CTLs), for cytolysis.[2, 3]

NK cells can, for example, be recruited by the TandAb™ AFM-13 (CD30-CD16; Affimed) designed for the treatment of Hodgkin Lymphoma.[18] Examples for T cell recruitment via scFv-based agents are the bispecific T cell engagers (BiTEs; Micromet/Amgen). Antibody-derivatives in the BiTE-format coat their tumor cell targets and engage effector memory T cells independent of their MHC : peptide specificity via the CD3ε chain of the T cell receptor-CD3 (TCR/CD3) complex.[7] Coupling between T cell and tumor cell leads to the formation of a cytolytic synapse and degranulation of the T cell. [7, 19] Moreover, the engagement of effector memory T cells via BiTEs leads to their proliferation and thus to an expansion of the effector cell population that is available for tumor cell lysis during the course of the treatment.[20-22] The CD19-specific BiTE Blinatumomab™ has shown impressive success in clinical studies with patients suffering from acute and chronic B cell malignancies.[20, 22-24] Other BiTEs targeting CD33 (CD33-CD3; AMG330) [25, 26], EpCAM (MT110; EpCAM-CD3)[27-29] and CEA (MT111; CEA-CD3)[30, 31], respectively, have produced promising results in recent pre-clinical studies and ongoing clinical trials.

However, despite their success, these bispecific agents still face limitations, which are difficult to overcome with this molecular format, including limitations in tumor cell specificity and "plasma retention time" ("plasma half-life").[22, 23] The drawback in specificity is due to the fact, that the BiTE-format is monospecific and monovalent for the tumor cell, recognizing only one target antigen. While mono-targeting has been successful in several applications, it may not confer sufficient specificity for cancer cells and sufficient discrimination between cancer and healthy cells in many other cases. Given that spontaneously arising cancer cells share many antigens with healthy cells, and that many of the most promising targets, such as growth factor receptors (e.g. EGF-receptor) and cell adhesion molecules (e.g. EpCAM) are not tumor-specific, this situation will occur. Therefore, monospecific agents have often caused side effects that are difficult to manage. In addition, under therapy with monospecific agents, escape mutants of tumor cells can emerge, which have lost the surface expression of the corresponding target antigen and have become resistant to treatment.[32] Dual-targeting agents, which address two different target antigens on the same cancer cell, may be capable of overcoming some of these limitations. Also, most BiTEs have a molecular mass below 65 kDa and thus below the kidney excretion limit, which results in a plasma half-life in the range of approximately 1 hour.[33] This shortcoming can be addressed by agents with a higher molecular mass and by extending the half-life by PEGylation, by fusion to human serum albumin (HSA) domains carrying a binding site for the FcRn shuttling receptor, or antibodies and antibody fragments with specificity for HSA.[34]

To take advantage of these added capabilities offered by multispecific scFv-based agents, the molecular format of "single chain triplebodies" ("triplebodies") has been developed by our group. A triplebody is composed of three scFvs connected via flexible $(Gly_4Ser)_4$ linkers, which results in a maximum computed distance of 20 nm between the two distal binding moieties[35] and a molecular mass of 85 to 95 kDa.[36] This mass exceeds the threshold for first-pass kidney excretion and consequently, triplebodies have a prolonged plasma half-life of approximately 4 hrs in mice. This corresponds to approx. 1 day in humans by allometric scaling.[9] Triplebodies can be designed to recruit different classes of effector cells via their central scFv, which is specific for an activating surface molecule such as CD16 on NK cells and macrophages[9, 10, 36], CD89 on polymorphonuclear granulocytes (PMNs)[37], or CD64 on macrophages and cytokine-stimulated PMNs.[3] The two distal binding moieties of the triplebody are capable of either monospecific bivalent targeting (example: 19-16-19)[9] or bispecific bivalent targeting ("dual-targeting") of two different target antigens on the same cancer cell (examples: 123-16-33[36], 33-16-19[10] and HLA-DR-16-19[11]). Dual-targeting triplebodies have been shown to achieve preferential binding[4] and to mediate preferential lysis[38] of double-positive over single-positive target cells by cytolytic effectors in a mixed environment. They even permitted preferential effector-cell mediated lysis of the double-positive cells when the single-positive cells were present in an up to 20-fold numerical excess. For some target antigen combinations the dual-targeting approach may not be successful, because individual target affinities, antigen surface densities and the genetically and epigenetically determined susceptibility of the target cell to effector cell-mediated lysis need to cooperate for enhanced potency. [28] Nevertheless, dual-targeting triplebodies have been successful in preclinical studies for a number of different combinations of target antigens, and therefore this concept deserves further exploration.

The ability of triplebodies to recruit T cells as effectors is unaddressed so far and it is uncertain whether the fine structure of an immunological synapse mediated by a triplebody would be functional, as demonstrated for NK cells. In the present study a single chain triplebody was constructed and tested for the ability to recruit cytotoxic T cells (CTLs) as effectors for the lysis of CD19-positive leukemia cells. As we demonstrate in our current study, the new triplebody anti-CD19/anti-CD3/anti-CD19 (19-3-19) is capable of activating resting T cells and of mediating redirected and serial lysis of tumor cells, both of established B-ALL cell lines and of primary cells isolated from the peripheral blood of patients suffering from different types of B cell malignancies. The successful recruitment of effector T cells via

19-3-19 indicates that the triplebody platform can be used to recruit an even broader range of effector cells. The thus highlighted ability of the triplebody format to choose an optimally suited effector cell for therapy by adjusting the central trigger scFv based on a patient's specific cancer type and the availability of these effectors in the tumor tissue increases the range of therapeutic options and may add an additional layer to individualized cancer therapy.

RESULTS

Design and production of triplebody 19-3-19.

Triplebody 19-3-19 carries a scFv domain derived from the murine hybridoma antibody OKT3 (directed against human CD3ε) in the central position, and CD19-specific scFv domains, targeting the B-lineage antigen CD19, derived from hybridoma 4G7 as previously described (Fig. 1).[9] In this fusion protein with an N-terminal Strep-tag and a C-terminal His-tag, the CD19-specific scFv components were humanized by CDR-grafting.[39] Triplebody 19-3-19 was expressed both in adherent HEK 293T cells and in suspension-adapted HEK 293F cells with yields between 0.9 and 5.1 mg protein/L culture supernatant in different experiments (Table 1). HEK 293F cells permitted cultivation in serum-free medium and efficient purification via Ni-NTA affinity chromatography. The N- and C-termini were intact and no degradation products were detected (Fig. 2). In addition, two new agents in the Bispecific T cell Engager (BiTE)-format were produced as controls. One carried our humanized CD19-specific scFv domain and was designated 19-3 ("Blinatumomab™-look-alike"), the other carried scFvs with specificity for Her2/NEU and CD3ε and was designated Her2-3. Finally, a control triplebody targeting Her2/NEU (designated Her2-3-Her2) was also produced. Expression of Her2-3-Her2 and Her2-3 was efficient with yields of 8.5 and 9.2 mg/L of culture supernatant, respectively (Table 1).

Triplebody 19-3-19 binds specifically both to its target antigens and the trigger protein.

Both the triplebody 19-3-19 and the BiTE 19-3 bound to primary human T cells isolated from *ex vivo* expanded mononuclear cells (Fig. 3A; left), as well as to CD19-positive Nalm-6 cells (a pre-B ALL-derived cell line; Fig. 3A, right), but it did not bind to antigen-negative HEK 293F cells (data not shown). The Her2-3-Her2 specificity control bound to T cells via the trigger CD3ε, but not to Her2- and CD3ε-negative Nalm-6 cells. At the saturating concentration of 15 µg/mL both the control triplebody Her2-3-Her2 and the 19-3 BiTE showed stronger binding to T cells than triplebody 19-3-19, as evidenced by a stronger shift in the mean fluorescence intensity (MFI) of the cell-bound fusion proteins detected by cytofluorimetry (Fig. 3A, left panel). Thus the binding capacity of the CD3ε-specific scFv domain was affected by its molecular context within a given fusion protein. The difference in binding strength was also reflected in the equilibrium dissociation constants (K_D values) of 19-3-19 and 19-3 for CD3ε exposed on primary T cells. The triplebody bound less strongly with an affinity of 53.3 ± 19 nM compared to 34.7 ± 14 nM for the BiTE 19-3 (Fig. 3B, left panel), but the difference was not significant. The overall avidity of the triplebody for CD19

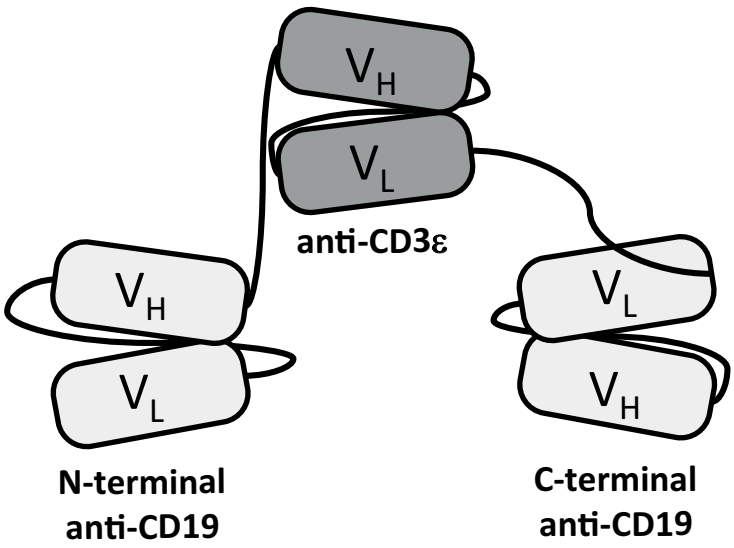

Figure 1: Domain architecture of T cell-recruiting triplebody 19-3-19. Triplebody 19-3-19 binds to the CD3ε chain of the TCR/CD3 complex via its central scFv and to two copies of CD19 on the surface of a malignant target cell via its two distal scFvs. The scFvs are connected by flexible $(G_4S)_4$-linkers (black lines), which gives the molecule a maximum computed span length (distance between the two distal binding sites) of 20 nm, when the flexible linkers are fully extended.

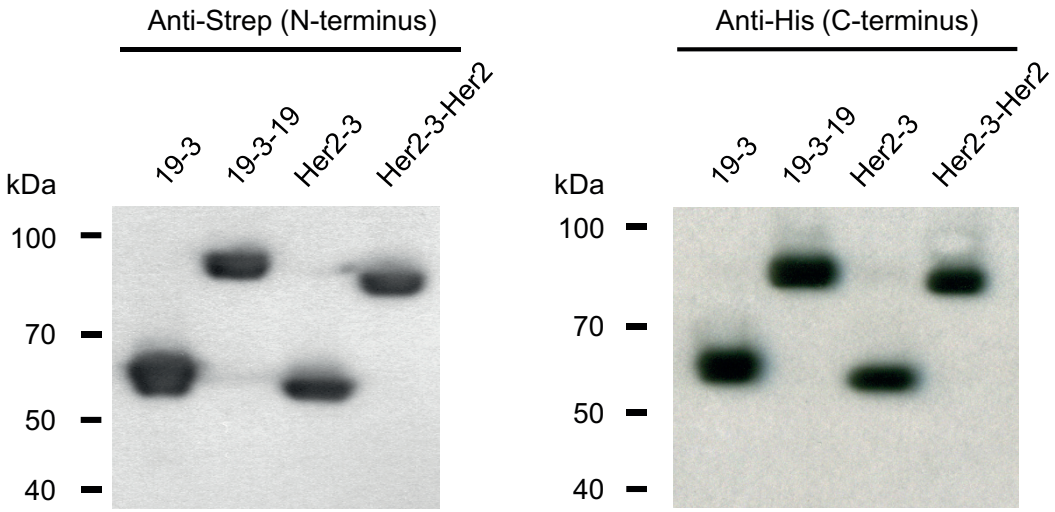

Figure 2: N- and C-termini of triplebody 19-3-19 and control proteins 19-3, Her2-3 and Her2-3-Her2 were intact. The fusion proteins carried N-terminal Strep and C-terminal hexa-histidine tags. Western blot analysis with antibodies reacting with the Strep- and His-tags, respectively, revealed that the fusion proteins carried intact N- and C-termini and provided no indication for incomplete synthesis or proteolytic degradation.

Table 1. Molecular masses and yields of T cell-engaging triplebodies and bispecific scFvs.
Proteins were expressed and purified as described in the Methods section. Buffer conditions were chosen to minimize protein aggregation. Proteins were concentrated to 150 - 300 ng/µL in the storage buffer by centrifugation, using centrifugal filters with a molecular weight cut-off (MWCO) of 50 kDa for the triplebodies and 10 kDa for bispecific scFvs. Theoretical molecular masses were computed from the known amino acid sequence composition of the molecules.

Protein	Computed Mass [kDa]	Yield [mg/L] (293F cells)	Storage Buffer
anti[CD19-CD3]	60.7	0.9 – 4.8	20mM L-Histidin 300mM NaCl 100mM D-Trehalose 5mM EDTA 10% Glycerol pH 6.5
anti[CD19-CD3-CD19]	89.9	0.9 – 5.1	
anti[Her2-CD3]	59.5	1.8 – 9.2	
anti[Her2-CD3-Her2]	87.2	6.0 – 8.5	

on the surface of SEM (pro-B ALL) cells was 14.7 ± 2 nM. Thus, the binding-strength of the triplebody for CD19 was approximately two-fold greater than the monovalent affinity of the CD19-specific scFv-domain carried in the control 19-3 with a K_D value of 28.4 ± 1 nM (Fig. 3B, right panel). These numerical values indicate that the two CD19-specific scFv domains of triplebody 19-3-19 contributed to the overall avidity of this protein in an additive rather than a synergistic manner, which was previously reported for the triplebody 19-16-19.[9] This observation suggests that the detailed spatial arrangement assumed by the two CD19-specific scFvs in a triplebody, which mediate the association with a target cell, is different between an NK- and a T cell-recruiting agent. The increase in avidity for CD19 on living cells observed for the triplebody relative to the BiTE is also evidence that both CD19-binding sites of the triplebody can simultaneously bind one copy each of CD19 on the same target cell.

Triplebody 19-3-19 mediates specific target cell lysis in combination with effector T cells.

To investigate whether the formation of a cytolytically productive synapse between an effector T cell and its tumor cell target can be mediated by triplebody 19-3-19, redirected lysis (RDL) assays were performed. For this purpose, a panel of CD19-positive leukemia- and lymphoma-derived cell lines representing different types of B cell-malignancies were used as targets with a

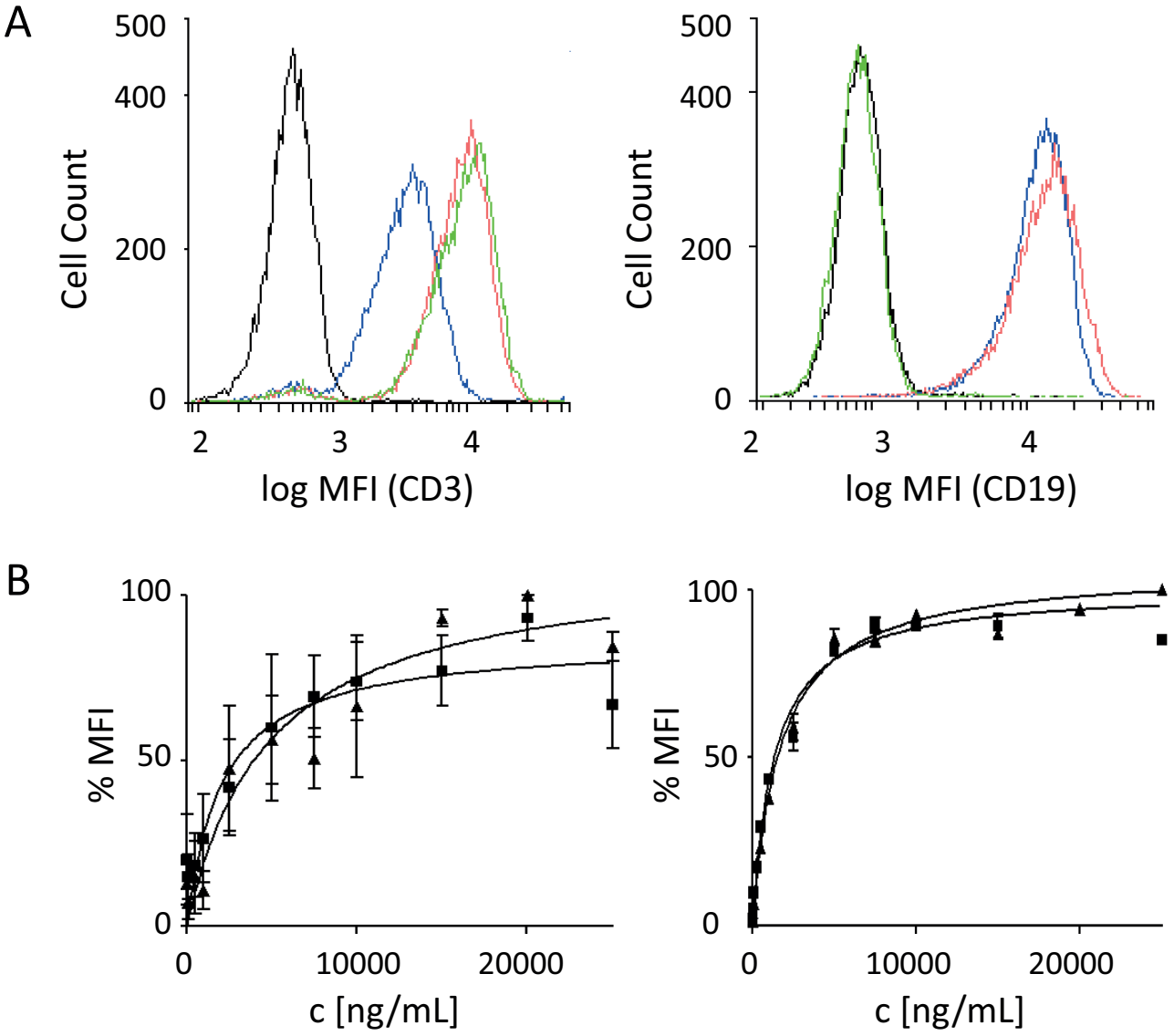

Figure 3: Binding specificities of the scFv components of triplebody 19-3-19. Target specificity of the 19-3 BiTE protein and triplebody 19-3-19 was examined by flow cytometry as described.[53] Molecules bound to the surface of single-positive target cells were detected with a secondary anti-His mAb and a Phycoerythrin (PE)-conjugated tertiary goat-anti-mouse IgG mAb. **(A)** Shift in mean fluorescence intensity (MFI) produced by binding to primary T cells (left), and Nalm-6 cells (right) at a saturating concentration of 15 µg/mL of either the BiTE or the triplebody. Black: isotype control; blue: triplebody 19-3-19; red: 19-3 BiTE; green: control triplebody Her2-3-Her2. MFIs are given as logarithms to the base of 10. **(B)** Determination of equilibrium dissociation constants K_D of 19-3 and the triplebody 19-3-19 for CD3 on primary T cells (n = 4), and for CD19 on SEM cells (n = 7). Error bars indicate standard error of the mean (SEM). The dissociation constants for CD3 were 34.7 ± 14 nM and 53.3 ± 19 nM for the BiTE and the triplebody, respectively. The dissociation constants for CD19 were 28.4 ± 1 nM for 19-3 and 14.7 ± 2 nM for triplebody 19-3-19, where the latter value refers to the overall (bivalent) avidity of the entire molecule, not to the monovalent affinity of the individual CD19-specific scFvs.

T cell : target cell ratio of 6 : 1. Triplebody 19-3-19 or control proteins 19-3 and Her2-3-Her2 were added at different concentrations and after a 3 hr reaction time target cell death was measured by Calcein release.[11, 38] 19-3-19 and 19-3 produced significant specific lysis of CD19-positive target cells in a dose-dependent manner (Fig. 4a). However, even at the highest concentration of 10 nM, the specificity control triplebody Her2-3-Her2 did not produce any significant specific lysis (3.5 ± 5 % background). This result is in accordance with an earlier report[40] describing that the sole binding of a BiTE protein to CD3ε on the T cell in the absence of binding to the target cell was not sufficient to induce bystander lysis of target cells by the T cells.

Lysis of SEM cells occurred with a sigmoidal dose-response with a maximum specific lysis of 89.8 ± 9 % after 3 hrs (mean of 4 experiments) and an EC50-value of 5.5 pM (95% CI: 3-9 pM). Dose-responses

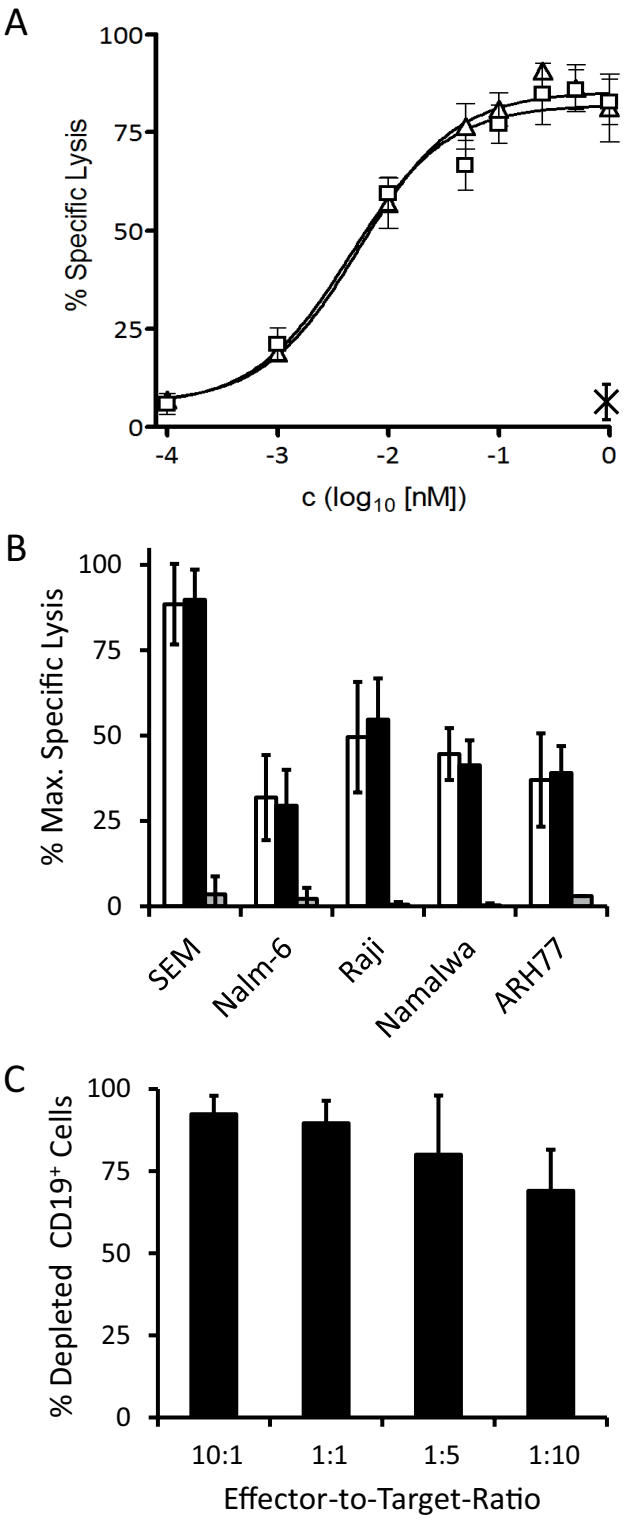

Figure 4: Specific redirected lysis of malignant target cell lines mediated by the 19-3 BiTE and triplebody 19-3-19 in conjunction with effector T cells. Standard Calcein Release Assays with an E : T ratio of 10 : 1 (MNCs : target cells) and a duration of 3 hrs were performed unless indicated otherwise. Error bars indicate SEM. **(A)** Dose-Response-Curve for SEM cells (triangles: triplebody 19-3-19; squares: 19-3 BiTE; cross: specificity control Her2-3-Her2; n=4). **(B)** Maximum specific lysis of several CD19-positive malignant B-lymphoid cell lines (n=4 each) induced by 19-3 (white bars), triplebody 19-3-19 (black bars) and specificity control Her2-3-Her2 (grey bars), respectively. **(C)** Serial lysis of unlabeled SEM target cells mediated by triplebody 19-3-19 at different E : T ratios. The reaction mixture (purified T cells and SEM target cells in RPMI1640 GlutaMAX medium containing 10% FCS) was incubated with or without 1nM triplebody overnight (approx. 15 hrs) (n = 3). The total number of viable cells in each reaction was determined and the fraction of CD19-positive target cells was established by FACS analysis.

were also recorded for Nalm-6 (pre-B ALL), Raji (Burkitt lymphoma), Namalwa (Burkitt lymphoma) and ARH77 (plasma cell leukemia) cells and EC50-values were in the low picomolar range (Table 2). The specificity control triplebody Her2-3-Her2 did not induce significant lysis of any of the target cell lines (Fig. 4B). Different surface antigen densities of CD19 on these cell lines are an explanation for the difference in lysis measured, because a loose correlation was observed between the copy number of CD19 molecules per cell and the degree of maximum specific lysis (Fig. 4B and Table 2). Copy numbers per cell (given in the parentheses) were measured by calibrated cytofluorimetry and gave rise to the following ranking: SEM (30,000 ± 8,000) > Raji (23,500 ± 19,000) > Nalm-6 (17,500 ± 7,000) > Namalwa (7,000 ± 4,000) > ARH77 (1,500 ± 2,000). Numbers of CD19 copies per cell were weakly correlated with the degree of maximum specific lysis achieved for these cell lines (Table 2) with the exception of Nalm-6 cells. Nalm-6 cells carried intermediate numbers of CD19 copies per cell but responded poorly to lysis mediated by the triplebody plus T cells. Finally, no statistically significant difference between the degree of maximum lysis of these cell lines reached by T cells in combination with either the triplebody 19-3-19 or the BiTE 19-3 was observed (p-values > 0.05; Table 2). Thus, both agents mediated comparable maximum lysis of different types of malignant B-lymphoid cells.

Triplebody 19-3-19 induces serial tumor cell lysis.

Cytolytic T cells alone and T cells recruited by Blinatumomab™ are capable of serial target cell lysis.[19] This is a valuable property for therapeutic efficacy, and therefore we sought to determine, whether T cells recruited by 19-3-19 were also capable of serial lysis. Redirected lysis experiments were performed for an extended reaction period of 15 hrs with a constant saturating concentration of 19-3-19 (1 nM), constant numbers of target cells, but decreasing effector-to-target cell ratios over the range from 10 : 1 to 1 : 10 (Fig. 4C). Even at an effector : target cell ratio of 1 : 10, 69 ± 13 % of the CD19-positive target cells were lysed, which provides clear evidence for serial lysis by T cells mediated by the triplebody.

Activation of resting T cells via synapse-formation mediated by 19-3-19.

Under physiological equilibrium conditions T cells in human blood are not activated unless an immune response is raised to a pathogen. Consequently, a therapeutic agent based on T cell-engagement may also require the activation of resting T cells to develop maximum efficacy. The BiTE Blinatumomab™ has already been shown to cause the activation of memory T cells, which (differing from naive T cells) do not require a second activation signal, and to trigger their proliferation. [20-22] To investigate whether triplebody 19-3-19 is capable of activating resting T cells when it connects the target and effector cell via the CD3ε-specific scFv domain, a long-term (72 hr) RDL assay was performed using non-stimulated PBMCs from healthy unrelated donors as a source of effector cells and SEM cells as targets at an E : T ratio of 10 : 1 (PBMCs : targets).

The population of PBMCs from healthy donors includes both CD19- and CD3-positive cells and therefore, the frequencies of these subsets within the PBMC populations were measured for each donor prior to their use in RDL assays. For the panel of donors tested, the CD19-positive subset ranged from 0.8 to 12.6 % and the T cell subset from 69.3 to 74.5 % of all PBMCs, respectively.

At the start of these experiments (time t_0) the CD19-positive cellular subset accounted for 11.6 to 19.6 % of all cells (PBMCs plus target SEM cells) in the reaction

Table 2. Maximum lysis and EC50 values of 19-3 bispecific scFv and triplebody 19-3-19 for different malignant B-lymphoid cell lines.

Cell Line		Maximum Specific Lysis [%]			EC50 [pM] (95% CI [pM])			n
		19-3	19-3-19	p-value	19-3	19-3-19	p-value	
pro-B ALL	**SEM**	88.5 ± 12	89.8 ± 9	0.33	4.5 (2 - 10)	5.5 (3 - 9)	0.43	4
	Nalm-6	31.9 ± 12	29.5 ± 11	0.08	12.7 (5 - 30)	22.3 (16 - 31)	0.21	4
Burkitt lymphoma	**Raji**	49.6 ± 16	54.7 ± 12	0.1	1.8 (0.5 - 7)	47.4 (11 - 201)	0.053	4
	Namalwa	44.6 ± 8	41.3 ± 7	0.12	6.2 (32 - 12)	19.9 (9 - 43)	0.071	4
plasma cell leukemia	**ARH77**	37.0 ± 14	39.0 ± 8	0.34	5.6 (0.3 - 95)	189.6 (54 - 664)	0.003	4

mixture. The decreasing fraction of CD19-positive cells, the number of memory T cells ($CD3^+$ $CD45RO^+$), the expression levels of the early T cell activation marker CD69 (trans-membrane C-type lectin) and of the late activation marker CD25 (α-subunit of the IL-2 receptor) on CD3-positive cells were then assessed every 24 hrs (Fig. 5).

T cell activation was induced in all donor samples tested, but with extensive inter-donor variability (data not shown). The T cell activation profile from one particular 28-yr old male donor is shown in Fig. 5. After 24 hrs 92.5 % (values ranging from 86.0 to 99.4 % lysis for different donors) of CD19-positive target cells were depleted (Fig. 5A). Maximum depletion of targeted cancer cells was generally achieved after 48 hrs (94.2 to 99.6 % lysis). The control triplebody Her2-3-Her2 did not induce T cell activation as determined by activation marker expression (Fig. 5B) and Interferon-γ release (data not shown).

In all donor samples the addition of 19-3-19 or PHA/IL-2 (positive control) to the reaction mixture caused a strong increase of the early activation marker CD69 on the surface of the CD3-positive cells (Fig. 5B, red) within the first 24 hrs. At later time points the CD69 levels dropped progressively for the rest of the time course. Surface expression of CD25 was also induced, but less intensely and slower than CD69 and also varied greatly among the different donor samples. CD25 expression levels, induced by the triplebody, peaked between 24 to 48 hrs and remained almost constant for the later time points (Figure 5B, black). In contrast, addition of the Her2-3-Her2 control triplebody caused no changes in CD69 or CD25 expression in the CD3-positive T cells. Addition of the triplebody 19-3-19 alone to the effector cells in the absence of CD19-positive target cells did not have any effect on the T cell population (data not shown).

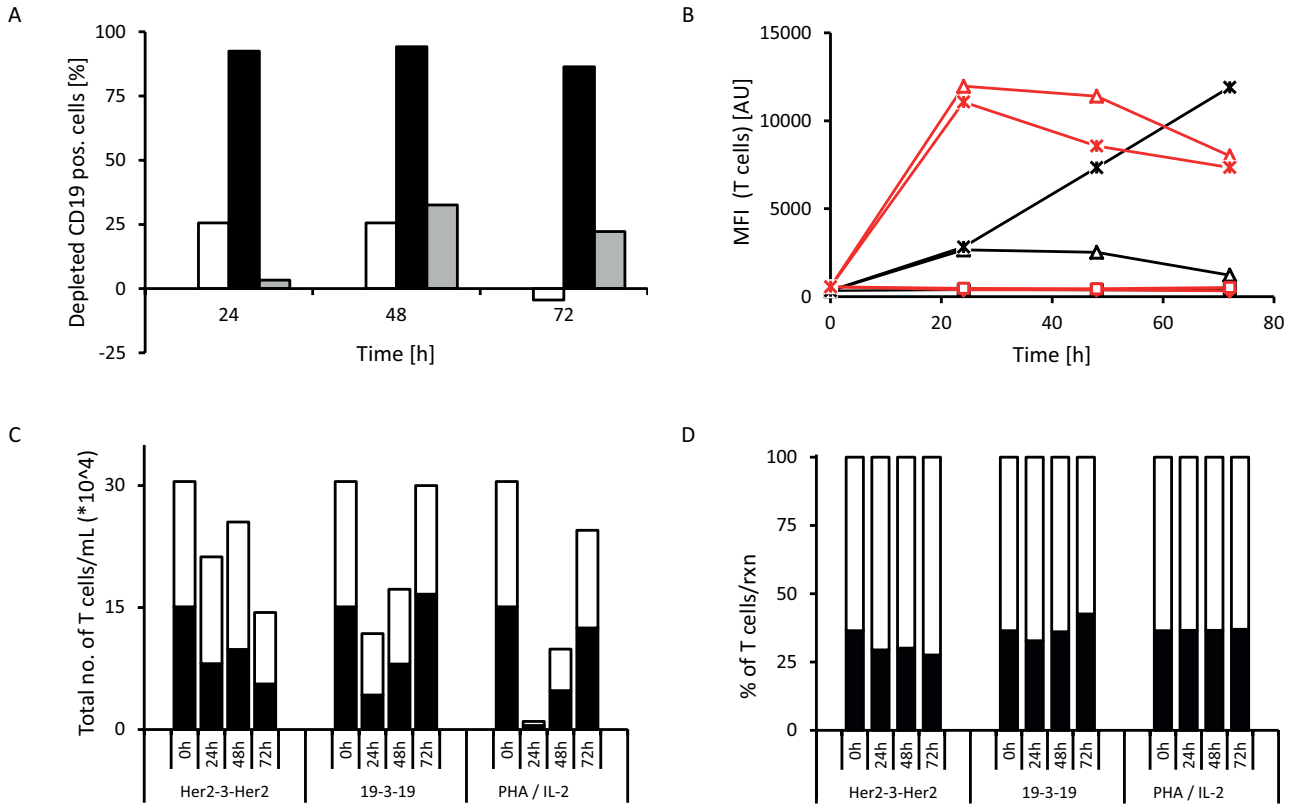

Figure 5: Example of T cell activation induced by triplebody 19-3-19. Long-term (72 hrs) redirected lysis assay with an E : T ratio of 10 : 1 non-stimulated PBMCs : SEM target cells and 1 nM triplebody or 2 % PHA/100 U/mL IL-2 (pos. control) were performed and the expression of activation markers by the effector T cells was assessed at 0, 24, 48 and 72 hrs (n=4). Representative data from one 28-yr old, healthy male donor are shown. The CD3-positive cells comprised 70.4 % of the donor's PBMC fraction and the CD19-positive cells of the donor comprised 4.5 % of his PBMCs. At time t_0 the overall content of CD19-positive cells in the reaction mixture (PBMCs + SEMs) was 14.6 %. **(A)** Depletion of CD19-positive target cells over time (white bars = triplebody Her2-3-Her2; black bars = triplebody 19-3-19; grey bars = 2 % PHA/100 U/mL IL-2). **(B)** Time course of expression of early T cell activation marker CD69 (red) and late activation marker CD25 (black) on the cell surface. The increase in activation marker expression coincided with elevated IFN-γ concentrations in the supernatant (data not shown). Diamonds: no treatment; squares: treatment with triplebody Her2-3-Her2; triangles: treated with triplebody 19-3-19; crosses: treated with 2 % PHA/100 U/mL of IL-2. **(C)** Absolute number of T cells ($CD3^+$ cells) and memory T cells ($CD3^+$ $CD45RO^+$, dark area) in the reaction mixture. **(D)** Fraction of memory T cells ($CD3^+$ $CD45RO^+$, dark area) in the total CD3-positive cellular compartment, which was set to 100 %.

Therefore, the triplebody only caused activation of the effector T cells, when it physically connected the effector and the target cells in an antigen-specific manner and engaged them to build a productive synapse.

In the redirected lysis (RDL) experiments with triplebody 19-3-19 or PHA/IL-2 the overall numbers of living T cells dropped during the first one to two days, but rose again and reached the numbers present in the starting population after 72 hrs (shown for the 28-yr old male donor sample in Fig. 5C). The subset of the CD3-positive population defined as memory T cells ($CD3^+$ $CD45RO^+$) also followed the drop and increase over time (Fig. 5D). We conclude that the T cell-recruiting triplebody can engage and activate memory T cells and induce their proliferation.

Triplebody 19-3-19 mediates efficient lysis of CD19-positive malignant cells in primary patient samples.

To determine the effect of an *ex vivo* treatment of patient cells with triplebody 19-3-19 plus effector cells, primary patient samples were used as malignant targets. PBMC fractions from five patients with different types of B cell malignancies were isolated by density gradient centrifugation and then employed as targets in our Calcein release RDL assays. The first patient suffered from an unusual case of tri-phenotypic acute leukemia (expressing B- and T-lymphoid plus myeloid lineage markers) and donated blood at diagnosis. Whole blood samples were also collected at diagnosis from an immunocytoma patient and two B-CLL patients. Finally, a blood sample from a B-CLL patient, who had relapsed 4 years after a complete remission and who had received 6 courses of combination therapy using MabThera® plus fludarabine and cyclophosphamide, was collected. This patient still displayed low expression of approximately 1,800 copies/cell of CD20 on its surface (Table 3, bottom). Patient characteristics are summarized in table 3.

Dose-responses for each patient sample were determined, using either our 19-3 BiTE, the triplebody 19-3-19, or the therapeutic CD20 antibody MabThera® and were assessed with standard 3 hr Calcein release-assays using allogeneic, *ex vivo* expanded MNC effector

Table 3. Synopsis of patient data. Patient characteristics (top), target and effector cell content (center) and specific antibody binding capacity for CD3, CD19, CD20 and CD33 of malignant cells in the peripheral blood as determined with the QIFIKIT (Dako) (bottom).

		Patient 1 (green)	Patient 2 (red)	Patient 3 (blue)	Patient 4 (yellow)	Patient 5 (purple)
Gender		Male	Male	Male	Female	Male
Age		19 years	86 years	78 years	67 years	52 years
Diagnosis		Mixed phenotype acute leukemia (MPAL (NOS))	CD19-positive NHL with leukemic progression	B-CLL	Relapsed B-CLL	B-CLL
Blast titer		93.4 % blasts in BM at diagnosis	58 % of lymphocytes in the PB are CD19-positive	29,000 B-CLL cells/µL	65 % lymphocytes in the PB (9 % atypical)	42 % lymphocytes in the PB
Case history		newly diagnosed	newly diagnosed	newly diagnosed	4 years prior: 6x MabThera® plus fludarabine and cyclophosphamide > CR	newly diagnosed
% CD19+ in PBMCs		94.8	21	89.8	68.8	73.2
% CD3+ in PBMCs		0.8	56.1	6.8	16.6	8.6
Specific antibody binding capacity (SABC) of tumour cells in the peripheral blood	CD3	211	n.d.	n.d.	n.d.	n.d.
	CD19	8,400 ± 2,800	14,600 ± 7,700	9,600 ± 500	6,500 ± 1,700	7,600 ± 1,900
	CD20	0	19,400 ± 2,200	4,000 ± 100	1,800 ± 300	3,900 ± 1,200
	CD33	317	n.d.	n.d.	n.d.	n.d.

cells (expanded in the presence of IL-2) from an unrelated healthy donor. The E : T ratio (MNCs : targets) was 10 : 1, which corresponded to an actual T cell : target ratio of 5 : 1 and an NK cell : target ratio of 2 : 1.

The maximum cytolytic response of the three CD20-positive B-CLL patient samples (patients 3, 4 and 5) to both CD19-targeting antibody-derivatives was more pronounced than the response to the standard-of-care reagent MabThera® (Fig. 6A). The malignant cells of these three patients had higher surface densities of CD19 than of CD20 (Table 3, bottom), which paralleled the higher maximum specific lysis mediated by 19-3 and 19-3-19 than by MabThera®. The sample from the immunocytoma patient (patient 2) responded more strongly to treatment with MabThera® than to treatment with either 19-3-19 or 19-3 (Fig. 6A). This coincides with a greater surface density of CD20 than CD19 on the malignant target cells from this patient (Table 3, bottom). The mixed phenotype acute leukemia (not otherwise specified) (MPAL(NOS)) patient sample (patient 1)

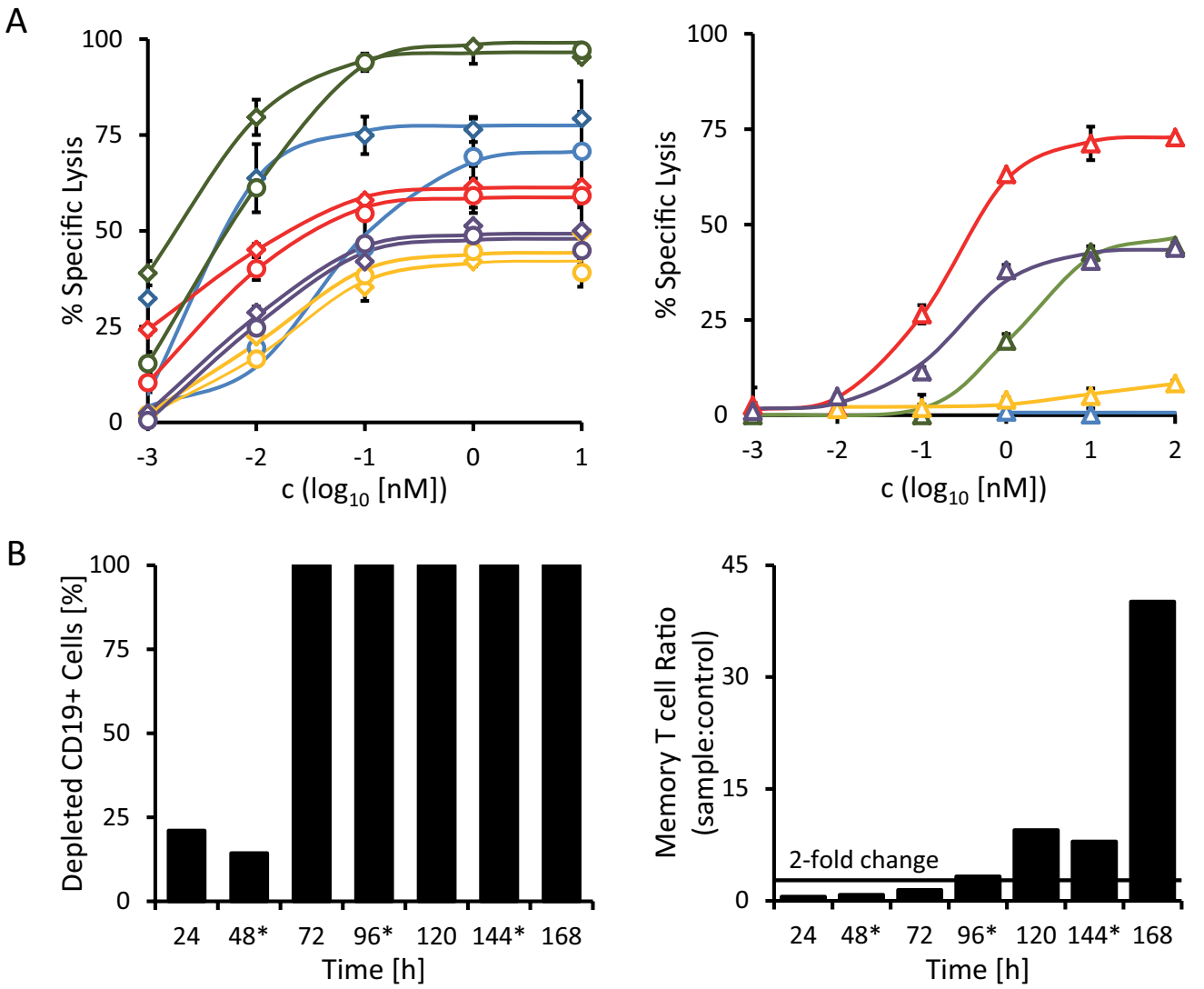

Figure 6: Redirected lysis of CD19-positive malignant cells from primary patient material mediated by triplebody 19-3-19. The ability of triplebody 19-3-19 to mediate the lysis of malignant cells isolated from the peripheral blood of patients with different B cell malignancies (see table 3) via allogeneic and autologous effector T cells was assessed in redirected lysis assays. Samples were assayed in triplicate. Error bars indicate intra-sample variation. **(A)** Specific lysis of malignant cells via allogeneic pre-stimulated effector T cells mediated at different concentrations of the 19-3 BiTE (diamonds) and triplebody 19-3-19 (circles) or the therapeutic antibody MabThera® (triangles) in a 3 hr assay, respectively. Patient 1 (MPAL (NOS)): blue; patient 2 (NHL): red; patient 3 (B-CLL): green; patient 4 (relapsed B-CLL): yellow; and patient 5 (B-CLL): purple. **(B)** Triplebody 19-3-19-induced depletion of CD19-positive cells by autologous effector T cells and expansion of memory T cells ($CD3^+$ $CD45RO^+$) in the PBMC fraction isolated from patient 2 (NHL) in a 7 d assay. 1 nM of fresh Triplebody 19-3-19 was added every 48 hrs (indicated by asterisks). A similar assay was performed with samples from patients 1 (MPAL (NOS)) and 3 (B-CLL) (data not shown), but no response was observed, possibly due to the relatively short observation time, T cell attenuation or too low initial numbers of effector T cells.

was CD20-negative and consequently failed to display any response to treatment with MabThera®, but it did respond to treatment with both the 19-3 and 19-3-19 reagents (Fig. 6A). The response profile of this MPAL patient is more typical for patients with acute B-lymphoblastic leukemia often found in children and young adults, where the malignant blasts have a phenotype resembling early stages of B cell differentiation. Blasts from B cell precursor leukemias (BCP-ALLs) of infants, children and young adults often fail to express CD20, and thus these patients are more likely to benefit from treatment with a CD19-directed rather than a CD20-specific agent.[41, 42]

Triplebody 19-3-19 and our 19-3 BiTE reagent were effective at far lower concentrations than MabThera®. Although inter-patient variation was substantial, the EC50-values for 19-3 and 19-3-19 generally were 30- to 925-fold lower than those determined for MabThera® for the panel of patient samples analyzed here (Table 4). No statistically significant differences between the BiTE reagent and the triplebody were observed with regard to the degree of maximum lysis and the EC50 values. Interestingly, maximum lysis achieved with the triplebody was marginally lower than the extent reached with 19-3. Maximum specific lysis and EC50 values are summarized in Table 4.

Triplebody 19-3-19 induces expansion of memory T cells in a sample from an NHL patient.

In patients with malignant hematopoietic diseases healthy immune effector cells are often displaced and suppressed. However, sufficient numbers of functioning effector cells are needed for a successful therapy with an agent critically relying on the recruitment of cytolytic effectors. By inducing the proliferation of memory T cells, the BiTE® agents Blinatumomab™ and AMG330 have caused an amplification of available effector cells.[20-22, 26] As the triplebody 19-3-19 also employs an OKT3-derived scFv-domain to trigger its effector cells, we investigated whether exposure to this triplebody was also capable of stimulating the proliferation of memory T cells in a patient sample. To this effect, the triplebody was added in a 1 nM saturating concentration to PBMCs isolated from an immunocytoma patient (patient 2) every 48 hrs for 7 days. At timepoint t_0, the sample contained 21 % CD19-positive cells and 56.1 % CD3-positive cells (Table 3). Approximately half of the CD3-positive cells (53.3 %) expressed the memory T cell marker CD45RO on their surface. In this particular patient sample, the T cell population displayed the same initial drop in numbers during the first 24 hrs that was also observed during the activation of T cells in the healthy donor samples reported above (Fig. 5). However, after 48 hrs, the T cells started to expand and the numbers of memory T cells had more than doubled after 96 hrs in comparison to the control reaction without added triplebody. On day 7, the numbers of memory T cells were increased by more than 42-fold in the triplebody-treated sample (Fig. 6B, right). The overall T cell population expanded 7-fold during the 7 d period of observation despite the absence of detectable numbers of CD19-positive target cells from 72 hrs on (Fig. 6B, left).

DISCUSSION

In the present study, the prototype T cell-recruiting triplebody 19-3-19 was constructed and shown to engage pre-activated as well as non-stimulated T cells efficiently for the redirected and serial lysis of malignant CD19-positive target cells. Moreover, 19-3-19 led to the activation and induced the proliferation of allogeneic and autologous effector T cells. The key new result of the present study is the observation that fusion proteins in the molecular format of single chain triplebodies are also suited for the engagement of cytolytic T cells (CTLs) via CD3ε to eliminate antigen-positive cancer cell targets.

The concept of an "individualized therapy" usually refers to the selection of a specific therapeutic target based on a patient's individual genotypic and phenotypic characteristics, as determined by molecular diagnostics. However, another important aspect of personalized medicine, especially when planning to exploit or boost the patient's own immune system, is the size and activity of a suitable population of immune effector cells available at the cancer site. As a patient's immune status varies with the type and stage of the disease, different effector cell populations may be best suited in different situations. NK cells, for example, recover more rapidly than T and B lymphocytes after chemotherapy, and they require little activation time. They are present in the human circulation in a pre-activated state and are instantaneously ready for antibody-mediated cytolysis. Thus NK cells may be a suitable choice of effector cells to combat minimal residual disease after an induction

Table 4. Synopsis of maximum lysis and EC50 values for patient samples.

	Maximum Specific Lysis [%]			EC50 [pM] (95% CI [pM])		
	19-3	19-3-19	MabThera®	19-3	19-3-19	MabThera®
Patient 1	79.3	70.8	n.d.	1.2 (0.3 - 5)	48.1 (9 - 270)	n.d.
Patient 2	61.5	59.2	72.8	6.1 (4 - 10)	4.8 (3 - 9)	185.7 (135 - 255)
Patient 3	98	100	44.5	2.8 (1 - 8)	6.4 (4 - 11)	1,300 (426 – 4,224)
Patient 4	49.4	44.7	8.4	10.7 (1 - 177)	13.9 (2 - 84)	9,900 (0.1 - 568 nM)
Patient 5	51.3	48.8	43.9	6.7 (1 - 36)	7.1 (2 - 29)	247.5 (89 - 688)

chemotherapy.[3] $CD8^+$ T cells, however, are frequently present in cancer tissues in abundance, have a greater intrinsic cytotoxic potential than NK cells, and are capable of more prolonged serial lysis.[43, 44] CTLs are therefore a particularly desirable class of cytolytic effectors for cancer therapy.

Ideally, for a fully individualized approach and to avoid successful immune evasion by the tumor cells, both the therapeutic target and the effector population should be chosen corresponding to the patient's individual disease properties. The molecular format of triplebodies may help to reach this goal, because triplebodies were found suited in this study to recruit not only NK cells but also T cells as cytolytic effectors.

Both the protein 19-3 in the BiTE-format and the newly constructed triplebody 19-3-19 were produced with similar expression yields and had similar cytolytic potential. Triplebody 19-3-19 led to efficient *in vitro* lysis of CD19-positive targets from both established malignant B-lymphoid cell lines and primary patient material at picomolar concentrations. Cell surface density of target antigens was a major, but not the only important determinant of cytolytic efficacy of the agent. A CD19-positive cell line with high antigen surface expression (SEM) showed a greater degree of maximum lysis in a standard 3 hr reaction interval in our redirected lysis experiments than cell lines with lower surface expression of the target antigen (Raji, Namalwa and ARH77).

The difference between maximum lysis of SEM cells (89.8 %) and Raji cells (54.7 %) was significant, even though CD19 copy numbers per cell differed by only 6,500 copies between these two cell lines. However, the determination of antigen copy numbers per cell by calibrated cytofluorimetry does not take the actual cell size into account and therefore produces copy numbers per cell, but not antigen density values. We have observed that Raji cells (Burkitt's lymphoma-derived) are much larger than SEM cells (pro-B ALL-derived), and therefore, the antigen density per surface unit may be lower for Raji cells than for SEMs. However, this argumentation does not fully explain the low specific lysis achieved for Nalm-6 cells. Nalm-6 cells have a relatively small cell volume that is comparable to SEMs and carried 17,500 copies of CD19/cell, but resulted in only 31.9 and 29.5 % specific lysis mediated by 19-3 and 19-3-19, respectively, which were the lowest values observed. Additional parameters other than antigen surface density appear to play important roles in determining the sensitivity of a target cell to T cell-mediated lysis, probably linked to the specific oncogenic genomic and epigenetic alterations of the particular target and their tumor-type specific susceptibilities to apoptosis.

The triplebody 19-3-19 induced a similar T cell response profile as Blinatumomab™. Activation of the T cell by this triplebody only occurred when the T cells were connected to the target cells by the triplebody in an antigen-specific manner, but was independent of specific MHC : peptide recognition. Furthermore, memory T cells rather than naïve T cells were engaged and induced to proliferate. Whether the triplebody also affects the activation state of naïve T cells, i.e. whether naïve T cells remain resting or are forced into anergy due to the interaction of 19-3-19 with CD3 in the absence of any "second signal" (co-stimulus), remains to be determined.

Interestingly, the CD3ε-specific scFv of 19-3-19 bound less efficiently to primary T cells than when this domain was embedded in our 19-3 BiTE protein or the Her2-3-Her2 control protein, when each was used at saturating concentrations. Together with the lower affinity of 19-3-19 for CD3ε in comparison to 19-3, these observations indicate that CD3ε on the surface of the T cells is less available for binding by the triplebody 19-3-19 than by triplebody Her2-3-Her2 and by the 19-3 protein. We cannot yet offer a definitive explanation for this observation, but the precise conformation of the CD3ε-specific scFv is likely different, when it is flanked at both sides by CD19-specific scFvs or Her2-specific scFvs, or only at one side by a single CD19-specific scFv. One possibility may be partial sterical hindrance of the CD3ε-specific scFv by the two distal CD19 scFvs, which may impact affinity.

A sensitivity of CD3ε-specific scFvs to their precise molecular surroundings has been previously reported by other authors. In the hands of M. Arndt and colleagues the CD3ε-specific scFv required optimization for every different BiTE construct, which led to the development of a new modular targeting system by these authors.[13] Further development of previously reported trispecific T cell-engaging antibody-derivatives, which employed an N-terminal tumor-associated antigen (TAA)-specific scFv, a central CD3ε-specific scFv or V_H domain, and a C-terminal CD28-specific V_H domain in one polypeptide chain,[45, 46] was discontinued. The question, whether the CD3ε-specific scFv domain in the central position of these fusion proteins was stable and functional, remained unanswered.

The value of triplebodies recruiting effector T cells can most likely be further increased by taking advantage of the unique capability of triplebodies for "dual-targeting". Dual-targeting has been reported to enhance the selectivity of triplebodies recruiting NK cells as cytolytic effectors,[38] but it needs to be determined whether a preferential lysis of antigen double-positive cells over simultaneously present antigen single-positive cells can also be achieved by dual-targeting triplebodies, which recruit T cells as effectors. This may not be a foregone conclusion, because results recently reported by Harms and colleagues about the cross-arm binding efficiencies of monoclonal antibodies and different multispecific antibody-derived formats[47] suggest, that not every target combination leads to an improved antibody-activity in spite of the higher combined target antigen density. This may be explained in part by the "protein island"-model of the cell membrane, which is currently one of the

most potent models for the surface architecture of human leukocytes.[48, 49] This model proposes that the surface of human leukocytes is composed of "protein islands" of approximately 200-300 nm in diameter. Particular groups of proteins are segregated in separate islands. They are anchored to the cytoskeleton by protein contacts, and the lipid composition within the islands is different from the areas outside of the islands. The islands have a degree of freedom for lateral movement on the surface, and specific events can cause the relocation of one island into the immediate vicinity of another to facilitate protein interaction. This has been reported for example for the T cell antigen receptor (TCR) and its co-factor Lat.[49] On the surface of resting T cells these two proteins were found in different protein islands, which concatenated upon T cell activation. If we assume this model to be valid, and if two antigens, which are targeted by a multispecific antibody-derivative such as our triplebody, reside in separate protein islands, and if the intrinsic cross-arm binding property of the employed molecule is unsuited for simultaneous binding, and if none of the two antigens can relocate to the other island, then there is no benefit in multispecificity. However, if two different antigens can be bound simultaneously on the same cell, then cancer cell selectivity may be possible and several immunotherapeutic mechanisms of action, such as growth factor receptor inhibition, neutralization of immune evasion mechanisms, or induction of apoptosis and ADCC (or RDL), can potentially be combined.

In this proof-of-principle study, we have demonstrated that triplebodies which are bivalent, but monospecific for the target antigen, can recruit one of the most desirable effector cell populations, the cytolytic T cells, for cancer cell lysis. It remains to be investigated in future studies, whether it is possible to further enhance the value of T cell-recruiting triplebodies as potential therapeutic agents by endowing them with the dual-targeting option, based on the rational choice of a pair of target antigens on the cancer cell, which is more abundant and/or more accessible on the surface of the cancer cell than on the corresponding healthy cells. It also remains to be seen, whether the triplebodies have the improved plasma half-life relative to the BiTE agents in humans, which has been demonstrated for them in mice. However, we anticipate that both of these goals are within reach, and therefore, that triplebodies have significant therapeutic potential for the treatment of cancer and other diseases.

METHODS

Bacterial strains and cell lines

DNA plasmids for the eukaryotic expression of antibody-derived fusion proteins were amplified in *Escherichia coli* strain XL-1. The mammalian production cell line 293F was purchased from Life Technologies™ and cultured in serum-free FreeStyle™ medium (Life Technologies™). The pro B-ALL cell line SEM has been continuously propagated in our laboratory since its establishment in 1995,[50] the CD19-positive pre-B cell line Nalm-6, the Burkitt lymphoma cell lines Raji and Namalwa and the plasma cell leukemia cell line ARH77 were purchased from the Leibniz Institute DSMZ (German Collection of Microorganisms and Cell Cultures).[51] All cell lines were cultured in RPMI 1640, GlutaMAX™ supplemented with 10 % fetal calf serum (FCS) and Penicillin (100 U/mL)/Streptomycin (100 µg/mL) (Gibco®, Life Technologies™). The medium for the Namalwa cell line was additionally supplemented with 1 mM sodium pyruvate.

Construction, expression and purification of triplebody 19-3-19 and control proteins

All antibody derivatives employed in this study were cloned into the mammalian expression vector pSecTag2-HygroC (Life Technologies™). The scFv building blocks for the bispecific scFv proteins 19-3 and the Her2-3, and for the triplebodies 19-3-19 and Her2-3-Her2 were developed by our team at the University of Erlangen (CD19-specific scFv) or provided by M. Peipp (University of Schleswig-Holstein, Kiel; CD3ε- and Her2-specific scFvs), respectively. The sequences coding for the disulfide-stabilized CD16-specific scFv in the gene encoding the triplebody 19-16-19 (derived from Kellner et al. 2008, but with humanized scFv sequences) were replaced with the murine CD3ε-specific scFv sequence amplified by polymerase chain reaction (PCR) from the sequence coding for Her2-3 by standard molecular cloning methods. Similarly, the sequences coding for the Her2-specific scFv in the Her2-3 construct were replaced with the sequences coding for the humanized CD19-specific scFv to produce the coding sequences for 19-3. The sequences coding for the CD19-specific scFvs in the coding construct for triplebody 19-3-19 were replaced with coding sequences for the Her2-specific scFv amplified by PCR from the construct coding for Her2-3 to produce the coding sequences for triplebody Her2-3-Her2. (Details of the construction scheme are listed in Supplementary Table S1). 293F cells were transfected with the respective expression vectors using the *Trans*IT®-LT1 transfection reagent (Mirus® Bio LLC) following manufacturer's instructions. Antibody-derived fusion proteins were purified by affinity chromatography from cell culture supernatants that were harvested 7 days post transfection. A Nickel-nitrilo triacetic acid (Ni-NTA) matrix was used. Protein concentrations were determined by measurement of their absorbance at 280 nm. Protein identity was confirmed and purity assessed by SDS-polyacrylamide gel electrophoresis and Western Blotting

(N-terminal integrity confirmed with anti-Strep- and C-terminal integrity confirmed with anti-His antibodies).

Preparation of peripheral blood mononuclear cells (PBMCs) from whole blood

10 - 60 mL of peripheral blood was drawn into EDTA monovettes (Sarstedt) from healthy unrelated donors and patients suffering from different types of B cell neoplasias, after informed written consent was obtained. This study is in accordance with the declaration of Helsinki and was approved by the ethics committee of the Medical Faculty of the Ludwig-Maximilians-Universität München (project no. 173-13). PBMCs were separated by density gradient centrifugation using Lymphoprep™ (Axis Shield PoC) medium, and residual erythrocytes were lysed by incubation with Ery-Lysis-Buffer (University Pharmacy, Munich) for 5 min. To generate effector cells for standard 3 hr cytotoxicity assays, an *ex vivo* expansion and stimulation of mononuclear cells (MNCs) was carried out for 20 d in the presence of IL-2 as described.[52] For T cell activation assays freshly isolated, non-stimulated PBMCs were used.

Enrichment of a pan T cell population by preparative magnetic cell separation

Pan T cells were isolated from *ex vivo* expanded MNCs or freshly isolated, non-stimulated PBMCs by negative selection using a commercial Pan T cell isolation kit (Miltenyi Biotec, Bergisch Gladbach, Germany) according to the manufacturer's instructions. The enriched T cells are referred to as "untouched cells" because they have no residual antibody bound to their surface and have been maintained under mild buffer/medium conditions. T cell purity was assessed by flow cytometry and the purified T cells were used for binding and T cell activation studies.

Flow cytometry

An Accuri C6 flow cytometer (BD Biosciences, Heidelberg, Germany) was used for flow cytometric analysis of the binding behavior of the antibody-derived fusion proteins and for the differential analysis of leukocyte/tumor cell subpopulations. In the Accuri C6 instrument the laser and optical alignments have been pre-set and locked. In this instrument the detector voltages are not adjustable as opposed to other machines. Equilibrium binding constants (affinity constants, K_D) for CD19 and CD3 were determined by calibrated cytofluorimetry. [53] The maximum mean fluorescence value was set to 100 % and all data points were normalized accordingly. Experiments were repeated 4 to 7 times and K_D values were calculated with the GraphPad Prism Software (GraphPad Software Inc., San Diego, CA, USA) using a nonlinear regression curve fit. Cell-bound antibody-derivatives were detected using a Penta-His™ AlexaFluor488-conjugated antibody (QIAGEN, Hilden, Germany). The CD3-, CD4-, CD8-, CD19-, CD25-, CD33-, CD45RA-, CD45RO-, CD56- and CD69-specific monoclonal antibodies (mAbs) used for the analysis of lymphocyte and myeloid cell content and for the detailed analysis of relevant T cell subpopulations as well as the respective isotype control mAbs were from Immunotech (Marseille, France). Specific antibody binding capacity of cells from established B-ALL lines and primary leukemia blasts for CD3 (unconjugated mAb from ebioscience, Frankfurt, Germany), CD19 (unconjugated mAb from DAKO, Hamburg, Germany), and CD33 (unconjugated mAbs from BD Pharmingen, Heidelberg, Germany) was determined with a commercial calibrated cytofluorimetric assay (QIFIKIT®, DAKO, Hamburg, Germany) as described.[54, 55]

Cytotoxicity assay

To quantitate cell-mediated cytolysis (referred to as redirected lysis, RDL) induced by the BiTE or triplebody proteins, target cells were pre-labelled with Calcein AM (Life Technologies) and mixed with effector cells in RPMI 1640 GlutaMAX medium supplemented with 10 % fetal calf serum at an E : T ratio of 10 : 1 unless otherwise stated. Either MNCs expanded *ex vivo* for 20 days and pre-stimulated with anti-CD3 mAb OKT3 and IL-2,[11, 56] or untouched T cells isolated via magnetic separation, were used as effector cells. After addition of different antibody-derived proteins to 200 µL reaction volume in round-bottom 96-well plates, the reactions were incubated at 37 °C with 5 % CO_2. Calcein release was determined by measuring the fluorescence intensity (relative light units, RLU) in the supernatant with a Berthold Mithras plate reader (Berthold technologies, Bad Wildbad, Germany). Maximum lysis was achieved by addition of 50 µL of a solution containing 10 % Triton X-100 in RPMI 1640 GlutaMAX medium supplemented with 10 % fetal calf serum and 1 % Penicillin/Streptomycin. Specific lysis was calculated as follows:

$$\%\,\text{specific Lysis} = 100*[\text{RLU (sample)} - \text{RLU (background)}] / [\text{RLU (maximal lysis)} - \text{RLU (background)}]$$

T cell activation assay

Activation of resting T cells was determined by measurement of IFN-γ release and the expression of the early activation surface marker CD69 and the late activation marker CD25, the alpha-subunit of the high-affinity receptor for interleukin-2 (IL-2R). Freshly isolated PBMCs from healthy unrelated donors remained either untouched, were depleted of CD19-positive cells by magnetic separation, or were mixed with SEM cells at an E : T ratio of 10 : 1. Triplebody was added at a

concentration of 1 nM to a 280 µL reaction mixture containing 1,4*10^5 PBMCs with or without 1.4*10^4 SEMs in RPMI 1640 + GlutaMAX™ medium with 10 % FCS and 1 % Pen/Strep (Gibco®, Life Technologies™). After incubation for 0, 24, 48 and 72 hrs the total number of living cells in the reaction mixture was determined with a hemocytometer (Marienfeld Superior, Lauda-Königshofen, Germany) using Trypan Blue staining (Gibco®, Life Technologies™). The surviving cells were stained for CD3/CD19, CD3/CD25, CD3/CD69 and CD3/CD45RO and the fraction of the relevant cell populations (CD19-positive targets, CD3-positive effectors, activated CD3-positive effectors and CD3 CD45RO double-positive memory T cells) was assessed by flow cytometry. The fraction of depleted B cells, i.e. the differential removed by the depletion, was computed with the help of the following formula:

$$\%\,\text{depleted B cells} = 100\% * (CD19^+ \text{ cells control} - CD19^+ \text{ cells sample}) / (CD19^+ \text{ cells control})$$

Measurement of IFN-γ release into peripheral blood samples

Induction of cytokine release by immune effector cells due to the presence of the triplebody or BiTE control molecule was determined in whole blood assays. Triplebodies 19-3-19 or Her2-3-Her2 or the protein 19-3 were added to 200 µL of peripheral blood in a round-bottom Nunc™ 96-Microwell plate (ThermoFisher Scientific, MA, USA) at different concentrations and were incubated for 6 hrs at 37 °C with 5 % CO_2. The samples were then diluted 1 : 1 with PBS and concentrations of IFN-γ were determined using commercial Ready-Set-Go ELISA kits (ebioscience, Frankfurt, Germany). Depending on sample availability, samples were run in duplicates or triplicates.

Statistical analysis

All statistical analyses were performed by GraphPad Prism Software (GraphPad Software Inc., San Diego, CA, USA) using Student's t-test for the determination of significance, defined by $p < 0.05$.

ABBREVIATIONS

ADCC: antibody-dependent cellular cytotoxicity, ALL: acute lymphoblastic leukemia, B-CLL: chronic B cell leukemia, BiTE: bispecific T cell engager, bsscFv: bispecific single chain Fv, CD: cluster of differentiation, CI: confidence interval, CR: complete remission, EC50: concentration at which half maximal effect is achieved, ELISA: enzyme-linked immunosorbent assay, FACS: fluorescence-assisted cell sorting, IFN-□: Interferon gamma, IL-2: Interleukin-2, MFI: Mean Fluorescence Intensity, MNC: mononuclear cells, MPAL (NOS): mixed phenotype acute leukemia (not otherwise specified); NHL: Non-Hodgkin Lymphoma, PB: peripheral blood, PBMC: peripheral blood mononuclear cells, PCR: polymerase chain reaction, PHA: Phytohemagglutinin, pI: isoelectric point, pre-B cells: □-positive, CD10 (CALLA)-positive; pro-B cells: □-negative, CD10 (CALLA)-negative, RDL: redirected lysis assay, scFv: single chain fragment variable, SEM: standard error of the mean, TAA: tumor-associated antigen, TNF□: tumor necrosis factor alpha.

Competing Interests

The authors declare that they have no competing interests.

AUTHORS' CONTRIBUTIONS

CCR carried out the experiments and statistical analyses, participated in the project design and coordination and drafted the manuscript. CBS performed the DNA sequence optimization, helped in the establishment of a protein production and purification strategy and revised the manuscript. TAB, SK and IAS participated in the design of the project and revised the manuscript. GHF conceived of the study, participated in its design and helped to draft the manuscript. KPH and FSO participated in project design and coordination. All authors read and approved the final manuscript.

ACKNOWLEDGEMENTS

We thank Dr. Matthias Peipp for providing the pSecTag2-HygroC vector with the Her2-CD3 BiTE construct and Kerstin Lämmermann, Brigitte Schnabel, Alexandra Schele and Stefanie Nowecki for technical assistance. Guidance and scientific advice from Profs. Stefan Endres and Uwe Jacob, and Drs. Sarah Wildenhain and Nadja Fenn are gratefully acknowledged as well as fruitful scientific discussions with Nadine Moritz and Monika Herrmann. We also thank the healthy donors and patients, who provided blood samples for this study.

This study was supported by awards from the charity "Chimney Sweeps Help Children with Cancer" (Schornsteinfeger Helfen Krebskranken Kindern e.V.) to GHF, by support from the M4 excellence award to KPH, GHF and FO from the Bavarian Government, by funding from the Munich Center for Integrated Protein Science (CiPSM) to KPH and by a Ph.D. student research fellowship awarded to CCR by the German José Carreras-Leukemia Foundation (www.carreras-stiftung.de, Scholarship No. DJCLS F 13/05). SK is supported by the Graduiertenkolleg 1202 "Oligonucleotides in cell biology and therapy" funded by the Deutsche Forschungsgemeinschaft, the international doctoral program "immunotargeting of cancer" funded by the Elite

Network of Bavaria, the Melanoma Research Alliance (grant number N269626) and the Deutsche Krebshilfe.

REFERENCES

1. Carter PJ. Potent antibody therapeutics by design. Nat Rev Immunol. 2006; 6(5):343–357.
2. Schubert I, Stein C and Fey GH. Dual-Targeting for the Elimination of Cancer Cells with Increased Selectivity. Antibodies. 2012; 1(1):2–18.
3. Stein C, Schubert I and Fey GH. Natural Killer (NK)- and T-Cell Engaging Antibody-Derived Therapeutics. Antibodies. 2012; 1(1):88–123.
4. Schwemmlein M, Peipp M, Barbin K, Saul D, Stockmeyer B, Repp R, Birkmann J, Oduncu F, Emmerich B and Fey GH. A CD33-specific single-chain immunotoxin mediates potent apoptosis of cultured human myeloid leukaemia cells. Br J Haematol. 2006; 133(2):141–151.
5. Schwemmlein M, Stieglmaier J, Kellner C, Peipp M, Saul D, Oduncu F, Emmerich B, Stockmeyer B, Lang P, Beck JD and Fey GH. A CD19-specific single-chain immunotoxin mediates potent apoptosis of B-lineage leukemic cells. Leukemia. 2007; 21(7):1405–1412.
6. Stieglmaier J, Bremer E, Kellner C, Liebig TM, ten Cate B, Peipp M, Schulze-Koops H, Pfeiffer M, Buhring HJ, Greil J, Oduncu F, Emmerich B, Fey GH and Helfrich W. Selective induction of apoptosis in leukemic B-lymphoid cells by a CD19-specific TRAIL fusion protein. Cancer Immunol Immunother. 2008; 57(2):233–246.
7. Hoffmann P, Hofmeister R, Brischwein K, Brandl C, Crommer S, Bargou R, Itin C, Prang N and Baeuerle PA. Serial killing of tumor cells by cytotoxic T cells redirected with a CD19-/CD3-bispecific single-chain antibody construct. Int J Cancer. 2005; 115(1):98–104.
8. Loffler A, Gruen M, Wuchter C, Schriever F, Kufer P, Dreier T, Hanakam F, Baeuerle PA, Bommert K, Karawajew L, Dorken B and Bargou RC. Efficient elimination of chronic lymphocytic leukaemia B cells by autologous T cells with a bispecific anti-CD19/anti-CD3 single-chain antibody construct. Leukemia. 2003; 17(5):900–909.
9. Kellner C, Bruenke J, Stieglmaier J, Schwemmlein M, Schwenkert M, Singer H, Mentz K, Peipp M, Lang P, Oduncu F, Stockmeyer B and Fey GH. A novel CD19-directed recombinant bispecific antibody derivative with enhanced immune effector functions for human leukemic cells. J Immunother. 2008; 31(9):871–884.
10. Schubert I, Kellner C, Stein C, Kugler M, Schwenkert M, Saul D, Mentz K, Singer H, Stockmeyer B, Hillen W, Mackensen A and Fey GH. A single-chain triplebody with specificity for CD19 and CD33 mediates effective lysis of mixed lineage leukemia cells by dual targeting. MAbs. 2011; 3(1):21–30.
11. Schubert I, Kellner C, Stein C, Kugler M, Schwenkert M, Saul D, Stockmeyer B, Berens C, Oduncu FS, Mackensen A and Fey GH. A recombinant triplebody with specificity for CD19 and HLA-DR mediates preferential binding to antigen double-positive cells by dual-targeting. MAbs. 2012; 4(1):45–56.
12. Stein C, Kellner C, Kugler M, Reiff N, Mentz K, Schwenkert M, Stockmeyer B, Mackensen A and Fey GH. Novel conjugates of single-chain Fv antibody fragments specific for stem cell antigen CD123 mediate potent death of acute myeloid leukaemia cells. Br J Haematol. 2010; 148(6):879–889.
13. Arndt C, Feldmann A, von Bonin M, Cartellieri M, Ewen EM, Koristka S, Michalk I, Stamova S, Berndt N, Gocht A, Bornhauser M, Ehninger G, Schmitz M and Bachmann M. Costimulation improves the killing capability of T cells redirected to tumor cells expressing low levels of CD33: description of a novel modular targeting system. Leukemia. 2014; 28(1):59–69.
14. Thurber GM, Schmidt MM and Wittrup KD. Antibody tumor penetration: transport opposed by systemic and antigen-mediated clearance. Adv Drug Deliv Rev. 2008; 60(12):1421–1434.
15. Yokota T, Milenic DE, Whitlow M and Schlom J. Rapid tumor penetration of a single-chain Fv and comparison with other immunoglobulin forms. Cancer Res. 1992; 52(12):3402–3408.
16. McDonagh CF, Huhalov A, Harms BD, Adams S, Paragas V, Oyama S, Zhang B, Luus L, Overland R, Nguyen S, Gu J, Kohli N, Wallace M, Feldhaus MJ, Kudla AJ, Schoeberl B and et al. Antitumor activity of a novel bispecific antibody that targets the ErbB2/ErbB3 oncogenic unit and inhibits heregulin-induced activation of ErbB3. Mol Cancer Ther. 2012; 11(3):582–593.
17. Jung G, Grosse-Hovest L, Krammer PH and Rammensee HG. Target cell-restricted triggering of the CD95 (APO-1/Fas) death receptor with bispecific antibody fragments. Cancer Res. 2001; 61(5):1846–1848.
18. Hartmann F, Renner C, Jung W, Sahin U and Pfreundschuh M. Treatment of Hodgkin's disease with bispecific antibodies. Ann Oncol. 1996; 7(Suppl 4): 143–146.
19. Dreier T, Lorenczewski G, Brandl C, Hoffmann P, Syring U, Hanakam F, Kufer P, Riethmuller G, Bargou R and Baeuerle PA. Extremely potent, rapid and costimulation-independent cytotoxic T-cell response against lymphoma cells catalyzed by a single-chain bispecific antibody. Int J Cancer. 2002; 100(6):690–697.
20. Bargou R, Leo E, Zugmaier G, Klinger M, Goebeler M, Knop S, Noppeney R, Viardot A, Hess G, Schuler M, Einsele H, Brandl C, Wolf A, Kirchinger P, Klappers P, Schmidt M and et al. Tumor regression in cancer patients by very low doses of a T cell-engaging antibody. Science. 2008; 321(5891):974–977.

21. Klinger M, Brandl C, Zugmaier G, Hijazi Y, Bargou RC, Topp MS, Gokbuget N, Neumann S, Goebeler M, Viardot A, Stelljes M, Bruggemann M, Hoelzer D, Degenhard E, Nagorsen D, Baeuerle PA and et al. Immunopharmacologic response of patients with B-lineage acute lymphoblastic leukemia to continuous infusion of T cell-engaging CD19/CD3-bispecific BiTE antibody blinatumomab. Blood. 2012; 119(26):6226–6233.

22. Topp MS, Kufer P, Gokbuget N, Goebeler M, Klinger M, Neumann S, Horst HA, Raff T, Viardot A, Schmid M, Stelljes M, Schaich M, Degenhard E, Kohne-Volland R, Bruggemann M, Ottmann O and et al. Targeted therapy with the T-cell-engaging antibody blinatumomab of chemotherapy-refractory minimal residual disease in B-lineage acute lymphoblastic leukemia patients results in high response rate and prolonged leukemia-free survival. J Clin Oncol. 2011; 29(18):2493–2498.

23. Handgretinger R, Zugmaier G, Henze G, Kreyenberg H, Lang P and von Stackelberg A. Complete remission after blinatumomab-induced donor T-cell activation in three pediatric patients with post-transplant relapsed acute lymphoblastic leukemia. Leukemia. 2011; 25(1): 181–184.

24. Topp MS, Gokbuget N, Zugmaier G, Degenhard E, Goebeler ME, Klinger M, Neumann SA, Horst HA, Raff T, Viardot A, Stelljes M, Schaich M, Kohne-Volland R, Bruggemann M, Ottmann OG, Burmeister T and et al. Long-term follow-up of hematologic relapse-free survival in a phase 2 study of blinatumomab in patients with MRD in B-lineage ALL. Blood. 2012; 120(26):5185–5187.

25. Aigner M, Feulner J, Schaffer S, Kischel R, Kufer P, Schneider K, Henn A, Rattel B, Friedrich M, Baeuerle PA, Mackensen A and Krause SW. T lymphocytes can be effectively recruited for ex vivo and in vivo lysis of AML blasts by a novel CD33/CD3-bispecific BiTE antibody construct. Leukemia. 2013; 27(5):1107–1115.

26. Krupka C, Kufer P, Kischel R, Zugmaier G, Bogeholz J, Kohnke T, Lichtenegger FS, Schneider S, Metzeler KH, Fiegl M, Spiekermann K, Baeuerle PA, Hiddemann W, Riethmuller G and Subklewe M. CD33 target validation and sustained depletion of AML blasts in long-term cultures by the bispecific T-cell-engaging antibody AMG 330. Blood. 2014; 123(3):356–365.

27. Brischwein K, Schlereth B, Guller B, Steiger C, Wolf A, Lutterbuese R, Offner S, Locher M, Urbig T, Raum T, Kleindienst P, Wimberger P, Kimmig R, Fichtner I, Kufer P, Hofmeister R and et al. MT110: a novel bispecific single-chain antibody construct with high efficacy in eradicating established tumors. Mol Immunol. 2006; 43(8):1129–1143.

28. Haas C, Krinner E, Brischwein K, Hoffmann P, Lutterbuse R, Schlereth B, Kufer P and Baeuerle PA. Mode of cytotoxic action of T cell-engaging BiTE antibody MT110. Immunobiology. 2009; 214(6):441–453.

29. Offner S, Hofmeister R, Romaniuk A, Kufer P and Baeuerle PA. Induction of regular cytolytic T cell synapses by bispecific single-chain antibody constructs on MHC class I-negative tumor cells. Mol Immunol. 2006; 43(6):763–771.

30. Osada T, Hsu D, Hammond S, Hobeika A, Devi G, Clay TM, Lyerly HK and Morse MA. Metastatic colorectal cancer cells from patients previously treated with chemotherapy are sensitive to T-cell killing mediated by CEA/CD3-bispecific T-cell-engaging BiTE antibody. Br J Cancer. 2010; 102(1):124–133.

31. Peng L, Oberst MD, Huang J, Brohawn P, Morehouse C, Lekstrom K, Baeuerle PA, Wu H, Yao Y, Coats SR, Dall'Acqua W, Damschroder M and Hammond SA. The CEA/CD3-bispecific antibody MEDI-565 (MT111) binds a nonlinear epitope in the full-length but not a short splice variant of CEA. PLoS One. 2012; 7(5):e36412.

32. Wortzel RD, Philipps C and Schreiber H. Multiple tumour-specific antigens expressed on a single tumour cell. Nature. 1983; 304(5922):165–167.

33. Schlereth B, Quadt C, Dreier T, Kufer P, Lorenczewski G, Prang N, Brandl C, Lippold S, Cobb K, Brasky K, Leo E, Bargou R, Murthy K and Baeuerle PA. T-cell activation and B-cell depletion in chimpanzees treated with a bispecific anti-CD19/anti-CD3 single-chain antibody construct. Cancer Immunol Immunother. 2006; 55(5):503–514.

34. Müller D and Kontermann R. Recombinant bispecific antibodies for cellular cancer immunotherapy. Curr Opin Mol Ther. 2007; 9(4):319–326.

35. Singer H, Kellner C, Lanig H, Aigner M, Stockmeyer B, Oduncu F, Schwemmlein M, Stein C, Mentz K, Mackensen A and Fey GH. Effective elimination of acute myeloid leukemic cells by recombinant bispecific antibody derivatives directed against CD33 and CD16. J Immunother. 2010; 33(6):599–608.

36. Kugler M, Stein C, Kellner C, Mentz K, Saul D, Schwenkert M, Schubert I, Singer H, Oduncu F, Stockmeyer B, Mackensen A and Fey GH. A recombinant trispecific single-chain Fv derivative directed against CD123 and CD33 mediates effective elimination of acute myeloid leukaemia cells by dual targeting. Br J Haematol. 2010; 150(5):574–586.

37. Guettinger Y, Barbin K, Peipp M, Bruenke J, Dechant M, Horner H, Thierschmidt D, Valerius T, Repp R, Fey GH and Stockmeyer B. A recombinant bispecific single-chain fragment variable specific for HLA class II and Fc alpha RI (CD89) recruits polymorphonuclear neutrophils for efficient lysis of malignant B lymphoid cells. J Immunol. 2010; 184(3):1210–1217.

38. Schubert I, Saul D, Nowecki S, Mackensen A, Fey GH and Oduncu F. A dual-targeting triplebody mediates preferential redirected lysis of antigen double-positive over single-positive leukemic cells. MAbs. 2013; 6(1).

39. Kugler M, Stein C, Schwenkert M, Saul D, Vockentanz L, Huber T, Wetzel SK, Scholz O, Pluckthun A, Honegger A

and Fey GH. Stabilization and humanization of a single-chain Fv antibody fragment specific for human lymphocyte antigen CD19 by designed point mutations and CDR-grafting onto a human framework. Protein Eng Des Sel. 2009; 22(3):135–147.

40. Brischwein K, Parr L, Pflanz S, Volkland J, Lumsden J, Klinger M, Locher M, Hammond SA, Kiener P, Kufer P, Schlereth B and Baeuerle PA. Strictly target cell-dependent activation of T cells by bispecific single-chain antibody constructs of the BiTE class. J Immunother. 2007; 30(8):798–807.
41. Gasteiger E, Hoogland C, Gattiker A, Duvaud S, Wilkins MR, Appel RD, Bairoch A, (2005) Protein Identification and Analysis Tools on the ExPASy Server. In: Walker JM, ed. The Proteomics Protocols Handbook: Humana Press), 571–607
42. Tallen G, Henze G, Von Stackelberg and A. Treatment of children and adolescents with relapsed ALL: therapy target long-term healing. Pharm Unserer Zeit. 2012; 41(3):214–221.
43. Restifo NP, Dudley ME and Rosenberg SA. Adoptive immunotherapy for cancer: harnessing the T cell response. Nat Rev Immunol. 2012; 12(4):269–281.
44. Baeuerle PA, Kufer P and Bargou R. BiTE: Teaching antibodies to engage T-cells for cancer therapy. Curr Opin Mol Ther. 2009; 11(1):22–30.
45. Wang XB, Zhao BF, Zhao Q, Piao JH, Liu J, Lin Q and Huang HL. A new recombinant single chain trispecific antibody recruits T lymphocytes to kill CEA (carcinoma embryonic antigen) positive tumor cells in vitro efficiently. J Biochem. 2004; 135(4):555–565.
46. Liu J, Zhao Q, Zhao B, Cheng J, Wang X, Song L, Zhong Z, Lin Q and Huang H. A new format of single chain trispecific antibody with diminished molecular size efficiently induces ovarian tumor cell killing. Biotechnol Lett. 2005; 27(22):1821–1827.
47. Harms BD, Kearns JD, Iadevaia S and Lugovskoy AA. Understanding the role of cross-arm binding efficiency in the activity of monoclonal and multispecific therapeutic antibodies. Methods. 2014; 65(1):95–104.
48. Lillemeier BF, Pfeiffer JR, Surviladze Z, Wilson BS and Davis MM. Plasma membrane-associated proteins are clustered into islands attached to the cytoskeleton. Proc Natl Acad Sci U S A. 2006; 103(50):18992–18997.
49. Lillemeier BF, Mortelmaier MA, Forstner MB, Huppa JB, Groves JT and Davis MM. TCR and Lat are expressed on separate protein islands on T cell membranes and concatenate during activation. Nat Immunol. 2010; 11(1):90–96.
50. Greil J, Gramatzki M, Burger R, Marschalek R, Peltner M, Trautmann U, Hansen-Hagge TE, Bartram CR, Fey GH, Stehr K and et al. The acute lymphoblastic leukaemia cell line SEM with t(4;11) chromosomal rearrangement is biphenotypic and responsive to interleukin-7. Br J Haematol. 1994; 86(2):275–283.
51. Drexler HG. 2010; Guide to Leukemia-Lymphoma Cell Lines. (Braunschweig).
52. Alici E, Sutlu T, Bjorkstrand B, Gilljam M, Stellan B, Nahi H, Quezada HC, Gahrton G, Ljunggren HG and Dilber MS. Autologous antitumor activity by NK cells expanded from myeloma patients using GMP-compliant components. Blood. 2008; 111(6):3155–3162.
53. Benedict CA, MacKrell AJ and Anderson WF. Determination of the binding affinity of an anti-CD34 single-chain antibody using a novel, flow cytometry based assay. J Immunol Methods. 1997; 201(2):223–231.
54. Braciak TA, Wildenhain S, Roskopf CC, Schubert IA, Fey GH, Jacob U, Hopfner KP and Oduncu FS. NK cells from an AML patient have recovered in remission and reached comparable cytolytic activity to that of a healthy monozygotic twin mediated by the single-chain triplebody SPM-2. J Transl Med. 2013; 11(1):289.
55. Olejniczak SH, Stewart CC, Donohue K and Czuczman MS. A quantitative exploration of surface antigen expression in common B-cell malignancies using flow cytometry. Immunol Invest. 2006; 35(1):93–114.
56. Fauriat C, Andersson S, Bjorklund AT, Carlsten M, Schaffer M, Bjorkstrom NK, Baumann BC, Michaelsson J, Ljunggren HG and Malmberg KJ. Estimation of the size of the alloreactive NK cell repertoire: studies in individuals homozygous for the group A KIR haplotype. J Immunol. 2008; 181(9):6010–6019.

SUPPLEMENTARY TABLE

Supplementary Table S1. Computed protein characteristics of the T cell-engaging bispecific scFv molecules and triplebodies. Protein parameters calculated from the primary sequences of the engineered T cell-engaging BiTEs and triplebodies with the ProtParam (http://web.expasy.org/protparam/) and PeptideCutter (http://web.expasy.org/peptide_cutter/) tools[41].

Protein	Length [aa]	MW [kDa]	ε [M^{-1} cm^{-1}]	computed pI	Construct	Relevant Proteinases
19-3	572	60.747	117,620	8.52	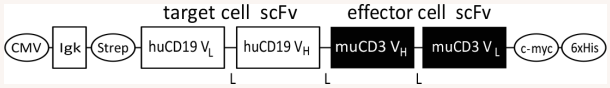	Chymotrypsin, Clostripain, Pepsin, *Proline endopeptidase (4 sites)*, Trypsin
19-3-19	854	89.94	168,180	8.53	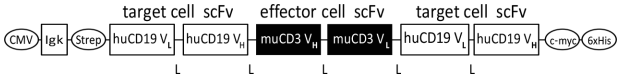	Chymotrypsin, Clostripain, Pepsin, *Proline endopeptidase (5 sites)*, Trypsin
Her2-3	563	59.503	117,160	8.66	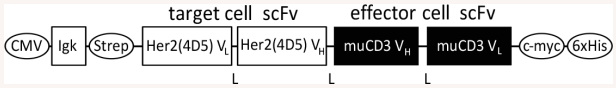	Chymotrypsin, Clostripain, Pepsin, *Proline endopeptidase (4 sites)*, Trypsin
Her2-3-Her2	834	87.249	167,260	8.71	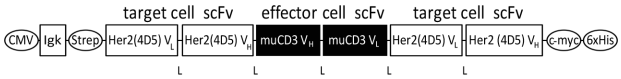	Chymotrypsin, Clostripain, Pepsin, *Proline endopeptidase (5 sites)*, Trypsin

2.3 Chip-based platform for dynamic analysis of NK cell cytolysis mediated by a triplebody

Elisavet I. Chatzopoulou, Claudia C. Roskopf, Farzad Sekhavati, Todd A. Braciak, Fuat S. Oduncu, Nadja C. Fenn, Karl-Peter Hopfner, Georg H. Fey & Joachim O. Rädler

Analyst 2016 Mar 21; **141** (7): 2284-2295

DOI: 10.1039/c5an02585k

2.3.1 Summary

In cancer patients, the leukocyte population is often functionally impaired or greatly reduced. It is difficult to take this parameter into account, when trying to predict whether an individual patient will benefit from an immunotherapeutic approach that relies on his autologous immune effector cells. Currently there are few methods available to monitor the cytolytic capacity of a patient's NK or CTL population in conjunction with therapeutic agents: on the one hand chromium and calcein release assays have a limited reaction period and provide average cytolysis values at single time points, but no details on the cellular interactions. On the other hand imaging techniques provide a more detailed insight into the cytolytic reaction, but have a low throughput. Therefore a single-cell cytometry (SCC) assay, which allows the observer to follow the cellular lysis of individual targets at high throughput for at least 15 hours, was developed and is introduced in this publication.

Active adhesion site arrays were prepared on microstructured hydrophobic surfaces of ibidi® channel slides and coated either with fibronectin for the adhesion of HEK 293.123 cells or with an anti-CD15 IgM antibody (SSEA-1) to immobilize MOLM-13 target cells. *Ex vivo* expanded NK cells from a healthy donor and triplebody SPM-2 were then added at different concentrations and time-lapse imaging was performed at 12 minute intervals for a period of 16 hours. Target cell lysis was assessed by uptake of propidium iodide (PI) and the time of cell death was determined to be the time at which the slope of the increasing PI signal reached its maximum.

The SCC method was compared to standard calcein release cytolysis assays with HEK 293.123 cells as targets. At an E : T ratio of 2 : 1 an isometric dose-response to increasing concentrations of SPM-2 was observed in both methods. The EC_{50}-values were comparable with 12.2 ± 0.1 pM in SCC and 10.2 ± 8 pM in the calcein release assay, respectively. The maximum specific lysis observed via SCC (25 ± 1%) was lower than that observed via calcein release (48 ± 2%), which was attributed to the lower target cell density and cell surface accessibility in SCC. In addition to its dose-dependence on SPM-2, the extent of NK cell-mediated lysis also increased with increasing E : T ratios. Moreover, more than one NK cell attacked a single target cell at an E : T ratio of 5 : 1 as observed by SCC.

For the dynamic analysis of NK cell-cytolysis, a killing rate was defined, which is the number of lytic events (lysed/total target cells) in an hour. Interestingly, a massive killing rate was generally observed in the first hour that dropped significantly in the second hour. Then the killing rate displayed a slow increase over the next 5 to 10 hours and a subsequent gradual decrease. Presumably the initial high killing rate was due to previous stimulation of NK cells and the resultant high stores of lytic granules. After the first attack, the depleted stores had to be replenished for further lytic events to occur. This resulted in the steady increase of the killing rate during the replenishment phase. At later time points medium exhaustion, accumulation of cell debris and partial apoptosis of NK cells was responsible for the gradual decrease in killing rate. The magnitude and speed of increase of the killing rate were affected by the concentration of SPM-2. At the example of AML-M5a cell line MOLM-13 it was shown that SCC can also be adapted to suspension cells as targets. They were immobilized with a CD15-specific IgM antibody and a natural NK cell-mediated lysis of 2.6% was observed.

In summary, the single-cell cytometry approach is reliable and suitable for the study of the dynamics and timing of cell-cell interactions and the influence of therapeutic agents. Therefore it may become a helpful technique to decide on optimal dosing and administration schedules for therapeutic agents and may be extended to biomarker assessment. SCC already has a low requirement for cellular material and may be further miniaturized and automated. Lastly, SCC is a suitable method to investigate the effect of therapeutic agents on cellular subset, for example the sensitivity of AML stem cells towards treatment with SPM-2 plus NK cells.

2.3.2 Contribution

I expanded peripheral blood mononuclear cells and isolated NK cells for single-cell cytometry. Furthermore, I performed the bulk assays (4 hour calcein release assay) for comparison with the SCC assays. I also helped with the interpretation of the results and reviewed the paper prior to submission.

Published on 09 March 2016. Downloaded by Ludwig Maximilians Universitaet Muenchen on 14/03/2016 09:19:59.

Analyst

PAPER

View Article Online
View Journal

Cite this: DOI: 10.1039/c5an02585k

Chip-based platform for dynamic analysis of NK cell cytolysis mediated by a triplebody†

Elisavet I. Chatzopoulou,[a] Claudia C. Roskopf,[b] Farzad Sekhavati,[a] Todd A. Braciak,[b] Nadja C. Fenn,[c] Karl-Peter Hopfner,[c] Fuat S. Oduncu,[b] Georg H. Fey[d] and Joachim O. Rädler*[a]

Cancer therapy *via* redirected lysis mediated by antibodies and antibody-derived agents relies on the availability of substantial numbers of sufficiently active immune effector cells. To monitor antitumor responses before and during therapy, sensitive methods are needed, capable of quantitating specific lysis of target cells. Here we present a chip-based single-cell cytometric assay, which uses adherent human target cells arrayed in structured micro-fields. Using a fluorescent indicator of cell death and time-lapse microscopy in an automated high-throughput mode, we measured specific target cell lysis by activated human NK cells, mediated by the therapeutic single chain triplebody SPM-2 (33-16-123). This antibody-derived tri-specific fusion protein carries binding sites for the myeloid antigens CD33 and CD123 and recruits NK cells *via* a binding site for the Fc-receptor CD16. Specific lysis increased with increasing triplebody concentration, and the single-cell assay was validated by direct comparison with a standard calcein-release assay. The chip-based approach allowed measurement of lysis events over 16 hours (compared to 4 hours for the calcein assay) and required far smaller numbers of primary cells. In addition, dynamic properties inaccessible to conventional methods provide new details about the activation of cytolytic effector cells by antibody-derived agents. Thus, the killing rate exhibited a dose-dependent maximum during the reaction interval. In clinical applications *ex vivo* monitoring of NK activity of patient's endogenous cells will likely help to choose appropriate therapy, to detect impaired or recovered NK function, and possibly to identify rare subsets of cancer cells with particular sensitivity to effector-cell mediated lysis.

Received 16th December 2015,
Accepted 29th February 2016

DOI: 10.1039/c5an02585k

www.rsc.org/analyst

Introduction

Several antibody-derived proteins used in cancer therapy function in conjunction with cytolytic effector cells, such as NK-cells and cytotoxic T-cells (T-CTLs). Examples are the CD20 antibody Rituximab (Rituxan™) and the CD19-directed bispecific agent Blinatumomab (Blincyto™), as well as the bispecific proteins AMG330 and MGD006, developed for the treatment of Acute Myeloid Leukemia (AML;[1–7]). The cytolytic activity of several therapeutic antibodies in the classic IgG format largely depends on the Fcγ RIII-receptor CD16 present on NK-cells, monocytes and macrophages,[8–12] while the activity of the mentioned bispecific agents depends on T-CTLs. Therapeutic use of these agents requires that the patient harbors the respective effector cells in substantial numbers and in a sufficiently active state. For AML originating in the bone marrow (BM), this requirement is often not met during the early stages of treatment. At diagnosis and during the first cycle of induction therapy of AML patients, NK- and T- cells are usually reduced by about 10- to 20-fold in numbers relative to a healthy BM, and the remaining cells are functionally impaired.[13–16] To determine a suitable therapeutic agent and time point for the start of treatment, it would therefore help, if investigators could monitor the capacity of a patient's NK- and/or T-cells to mediate cancer cell lysis in conjunction with the therapeutic agent. This requires the availability of reliable functional assays permitting a quantitative assessment of the cytolytic potential of a patient's NK- and/or T-cells by using only small numbers of these cells, which are available in limited supply.

Chromium-51 and Calcein-release assays have been used extensively to measure cytotoxicity induced by therapeutic agents.[17,18] However, they cannot be used for reaction periods in excess of approximately 4 hours due to increasing spon-

[a]Faculty of Physics and Graduate School of Quantitative Biosciences (QBM), Ludwig-Maximilians-Universität, Munich, Germany. E-mail: raedler@lmu.de; Fax: +0049-(0)2180-3182; Tel: +0049-(0)89-2180-2438
[b]Division of Hematology and Oncology, Medizinische Klinik und Poliklinik IV, Klinikum der Universität München, Munich, Germany
[c]Department of Biochemistry and Gene Center, Ludwig-Maximilians-Universität, Munich, Germany
[d]Department of Biology, Friedrich-Alexander-University Erlangen-Nürnberg, Erlangen, Germany

†Electronic supplementary information (ESI) available. See DOI: 10.1039/c5an02585k

Published on 09 March 2016. Downloaded by Ludwig Maximilians Universitaet Muenchen on 14/03/2016 09:19:59.

taneous release of the label from target cells.[19] They also do not provide further information regarding the intrinsic aspects of the investigated cellular interaction. On the other hand, imaging techniques traditionally offered a more detailed insight into the interrogated phenomenon, however at low-throughput. This led to the concomitant use of microscopy to visualize processes that have previously been hypothesized based on data averaged over large cell populations and produced with the standard assays.[20] Nevertheless, time-lapse microscopy has evolved significantly over the past decade and now permits us to follow the death of individual cells at high throughput and for observation periods of up to 15 hours and beyond.[21] These newly developed microscopy-based approaches have uncovered detailed features of NK physiology and their innate ability to direct lysis of tumor cells, the "natural killing mode of NK cells". Furthermore, different types of NK cells have been used in these studies, including both NK-cell lines and primary NK cells activated by IL-2 as well as unstimulated NK cells isolated from healthy donors. As a result, many different approaches have been implemented to uncover new aspects of the complex physiology of NK cells, such as the kinetics of their natural killing mode[22] and their "kinetic boosting" by Fc-engineered antibodies.[23] Moreover, the NK population was classified based on migratory behavior and cytotoxic response of individual cells.[24,25] Finally, altered NK cell cytotoxicity, migratory behavior and contact dynamics have been reported between IL-2 stimulated and non-stimulated NK cells.[26]

In oncology Antibody Dependent Cellular Cytotoxicity (ADCC) makes use of antibodies to enhance the natural killing mode of NK cells.[27,28] This process more generally is called "redirected lysis; RDL" when the mediator protein is not an antibody, but an antibody-derived agent. Although unmodified antibodies in the classic immunoglobulin (IgG) format have been successful in the treatment of selected types of cancer, in particular of hematologic malignancies, their broader use for the treatment of solid tumors is limited. Antibody engineering has led to the development of more broadly applicable derived proteins.[29–32] Some of these new molecular formats no longer carry the full antigen-binding-domains of classic IgGs (Fv-domains) but employ antibody fragments, termed "single-chain Fragment variables (scFvs)", as recognition domains. Bispecific tandem diabodies are a class of recombinant fusion proteins based on scFv-recognition domains, and Blinatumomab, the prototype of this class of agents, is approved for the treatment of certain types of lymphomas and leukemias.[3,4] An extension of the molecular format of tandem diabodies are the "single-chain tandem triplebodies" ("triplebodies" for simplicity), which carry two scFv recognition domains for target antigens on the cancer cell plus an scFv module specific for a trigger molecule on an effector cell, arranged in tandem in a single polypypeptide chain.[33–35] They can be designed to bind either two copies of the same target antigen or one copy each of two different antigens on the surface of the same cancer cell. The latter "dual-targeting" mode of binding leads to an increased selectivity of cancer cells bearing both antigens in high combined density.[18,36] Triplebody SPM-2 (33-16-123) was designed for the elimination of AML cells. It carries one binding site for CD16 and two binding sites for the tumor-antigens CD123 and CD33, present on AML cells.[16,34] Triplebodies can bind their target cells either monovalently with only one of the two target binding modules, leaving the other module non-engaged, or bi-valently, employing both target binding modules simultaneously.

Here we use single-cell cytometry (SCC) to assess the efficiency of SPM-2-mediated killing of malignant target cells by NK cells in a time-lapse mode. We use a design where target cells are arranged in arrays of microstructured adhesion sites, allowing for a facilitated assessment of the fraction of cells specifically lysed by NK cells, which are added to the assay. We recorded time-lapse movies over a period of 16 hours and followed the action of SPM-2 by the apoptosis marker propidium iodide (PI). Our main objective was to implement a single-cell assay for time-resolved studies of the triplebody and NK cell-mediated lysis in accordance with existing standard assays. The platform presented herein facilitated a dynamic analysis of the cytotoxic response of the NK cell population triggered by the triplebody. As model target cells, HEK293.123 cells were used. Our results open the possibility for future use of the assay to study not only the quality of primary effector cells from human donors, but also to study mechanistic details of the mode of action of the therapeutic agent on different subsets of target cells.

Results and discussion

To quantitate the extent of re-directed lysis of tumor cells by NK cells mediated by the triplebody SPM-2, we developed a single-cell assay based on fluorescence microscopy and microstructured arrays. Arrays of adhesion sites spaced by 60 μm were fabricated as previously reported[37,38] and further described in the Methods section. The 60 μm spacing of the adhesion sites was found to be the optimal distance for generating a single-cell array of the adherent HEK293.123 cells, after having tested smaller and larger distances in preliminary tests (data not shown). Triplebody SPM-2 (33-16-123) was synthesized as previously described,[16] following rearrangement, humanization, and stabilization of the DNA sequences of an earlier prototype of this agent.[34] Target cells (the established human cell line HEK293.123) were seeded on the microstructured topas surfaces using ibidi® channel slides. Fig. 1 illustrates the basic experimental imaging platform (Fig. 1A) and a typical image of a HEK-cell array after addition of NK cells (Fig. 1B). NK cells were derived from a healthy donor and activated as previously described.[18,39] Image acquisition started immediately after NK cell addition. Images were acquired in 12 min intervals over a time course of 16 hours. The time-lapse sequences were analyzed using custom-made image-analysis software integrating the fluorescence intensities from each individual adhesion site at each time-point.

We determined the fraction of specifically lysed cells (% specific lysis), representing the incremental lysis mediated by NK cells in the presence of the triplebody SPM-2 over the

 This journal is © The Royal Society of Chemistry 2016

Published on 09 March 2016. Downloaded by Ludwig Maximilians Universitaet Muenchen on 14/03/2016 09:19:59.

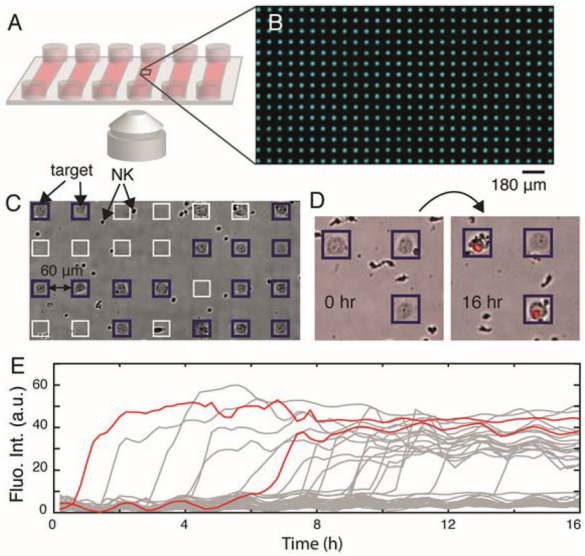

Fig. 1 Experimental set-up of the single-cell cytometry (SCC) assay. Chemically modified patterned surfaces (arrays) were prepared on 6-channel microscope slides (A). Protein-coated arrays were generated by plasma-induced patterning. (B): Squares with a side-length of 30 µm were coated with fibronectin (here fibronectin labeled with Alexa Fluor 488) and the backfilling (black) area with PLL(20k)-g(3.5)-PEG(2k) (PEG (2)). Each channel on the carrier surface, shown in (A), contained 4400 adhesive squares for cell attachment. In (B) a part of an overview microscopic scan of one coated channel of the slide is shown. (C): Arrays of adherent HEK293.123 target cells were prepared on the chemically modified surfaces (surfaces seeded with cells have adhesive squares with unlabeled fibronectin). NK cells were added and squares occupied by single target cells (framed in blue) were selected and tracked in a time-lapse mode. NK cells were identified cinematographically by their size and motility. The distance between the squares was 60 µm in our experiments, but arrays with different spacing can be produced. (D): The cell-impermeable red fluorescent marker PI (propidium iodide) was used to identify dead cells. Overlay of brightfield and PI emission is presented for the first and last frame of a measurement. (E): The mean fluorescence intensity of 40 cells over time is plotted (in the presence of 10 nM SPM-2 triplebody). Each track ("fate plot") represents the fluorescence intensity of one cell in the PI channel. Tracks exceeding an intensity threshold (defined by a supervised selection process as described under Methods) represent lysed cells. Two exemplary time-courses of two target cells that were lysed are highlighted in red.

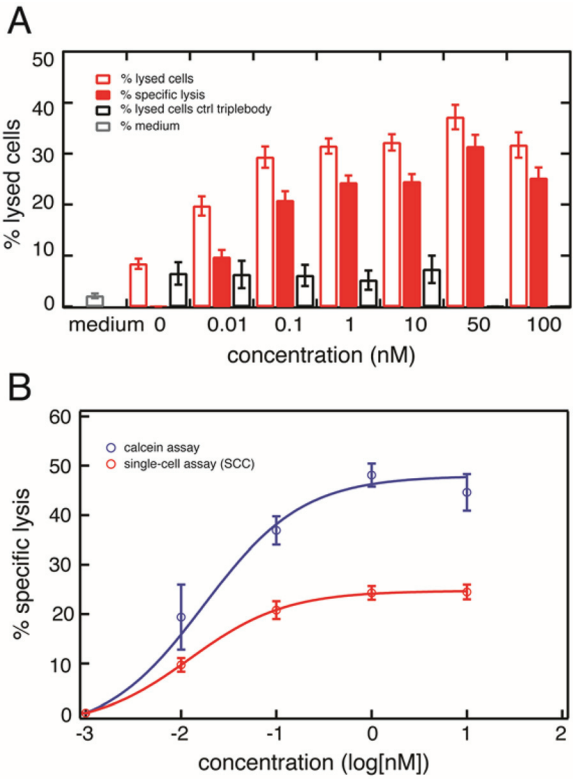

Fig. 2 Validation of the SCC assay by direct comparison with the bulk assay. A: Data obtained with the SCC assay. Red open bars: percentage of dead target cells relative to the total number of target cells analyzed ("overall lysis"). Red filled bars: percentage of specific lysis induced by SPM-2 after subtraction of natural killing by NK cells alone (the numbers shown for 0 nM concentration). Black open bars: overall lysis produced by addition of control triplebody SPM-1 (19-16-19), a triplebody in the same molecular format as SPM-2, but recognizing the target antigen CD19, which is absent from HEK293.123 cells. This control was not performed for 50 and 100 nM concentrations of the control protein. Medium control: without added NK cells and triplebodies; this control measures the extent of spontaneous death of target cells over the measurement interval. The averaged value of all the dose-dependent measurements is shown. (B) Comparison of data obtained with the SCC assay (red circles) over a 16 hour measurement and the bulk assay (calcein release assay; blue circles) over a 4 hour period. Data points of the calcein assay represent the mean value of the percentage of specific lysis averaged over triplicate reaction wells on the same microtiter plate, and error bars represent the SEM (standard error of the mean). Effector cells were MACS-purified NK cells from a healthy donor, pre-stimulated with IL-2 (LAK cells), and seeded at an E : T ratio of 2 : 1.

background of natural killing by NK cells alone according to the formula given in Methods section. Lysed cells were accounted for based on a threshold in the PI fluorescence signal. Fig. 2 shows the percentage of lysed cells as a function of triplebody dose. For clarity the percentage of total lysed cells and the percentage of natural killing by NK-cells are shown together with the calculated extent of specific lysis.

Dose-dependence measurements and comparison with calcein release assay

Dose-dependence measurements were also performed with the established calcein release assay (Fig. 2B). For these measurements the effector-to-target cell (E : T) ratio was kept constant at 2 : 1 and the concentration of the SPM-2 triplebody varied from 0–100 nM for the SCC assay and from 0–10 nM for the calcein release assay. As effector cells immunomagnetically (MACS) purified pre-stimulated NK cells from the same healthy donor were used. The average percentage of NK cells ($CD56^{bright}CD16^{bright}$) after the MACS purification was 83.3% ± 4.6%. This percentage was taken into account in order to achieve an actual NK-to-target ratio of 2 : 1 as mentioned above. The total number of target cells analyzed in this set of measurements is given in Table 1. Over a 16 hour measurement period, a maximum of about 35% of the cells analyzed were lysed in the SSC assay in the presence of triplebody SPM-2 (Fig. 2A, red open bars). The fraction of specifically

Published on 09 March 2016. Downloaded by Ludwig Maximilians Universitaet Muenchen on 14/03/2016 09:19:59.

Table 1 Total number of target cells analyzed in dose-dependence measurements

nM	SPM-2	Control triplebody
0	3099	465
0.01	1648	303
0.1	1888	507
1	3482	524
10	3254	344
50	1528	—
100	1364	—
Medium	3075	489

lysed cells (% specific lysis) steadily increased with triplebody concentration and reached a plateau at about 25% for concentrations from 1 nM upwards (Fig. 2A, red bars). As a negative control the triplebody SPM-1 (19-16-19) was used, a protein in the same molecular format as SPM-2 and carrying the same scFv binding site for CD16, but with specificity for the target antigen CD19, which is absent from the surface of HEK293.123 cells. In separate experiments with CD19-positive target cells this control triplebody mediated cytolysis by NK cells,[33] but it did not produce specific lysis of HEK293.123 targets in the SCC assay (Fig. 2A, black open bars). The fraction of specific lysis induced by SPM-2 showed comparable dose-dependence in the SSC and the calcein-release assays (Fig. 2B). In both cases specific lysis reached plateau values for concentrations from 1 nM upwards, and the shape of the curves was similar (isometric). The EC50 values (half-maximum effector concentrations; the concentrations, at which half of the maximum lysis was reached) derived from both curves were (10.2 ± 8.0) and (12.2 ± 0.1) pM for the calcein and the SCC assays, respectively. The errors represent the standard deviation computed by statistical modeling of the two assays (see Methods section). While the EC50 values derived from both data sets were very similar, the maximum fractions of specifically lysed cells were (48 ± 2)% for the calcein assay and (25 ± 1)% for the SCC assay. This difference most likely is explained by the fact that in the calcein assay both effector and target cells were present in the fluid phase, whereas in the SSC assay the targets were anchored to the substrate and were therefore less accessible to the effector cells. In addition, in the SCC assay the density of cells per unit volume was less than half of the density reached in the calcein assay. However, this quantitative difference in the maximum levels of specific lysis recorded with both assays does not affect the key conclusion that the SSC assay is validated by this comparison, as it captured the dose-dependence of the triplebody's lytic potential in the same qualitative manner as the calcein assay.

Dependence of the extent of cytolysis on the E : T ratio

Next we measured the efficiency of lysis as a function of the effector-to-target cell (E : T) ratio (Fig. 3). For measurements of the dependence of this variable on the E : T ratio, the concentration of the SPM-2 triplebody was kept constant at 1 nM, while the E : T ratios tested were 0.2 : 1, 1 : 1, 2 : 1 and 5 : 1. The

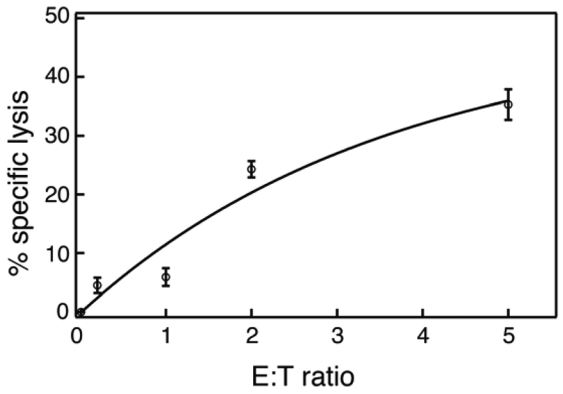

Fig. 3 Dependence of specific lysis measured with the SCC assay on the E : T ratio. Lysis induced over a range of different Effector to Target (E : T) cell ratios by SPM-2 at a 1 nM saturating concentration. Data points are fitted to an exponential curve. Effector cells were MACS-purified NK cells from a healthy donor, pre-stimulated with IL-2 (LAK cells).

total number of target cells analyzed in this set of measurements is given in Table 2. The effector cells used were MACS-purified NK cells. The mean final percentage of the NK cells ($CD56^{bright}CD16^{bright}$) after the enrichment was 90.2% ± 3.0%. This percentage was taken into account in order to reach the actual NK to target cell ratio for each of the conditions mentioned above. The specifically lysed fraction increased as a function of the E : T ratio (Fig. 3). When the number of effector cells increased the probability for cell encounters increased too, explaining the increase in lytic events. Furthermore, in the case of the E : T = 5 : 1 the number of effector cells attacking one single target cell was also increased. In this case, we observed that more than one effector cells were able to form a synapse with one specific target cell at the same time. The maximum extent of specific lysis was achieved at the E : T = 5 : 1 condition.

Dynamic analysis of the lytic events

The automated SCC assay allowed us to monitor cellular lysis over a long period of time with high numeric precision. Focusing on the target cells enabled us to track the activity of the NK cell population, regarding their cytotoxic activity and how the SPM-2 agent affected it. In the following, we quantified the killing rate *i.e.* the number of lytic events that occurred per hour. This percentage corresponds to the number of lysed cells *versus* the total number of target cells analyzed. In

Table 2 Total number of target cells analyzed in measurements of the dependence on the E : T ratio

E : T	1 nM	0 nM
0.2 : 1	1061	1300
1 : 1	992	815
2 : 1	3482	744
5 : 1	1309	867
Medium	1909	1909

 This journal is © The Royal Society of Chemistry 2016

Published on 09 March 2016. Downloaded by Ludwig Maximilians Universitaet Muenchen on 14/03/2016 09:19:59.

Fig. 4B, the mean fluorescence intensity of 3 arbitrary single target cells is illustrated, while for one of these cells the corresponding time-lapse frames of selected time points are presented (Fig. 4A). We determined the individual time points of target cell lysis using the maximum slope of the fluorescence signal increase as an indicator. From such data, the cumulative percentage of lysed cells was computed and plotted for 3 different concentrations of SPM-2: 0, 1 and 100 nM (Fig. 4C). The variation of the killing rate over the course of 16 hours for various SPM-2 concentrations and for constant numbers of NK cells is plotted in Fig. 4D. For comparison, the first plot shows the rate of background lysis rate in the absence of NK cells and the SPM-2 agent (labeled "medium"). When the SPM-2 agent was absent or present in low concentration, the killing rate of the NK cells was almost constant, 0.5 ± 0.2 target cells were killed per hour at 0 nM and 1.3 ± 0.5 at 0.01 nM (Fig. 4D, 2nd and 3rd panel from the left). The killing rate increased until a maximum was reached after several hours into the measurement and then gradually decreased. The maximum rate was greater for higher concentrations of SPM-2 (50 and 100 nM; last 2 panels to the right in Fig. 4D) than for intermediate concentrations (0.1 to 10 nM; central panels in Fig. 4D), and therefore, the agent clearly influenced the maximum killing rate of the NK cells. The maximum rate also occurred earlier at high concentrations of the agent than at lower concentrations (Fig. 4D; 2 panels at right). Importantly, the rates of lysis were elevated in the 1st hour of the reaction (highlighted in yellow in Fig. 4D) and dropped strongly in the 2nd hour for all tested

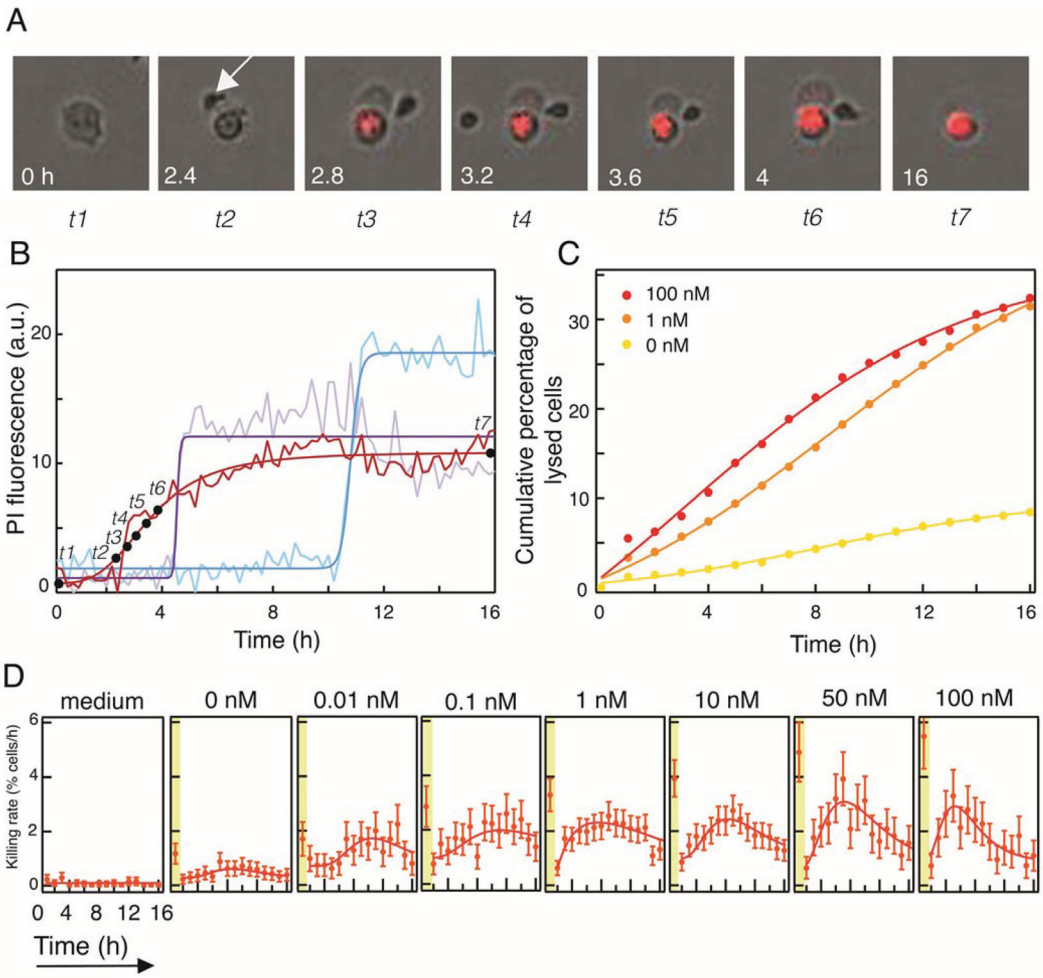

Fig. 4 Dynamic analysis of lytic events with the SCC assay. (A) Time-lapse images of an exemplary target cell being killed by an NK cell (arrow). The progressively increased PI fluorescence intensity reflects progressive nuclear membrane disintegration (irreversible apoptosis). (B) PI fluorescence intensity of 3 exemplary target cells over the course of 16 hours, including the cell shown in (A) (red curve). Raw intensities were fitted with the Hill Equation. (C) Cumulative percentage of lysed target cells for 3 different concentrations of SPM-2: 0, 1 and 100 nM. Data points were fitted with the sigmoid function. (D) Killing rate as a function of time for increasing concentrations of SPM-2 by a constant number of NK cells. The left panel ("medium") shows the dynamic of spontaneous cell death events, in the absence of NK cells. Data points were fitted with a log normal distribution curve. Data points for the first hour of the reaction (highlighted in yellow) represent natural killing by the NK cells but not specific lysis mediated by the triplebody. These events also occurred in the absence of added triplebody (2nd panel from the left), and were therefore excluded from the fitting.

Published on 09 March 2016. Downloaded by Ludwig Maximilians Universitaet Muenchen on 14/03/2016 09:19:59.

concentrations of the mediator protein, even without added mediator protein (Fig. 4D, 2nd panel from the left). Thereafter the rates increased until maximum rates were reached between 5–10 hours into the reaction, and then the rates declined again. The log normal distribution was fitted to the data points. In all cases, the first data point, indicated in the yellow region (Fig. 4D) was excluded from the fitting, because it consistently was an outlier. We explain this excessively high lytic rate as being probably owed to the previous stimulation of the NK cells by long-term culture in the presence of IL-2.

NK cells are "ready-to-kill" cells and the most common way to kill is through perforin/granzyme granule-mediated exocytosis.[40] In this study, LAK (Lymphokine Activated Killer cells) NK cells, pre-stimulated with IL-2 from a healthy donor, were used. These cells exhibit greater cytotoxicity due to increased intracellular concentrations of effector molecules such as perforin and granzymes.[41] They form a synapse with the target cell and then degranulation occurs which leads to apoptotic death of the target. At the beginning of the measurement the cytosol of the NK cells is full of granzymes, which then degranulate to lyse the large number of target cells at the beginning of the measurement. These distinctly large killing rates during the first hour of the measurement were further boosted by the triplebody in a dose-dependent manner. Subsequently, the NK cells were exhausted and gradually resumed their cytotoxic activity by producing again new granzymes. The triplebody played a role in the early hours of the reaction interval, either in the replenishment process or the subsequent lytic events or both, because the maximum rates of lysis were clearly augmented by the triplebody in a dose-dependent manner (Fig. 4D). The observed increase in lytic rates with time suggests an influence of the triplebody on the speed of replenishment or on other metabolic processes preparing the NK cell for the next degranulation event and on an acceleration of the cadence of lytic bursts. Furthermore, the initial increases in the rate during the first few hours of the reaction may also be a consequence of the lytic events themselves; either the NK cells or the targets or both may have released soluble mediators (*e.g.* cytokines and others) which favored the lytic process in a positive feedback manner (a paracrine loop). At the same time, the medium was progressively exhausted and cellular debris from dead target and effector cells accumulated, which must have inhibited the lytic activity. The system was a closed system in our set-up and the medium was not renewed. Therefore, these inhibitory influences eventually may have outpaced the positive feedback mechanisms, an optimum was passed, and beyond this point the reaction rates began to decline. Moreover, it has been previously shown[42] that NK cells isolated from healthy donors and stimulated with IL-2 do not have a uniform cytotoxic activity. In essence a small subset of the NK cells are responsible for the majority of kills. Finally, taking into consideration that tumor cells can also induce the apoptosis of IL-2 activated NK cells[43,44] we propose that the decrease of the reaction rates after a certain time point most likely was due to a partial apoptosis of the active cytotoxic subpopulation in combination with the exhaustion of the medium.

Natural killing dynamic analysis against non-adherent AML target cells

Many samples of primary cancer cells, especially those derived from hematologic malignacies, consist of non-adherent cells. To address this matter and to render the proposed assay suitable for non-adherent cells we developed a second version of the chip, in which the patterns of squares covered with fibronectin were replaced by squares covered with an antibody of IgM isotype. To test this variant of our assay, we measured the natural killing potency of primary NK cells from another healthy donor for the human AML-derived target cell line MOLM-13.

A suitable antibody candidate for anchoring MOLM-13 cells to the micro-patterns, without interfering with the NK cells, is a CD15-specific antibody. The myeloid marker CD15 is present on the surface of the MOLM-13 cells[45] but not on the primary NK cells (Fig. S1†). Both IgG1- and IgM-types were tested and MOLM-13 cell arrays of greater occupancy and greater stability for longer periods of time (up to 24 h) were achieved with the IgM antibody, probably due to more favorable stereochemical properties of the IgM relative to the IgG1 isotype. Patterns of squares with 25 μm side-length were used for the MOLM-13 cell line, because these cells were smaller than the adherent HEK-cells used so far. As a result, smaller square patterns led to a greater percentage of single-cell occupied patterns. Even though we could have chosen smaller distances between the squares for the non-adherent MOLM-13 cells, we chose to maintain the 60 μm for better comparability with the measurements of the adherent target cells and to avoid introducing a new variable into the experimental setup. An array of MOLM-13 cells in the presence of NK cells is shown in Fig. 5A. Size and morphology of MOLM-13 and NK cells are very similar, therefore MOLM-13 cells were stained with fluorescent tracker dye Green CMFDA to permit the distinction from the NK cells.

To test this version of the assay for non-adherent cells we measured the natural killing of MOLM-13 targets by NK cells alone without addition of a mediating protein. For the measurements with the non-adherent cells, NK cells were derived from a second healthy donor and activated by long-term culture in the presence of IL-2 as previously described.[18,39] Preparation of the samples, image acquisition and analysis were performed as described for the measurements with the adherent HEK293.123 cells. The E : T ratio was 2 : 1 and after a 16 hour measurements period 2.6% of the cells analyzed (Table 3) were lysed (Fig. 5C). This percentage was lower than the average natural killing observed for the NK cells from the first donor at the same E : T ratio (8.4%) (Fig. 2A), which probably reflects donor-to-donor variability and the different types of target cells used. Time-lapse frames of an NK cell progressively killing a MOLM-13 cell are presented in Fig. 5B. The variation of the killing rate over

Table 3 Total number of target cells analyzed in measurements with the non-adherent cells

E : T = 2 : 1	Medium
1775	2276

This journal is © The Royal Society of Chemistry 2016

Published on 09 March 2016. Downloaded by Ludwig Maximilians Universitaet Muenchen on 14/03/2016 09:19:59.

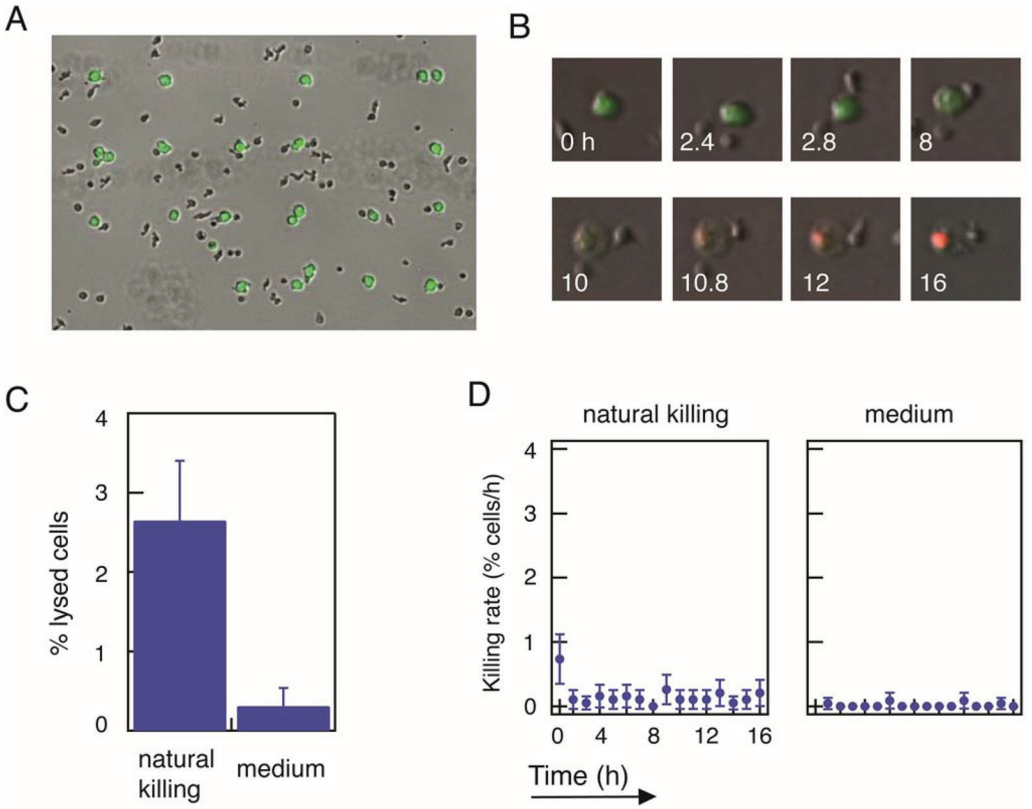

Fig. 5 Variation of the SCC assay adapted to non-adherent target cells. Arrays of antibody coated square patterns were generated with the same procedure as the fibronectin arrays, by substituting fibronectin with an anti-human CD15 antibody. Arrays of stained MOLM-13 cells (CellTracker™ Green CMFDA) were prepared on the chemically modified surfaces and then NK cells (unstained) were added (A). (B) Time-lapse images of an exemplary MOLM-13 target cell (green) being killed by an NK cell (unstained). The progressively increased PI fluorescence intensity reflects progressive nuclear membrane disintegration (irreversible apoptosis). (C) Data obtained with the SCC assay showing the natural killing potency of NK cells against MOLM-13 cells. The bars represent the percentage of dead target cells relative to the total number of target cells analyzed. (D) Dynamic analysis of the natural killing mode of NK cells against the MOLM-13 target cells. The right panel ("medium") shows the dynamic of spontaneous cell death events, in the absence of NK cells.

the course of 16 hours for the natural killing of the NK cells measured is presented in Fig. 5D. A slightly greater killing rate during the 1st hour was also observed in this case and probably reflects the preceding stimulation of the NK cells with IL-2 as was discussed above.

Compared with existing methods, single-cell cytometry allows for time-resolved studies of NK cell activity. Chromium-51 and calcein release assays offer a statistically valid measurement of cytotoxity, but they are restricted in duration due to spontaneous release of the label, and they produce time- and population-averaged data. Flow cytometry and ELISPOT assays offer single-cell data for large number of cells, but also only for at a single time point. Moreover, they measure cytotoxicity in an indirect manner, as with flow cytometry usually target cells that have survived are counted, while in ELISPOT assays usually IFN-γ secretion or degranulation of the effector cells is measured.[46,47] The SCC assay presented here fills the gap between these two different approaches of measuring cytotoxicity. SCC is capable of following the progression of NK cytotoxic activity over an extended duration of 16 hours. Due to spatial ordering of the target cells, image analysis is feasible with limited computational means generating data that contain full information on the time course of killing events relevant to therapeutic applications.

To better understand the mode of action of novel therapeutics based on the recruitment of effector cells and the functional properties of the effector cells involved, it is essential to have the ability to study also the dynamics of these processes. Additional studies will likely produce suggestions for optimal dosing and administration schedules in clinical applications. Time-lapse methods are promising in this regard, since meta-analysis can be extended to the use of additional markers including biomarkers of therapy success, disease progression and impending relapse, and because they lend themselves to further automatization.

An additional advantage of single cell assays is that they generate reliable data with substantially smaller numbers of effector cells. For an SCC assay typically only 2×10^4 NK cells are needed per measurement point, 5-times fewer than the $>10^5$ cells needed for each measurement point in a calcein release assay. Patient-derived NK cells are a scarce resource, in particular to monitor disease status and therapy outcome for AML patients. Further miniaturization of the new method is

Published on 09 March 2016. Downloaded by Ludwig Maximilians Universitaet Muenchen on 14/03/2016 09:19:59.

possible, so that reliable measurements will likely become possible with as few as 5000–10 000 NK cells. Furthermore, patterned arrays provide uniform micro-environments and spacing of target cells and hence potentially improve the standardization of cell–cell encounters. Hence, chip-based single cell assays are potentially valuable for clinical monitoring of the patients NK response and for the choice of personalized treatment for individual AML patients. They can also be applied to T-CTL as effector cells in combination with corresponding triplebodies and with other antibody-derived proteins recruiting T-cells as cytolytic effectors.[4–7,48]

Assays employing spatially arrayed target cells can also be useful to study questions regarding the timing in cell–cell recognition and immune response, such as for example the "memory" effect described for NK cells.[22] In the experiments presented here the full potential of the dual-targeting triplebody SPM-2 has not yet been analyzed. Here we have so far only used the CD123-binding site of this agent. In the future the effect of simultaneous engagement of both binding sites by one copy each of CD33 and CD123 on the lytic activity of NK cells can be studied. Dual-targeting renders the SPM-2 agent particularly promising for the therapy of AML because virtually all patients expressed either one or the other of the two antigens.[49] Indeed, in cell culture cytolysis assays with primary cells from a broad range of AML patients with different subtypes of AML and with a standard batch of NK cells from an unrelated healthy donor, all samples showed very effective lysis.[50] This is an unusually high degree of responsiveness, considering that the response rate to the best antibody-derived agent available so far for the treatment of AML (Mylotarg™ [51]) was in the range of 40% for blasts from patients with different subtypes of AML.[52] Even blasts from patients with AML subtypes that typically show a poor response to conventional chemotherapy were lysed efficiently by SPM-2 plus NK cells.[50] Moreover, the pair of CD33 plus CD123 is highly expressed on AML leukemia stem cells (AML-LSCs) but far less on normal hematopoietic stem cells (HSCs;[52–54]). Therefore, a therapeutic window appears to exist, which may permit a preferential elimination of the AML-LSCs over the normal HSCs of the patient and a reconstitution of the patient's hematopoietic system after the end of therapy from the patient's own HSCs, without the need for an allogeneic or autologous stem cell transplantation. If this could be achieved in the future, then this result would constitute major progress in the therapy of AML. Therefore, in the future it is important to study in detail not only how a patient's autologous NK cells in conjunction with this agent lyse the patient's bulk AML blasts, but also whether and how they lyse subsets of blasts progressively closer and closer to the leukemia initiating cells (LICs) and relapse initiating MRD cells, which are likely to be encompassed in the $CD34^{pos}CD38^{-neg}CD123^{high}$ compartment of BM and peripheral blood cells, which comprises between 0.01 and 67% of all malignant cells for different AML patients.[55] To this end cytolysis assays with rare subsets of patient-derived AML cells and NK- or T cells are required, which will be available in small numbers only. Finally, agents targeting the same pair of antigens, but recruiting T-cells as cytolytic effectors are also under development,[56] and similar experiments as those outlined above will also need to be performed with the corresponding T-cell-recruiting agents in order to find the best suited agent for individual patients in the sense of a personalized medicine. Developments are well under way that personalized medicine will clearly become more prevalent in the future. Time-resolved SSC assays are promising means to further investigate the capabilities of Fc engineered antibodies and other bi- and trispecific antibody-derived agents such as the triplebodies described here for enhanced target cell lysis. They therefore offer the potential to assist treatment decisions and monitoring of treatment success in cancer therapy.

Experimental

Cell culture

Human Embryonic Kindey 293 cells (HEK 293), obtained from the American Type Cell Culture Collection (ATCC, Manassas, VA, USA), were transfected with cDNA expression constructs for human CD123 and sublines were selected, which stably expressed CD123 over many passages in culture. The subline employed here has been in culture for several years and stably expresses approx. 360 000 copies of CD123 per cell on the surface.[57] It was cultured in RPMI 1640 medium (Biochrom; Merck Millipore, Berlin, Germany) supplemented with 10% (vol/vol) Fetal Bovine Serum (FBS; Gibco®, Life Technologies GmbH, Darmstadt, Germany) and 400 μg ml^{-1} Geneticin Selective Antibiotic G418 Sulfate (Roth, Karlsruhe, Germany). MOLM-13 cells were cultured in RPMI 1640 medium supplemented with 10% (vol/vol) FBS.

Ex vivo expansion of MNCs from healthy donors in the presence of IL-2 and immunomagnetic enrichment of NK cells

Mononuclear cells (MNCs) from peripheral blood (PBMCs) were expanded *ex vivo* in RPMI medium containing Interleukin-2 (IL-2) plus 5% (vol/vol) human serum (Life Technologies) for 20 days as described[18,39] and were then frozen in aliquots for subsequent use. Prior to use in cytolysis experiments, the cells were thawed and cultured overnight in RPMI medium containing 5% (vol/vol) human serum plus 50 units per ml of penicillin and 50 μg ml^{-1} of streptomycin (PS; Life Technologies) respectively, but no additional IL-2. NK cells were then enriched by negative selection using the human NK Cell Isolation Kit (Miltenyi Biotec; Cat. No. 130-092-657; Bergisch Gladbach, Germany) according to the provider's instructions. The enriched batches contained 83–90% of $CD56^{bright}$ $CD16^{bright}$ NK cells.

Surface patterning

Protein-coated arrays were prepared on polymer coverslips for 6-channel sticky slides (ibidi GmbH, Munich, Germany). First, coverslips were treated selectively with oxygen plasma (40 W for 3 min; Femto, Diener Electronic GmbH+Co. KG, Ebhausen, Germany). Selectivity was achieved using a polydimethylsiloxane (PDMS) stamp (cast from a master produced by photo-

 This journal is © The Royal Society of Chemistry 2016

Published on 09 March 2016. Downloaded by Ludwig Maximilians Universitaet Muenchen on 14/03/2016 09:19:59.

lithography) as a mask. The area exposed to plasma was passivated with PLL(20k)-g(3.5)-PEG(2k) (SuSoS AG; Dübendorf, Switzerland) at 1 mg ml^{-1} in aqueous buffer (10 mM HEPES pH 7.4 and 150 mM NaCl). Then the PDMS stamp was removed and the remaining hydrophobic areas (squares 30 × 30 μm) were exposed to fibronectin (50 μg ml^{-1}; YO Proteins AB, Huddinge, Sweden) for 1 hour. Finally, channels were rinsed thoroughly with PBS and the slides were stored at 4 °C for a maximum of 5 days. Before cell seeding, PBS was exchanged with culture medium (RPMI with 10% (vol/vol) FBS) and kept for 1 hour at 37 °C.

The same procedure was followed for the antibody-coated arrays with the following alterations: arrays were prepared on uncoated 8-well μ-slides (ibidi GmbH, Munich, Germany). After treatment with plasma, the PDMS stamp was removed and the remaining hydrophobic areas (squares 25 × 25 μm) were exposed to purified anti-human CD15 (SSEA-1) antibody (15 μg ml^{-1}; BioLegend®, San Diego, CA USA) for 1 hour at room temperature.

Time-resolved fluorescence microscopy

Sample preparation. For the fluorescence microscopy measurements 6-channel/8-well slides were used (ibidi GmbH) with protein-coated arrays. HEK293.123 cells were added to the channels (10 000 cells per channel) and incubated at 37 °C, in culture medium for approx. 4 hours, until the cells were deposited in an array. MOLM-13 cells were stained in 1 μM CellTracker™ Green CMFDA dye (Thermo Fischer Scientific, Waltham, MA USA) for 15 min in serum-free media in 37 °C, followed by 1 h of recovery in complete media. Then stained cells were seeded into the wells (10 000 cells per well), and after 2 hours the culture medium was exchanged to Leibovitz's L15 medium with GlutaMAX (Gibco®, Life Technologies) supplemented with 10% (vol/vol) FBS. Meanwhile, final solutions with the appropriate number of MACS enriched NK cells and the desired concentration of the SPM-2 triplebody or control agents were prepared and added to the channels/wells. A trypan blue exclusion test of the NK cells was performed immediately before the preparation of the final solutions.

Imaging was performed under an inverted Nikon Ti eclipse microscope with a motorized stage, a Plan Apochromat 4×/0.2 N.A. objective, an Andor Clara-E camera, and a Lumencor SOLA LED lamp. For detection of PI fluorescence a filter cube with 540/25 nm (excitation) and 630/60 nm (emission) filters was used. For the stained MOLM-13 cells a filter cube with 470/40 nm (excitation) and 525/50 nm (emission) filters was used. Images were taken with constant exposure times of 10 and 300 ms in the brightfield and the PI/Green CMFDA channels respectively at 12 min intervals for 16 hours. A pre-determined *X*–*Y* position list was used for the automated time-lapse recording of 84 positions for each measurement. During the recording samples were kept at a constant temperature of 37 °C using an ibidi heating system (ibidi GmbH).

Image and data analysis

Raw images were pre-processed with ImageJ (http://imagej.nih.gov/ij/). Using an in-house plugin, Microwell Analysis, an orthogonal grid was aligned over cells and single-cell occupied grid positions were selected. The mean intensities over the selected positions of the grid were extracted and exported to a data file. Custom Matlab scripts (MATLAB version R2014b Natick, Massachusetts: The MathWorks Inc., 2014) were employed to quantify the number of dead target cells and to find their lysis time-points based on the maximum slope of the signal increase in the PI channel. In the representative set of data, a threshold was chosen as a maximum value that can separate the weakest signal of a dead target cell from the background signals *e.g.* from healthy cells. Further analysis confirmed that the threshold was at least 4 times higher than the background fluorescence intensity of the healthy cells in the PI channel. Specific lysis was calculated as:

$$\text{specific lysis\%} = \left(\frac{\text{fraction lysed with SPM2} - \text{fraction lysed without SPM2}}{\text{total cells} - \text{spontaneous cell deaths}}\right) \times 100\%$$

Redirected lysis (RDL) assays using calcein release

Target cells HEK293.123 were pre-labeled with Calcein AM (Life Technologies) and mixed with MACS-purified NK cells in RPMI 1640 GlutaMAX medium supplemented with 10% (vol/vol) FBS at E : T = 2 : 1. SPM-2 triplebody was added at the desired concentration to a 200 μL reaction volume in round-bottom 96-well plates. Reactions were incubated at 37 °C with 5% CO_2 for 4 hours. Calcein release was quantitated by measuring the fluorescence intensity (relative light units, RLU) in the supernatant using a fluorimeter/ELISA plate reader at 485/535 nm. Maximum lysis was achieved by addition of 50 μL of a solution containing 10% Triton X-100 in RPMI 1640 GlutaMAX medium supplemented with 10% (vol/vol) FBS and 1% (vol/vol) PS. Specific cellular cytotoxicity was expressed as overall lysis minus the background of spontaneous lysis mediated by the NK cells alone, in the absence of added antibody-reagents. Specific lysis was evaluated by the formula:

$$\text{specific lysis\%} = \left(\frac{\text{RLU(sample)} - \text{RLU(background)}}{\text{RLU(maximum lysis)} - \text{RLU(background)}}\right) \times 100\%$$

Statistical analysis

In the case of the single-cell cytometry (SCC) assay we hypothesized that data follow the binomial distribution and error bars were calculated with a confidence level of 95%.

Statistical modeling of the calcein assay and single cell assay results

Statistical modeling of the single cell assay. Five different conditions were interrogated (0, 0.01, 0.1, 1, and 10 nM). For every condition we considered the number of dead cells and

Published on 09 March 2016. Downloaded by Ludwig Maximilians Universitaet Muenchen on 14/03/2016 09:19:59.

the number of cells in total. The problem at hand was to calculate the EC50 and its confidence interval of the dose response curve with measurements in these 5 conditions/concentrations. The concentrations correspond to the independent variable, and the ratio of dead cells/total cells corresponds to the response variable of the model (curve). From here on the $\log_{10}$ of the concentrations was used.

We hypothesized that the killing events in every condition can be modeled using a binomial distribution. The metrics of the binomial distributions were calculated using the binofit() function in Matlab. Then, these binomial distributions were sampled with replacement to generate 1000 random measurements (in terms of dead cells) per condition (concentration). From this random sampled number of dead cells we subtracted the number of dead cells observed for the 0 nM condition and divided by the corresponding number of total cells, having subtracted the number of spontaneous cell death events. This number corresponds to the specific killing ratio. Dose response curves in the form of a sigmoid curve were fitted for every set of random killing ratios, yielding 1000 random sampled dose response curves. The fit of the sigmoid curves was performed using the nlinfit() function in Matlab. From the sigmoid curves the parameters corresponding to the EC50 values were extracted and averaged across all 1000 random samplings yielding a mean value and a standard deviation.

Statistical modeling of the calcein assay. Here, we considered the specific lysis ratio measured directly using the calcein assay. The mean specific lysis ratios and corresponding standard deviations for the 5 conditions discussed above were used as an input to this analysis. We hypothesized that the lysis ratios in every condition can be modeled by using a normal distribution. We used these distributions in similar fashion as above to generate random measurements in terms of lysis ratios for every condition and to fit sigmoid curves to model dose response. From the sigmoid curves the terms corresponding to the EC50 were extracted and averaged across all random samplings to yield a mean and a standard deviation.

Conclusions

Single cell arrays combined with time-resolved fluorescence microscopy were used to study the interaction of primary human NK cells with human target cells mediated by triplebody SPM-2, an antibody-derived protein, which recruits NK cells for target cell lysis. The arrayed pattern of target cells allowed for highly efficient and automated counting of lytic events under standardized conditions. Lysis depended on the dose of the agent and the E : T ratio in a manner typical for standard cytolysis assays, and therefore this new assay was validated relative to existing standard procedures (calcein release assay). Use of the new SCC assay revealed so far unreported changes in the killing rate over long-term reaction periods (16 hours). Finally, a variation of the assay employing surface-coated antibodies demonstrated the feasibility to array non-adherent target cells in the chip-based single-cell cytometric assay. The proposed platform facilitates testing the susceptibility of many tumor-derived cell types to lysis by NK cells with or without an added mediator protein and can become a useful tool for the design of personalized therapies.

Disclosure of potential conflict of interest

The authors declare no conflict of interest.

Acknowledgements

Financial support by the Deutsche Forschungsgemeinschaft within the Excellence Graduate School Quantitative Bio-Sciences (QBM) and the program project grant (Sonderforschungsbereich) SFB 1032 (project B01) is gratefully acknowledged. Drs. Oduncu, Hopfner and Fey were funded by an M4 Excellence Award for Personalized Medicine from the Bavarian Ministry for Trade and the Economy. We thank Dr. Christoph Stein, Fraunhofer Institute, Aachen, Germany, for the kind gift of the HEK293.123 cell line. We are grateful to Max Albert for wafer and chip fabrication, and to Peter J. Röttgermann for microscopic pictures of the fibronectin-coated arrays.

References

1 L. Weiner, J. Murray and C. Shuptrine, *Cell*, 2012, **148**, 1081–1084.
2 P. McLaughlin, A. J. Grillo-López, B. K. Link, R. Levy, M. S. Czuczman, M. E. Williams, M. R. Heyman, I. Bence-Bruckler, C. A. White, F. Cabanillas, V. Jain, A. D. Ho, J. Lister, K. Wey, D. Shen and B. K. Dallaire, *J. Clin. Oncol.*, 1998, **16**, 2825–2833.
3 T. Dreier, G. Lorenczewski, C. Brandl, P. Hoffmann, U. Syring, F. Hanakam, P. Kufer, G. Riethmuller, R. Bargou and P. A. Baeuerle, *Int. J. Cancer*, 2002, **100**, 690–697.
4 R. Bargou, E. Leo, G. Zugmaier, M. Klinger, M. Goebeler, S. Knop, R. Noppeney, A. Viardot, G. Hess, M. Schuler, H. Einsele, C. Brandl, A. Wolf, P. Kirchinger, P. Klappers, M. Schmidt, G. Riethmüller, C. Reinhardt, P. Baeuerle and P. Kufer, *Science*, 2008, **321**, 974–977.
5 M. Aigner, J. Feulner, S. Schaffer, R. Kischel, P. Kufer, K. Schneider, A. Henn, B. Rattel, M. Friedrich, P. A. Baeuerle, A. Mackensen and S. W. Krause, *Leukemia*, 2013, **27**, 1107–1115.
6 M. Friedrich, A. Henn, T. Raum, M. Bajtus, K. Matthes, L. Hendrich, J. Wahl, P. Hoffmann, R. Kischel, M. Kvesic, J. W. Slootstra, P. A. Baeuerle, P. Kufer and B. Rattel, *Mol. Cancer Ther.*, 2014, **13**, 1549–1557.
7 C. go. identifier NCT02152956.

 This journal is © The Royal Society of Chemistry 2016

Published on 09 March 2016. Downloaded by Ludwig Maximilians Universitaet Muenchen on 14/03/2016 09:19:59.

8 T. Takai, M. Li, D. Sylvestre, R. Clynes and J. V. Ravetch, *Cell*, 1994, **76**, 519–529.
9 G. Cartron, L. Dacheux, G. Salles, P. Solal-Celigny, P. Bardos, P. Colombat and H. Watier, *Blood*, 2002, **99**, 754–758.
10 W.-K. K. Weng and R. Levy, *J. Clin. Oncol.*, 2003, **21**, 3940–3947.
11 M. Albanesi, D. A. Mancardi, L. E. Macdonald, B. Iannascoli, L. Zitvogel, A. J. Murphy, M. Daëron, J. H. Leusen and P. Bruhns, *J. Immunol.*, 2012, **189**, 5513–5517.
12 F. Nimmerjahn and J. V. Ravetch, *Nat. Rev. Immunol.*, 2008, **8**, 34–47.
13 R. T. T. Costello, S. Sivori, E. Marcenaro, M. Lafage-Pochitaloff, M.-J. J. Mozziconacci, D. Reviron, J.-A. A. Gastaut, D. Pende, D. Olive and A. Moretta, *Blood*, 2002, **99**, 3661–3667.
14 C. Fauriat, S. Just-Landi, F. Mallet, C. Arnoulet, D. Sainty, D. Olive and R. T. Costello, *Blood*, 2007, **109**, 323–330.
15 E. Lion, Y. Willemen, Z. N. Berneman, V. F. Van Tendeloo and E. L. Smits, *Leukemia*, 2012, **26**, 2019–2026.
16 T. Braciak, S. Wildenhain, C. Roskopf, I. Schubert, G. Fey, U. Jacob, K.-P. Hopfner and F. Oduncu, *J. Transl. Med.*, 2013, **11**, 289.
17 K. T. Brunner, J. Mauel, J. C. Cerottini and B. Chapuis, *Immunology*, 1968, **14**, 181–196.
18 I. Schubert, D. Saul, S. Nowecki, A. Mackensen, G. H. Fey and F. S. Oduncu, *mAbs*, 2014, **6**, 286–296.
19 D. L. Nelson, C. C. Kurman and D. E. Serbousek, *Curr. Protoc. Immunol.*, 2001, Ch. 7, Unit 7.27.
20 R. Bhat and C. Watzl, *PLoS One*, 2007, **2**, e326.
21 J. Albeck, J. Burke, B. Aldridge, M. Zhang, D. Lauffenburger and P. Sorger, *Mol. Cell.*, 2008, **30**, 11–25.
22 P. Choi and T. Mitchison, *Proc. Natl. Acad. Sci. U. S. A.*, 2013, **110**, 6488–6493.
23 G. Romain, V. Senyukov, N. Rey-Villamizar, A. Merouane, W. Kelton, I. Liadi, A. Mahendra, W. Charab, G. Georgiou, B. Roysam, D. A. Lee and N. Varadarajan, *Blood*, 2014, **124**, 3241–3249.
24 E. Forslund, K. Guldevall, P. E. Olofsson, T. Frisk, A. E. Christakou, M. Wiklund and B. Onfelt, *Front. Immunol.*, 2012, **3**, 300.
25 Unknown.
26 P. E. Olofsson, E. Forslund, B. Vanherberghen, K. Chechet, O. Mickelin, A. R. Ahlin, T. Everhorn and B. Onfelt, *Front. Immunol.*, 2014, **5**, 80.
27 C. Shuptrine, R. Surana and L. Weiner, *Semin. Cancer Biol.*, 2012, **22**, 3–13.
28 A. Scott, J. Wolchok and L. Old, *Nat. Rev. Cancer*, 2012, **12**, 278–287.
29 P. J. Carter, *Nat. Rev. Immunol.*, 2006, **6**, 343–357.
30 R. E. Kontermann, *mAbs*, 2012, **4**, 182–197.
31 R. Kontermann and U. Brinkmann, *Drug Discovery Today*, 2015, 838–847.
32 C. Spiess, Q. Zhai and P. J. Carter, *Mol. Immunol.*, 2015, 95–106.
33 C. Kellner, J. Bruenke, J. Stieglmaier, M. Schwemmlein, M. Schwenkert, H. Singer, K. Mentz, M. Peipp, P. Lang, F. Oduncu, B. Stockmeyer and G. H. Fey, *J. Immunother.*, 2008, **31**, 871–884.
34 M. Kügler, C. Stein, C. Kellner, K. Mentz, D. Saul, M. Schwenkert, I. Schubert, H. Singer, F. Oduncu, B. Stockmeyer, A. Mackensen and G. H. Fey, *Br. J. Haematol.*, 2010, **150**, 574–586.
35 H. Singer, C. Kellner, H. Lanig, M. Aigner, B. Stockmeyer, F. Oduncu, M. Schwemmlein, C. Stein, K. Mentz, A. Mackensen and G. H. Fey, *J. Immunother.*, 2010, **33**, 599–608.
36 J. M. Rowe and B. Löwenberg, *Blood*, 2013, **121**, 4838–4841.
37 P. J. Röttgermann, A. P. Alberola and J. O. Rädler, *Soft Matter*, 2014, **10**, 2397–2404.
38 M. Ferizi, C. Leonhardt, C. Meggle, M. Aneja, C. Rudolph, C. Plank and J. Rädler, *Lab on a Chip*, 2015, **15**, 3561–3571.
39 E. Alici, T. Sutlu, B. Björkstrand, M. Gilljam, B. Stellan, H. Nahi, H. C. Quezada, G. Gahrton, H.-G. G. Ljunggren and M. S. Dilber, *Blood*, 2008, **111**, 3155–3162.
40 M. J. Smyth, E. Cretney, J. M. Kelly, J. A. Westwood, S. E. Street, H. Yagita, K. Takeda, S. L. van Dommelen, M. A. Degli-Esposti and Y. Hayakawa, *Mol. Immunol.*, 2005, **42**, 501–510.
41 M. Cheng, Y. Chen, W. Xiao, R. Sun and Z. Tian, *Cell. Mol. Immunol.*, 2013, **10**, 230–252.
42 B. Vanherberghen, P. E. Olofsson, E. Forslund, M. Sternberg-Simon, M. A. Khorshidi, S. Pacouret, K. Guldevall, M. Enqvist, K.-J. J. Malmberg, R. Mehr and B. Önfelt, *Blood*, 2013, **121**, 1326–1334.
43 A. Poggi, A.-M. Massaro, S. Negrini, P. Contini and M. Zocchi, *J. Immunol.*, 2005, **174**, 2653–2660.
44 G. M. Spaggiari, P. Contini, A. Dondero, R. Carosio, F. Puppo, F. Indiveri, M. R. Zocchi and A. Poggi, *Blood*, 2002, **100**, 4098–4107.
45 Y. Matsuo, R. A. MacLeod, C. C. Uphoff, H. G. Drexler, C. Nishizaki, Y. Katayama, G. Kimura, N. Fujii, E. Omoto, M. Harada and K. Orita, *Leukemia*, 1997, **11**, 1469–1477.
46 A. Malyguine, S. Strobl, K. Dunham, M. Shurin and T. Sayers, *Cells*, 2012, **1**, 111–126.
47 E. Ranieri, I. Popescu and M. Gigante, *Methods Mol. Biol.*, 2014, **1186**, 75–86.
48 C. C. Roskopf, C. B. Schiller, T. A. Braciak, S. Kobold, I. A. Schubert, G. H. Fey, K.-P. P. Hopfner and F. S. Oduncu, *OncoTargets Ther.*, 2014, **5**, 6466–6483.
49 A. Ehninger, M. Kramer, C. Röllig, C. Thiede, M. Bornhäuser, M. von Bonin, M. Wermke, A. Feldmann, M. Bachmann, G. Ehninger and U. Oelschlägel, *Blood Cancer J.*, 2014, **4**, e218.
50 T. A. Braciak, C. C. Roskopf, S. Wildenhain, N. Fenn, C. Schiller, I. A. Schubert, U. Jacob, A. Honegger, C. Krupka, M. Subklewe, K. Spiekermann, K.-P. Hopfner, G. H. Fey, M. Aigner, S. Krause, A. Machensen and F. S. Oduncu, *OncoTargets Ther.*, in press.

Published on 09 March 2016. Downloaded by Ludwig Maximilians Universitaet Muenchen on 14/03/2016 09:19:59.

51 A. Burnett, M. Wetzler and B. Löwenberg, *J. Clin. Oncol.*, 2011, **29**, 487–494.
52 C. T. Jordan, D. Upchurch, S. J. Szilvassy, M. L. Guzman, D. S. Howard, A. L. Pettigrew, T. Meyerrose, R. Rossi, B. Grimes, D. A. Rizzieri, S. M. Luger and G. L. Phillips, *Leukemia*, 2000, **14**, 1777–1784.
53 A. W. Hauswirth, S. Florian, D. Printz, K. Sotlar, M.-T. T. Krauth, G. Fritsch, G.-H. H. Schernthaner, V. Wacheck, E. Selzer, W. R. Sperr and P. Valent, *Eur. J. Clin. Invest.*, 2007, **37**, 73–82.
54 R. B. Walter, F. R. Appelbaum, E. H. Estey and I. D. Bernstein, *Blood*, 2012, **119**, 6198–6208.
55 F. Vergez, A. S. Green, J. Tamburini, J.-E. E. Sarry, B. Gaillard, P. Cornillet-Lefebvre, M. Pannetier, A. Neyret, N. Chapuis, N. Ifrah, F. Dreyfus, S. Manenti, C. Demur, E. Delabesse, C. Lacombe, P. Mayeux, D. Bouscary, C. Recher and V. Bardet, *Haematologica*, 2011, **96**, 1792–1798.
56 C. Arndt, A. Feldmann, M. von Bonin, M. Cartellieri, E.-M. M. Ewen, S. Koristka, I. Michalk, S. Stamova, N. Berndt, A. Gocht, M. Bornhäuser, G. Ehninger, M. Schmitz and M. Bachmann, *Leukemia*, 2014, **28**, 59–69.
57 C. Stein, C. Kellner, M. Kügler, N. Reiff, K. Mentz, M. Schwenkert, B. Stockmeyer, A. Mackensen and G. Fey, *Br. J. Haematol.*, 2010, **148**, 879–889.

This journal is © The Royal Society of Chemistry 2016

Electronic Supplementary Material (ESI) for Analyst.
This journal is © The Royal Society of Chemistry 2016

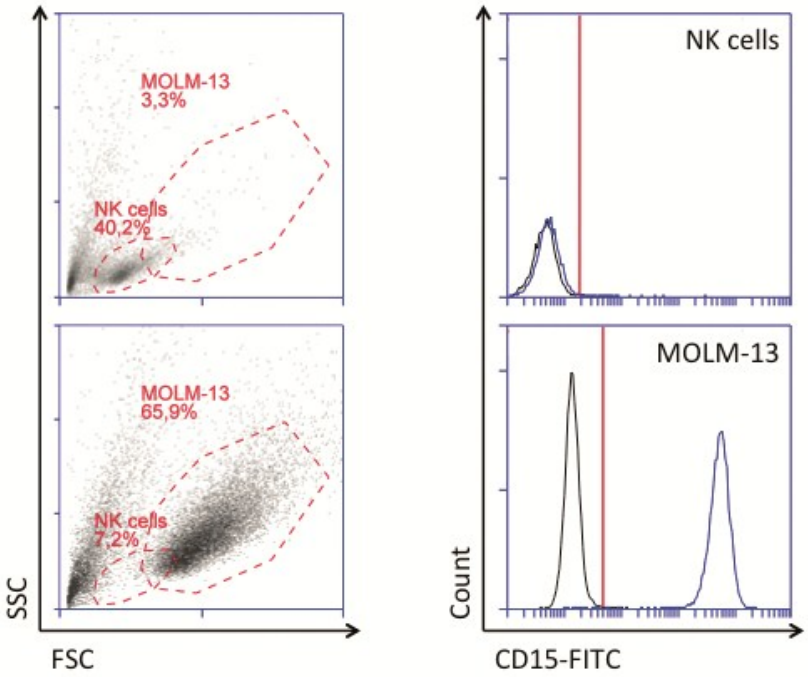

Expression profile of the cd15 myeloid expression marker on molm-13 and nk cells.

2.4 Dual-targeting triplebody 33-3-19 mediates selective lysis of biphenotypic CD19$^+$ CD33$^+$ leukemia cells

Claudia C. Roskopf, Todd A. Braciak, Nadja C. Fenn, Sebastian Kobold, Georg H. Fey,
Karl-Peter Hopfner & Fuat S. Oduncu

Oncotarget 2016 Apr 19; **7** (16): 22579-22589
DOI: 10.18632/oncotarget.8022

2.4.1 Summary

Targeted immunotherapy is limited by the lack of tumor-specific antigens. However, cancer cells can sometimes be distinguished immunophenotypically by the co-expression of two or more TAA. Such cases offer an intriguing opportunity for selective and individualized immunotherapy with multi-specific antibody derivatives such as single-chain triplebodies. The blasts in mixed phenotype acute leukemia, for instance biphenotypic B/myeloid leukemia cells, are an example for co-expression-dependent immunophenotypic distinction. In the present study, the T cell-engaging triplebody 33-3-19 was constructed and found to lyse biphenotypic CD19$^+$ CD33$^+$ leukemia cells preferentially over CD19 single-positive cells.

Triplebody 33-3-19 was generated by replacing the N-terminal CD19 scFv from the previously characterized 19-3-19^{248} construct with a humanized CD33-specific scFv. It was produced in stably transfected FreeStyle™ 293F production cell pools and purified by Ni-NTA affinity and size exclusion chromatography to yield 0.5 to 1.5 mg monomeric protein per liter supernatant. The triplebody displayed a marked aggregation tendency and had two melting points at 58.5°C (CD19 and CD3ε scFv) and 70°C (CD33 scFv). Stabilization attempts by targeted mutagenesis and disulfide-stabilization failed.

33-3-19 bound specifically to its three target antigens and had a strong biological activity, which decreased after two months of storage at -80°C. Similar to prototype 19-3-19, triplebody 33-3-19 activated freshly isolated, non-stimulated T cells in cytolysis assays. T cell activation dynamics were donor-dependent, but maximum target cell depletion (94.2 to 99.6%) was generally achieved after 48 hours. For the induction of redirected lysis (RDL) the presence of either CD19 or CD33 on the target cell surface was sufficient, but no activation occurred in the absence of both targets. B lymphoid and myeloid cancer cell lines responded in a dose-dependent manner to 33-3-19 treatment with EC_{50}-values for the B lymphoid targets ranging from 3 to 460 pM and ranging from 0.1 to 2.4 nM for the myeloid targets. Higher maximum lysis and lower EC_{50}-values correlated with

higher target antigen densities. In addition to depletion of the bulk leukemia cells, 33-3-19 also led to the lysis of more than 97% of colony forming cells (CFC) from the BV173 and MOLM-13 cell lines. 33-3-19 in combination with T cells also depleted primary blasts from patients with MPAL, B-ALL and B-CLL in a dose-dependent manner.

Finally, the selectivity of lysis that is mediated by dual-targeting triplebody 33-3-19 was assessed in cytolysis assays with mixed CD19 single-positive (sp; SEM) and CD19 and CD33 double-positive (dp; BV173) target cell populations with comparable target antigen densities: In a flow cytometric approach three times more sp SEM target cells survived cytolysis than dp BV173 target cells. The ratio of surviving cells (BV173/SEM) was 0.13, whereas the ratios of survivors upon treatment with monospecific triplebody 19-3-19 or the bispecific scFv (19-3 plus 33-3) were 0.68 and 0.66, respectively. Similarly, in a complementary calcein release-based cytolysis assay, the dp BV173 target cells displayed a 145-fold higher sensitivity towards 33-3-19 than the sp SEM cells, when both target cell populations were present in the reaction volume simultaneously. EC_{50}-values were 4.6 pM for BV173 and 667.7 pM for SEM cells. The dose-response of both cell lines was identical when the combination of bispecific scFv (19-3 plus 33-3) was used. EC_{50}-values were 6.1 pM (BV173) and 5.9 pM (SEM), respectively.

In conclusion, although the presence of one target antigen is sufficient to induce redirected lysis of cancer cells by T cell-engaging triplebody 33-3-19, the dual-targeting of CD19 and CD33 achieves target cell selectivity. A therapeutic window for this “selectivity effect” exists provided that sub-saturating triplebody concentrations are used. The therapeutic window as well as the limiting proteinchemical characteristics of 33-3-19 may be improved via affinity and stability engineering to provide a potentially useful therapeutic agent for the treatment of B/myeloid leukemias.

2.4.2 Contribution

I designed, purified and characterized triplebody 33-3-19 and control molecules, performed activation studies on T cells and investigated the cytolytic potential of triplebody 33-3-19 with respect to ALL and AML cell line targets, including their colony forming cells, and with respect to primary target cells from patients with different hematologic malignancies. Furthermore, I established two different approaches to determine selective lysis of $CD19^+CD33^+$ biphenotypic leukemia cells by 33-3-19 plus T cells in a reaction environment with mixed target cell populations. I am also the author of the manuscript, which was edited by Prof. Fey and reviewed by all co-authors.

Dual-targeting triplebody 33-3-19 mediates selective lysis of biphenotypic CD19+ CD33+ leukemia cells

Claudia C. Roskopf[1], Todd A. Braciak[1], Nadja C. Fenn[2], Sebastian Kobold[3], Georg H. Fey[4], Karl-Peter Hopfner[2], Fuat S. Oduncu[1]

[1]Klinikum der Universität München, Medizinische Klinik und Poliklinik IV, Hematology/Oncology, Munich, Germany

[2]Ludwig-Maximilians-Universität München, Department of Biochemistry and Gene Center, Munich, Germany

[3]Center for Integrated Protein Science (CIPSM) and Klinikum der Universität München, Medizinische Klinik und Poliklinik IV, Division of Clinical Pharmacology, Munich, Germany

[4]Friedrich-Alexander-University Erlangen-Nuremberg, Department of Biology, Erlangen, Germany

Correspondence to: *Claudia C. Roskopf,* ***e-mail:*** *Claudia.Roskopf@med.uni-muenchen.de*

Keywords: *leukemia, mixed phenotype acute leukemia (MPAL), immunotherapy, dual-targeting triplebody, selectivity*

Received: *November 11, 2015* ***Accepted:*** *February 23, 2016* ***Published:*** *March 10, 2016*

ABSTRACT

Simultaneous targeting of multiple tumor-associated antigens (TAAs) in cancer immunotherapy is presumed to enhance tumor cell selectivity and to reduce immune escape.

The combination of B lymphoid marker CD19 and myeloid marker CD33 is exclusively present on biphenotypic B/myeloid leukemia cells. Triplebody 33-3-19 binds specifically to both of these TAAs and activates T cells as immune effectors. Thereby it induces specific lysis of established myeloid (MOLM13, THP-1) and B-lymphoid cell lines (BV173, SEM, Raji, ARH77) as well as of primary patient cells. EC_{50} values range from 3 pM to 2.4 nM. In accordance with our hypothesis, 33-3-19 is able to induce preferential lysis of double- rather than single-positive leukemia cells in a target cell mixture: CD19/CD33 double-positive BV173 cells were eliminated to a significantly greater extent than CD19 single-positive SEM cells (36.6% vs. 20.9% in 3 hours, p = 0.0048) in the presence of both cell lines. In contrast, equivalent elimination efficiencies were observed for both cell lines, when control triplebody 19-3-19 or a mixture of the bispecific single chain variable fragments 19-3 and 33-3 were used. This result highlights the potential of dual-targeting agents for efficient and selective immune-intervention in leukemia patients.

INTRODUCTION

In acute leukemia of ambiguous origin with B/myeloid or trilineage phenotype (ca. 2 – 3% of all acute leukemias) and B-ALL or AML with aberrant antigen expression, the B lymphoid lineage marker CD19 and myeloid lineage marker CD33 are simultaneously displayed on the blast cell surface [1, 2]. Acute leukemias with co-expression of CD19 and CD33 usually have a poor prognosis [1, 3, 4]. In addition, there is no consensus regarding treatment protocols for mixed phenotype acute leukemias (MPAL) due to the rarity of these hematopoietic neoplasms and lack of clinical studies in this specific patient population [3, 5–7]. However, both CD19 and CD33 are validated therapeutic targets. The co-expression of these two lineage markers may offer unique opportunities for selective, individualized immunotherapy with novel antibody-derived agents, because the leukemia cells are immunophenotypically distinct from the corresponding healthy cells. By targeting both tumor-associated antigens, i.e. CD19 and CD33, at the same time, selectivity of elimination may be achieved and immune escape will likely be reduced, because antigen double-negative leukemia cell clones are less likely to be selected than single-negative ones [8, 9].

A number of multi-specific antibody-derived molecular formats have emerged over the past 25 years [8, 10] including the single chain triplebody platform. Single chain triplebodies are polypeptides that are composed of three single chain variable fragments

(scFvs) connected by flexible linkers. They are bi-specific for the target cell and mono-specific for the effector cell [11, 12]. In the classical triplebody format immune effector cells are engaged and activated via the central scFv, which binds to a trigger antigen such as FcγRIII (CD16) on NK cells and macrophages, CD64 or CD89 on neutrophilic granulocytes or the CD3-epsilon chain on T cells. The two distal scFvs in dual-targeting triplebodies bind to two different TAAs on the cancer cell surface. By coupling the recruited immune effector cell to the targeted cancer cell in an Fc receptor- and MHC:peptide-complex-independent manner, the immune effectors are activated and redirected against the target cells [11, 12]. This mode of action - referred to as redirected lysis (RDL) - is also employed by Bispecific T cell Engagers (BiTE®s), including Blinatumomab (BlinCyto™) and AMG330, which target CD19 and CD33, respectively [13–15]. Blinatumomab is the first-in-class of a new group of biotherapeutics after its FDA-approval for the treatment of relapsed and refractory adult B-ALL in December 2014. However, BiTE®s have a number of limitations including their low molecular weight (55 – 60 kD), which results in a serum half-life of only 1.5 to 2 hours [14, 15], and targeting of a single tumor-associated antigen (TAA). Since the latter is not tumor-specific, it does not allow for a very strong discrimination between malignant and normal antigen-positive target cells.

Triplebodies have a molecular mass of 80 to 90 kDa, which is above the threshold of immediate renal clearance. This is reflected in their extended serum half-life of 4 hours in mice in comparison to 2 hours for bispecific single chain Fvs (bsscFvs) [16]. Based on the slower clearance rate compared to bsscFvs, the smaller size compared to monoclonal antibodies and their capacity for multivalent tumor targeting, triplebodies are expected to achieve an efficient penetration of solid tissues [10, 11, 17]. A number of different triplebodies have been developed, which are capable of recruiting NK cells, γδ T cells and T cells as immune effector cell populations for RDL and of targeting a variety of different TAAs that are relevant in hematopoietic malignancies [16, 18–23].

In the present study, we constructed a T cell-recruiting triplebody 33-3-19 to explore the question whether preferential lysis of B/myeloid cancer cells relative to cells expressing only one lineage marker is also possible with the help of T cells as cytolytic effectors. Triplebody 33-3-19 was able to activate resting T cells to induce their proliferation and effector cell activity. Moreover, it enhanced the selective lysis of CD19/CD33 double-positive leukemia cells relative to CD19 single-positive targets with comparable target antigen density, which were present in the same reaction environment. These results lend further support to the concept of enhanced selectivity of lysis mediated by dual-targeting.

RESULTS

Construction and properties of dual-targeting T cell-engaging triplebody 33-3-19

To clone the triplebody 33-3-19 (Figure 1A), the N-terminal anti-CD19 single chain variable fragment (scFv), which was encoded at the 5'-end of the 19-3-19 gene in a pSecTag2-HygroC mammalian expression vector [21], was replaced by a humanized anti-CD33 scFv. Triplebody 33-3-19 and control proteins were purified from the supernatant of stably transfected Freestyle 293F cell pools by Ni-NTA affinity (Figure S1A) and size exclusion (Figure S1B) chromatography. Between 0.5 to 1.5 mg monomeric triplebody were obtained on average from 1 L of culture supernatant. As can be inferred from the size exclusion chromatogram (Figure S1B), triplebody 33-3-19 displayed a marked aggregation tendency. The protein's thermostability was measured by thermal shift assays and two melting points at 58.5 °C (CD19 and CD3 scFvs) and at 70 °C (CD33 scFv) were recorded. The biological activity of 33-3-19, which was determined from its EC_{50}-value in a standard redirected lysis (RDL) experiment against SEM target cells at different time points post production (data not shown), weakened over time, in spite of stabilization attempts via a variety of formulation-buffers, disulfide stabilization and site-directed mutagenesis (data not shown). However, triplebody 33-3-19 was suitable for proof-of-concept studies as it bound specifically to its three target antigens CD33, CD3-epsilon and CD19 (Figure 1B) and displayed a strong biological activity when used within one to two months after production.

Activation of resting T cells by triplebody 33-3-19

We first tested the ability of 33-3-19 to activate resting T cells. 33-3-19 was added to cytolysis reactions of unstimulated mononuclear cells (MNCs) from healthy donors, which were mixed with SEM (CD19-positive pre-B ALL cell line) target cells at an effector-to-target (E : T) ratio of 1 : 2. Within 24 to 48 hours after treatment with 33-3-19, the expression of early activation marker CD69 on the surface of the $CD3^+$ cell population was strongly increased (Figure 1C). Expression of CD25, the alpha-chain of the IL-2 receptor, on the T cell surface was also increased (Figure 1C) with different kinetics than CD69. The response patterns for the expression of activation markers varied considerably between different blood donors, but upon reaching peak cytolysis levels of 94.2 - 99.6 % of target cells after 48 hours, the levels of both CD69 and CD25 on the T cell surface began to drop again in each case. Addition of triplebody 33-3-19 to T cells without antigen-positive target cells did not lead to the elevation of activation marker levels (data not shown),

nor did the addition of a Her2-3-Her2 control triplebody to a reaction mixture containing T lymphocytes and leukemia cells (Figure 1C). This result suggests that T cell activation was not due to HLA-mismatch between donor and leukemia cells. Further, the presence of target antigen, which was physically linked to the surface of the T cell via the mediator protein, was thus an essential requirement for triplebody-mediated activation of T lymphocytes.

In parallel to the elevation of activation markers on the T cell surface, a donor-dependent elevation of the concentration of cytokines IL-2, IL-6, IL-10, TNFα and IFN-γ in the supernatant was detected (Figure S2A). To further analyze the impact of 33-3-19 on T cell proliferation, MNCs were fluorescently labelled with the cell proliferation dye CellTrace™ CFSE prior to the cytolysis reaction. More than 60 % of $CD3^+$ cells had already run through 1 to 3 cell cycles after 72 hours (Figure 1D). After 120 hours more than 97 % of T cells had proliferated (Figure S2B). No cytokine release or T cell proliferation was observed in control reactions without triplebody or with the specificity-control triplebody Her2-3-Her2.

Efficient redirected lysis of ALL and AML target cell lines

To determine the efficiency of 33-3-19-induced, T cell-mediated cytolysis of target antigen-positive cells, redirected lysis assays were performed with different AML and B cell lines as targets and with *ex vivo* expanded, pre-stimulated, allogeneic MNCs as effectors. An effector-to-target-cell ratio of 10 : 1 and an incubation time of 3 hours were employed. The expression of either CD19 or CD33 on the cancer cell surface was sufficient to induce cytolysis via 33-3-19 plus T cells (Figure 2A). However, cytolysis was not induced in the absence of target antigen on the cancer cells as determined with the specificity control Her2-3-Her2 (data not shown). The extent of cytolysis was concentration-dependent and a trend towards higher maximum lysis and

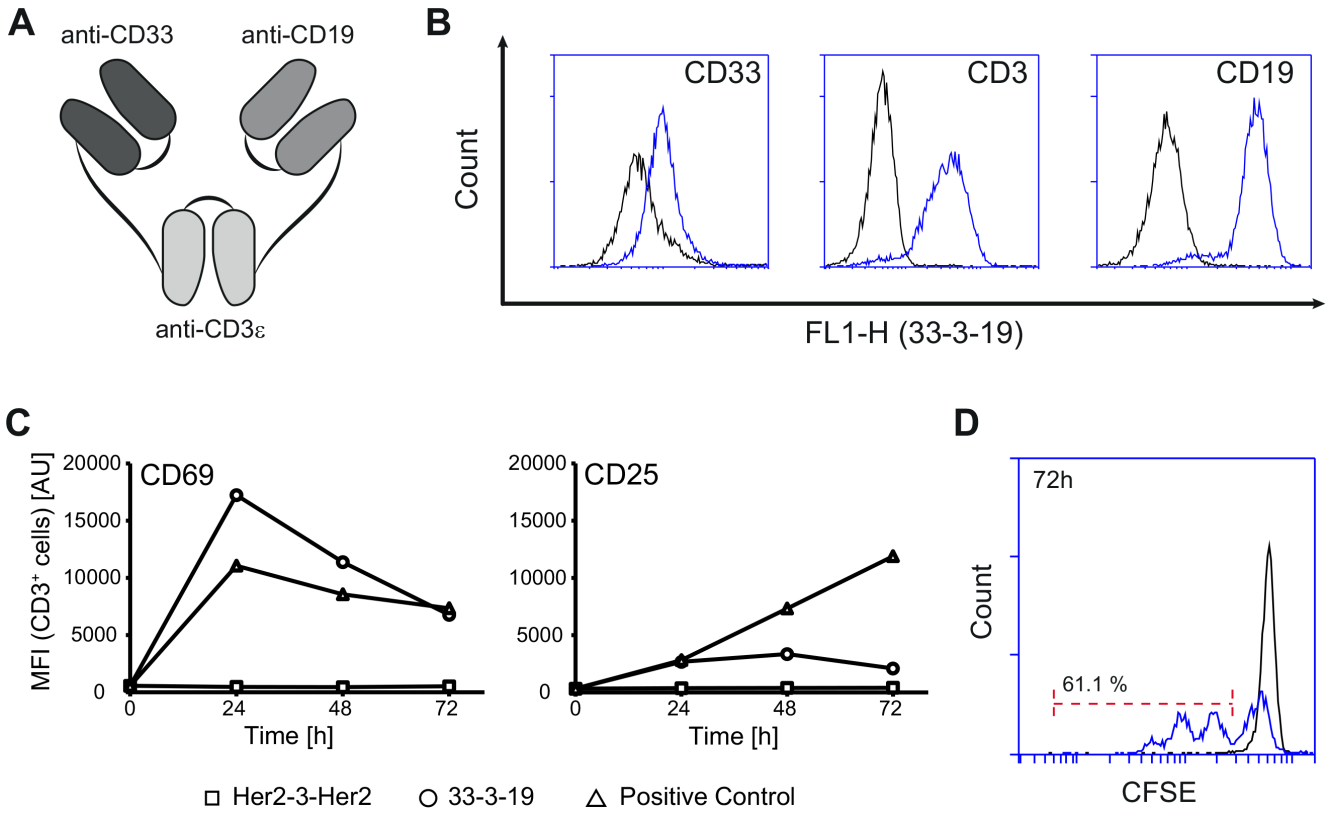

Figure 1: Specific binding and T cell-activation induced by dual-targeting triplebody 33-3-19. A. Design principle of 33-3-19. **B.** Specific binding of 33-3-19 to its target antigens as determined by cytofluorimetry. The antigen-positive targets used were the MOLM-13 (CD33) and SEM (CD19) cell lines and primary T cells (CD3) isolated from a healthy donor. No binding was observed to antigen-negative cells (HEK 293, data not shown). **C.** Non-stimulated PBMCs were incubated at an E : T ratio of 1 : 2 with SEM target cells and 1 nM triplebody or 2% PHA/100 U/mL IL-2 (pos. control) for 72 hours. The expression of activation markers CD69 and CD25 by effector T cells was assessed (n = 4). Representative data from one 28-yr old, healthy, male donor (70.4% $CD3^+$, 4.5% $CD19^+$) are shown. At time t_0 the overall content of CD19-positive cells in the reaction mixture (PBMCs + SEMs) was 14.6%. **D.** Non-stimulated PBMCs were labelled with 5 µM CFSE prior to incubation with SEM target cells at an E : T ratio of 1 : 2 and a cell density of $3 * 10^5$ / mL at t_0. T cell proliferation was assessed based on dilution of the CFSE cell proliferation dye (n = 3). Black = reaction without triplebody; blue = reaction with 1 nM 33-3-19.

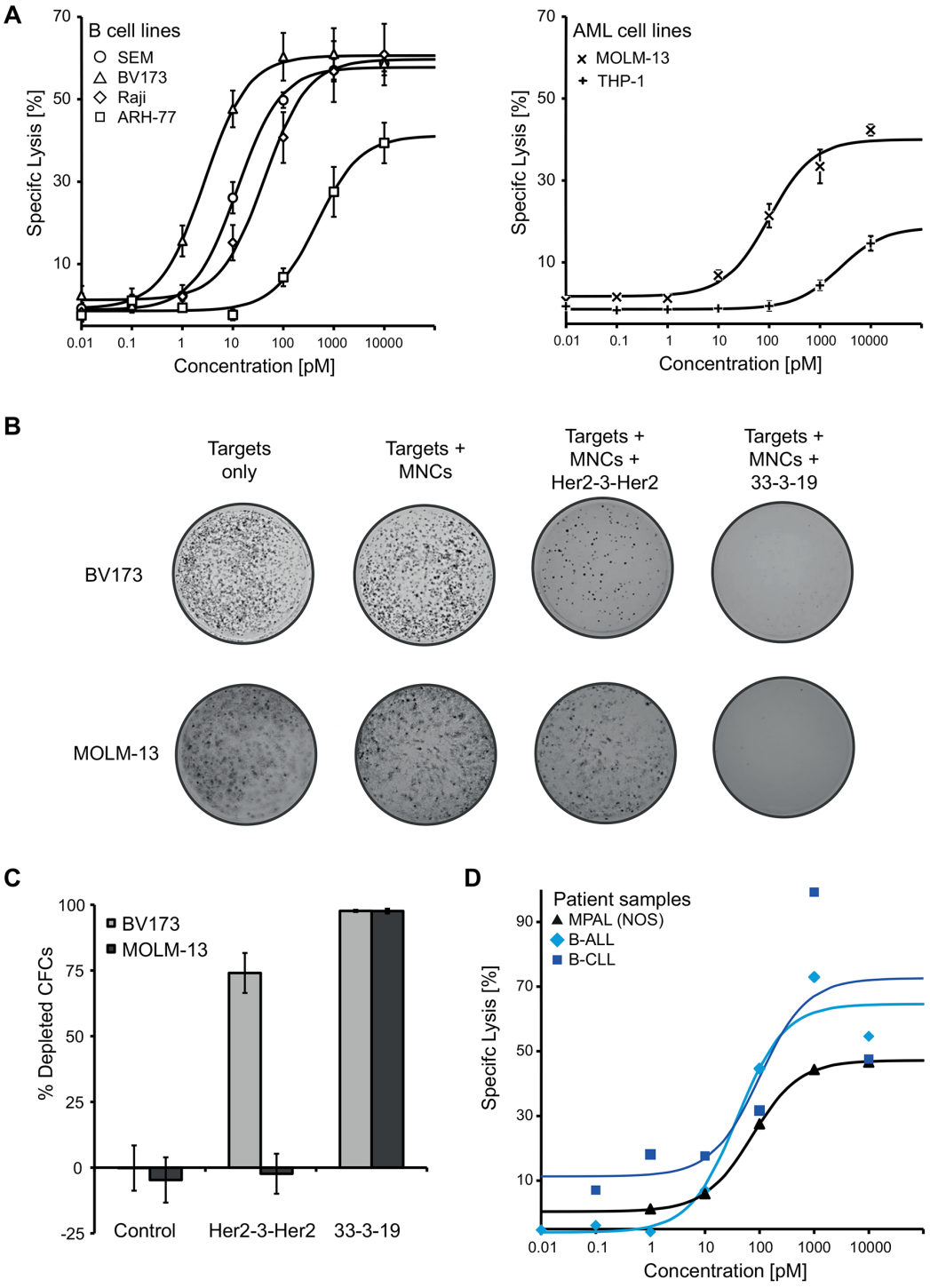

Figure 2: 33-3-19-mediated lysis of B and AML cell lines including their colony forming cells (CFCs), as well as of primary patient material. A. Dose-response of several B-lymphoid (left) and AML cell lines (right) representing different types of hematologic malignancies. No cytolytic response was observed, when the specificity-control triplebody Her2-3-Her2 was employed (data not shown). **B + C.** Cells were harvested post cytolysis and used in a human colony-forming cell (CFC) assay. 5.5 * 10^4 (MOLM-13 targets) or 1.1 * 10^5 cells (BV173 targets) were seeded into each well, respectively, which corresponds to 5,000 seeded MOLM-13 and 10,000 seeded BV173 cells (the remaining cells are the MNC effector cells). After 7 days, cells were stained with 1 mg/mL iodonitrotetrazolium-chloride solution overnight. Images were taken on the following day and colonies counted manually (n = 3 for each cell line). **D.** Dose-response of primary patient material (PBMCs) to treatment with triplebody 33-3-19 plus allogeneic PBMCs. All patient samples were collected at first diagnosis. The MPAL (NOS) patient displayed a trilineage phenotype (B lineage: $CD19^{high}$, $CD79a^{high}$; T lineage: $cyCD3^{+}$, $CD2^{+}$, $CD5^{high}$, $CD7^{high}$; myeloid lineage: MPO detectable, $CD33^{+}$, $CD117^{high}$).

Table 1: EC_{50}-values, maximum specific lysis and antigen density for 33-3-19-sensitive cell lines and patient samples

		Disease	EC_{50} (95% CI) [pM]	Max. spec. lysis [%]	Antigen Density [molecules/cell]	
					CD19	CD33
B cell lines	**SEM**	*Pre-B ALL*	12 (8 – 18)	58.7	50,000 ± 17,000	< 100
	BV173	*Pre-B ALL*	3 (1 – 6)	61.0	60,000 ± 11,000	4,500 ± 800
	Raji	*Burkitt's lymphoma*	42 (18 – 98)	60.8	31,000 ± 19,000	650 ± 100
	ARH77	*Plasma cell leukemia*	460 (179 – 1,177)	39.4	3,000 ± 2,000	< 100
AML cell lines	**MOLM-13**	*AML-M5a*	100 (58 – 173)	42.3	0	32,000 ± 6,500
	THP-1	*AML-M5*	2,442 (1,105 – 5,311)	14.6	0	17,000 ± 4,000
Patient samples		*ALL*	39 (9 – 165)	72.9	n.d	n.d.
		MPAL(NOS)	72 (63 – 84)	46.6	8,500 ± 3,000	300
		B-CLL	101 (1 – 44,550)	99.2	n.d.	n.d.

EC_{50}-values and maximum specific lysis were determined from the sigmoidal dose-response in 3 hour Calcein release cytolysis assays with an E : T Ratio of 10 : 1. Antigen density was determined by calibrated cytofluorimetry using the QifiKit (Dako) [28]. N.d. = not determined.

lower EC_{50}-values was observed with higher target antigen density on the cell surface (Table 1). EC_{50}-values for the B lymphoid cell lines were in the low picomolar range (3 – 460 pM). The tested AML-cell lines responded at higher triplebody concentrations with EC_{50}-values of 0.1 nM (MOLM-13) and 2.4 nM (THP-1), respectively (Table 1).

Elimination of potential leukemia-initiating cells

To achieve long-lasting remissions, it is necessary to eliminate those cancer cells that are capable of repopulating the cancer tissue, i.e. the leukemia-initiating cells (LICs) and especially the leukemia stem cells (LSCs). One hallmark of LICs is their colony-forming capacity. To investigate whether treatment with 33-3-19 leads to the eradication of LICs as well as bulk cancer cells, we performed colony forming cell (CFC) assays with the cells that had survived a 4 hour redirected lysis assay with or without triplebody. The addition of 33-3-19 resulted in the elimination of more than 97% of CFCs from a biphenotypic Philadelphia chromosome-positive B-precursor ALL cell line (BV173) as well as a $CD33^+$ AML M5a cell line (MOLM-13) (Figure 2B and 2C). This result points towards the capacity of triplebodies to eradicate potential LICs and warrants further careful examination in the future with primary patient cells as targets.

Redirected lysis of primary material from patients with different disease entities

To determine, whether triplebody 33-3-19 was also effective against primary cancer cells, redirected lysis assays were performed with primary cells from three patients, diagnosed with B-CLL, B-ALL and mixed phenotype acute leukemia (no other specification) (MPAL (NOS)), respectively. Each leukemia cell sample responded to treatment with 33-3-19 plus allogeneic effector cells in a dose-dependent manner, and maximum specific lysis values of 46.6% (MPAL (NOS)), 72.9% (B-ALL) and 99.2% (B-CLL) were achieved within 3 hours (Figure 2D, Table 1). EC_{50}-values ranged from 40 to 100 pM. The blasts from the patient with MPAL (NOS) displayed a combined (CD19 plus CD33) target antigen density of approximately 9,000 molecules/cell (Table 1). This - together with its maximum lysis and EC_{50}-value - supports the notion that combined target antigen density correlates with higher maximum specific lysis/lower EC_{50}-value. In the samples from the B-CLL and B-ALL patient a higher degree of specific lysis was achieved with 1 nM than with 10 nM triplebody (Figure 2D).

Enhanced selectivity of lysis for biphenotypic $CD19^+$ $CD33^+$ target cells

To assess whether the dual-targeting of CD19 and CD33 with a single molecule actually enhanced the selectivity of target cell lysis in a mixed environment, cytolysis experiments with mixed target cell populations were performed. The target cell population was composed of a mixture of CD19 single-positive SEM cells and CD19/CD33 double-positive BV173 cells. The SEM cell line was chosen, because of its comparably high target antigen density: SEM cells carried approximately 50,000 CD19 molecules and no detectable CD33 molecules on their surface, BV173 cells carried approximately 60,000 copies of CD19 and 4,500 copies of CD33 on their surface (Table 1).

In a first approach, the target cell populations were labelled with different concentrations of a permanent fluorescent dye and mixed with pre-stimulated MNCs at an E : T ratio of 1 : 6. After 12 hours the surviving target cells were enumerated cytofluorimetrically. Upon addition of 1 nM dual-targeting triplebody 33-3-19, the double-positive BV173 target cells were lysed preferentially over the single-positive SEM target cells, as demonstrated by a three-fold higher viability of the SEM cells (Figure 3A). In contrast, the monospecific bivalent triplebody 19-3-19 or a mixture of the bsscFvs (19-3 plus 33-3) reduced both populations to a similar extent: treatment with 33-3-19 resulted in a ratio of 0.13 for surviving BV173-to-SEM target cells (Figure 3B), while treatment with the bsscFv mixture (19-3 plus 33-3) resulted in a significantly different ratio of 0.66 (t-test, p = 0.007). Treatment with 19-3-19 resulted in a ratio of 0.68 for surviving BV173-to-SEM target cells (t-test, p = 0.067).

To confirm these results by a complementary method, we now labeled each cell type independently with

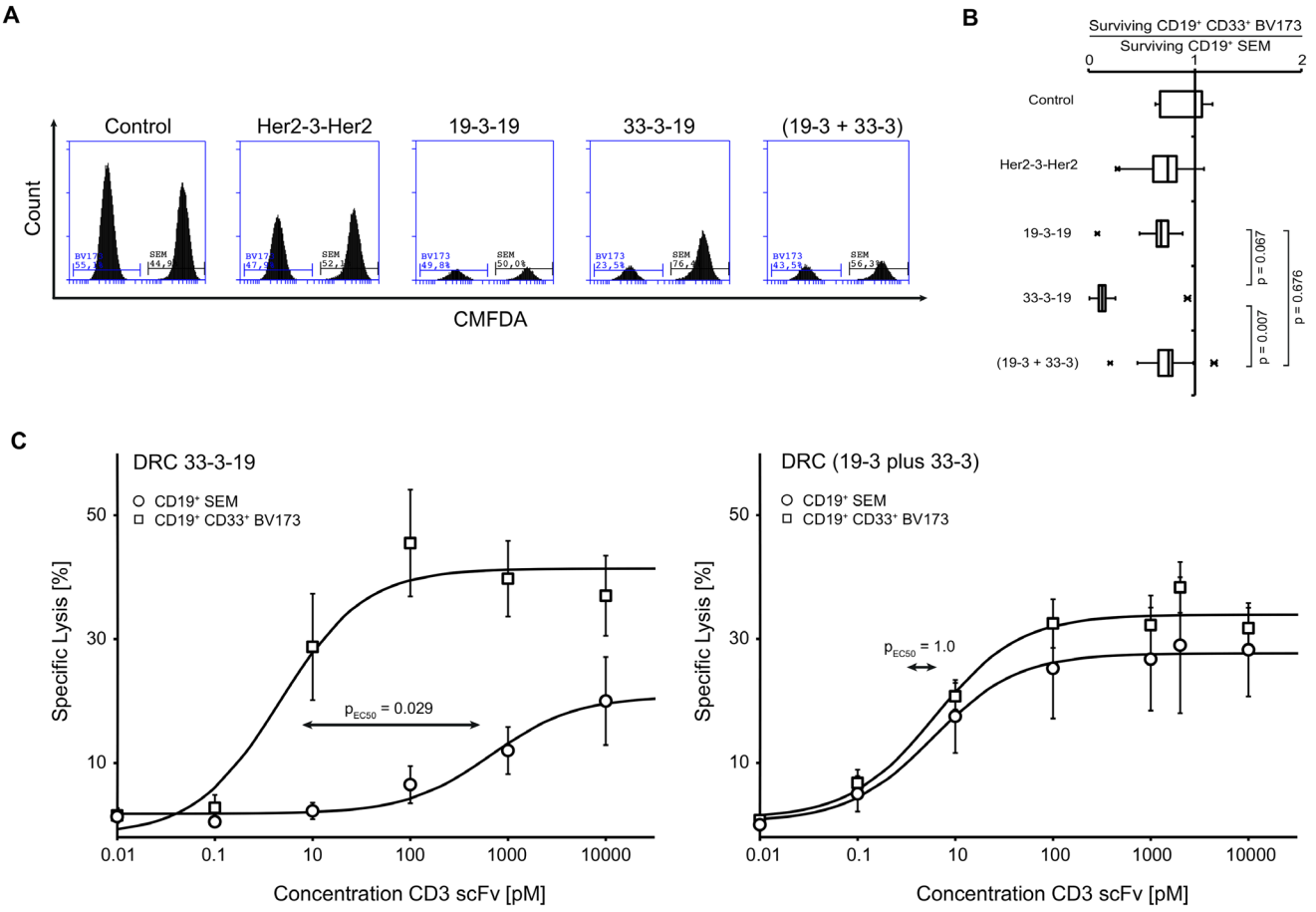

Figure 3: Selective lysis of CD19/CD33 double-positive target cells induced by dual-targeting triplebody 33-3-19 plus allogeneic T cells. Cytolysis assays with mixed CD19 single-positive (sp) and CD19/CD33 double-positive (dp) target cell populations were performed to investigate whether dual-targeting triplebody 33-3-19 achieved selectivity of lysis. **A.** PBMCs were labelled with 2 µM CellTracker™ Deep Red and sp SEM and dp BV173 target cells were labelled with 2 µM and 20 nM CellTracker™ Green CMFDA, respectively, and mixed at an E : sp T : dp T ratio of 1 : 3 : 3. After incubation for 12 hours cells were stained with 7-AAD to exclude dead/dying cells and the number of surviving sp and dp target cells was assessed by flow cytometry (n = 5). Figure 3A shows an example of the histograms for surviving $CMFDA^+$ $7\text{-}AAD^-$ Deep Red^- target cells from each reaction. **B.** The ratio of surviving dp BV173 to sp SEM target cells was calculated from absolute cell numbers in a set sample volume (250 µL). The box plot in Figure 3B is based on five independent measurements. On average, three-times more sp SEM target cells survived treatment with 1 nM dual-targeting triplebody 33-3-19 than dp BV173 target cells. Treatment with 1 nM mono-targeting triplebody 19-3-19 or an equimolar concentration of bsscFvs (19-3 plus 33-3) reduced both target cell lines to a similar extent. **C.** sp SEM target cells were Calcein-labelled in one and dp BV173 target cells were labelled in the other arm of a 3 hour Calcein release cytolysis assay with mixed target cell populations (E : sp T : dp T is 2 : 1 : 1). The concentrations of dual-targeting triplebody 33-3-19 and an equimolar mixture of the CD3 bsscFvs (19-3 plus 33-3) were titrated. The ratio of killed sp-to-dp target cells was determined from the ratio of specific lysis achieved in each arm of the experiment, respectively (n = 4). While both cell lines were equally sensitive towards treatment with the bsscFv mixture (EC_{50}-values are 6.1 pM for BV173 and 5.9 pM for SEM), the double-positive cell line BV173 was 145-times more sensitive towards treatment with 33-3-19 (EC_{50}-value = 4.6 pM) than the single-positive cell line SEM (EC_{50}-value = 667.7 pM), when both target cell lines were present in the same reaction volume.

Calcein green in a cytolysis test to determine specific lysis of each target cell population individually (Figure S3A). Again, the BV173 population was lysed to a significantly greater extent than the SEM population upon treatment with 33-3-19, but not after treatment with 19-3-19 or an equimolar mixture of (19-3 plus 33-3) (Figure S3B). Dose-response curves were established for each population in the target cell mixture treated with either 33-3-19 or the bsscFv mixture (19-3 plus 33-3). The concentration of the CD3-epsilon scFv was equimolar between the treatment groups, i.e. 1 nM 33-3-19 corresponded to (0.5 nM 19-3 plus 0.5 nM 33-3). $CD19^+$ $CD33^+$ BV173 target cells responded to far lower doses of dual-targeting triplebody 33-3-19 than the $CD19^+$ SEM target cells, when both were simultaneously present in the reaction mixture (Figure 3C, left panel). The EC_{50}-values of 33-3-19 for the double- and single-positive cell lines were 4.6 pM and 667.7 pM, respectively. This is a significant 145-fold difference in sensitivity (Mann-Whitney u-test, $p = 0.029$) towards 33-3-19 treatment between the two target cell populations. In contrast both, the double- and the single-positive cell lines, displayed equal sensitivity towards treatment with the mixture of bsscFvs (19-3 plus 33-3) with EC_{50}-values of 6.1 and 5.9 pM, respectively (Figure 3C, right panel).

DISCUSSION

In the present study, we characterized a dual-targeting T cell-recruiting triplebody 33-3-19 that was designed for the selective lysis of CD19/CD33 double-positive B/myeloid leukemia cells over CD19 single-positive normal cells. The results emphasize that dual-targeting agents have the capacity to achieve better target cell selectivity and reduced off-target toxicity.

To activate CTLs, to redirect their effector cell functions, and to induce T cell proliferation, the simultaneous binding of the CD3-epsilon trigger antigen on the T lymphocytes and tumor-associated antigen (TAA) on the cancer cell surface by triplebody 33-3-19 was required. This observation as well as our previous experiences with the mono-targeting triplebody 19-3-19 [21] suggest that the mode of action of T cell-recruiting triplebodies is very similar to that postulated for BiTE®s [24–26]: the higher affinity of these antibody derivatives for the TAAs rather than the effector cell antigen leads to a preferential coating of the cancer cells. Once a T cell has come into proximity of the target cell, multiple specific binding events to the triplebodies coating the cancer cell result in CD3-receptor cross-linking and subsequent T cell activation. However, in contrast to BiTE®s, antibody derivatives with multiple targeting domains such as 33-3-19 bind bi-(or multi-)valently to the target cell and can thus profit from a cooperativity or avidity effect, which has previously been demonstrated for several triplebodies [16, 19–21]. Therefore the difference in affinity for the TAA and trigger antigens may not need to be as pronounced as for BiTE® molecules [25]. This may also give rise to lower off-target toxicity, because the affinity for single-positive non-target cells may be too low to induce a prolonged contact with CTLs or other immune effector cells.

Since the mode of action of BiTE®s and T cell-recruiting triplebodies appears to have common components, it is not surprising that the release of cytokines IL-2, IL-6, IL-10, TNFα and IFN-γ was observed after treatment of target cells *in vitro* with 33-3-19 and effector T cells. This result leads to the prediction that T cell-engaging triplebodies may also induce a cytokine release syndrome (CRS) similar to the one described clinically for Blinatumomab [14, 15]. However, the clinical experience with this T cell-activating agent and with the use of (CAR) T cells for therapy have helped to implement CRS treatment strategies, which are effective in most cases [27].

In this study, we also provided clear evidence suggesting that dual-targeting of (CD19 plus CD33) improved target cell selectivity, in particular at sub-saturating concentrations. The presence of only one of the TAAs on the target cell surface was sufficient to redirect T cell function; however, CD19/CD33 double-positive target cells displayed a 145-fold greater sensitivity towards treatment with 33-3-19 than CD19 single-positive cells, when both populations were present in the same reaction environment. This observation points to a possible concentration-dependent therapeutic window for the selectivity of dual-targeting agents: at concentrations of the agent, which fall into this window, double-positive cancer cells are largely eradicated, but single-positive cells are mostly spared. It may be possible to maximize this "selectivity window" by affinity engineering of the individual arms of dual-targeting agents as was recently shown by Mazor *et al.* for an anti-CD4/CD70 DuetMab® [9].

Another important parameter is the combined and individual target antigen density on the target and non-target tissues. The antigen density limits the number of triplebody molecules that can be bound to the cancer cell surface. We frequently observe - for example in the case of the B-CLL and B-ALL patient samples in this study - that target cells display a higher specific lysis at 1 nM triplebody than at 10 nM triplebody. This pattern might be attributed to an "oversaturation" effect: when the amount of triplebody exceeds the number of available binding sites on the cancer cells, the effector cells may be coated in addition to the targets and a successful interaction between effectors and targets to form a cytolytic synapse is mediated less frequently or less efficiently. Thus, the most effective concentration of a dual-targeting agent such as 33-3-19 may depend on the combined target antigen density of an individual patient's target cells. This may pose a challenge for the determination of an appropriate dosing regimen: target antigen densities vary significantly between individuals [28] and can even vary between the bulk of leukemia cells and the leukemia-initiating stem- or

progenitor cells (as is the case for the combined density of CD33 and CD123 on AML LSCs [29], for example). Thus, the suitable concentration to achieve a selective eradication of target cells may also vary between patients.

Triplebody 33-3-19 has not yet undergone late-stage preclinical development. Most of the limiting protein-chemical properties described above and in particular the tendency to form aggregates can probably be attributed to intra- and intermolecular shuffling of V-chain subdomains, because the individual scFvs used here were stable in other triplebody constructs. However, recent advances in antibody engineering [30] offer the opportunity to improve the intrinsic stability of antibody derivatives such as 33-3-19. If such stability engineering were combined with affinity engineering to further increase the "selectivity window", then later-stage versions of 33-3-19 may become potent and clinically useful therapeutic agents for a selective targeting of $CD19^+$ $CD33^+$ B/myeloid leukemia cells.

MATERIALS AND METHODS

Cloning, production and purification

Triplebody 33-3-19 and bsscFv 33-3 were constructed using standard molecular biology techniques. Briefly, the 5' (i.e. N-terminal) CD19-scFv in our previously described 19-3-19 and 19-3 constructs [21] were replaced with the humanized CD33-specific scFv, which was isolated by polymerase chain reaction (PCR) from the SPM-2 gene cassette [22]. All triplebody- and bsscFv-encoding genes were cloned into the pSecTag2-HygroC vector for mammalian expression. Freestyle 293F cells were transfected with TransIT-LT1 transfection reagent and a stable production cell pool was generated by Hygromycin B selection for 8 weeks. The recombinant protein was purified from the supernatant via Ni-NTA affinity chromatography followed by analytical size exclusion chromatography. Protein aliquots were stored at -80 °C.

Thermal shift assay

SYPRO Orange (Thermo Fisher Scientific, Darmstadt), which only fluoresces upon binding to denatured protein, was added to 45 µL aliquots of a 0.1 mg/mL protein solution at a dilution of 1 : 5,000. Fluorescence emitted by the labeled denatured triplebody was monitored on a Biorad CFX 96 instrument during a temperature increase from 10 °C to 95 °C at 0.5 °C intervals (10 sec/interval).

Cell culture methods

Cell lines BV173, Raji, ARH77, THP-1 and MOLM-13 were purchased from the German Collection of Microorganisms and Cell Lines (Leibniz-Institut DSMZ, Braunschweig). The SEM cell line was purchased from the American Type Culture Collection (ATCC). SEM, Raji, ARH77 and THP-1 were cultured in RPMI 1640 (Gibco, Thermo Fisher Scientific, Darmstadt) supplemented with 10% fetal bovine serum (FBS) and Penicillin (100 U/mL) / Streptomycin (100 µg/mL). Medium for BV173 and MOLM-13 was supplemented with 20% FBS. Freestyle 293F cells were purchased from Life Technologies and grown in FreeStyle™ medium in a shaking incubator.

Blood samples from healthy donors and patients with hematologic malignancies were drawn into EDTA-monovettes (Sarstedt) after informed written consent had been obtained. This study is in compliance with the declaration of Helsinki and was approved by the ethics committee of the Medical Faculty of the Ludwig-Maximilians-Universität München (project no. 173-13). PBMCs were separated by density gradient centrifugation using Lymphoprep™ (Axis Shield PoC) medium, and residual erythrocytes were lysed by incubation with erythrocyte-lysis-buffer (University Pharmacy, Munich) for 5 minutes. To generate effector cells for standard 3 hours cytotoxicity assays an *ex vivo* expansion and stimulation of mononuclear cells (MNCs) was carried out for 20 days in the presence of IL-2 as described [23, 31]. For T cell activation and proliferation assays freshly isolated, non-stimulated PBMCs were used.

Flow cytometry

Flow cytometric analyses were carried out on a BD Accuri C6 or a Millipore Guava instrument. For binding studies target antigen-positive cells were incubated with 15 µg/mL antibody derivatives and washed. Bound antibody derivatives were then detected with an AlexaFluor488-conjugated anti-His_5 antibody (1 : 200 dilution, Qiagen). CD3, CD4, CD8, CD16, CD19, CD25, CD33, CD56, CD69 and isotype control antibodies conjugated with different fluorophores were purchased from Immunotech (Beckmann-Coulter, Marseille). For cell-surface marker analysis, target cells were fixed in 3.7 % paraformaldehyde (PFA) solution at room temperature for 15 minutes, subsequently stained with the required antibody cocktail at 4 °C for 30 minutes, washed with phosphate buffered saline (PBS) and analyzed. The viability dye 7-AAD and the Cytometric Bead Array™ Human Th1/Th2 Cytokine Kit II were purchased from BD Biosciences (San Diego, CA) and used according to the manufacturer's instructions. The CellTrace™ CFSE proliferation dye (Molecular Probes, Darmstadt) and the QifiKit (Dako, Eching) for the quantification of surface antigens were used according to the manufacturer's instructions.

Calcein release assay/redirected lysis assay (RDL)

Target cells were labelled with 15 µM Calcein Green AM (Molecular Probes, Darmstadt), washed, and

mixed with *ex vivo* expanded and stimulated PBMCs from healthy unrelated donors in RPMI 1640 GlutaMAX™ supplemented with 10 % FBS and Penicillin (100 U/mL)/Streptomycin (100 µg/mL) (Gibco, Thermo Fisher Scientific, Darmstadt) at an E : T ratio of 10 : 1. Antibody derivatives were diluted to the desired concentration with medium and added to 200 µL reaction volumes in a 96-well round bottom tissue culture plate (CellStar, Greiner bio-one). After a 3 hour incubation period at 37 °C, 5 % CO_2, 100 µL supernatant was transferred to a black 96-well flat bottom plate (Nunc) and fluorescence was determined on a Berthold Mithras plate reader (Berthold Technologies, Bad Wildbad). Maximum lysis was achieved by addition of 2.5 % Triton X-100. Specific lysis was calculated as follows:

% Specific Lysis = 100 * [(RLU (sample) – RLU (background)) / (RLU (max. lysis) – RLU (background))]

, where RLU = relative light units and the background is the degree of lysis obtained with effector cells alone in the absence of added triplebody.

Selective lysis studied by flow cytometry

To investigate whether 33-3-19 induces a selective lysis of target antigen double-positive (dp) cells, single-positive (sp) $CD19^+$ SEM cells and dp $CD19^+$ $CD33^+$ BV173 cells were differentially labeled with CellTracker™ Green CMFDA (i.e. 2 µM and 20 nM, respectively) and mixed with *ex vivo* expanded and stimulated, CellTracker™ Deep Red (2 µM)-labelled PBMCs at an E : sp T : dp T Ratio of 1 : 3 : 3. Triplebodies 19-3-19, 33-3-19, Her2-3-Her2 or a mixture of the bsscFvs (19-3 plus 33-3) were added to give 1 nM concentration. After a 12 hour incubation period at 37 °C/5 % CO_2 cells were harvested, stained with the viability dye 7-AAD and resuspended in 500 µL PBS. 250 µL of each sample were analyzed by flow cytometry. Surviving target cells were identified by gating on $CMFDA^+$, Deep Red^-, 7-AAD^- cells.

Selective lysis studied by Calcein release

In an alternative approach to investigate the hypothesized target cell selectivity of 33-3-19, cell death of sp and dp target cells in a mixed population was measured by Calcein release in parallel reactions. In one reaction mixture sp SEM cells were labeled and in the parallel reaction dp BV173 cells were labeled with 15 µM Calcein Green AM. Cell death was determined by fluorescence from released Calcein Green in the supernatant after an incubation period of 3 hours with pre-stimulated PBMCs from healthy unrelated donors at an E : sp T : dp T ratio of 2 : 1 : 1. Triplebodies Her2-3-Her2, 19-3-19, 33-3-19 and the mixture of bsscFvs (19-3 plus 33-3) were adjusted to the desired concentrations. Maximum lysis was achieved by addition of 2.5 % Triton X-100 and specific lysis was calculated as described above.

Colony formation assays

Colony formation assays in MethoCult™ were performed after a 4 hour cytolysis reaction with an E : T ratio of 10 : 1 PBMCs to target cells and 1 nM triplebody Her2-3-Her2 or 33-3-19. Colony Forming Cells (CFCs) were detected and counted using the MethoCult™ H4434 Classic medium (Stem Cell Technologies, Munich). Briefly, cells were harvested and washed with Iscove's Modified Dulbecco's Medium after the cytolysis reaction. 5,000 to 10,000 target cells were seeded to 1 mL of rigorously vortexed MethoCult™ medium and transferred to a 24-well tissue culture plate. The sample well was surrounded with water-containing wells and the dish was incubated at 37 °C/5 % CO_2 for 7 days. On day seven, 100 µL of a 1 mg/mL iodonitrotetrazolium chloride (INT) solution in PBS was added and after an overnight incubation at 37 °C/5 % CO_2 the number of colonies was counted.

Statistical analysis

All statistical analyses were performed by GraphPad Prism Software (GraphPad Software Inc., San Diego, CA, USA) using Student's t-test for the determination of significance in normally distributed, and using the Mann-Whitney u test in samples with unknown distribution. Statistical significance was defined as $p < 0.05$.

ACKNOWLEDGMENTS

We thank Prof. Matthias Peipp for providing the pSecTag2-HygroC vector with the Her2-CD3 bsscFv construct and Kerstin Lämmermann, Brigitte Schnabel, Alexandra Schele, Kristin Leike and Stefanie Nowecki for technical assistance. Dr. J Seissler kindly provided access to the Accuri C6 cytofluorimeter. Guidance and scientific advice from Profs. Stefan Endres and Uwe Jacob, and Drs. Sarah Wildenhain, Christian B. Schiller and Ingo A. Schubert are gratefully acknowledged as well as fruitful scientific discussions with Nadine Moritz, Monika Herrmann, Elisavet Chatzopoulou and Laia Pascual-Ponce. We also thank the healthy donors and patients, who provided blood samples for this study.

CONFLICTS OF INTEREST

No conflicts of interest are reported.

GRANT SUPPORT

This study was supported by awards from the charity "Chimney Sweeps Help Children with Cancer" (Schornsteinfeger Helfen Krebskranken Kindern e.V.) to GHF, by support from the M4 excellence award to KPH, GHF and FO from the Bavarian Government, by

funding from the Center for Integrated Protein Science Munich (CiPSM) and Quantitative Biosciences Munich (QBM) to KPH and by a Ph.D. student research fellowship awarded to CCR by the German José Carreras-Leukemia Foundation (www.carreras-stiftung.de, Scholarship No. DJCLS F 13/05). SK was supported by the international doctoral program "i-Target: immunotargeting of cancer" funded by the Elite Network of Bavaria, the Melanoma Research Alliance (grant number N269626), the Wilhelm-Sander-Stiftung (grant number 2014.018.1), the German Cancer Aid, the Else-Kröner-Fresenius Stiftung (grant number 2014 A204), the Ernst-Jung-Stiftung, the Marie-Slodowska Curie innovative training network "IMMUTRAIN: training network for the immunotherapy of cancer" funded under the H2020 program of the European Union and by LMU Munich's Institutional Strategy LMUexcellent within the framework of the German Excellence Initiative.

Abbreviations

ALL = Acute Lymphoid Leukemia; AML = Acute Myeloid Leukemia; bsscFv = bispecific scFv, CD = Cluster of Differentiation; CFC = colony forming cell; CLL = Chronic Lymphoid Leukemia; CNS = central nervous system; CRS = cytokine release syndrome; CTL = cytotoxic T lymphocyte; dp = double-positive; DRC = dose-response curve; EC_{50} = Effective Concentration, at which 50% of targets are killed; INT = iodonitrotetrazolium chloride; LIC = leukemia initiating cells; LSC = leukemia stem cell; MNC = mononuclear cell; MPAL (NOS) = Mixed Phenotype Acute Leukemia (No Other Specification); n.d. = not determined; PB = peripheral blood; PBMC = peripheral blood mononuclear cells; PBS = phosphate-buffered saline; PHA = phytohemagglutinin; PFA = paraformaldehyde; RDL = redirected lysis; RLU = relative light units; scFv =single chain variable fragment; sp = single-positive

REFERENCES

1. Porwit A, Bene MC. Acute Leukemias of Ambiguous Origin. American journal of clinical pathology. 2015; 144:361-376.
2. Weinberg OK, Arber DA. Mixed-phenotype acute leukemia: historical overview and a new definition. Leukemia. 2010; 24:1844-1851.
3. Matutes E, Pickl WF, Van't Veer M, Morilla R, Swansbury J, Strobl H, Attarbaschi A, Hopfinger G, Ashley S, Bene MC, Porwit A, Orfao A, Lemez P, Schabath R, Ludwig WD. Mixed-phenotype acute leukemia: clinical and laboratory features and outcome in 100 patients defined according to the WHO 2008 classification. Blood. 2011; 117:3163-3171.
4. Mejstrikova E, Kalina T, Trka J, Stary J, Hrusak O. Correlation of CD33 with poorer prognosis in childhood ALL implicates a potential of anti-CD33 frontline therapy. Leukemia. 2005; 19:1092-1094.
5. Al-Seraihy AS, Owaidah TM, Ayas M, El-Solh H, Al-Mahr M, Al-Ahmari A, Belgaumi AF. Clinical characteristics and outcome of children with biphenotypic acute leukemia. Haematologica. 2009; 94:1682-1690.
6. Mejstrikova E, Volejnikova J, Fronkova E, Zdrahalova K, Kalina T, Sterba J, Jabali Y, Mihal V, Blazek B, Cerna Z, Prochazkova D, Hak J, Zemanova Z, Jarosova M, Oltova A, Sedlacek P, et al. Prognosis of children with mixed phenotype acute leukemia treated on the basis of consistent immunophenotypic criteria. Haematologica. 2010; 95:928-935.
7. Weinberg OK, Seetharam M, Ren L, Alizadeh A, Arber DA. Mixed phenotype acute leukemia: A study of 61 cases using World Health Organization and European Group for the Immunological Classification of Leukaemias criteria. American journal of clinical pathology. 2014; 142:803-808.
8. Kontermann R. Dual targeting strategies with bispecific antibodies. mAbs. 2012; 4.
9. Mazor Y, Hansen A, Yang C, Chowdhury PS, Wang J, Stephens G, Wu H, Dall'Acqua WF. Insights into the molecular basis of a bispecific antibody's target selectivity. mAbs. 2015; 7:461-469.
10. Cuesta AM, Sainz-Pastor N, Bonet J, Oliva B, Alvarez-Vallina L. Multivalent antibodies: when design surpasses evolution. Trends in biotechnology. 2010; 28:355-362.
11. Schubert I, Stein C, Fey GH. Dual-Targeting for the Elimination of Cancer Cells with Increased Selectivity. Antibodies. 2012; 1:2-18.
12. Stein C, Schubert I, Fey GH. Natural Killer (NK)- and T-Cell Engaging Antibody-Derived Therapeutics. Antibodies. 2012; 1:88-123.
13. Baeuerle PA, Kufer P, Bargou R. BiTE: Teaching antibodies to engage T-cells for cancer therapy. Curr Opin Mol Ther. 2009; 11:22-30.
14. Ribera JM, Ferrer A, Ribera J, Genesca E. Profile of blinatumomab and its potential in the treatment of relapsed/refractory acute lymphoblastic leukemia. OncoTargets and therapy. 2015; 8:1567-1574.
15. Zugmaier G, Klinger M, Schmidt M, Subklewe M. Clinical overview of anti-CD19 BiTE((R)) and *ex vivo* data from anti-CD33 BiTE((R)) as examples for retargeting T cells in hematologic malignancies. Molecular immunology. 2015; 67:58-66.
16. Kellner C, Bruenke J, Stieglmaier J, Schwemmlein M, Schwenkert M, Singer H, Mentz K, Peipp M, Lang P, Oduncu F, Stockmeyer B, Fey GH. A novel CD19-directed recombinant bispecific antibody derivative with enhanced immune effector functions for human leukemic cells. J Immunother. 2008; 31:871-884.
17. Schmidt MM, Wittrup KD. A modeling analysis of the effects of molecular size and binding affinity on tumor targeting. Molecular cancer therapeutics. 2009; 8:2861-2871.

18. Kugler M, Stein C, Kellner C, Mentz K, Saul D, Schwenkert M, Schubert I, Singer H, Oduncu F, Stockmeyer B, Mackensen A, Fey GH. A recombinant trispecific single-chain Fv derivative directed against CD123 and CD33 mediates effective elimination of acute myeloid leukaemia cells by dual targeting. British journal of haematology. 2010; 150:574-586.

19. Schubert I, Kellner C, Stein C, Kugler M, Schwenkert M, Saul D, Mentz K, Singer H, Stockmeyer B, Hillen W, Mackensen A, Fey GH. A single-chain triplebody with specificity for CD19 and CD33 mediates effective lysis of mixed lineage leukemia cells by dual targeting. mAbs. 2011; 3:21-30.

20. Schubert I, Kellner C, Stein C, Kugler M, Schwenkert M, Saul D, Stockmeyer B, Berens C, Oduncu FS, Mackensen A, Fey GH. A recombinant triplebody with specificity for CD19 and HLA-DR mediates preferential binding to antigen double-positive cells by dual-targeting. mAbs. 2012; 4:45-56.

21. Roskopf CC, Schiller CB, Braciak TA, Kobold S, Schubert IA, Fey GH, Hopfner KP, Oduncu FS. T cell-recruiting triplebody 19-3-19 mediates serial lysis of malignant B-lymphoid cells by a single T cell. Oncotarget. 2014; 5:6466-6483. doi: 10.18632/oncotarget.2238.

22. Braciak TA, Wildenhain S, Roskopf CC, Schubert IA, Fey GH, Jacob U, Hopfner KP, Oduncu FS. NK cells from an AML patient have recovered in remission and reached comparable cytolytic activity to that of a healthy monozygotic twin mediated by the single-chain triplebody SPM-2. Journal of translational medicine. 2013; 11:289.

23. Schubert I, Saul D, Nowecki S, Mackensen A, Fey GH, Oduncu FS. A dual-targeting triplebody mediates preferential redirected lysis of antigen double-positive over single-positive leukemic cells. mAbs. 2014; 6:286-296.

24. Dreier T, Lorenczewski G, Brandl C, Hoffmann P, Syring U, Hanakam F, Kufer P, Riethmuller G, Bargou R, Baeuerle PA. Extremely potent, rapid and costimulation-independent cytotoxic T-cell response against lymphoma cells catalyzed by a single-chain bispecific antibody. International journal of cancer. 2002; 100:690-697.

25. Hoffmann P, Hofmeister R, Brischwein K, Brandl C, Crommer S, Bargou R, Itin C, Prang N, Baeuerle PA. Serial killing of tumor cells by cytotoxic T cells redirected with a CD19-/CD3-bispecific single-chain antibody construct. International journal of cancer. 2005; 115:98-104.

26. Loffler A, Gruen M, Wuchter C, Schriever F, Kufer P, Dreier T, Hanakam F, Baeuerle PA, Bommert K, Karawajew L, Dorken B, Bargou RC. Efficient elimination of chronic lymphocytic leukaemia B cells by autologous T cells with a bispecific anti-CD19/anti-CD3 single-chain antibody construct. Leukemia. 2003; 17:900-909.

27. Barrett DM, Teachey DT, Grupp SA. Toxicity management for patients receiving novel T-cell engaging therapies. Current opinion in pediatrics. 2014; 26:43-49.

28. Olejniczak SH, Stewart CC, Donohue K, Czuczman MS. A quantitative exploration of surface antigen expression in common B-cell malignancies using flow cytometry. Immunol Invest. 2006; 35:93-114.

29. Ehninger A, Kramer M, Rollig C, Thiede C, Bornhauser M, von Bonin M, Wermke M, Feldmann A, Bachmann M, Ehninger G, Oelschlagel U. Distribution and levels of cell surface expression of CD33 and CD123 in acute myeloid leukemia. Blood cancer journal. 2014; 4:e218.

30. Xu L, Kohli N, Rennard R, Jiao Y, Razlog M, Zhang K, Baum J, Johnson B, Tang J, Schoeberl B, Fitzgerald J, Nielsen U, Lugovskoy AA. Rapid optimization and prototyping for therapeutic antibody-like molecules. mAbs. 2013; 5:237-254.

31. Alici E, Sutlu T, Bjorkstrand B, Gilljam M, Stellan B, Nahi H, Quezada HC, Gahrton G, Ljunggren HG, Dilber MS. Autologous antitumor activity by NK cells expanded from myeloma patients using GMP-compliant components. Blood. 2008; 111:3155-3162.

SUPPLEMENTARY FIGURES

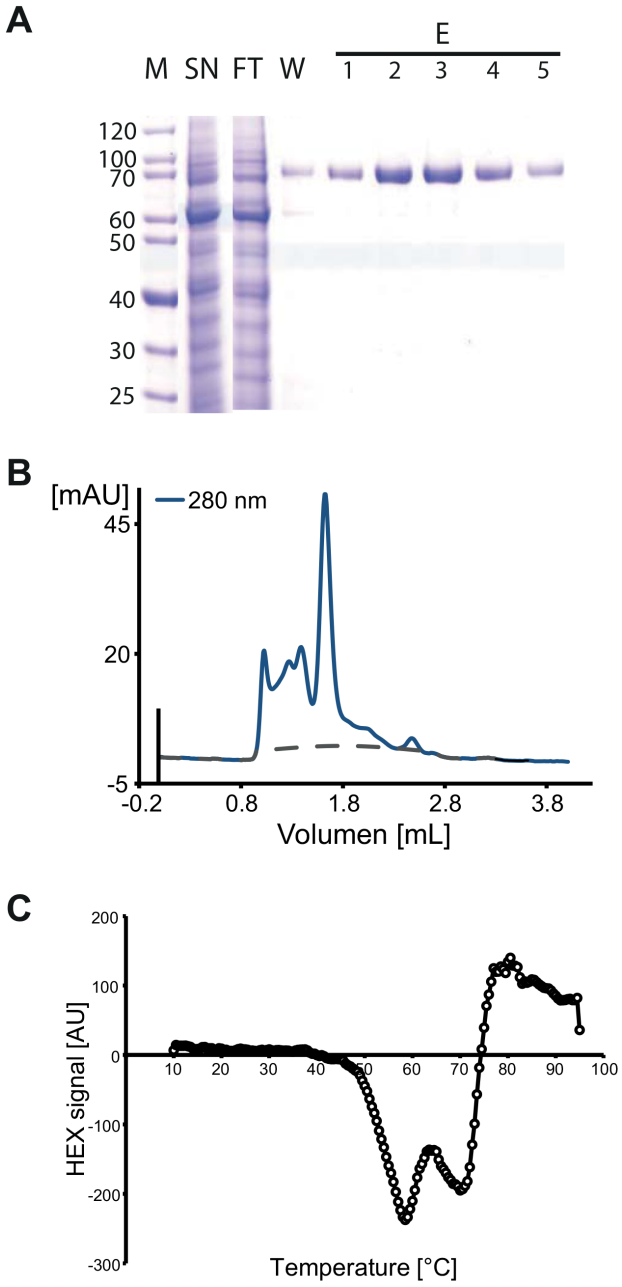

Supplementary Figure S1: Protein-chemical properties of dual-targeting T cell-engaging triplebody 33-3-19. A. SDS-polyacrylamide gel electrophoresis of protein fractions post Ni-NTA enrichment of triplebody 33-3-19 from the supernatant of a stable Freestyle 293F production cell pool (yield = 0.5 – 1.5 mg/L supernatant). M = protein marker, SN = supernatant, FT = flow through, W = wash fraction, E = elution fraction. **B.** Size exclusion chromatogram of triplebody 33-3-19. The monomer fraction (main peak) was collected and concentrated. Aliquots were flash-frozen in liquid nitrogen and stored at -80 °C until use (max. 2 months). **C.** Melting curve of 33-3-19 monomer as determined by a thermal shift assay. Melting point 1 (CD19 and CD3 scFvs) = 58.5°C; melting point 2 (CD33 scFv) = 70°C. Identification of the peaks from comparison of similar experiments performed earlier by our team with the triplebodies 33-16-123 (SPM-2) (N.C. Fenn, unpublished data) permitting identification of the transition caused by the CD33-specific scFv component and 19-3-19 (C.C. Roskopf, unpublished data) permitting identification of the transitions attributed to the CD19- and CD3-specific scFv components.

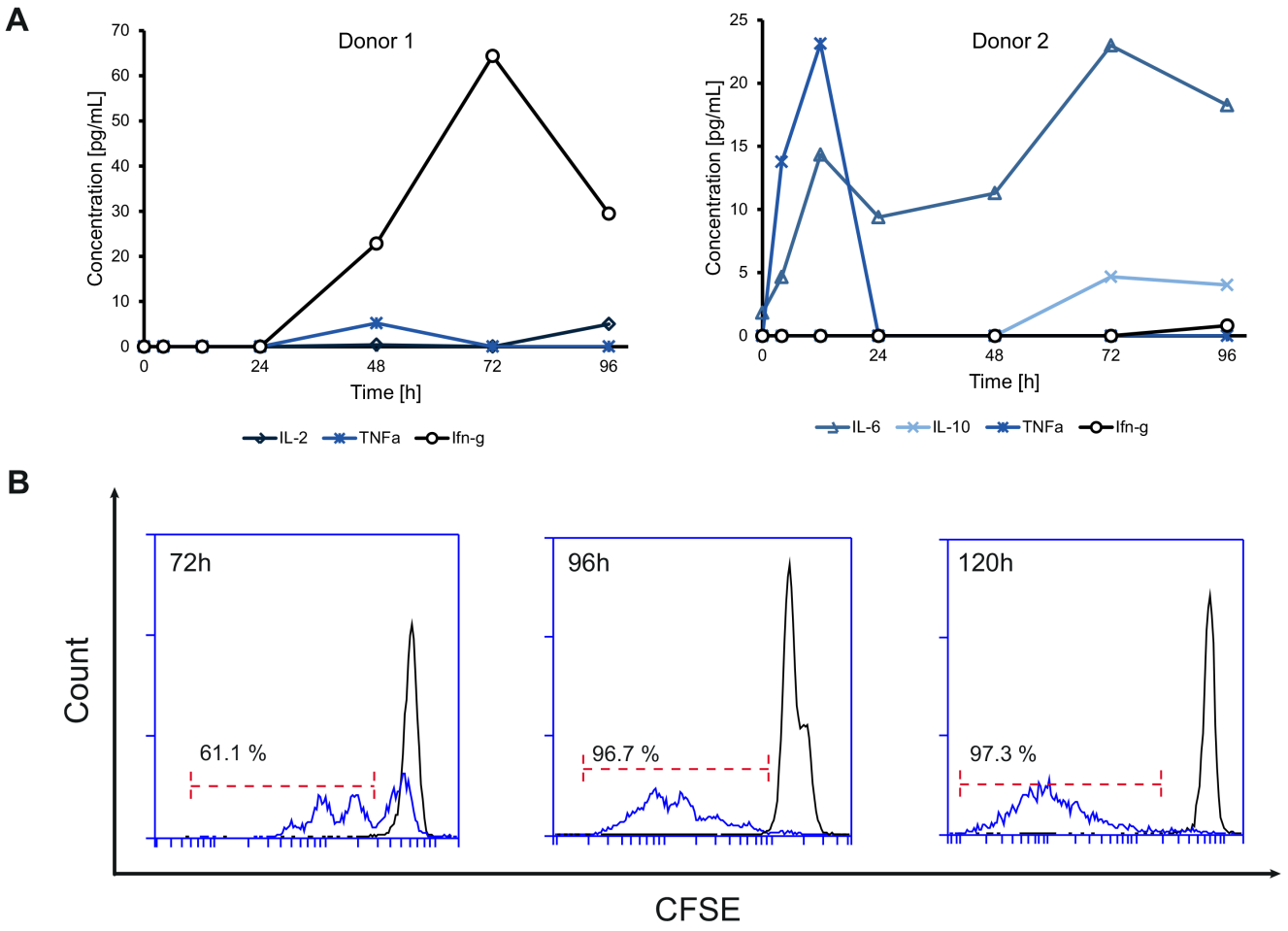

Supplementary Figure S2: T cell-activation induced by triplebody 33-3-19 and targets. Non-stimulated PBMCs from healthy unrelated donors were labelled with 5 µM CFSE and incubated with SEM target cells at an E : T ratio of 1 : 2 and a cell density of 3 * 10^5/ mL at t_0 (n = 3). **A.** After 0, 4, 12, 24, 48, 72 and 96 hours, cytokine levels in the medium were determined using the BD CBA™ Human Th1/Th2 Cytokine Kit II. Cytokine secretion profiles from 2 donors are shown. Both donors displayed complete target cell depletion and T cell proliferation was induced. Probably due to the very low cell numbers, cytokine concentrations increased slightly only, but IL-2, IL-6, IL-10, TNFα and IFN-γ were detectable, a similar profile to the one seen after treatment with the BiTE®s Blinatumomab and AMG330 [14, 15]. **B.** After 72, 96 and 120 hours T cell proliferation was assessed based on the dilution of the CellTrace™ CFSE proliferation dye.

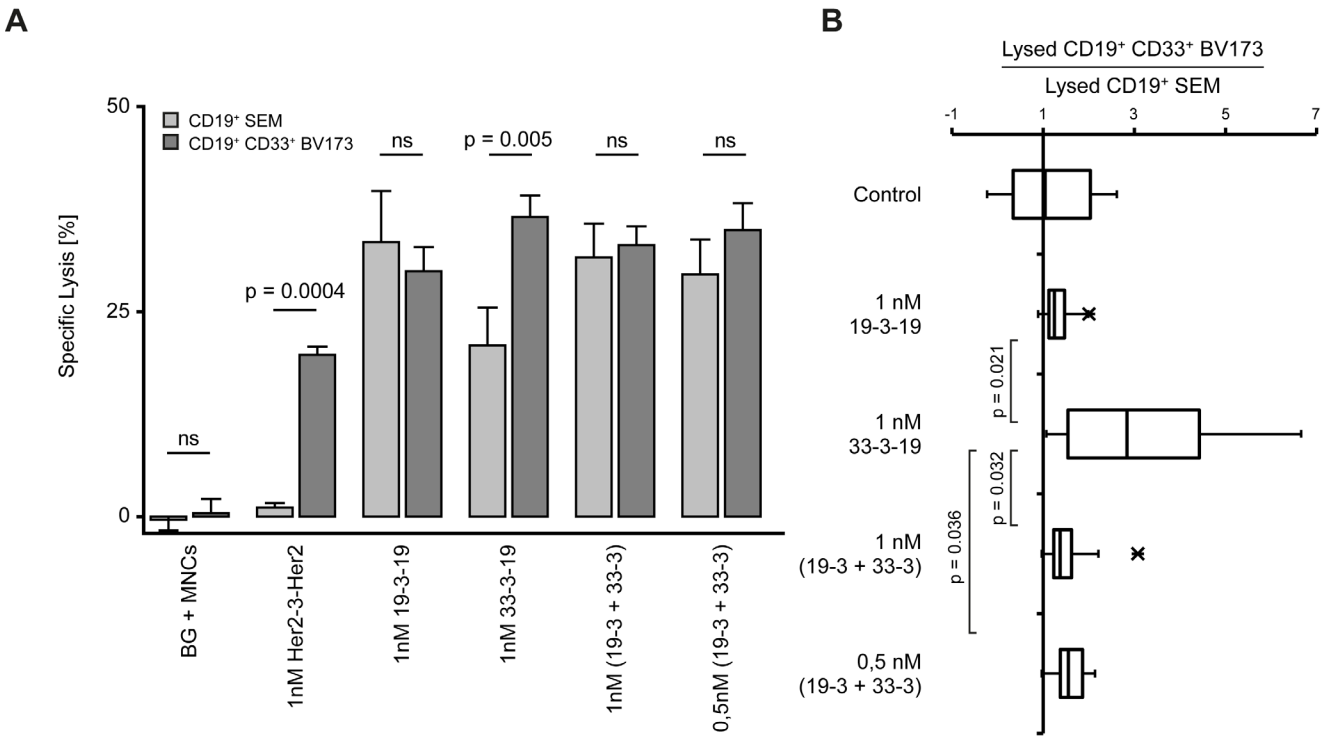

Supplementary Figure S3: Selective lysis of CD19+ CD33+ target cells at 1 nM 33-3-19. CD19 single-positive (sp) SEM target cells were Calcein-labelled in one and CD19/CD33 double-positive (dp) BV173 target cells were labelled in the other arm of a 3 hour Calcein release cytolysis assay with mixed target cell populations (E : sp T : dp T is 2 : 1 : 1; n = 11). **A.** Specific lysis of individual target cell populations in parallel reactions. In the presence of 1 nM dual-targeting triplebody 33-3-19, roughly twice as many BV173 target cells were lysed as SEM target cells (p = 0.0048). **B.** Box plot of the ratio of lysed dp-to-sp target cells, which was determined from the ratio of specific lysis achieved in each arm of the experiment, respectively.

2.5 CD19-specific triplebody SPM-1 engages NK and γδ T cells for rapid and efficient lysis of malignant B lymphoid cells

Christian B. Schiller*, Todd A. Braciak*, Nadja C. Fenn*, Ursula J. Seidel*, Claudia C. Roskopf*, Sarah Wildenhain*, Annemarie Honegger, Ingo A. Schubert, Alexandra Schele, Kerstin Lämmermann, Georg H. Fey , Uwe Jacob, Peter Lang, Karl-Peter Hopfner[$] & Fuat S. Oduncu[$]

*: equal contribution

[$]: co-senior authors

Oncotarget 2016 Dec 13; **7** (50): 83392-83408

DOI: 10.18632/oncotarget.13110

2.5.1 Summary

CD16 (FcγRIIIa) is not only expressed by NK cells, but also by γδ T cells. Both of these immune effector populations already have natural roles in fighting cancer and thus engaging them via immunotherapeutic agents appears to be a promising approach to boost anti-cancer responses. Aside from the interaction of IgG Fc-domains with CD16, antibody-derived molecules with a scFv directed against CD16 have been shown to successfully engage NK cells for the redirected lysis of cancer cells. However, many antibody derivatives have been difficult to produce in large scale or under conditions that reflect the industrial standard. In this publication, humanized triplebody SPM-1 with dual specificity for CD19 and CD16 is presented, whose manufacturing protocols follow industry standard. Furthermore, SPM-1 is capable of engaging both NK and γδ T cells for the redirected lysis of malignant B lymphoid cells with the same efficiency as an Fc-optimized antibody.

The binding moieties of triplebody SPM-1 derive from the previously described triplebody ds[19-16-19][211] and were humanized by CDR-grafting.[249] Homologous recombination was minimized by codon optimization. Using a three-step chromatographic procedure that reflects industrial purification procedures highly pure, monomeric protein was obtained at a yield of 1.7 to 5.5 mg/L supernatant. With a K_D value of (12 ± 1.5 nM), the disulfide-stabilized humanized CD16 binding head displayed a higher affinity for the FcγRIIIa than its murine predecessor. The avidity of the two CD19 scFv for CD19 was comparable to the parental molecule with a K_D value of (17.5 ± 0.4 nM). In redirected lysis assays with either B lymphoid cell lines or primary patient material as targets and *ex vivo* expanded, prestimulated NK cells from healthy donors as effectors, highly efficient cytolysis was achieved with EC_{50}-values in the picomolar range. In patient samples, the EC_{50}-values were 5 to 430-fold lower than those achieved with the commercially available anti-CD20 antibody rituximab (MabThera®). In fact, the triplebody displayed the same cytolytic efficiency as a CD19-specific

Fc-optimized antibody (i. e. 4G7SDIE) and minibody, while a minibody with an unmodified IgG1 Fc-domain was ineffective.

To investigate the activation potential of SPM-1 for γδ T cells, which were present at an average of (2.3 ± 12%) in the PBMC fraction of healthy donors, the level of degranulation marker CD107a on the γδ T cell surface and the levels of intracellular TNF-α and IFN-γ were examined by FACS after cytolysis assays. All levels were elevated upon exposure to SPM-1 plus target cells. Moreover, SPM-1 mediated 100% lysis of immobilized CD19-transfected MCF7 cells (i. e. MCF7-CD19 tm^{250}) by freshly isolated and *ex vivo* expanded γδ T cells at E : T ratios of 10 : 1 and 20 : 1 in an impedance-based cytotoxicity assay (xCELLigence technology) within 12 hours. In this assay, the triplebody displayed biphasic killing kinetics with a faster initial rise in killing rate than monoclonal antibody 4G7SDIE. This suggests a faster on-rate of the triplebody compared to the mAb.

In conclusion, triplebody SPM-1 was sufficiently optimized biochemically to be a candidate for future clinical studies. It has highly efficient cytolytic properties in conjunction with NK cells and γδ T cells that match those of Fc-engineered antibodies and may thus be suitable for the treatment of B cell malignancies or B cell-mediated autoimmune disorders.

2.5.2 Contribution

I prepared the patient samples and performed the corresponding redirected lysis assays with SPM-1, provided by Dr. Schiller, and rituximab. Furthermore I determined the antigen densities of CD19 and CD20 on the surface of different B cell lines and of primary leukemia blasts. I also constructed control triplebody Her2-16-Her2. Finally, I wrote the first draft of the manuscript, which was edited by Prof. Fey, and implemented the changes requested by the co-authors.

www.impactjournals.com/oncotarget/ Oncotarget, 2016, Vol. 7, (No. 50), pp: 83392-83408

Research Paper

CD19-specific triplebody SPM-1 engages NK and gd T cells for rapid and efficient lysis of malignant B-lymphoid cells

Christian B. Schiller[1,*], Todd A. Braciak[2,*], Nadja C. Fenn[1,*], Ursula J. E. Seidel[3,*], Claudia C. Roskopf[2,*], Sarah Wildenhain[1,*], Annemarie Honegger[*], Ingo A. Schubert[5], Alexandra Schele[1], Kerstin Lämmermann[2], Georg H. Fey[6], Uwe Jacob[6], Peter Lang[3], Karl-Peter Hopfner[1,#], Fuat S. Oduncu[2,#]

[1]Department of Biochemistry and Gene Center, Ludwig-Maximilians-University, Munich, Germany

[2]Division of Hematology and Oncology, Medizinische Klinik und Poliklinik IV, Klinikum der Universität München, Munich, Germany

[3]Department of General Paediatrics, Oncology/Haematology, University Children's Hospital Tübingen, Tübingen, Germany

[4]Department of Biochemistry, University of Zurich, Zurich, Switzerland

[5]Department of Biology, University of Erlangen-Nuremberg, Erlangen, Germany

[6]Westend-Innovation, Munich, Germany

[*]CBS, TAB, NCF, UJES, CCR and SW are co-first authors in this study

[#]KPH and FSO are co-senior authors in this study

Correspondence to: *Claudia C. Roskopf,* ***email:*** *Claudia.Roskopf@med.uni-muenchen.de*

Keywords: *single chain triplebody, antibody-dependent cellular cytotoxicity, gamma delta T cell, leukemia, immunotherapy*

Received: *June 30, 2016* ***Accepted:*** *October 03, 2016* ***Published:*** *November 04, 2016*

ABSTRACT

Triplebodies are antibody-derived recombinant proteins carrying 3 antigen-binding domains in a single polypeptide chain. Triplebody SPM-1 was designed for lysis of CD19-bearing malignant B-lymphoid cells through the engagement of CD16-expressing cytolytic effectors, including NK and gd T cells.

SPM-1 is an optimized version of triplebody ds(19-16-19) and includes humanization, disulfide stabilization and the removal of potentially immunogenic sequences. A three-step chromatographic procedure yielded 1.7 - 5.5 mg of purified, monomeric protein per liter of culture medium. In cytolysis assays with NK cell effectors, SPM-1 mediated potent lysis of cancer-derived B cell lines and primary cells from patients with various B-lymphoid malignancies, which surpassed the ADCC activity of the therapeutic antibody Rituximab. EC_{50}-values ranged from 3 to 86 pM. Finally, in an impedance-based assay, SPM-1 mediated a particularly rapid lysis of CD19-bearing target cells by engaging and activating both primary and expanded human gd T cells from healthy donors as effectors.

These data establish SPM-1 as a useful tool for a kinetic analysis of the cytolytic reactions mediated by gd T and NK cells and as an agent deserving further development towards clinical use for the treatment of B-lymphoid malignancies.

INTRODUCTION

CD19 is a type I transmembrane glycoprotein and a signaling receptor of the immunoglobulin superfamily. It is a component of the B cell receptor (BCR) co-complex, and is expressed from early to late stages of B cell development. Signaling through CD19 promotes proliferation and differentiation [1–4]. The antigen is particularly promising for targeted immunotherapy of B-lymphoid malignancies, because of its relatively high and lineage-specific expression on B cells of different maturation stages and its presence on the surface of cancer progenitor cells [5–7]. However, the results of initial clinical trials with CD19-antibodies were disappointing [5, 8], presumably due at least in part to a far lower surface density of CD19 on the malignant cells than of CD20 on lymphoma cells, the target antigen for the clinically successful antibody Rituximab.

A second generation of improved CD19-targeting proteins and cellular agents has been developed, which

includes Fc- and glyco-engineered immunoglobulins, such as the antibodies XmAb5574 (MOR208) and MEDI-551 [9, 10], the bispecific T cell engager (BiTE®) Blinatumomab (Blincyto®) [11, 12], and the adoptive transfer of genetically modified T cells, obtained by stable transfection with chimeric antigen receptors (CARs). Genetically modified CAR-T cells (CAR-Ts) have been remarkably successful in the treatment of various B-lymphoid malignancies, in particular of Acute Lymphoblastic Leukemia (ALL) in children and young adults with poor prognosis [13–16]. CD19 therefore clearly is a useful target for antigen-specific immunotherapy, provided an appropriate molecular format of the therapeutic agent is chosen.

BiTE and CAR-T cell approaches rely on cytotoxic T lymphocytes (CTLs) for the elimination of cancer cells [11, 13–16]. Although highly effective in many cases, these approaches still leave room for future improvements. In rare cases, undesirable adverse events have been reported after treatment of patients with CD19-directed BiTEs and CD19-directed CAR-Ts. These include cytokine release syndromes and involvement of the central nervous system [17] as well as tumor lysis syndrome and the occasional outgrowth of target antigen-negative tumor cell clones ("antigen-loss" or "escape" variants) [12, 17, 18]. A short serum half-life in the case of BiTEs, potentially durable lymphopenia in the case of CARTs and finally, the associated high costs limit the availability of these therapies for a significant segment of patients.

The use of antibodies for therapeutic purposes, on the other hand, is well-established and effective, and is generally less expensive, but also suffers from certain limitations. These agents rely on the presence of Fc-receptor-bearing effector cells, which can be activated by the mediator protein to assemble a productive synapse with the target cell. In some cases, the needed effector cells are not available in sufficient quantity and quality at certain stages of disease development. An example are limiting numbers of functionally active NK cells in the bone marrow of AML patients at diagnosis, which limit the use of IgGs as front-line therapeutic agents [19–22]. Immunoglobulins further suffer from limited penetration into solid tumor tissues, owed to their large mass [23–25].

To address some of these limitations of mono-targeting IgGs, our team has developed the molecular format of single chain triplebodies. These proteins consist of 3 single chain variable antibody fragments (scFvs) connected by flexible $(G_4S)_n$ linkers [26–31]. Triplebodies are anticipated to have improved pharmacokinetic properties due to their smaller size of approximately 90 kD. Based on experimental and theoretical data from other groups, this is expected to result in a faster equilibration of these molecules in the mammalian blood circulation and in an easier penetration into solid tumor tissues compared to full-length antibodies [23, 32, 33]. Furthermore, triplebody SPM-2 was shown to mediate an efficient elimination of AML blasts from an AML patient in remission by autologous NK cells [34].

Triplebodies developed so far were designed for bivalent binding of a tumor cell via their two distal scFvs, and for monovalent binding to a trigger molecule on a cytolytic effector cell through their central scFv. Effector cells engaged by triplebodies to date include NK cells, CTLs, and neutrophilic granulocytes, which were activated for cytolysis via the triggers CD16, CD3ε, and CD64, respectively [35]. CD16, the human Fcγ-receptor III (FcγRIII), is expressed by NK cells, macrophages, γδ T cells and a subset of cytokine-stimulated dendritic cells (DCs). Upon cross-linking, signaling via CD16, which associates with the FcR γ-chain or CD3ζ, elicits potent effector functions including ADCC and phagocytosis [36].

NK cells and γδ T cells are capable of recognizing and eliminating malignant cells in a natural killing mode in the absence of mediator proteins such as antibodies. NK cells respond to the absence of MHC class I proteins on cancer cells ("missing self"). γδ T cells are independent of MHC : peptide recognition, but can react to non-peptidic phosphoantigens, which are preferentially displayed on the surface of cancer cells. Therefore, both of these effector cell classes can bypass immune evasion of cancer cells by downregulation of MHC class I [37, 38]. In addition, NK cells and γδ T cells are major anti-viral effectors after transplantation of hematopoietic stem cells (HSCT), but do not cause graft-versus-host-disease (GvHD) [37]. Enhancing the cytolytic activity of NK cells and γδ T cells via CD16-triggering therapeutic agents therefore is a promising strategy for cancer treatment, which may also lead to a systemic cellular immune response following an initial lysis of cancer cells by ADCC, in the sense of a tumor-vaccination effect.

The capacity to recruit γδ T cells as cytolytic effectors has not yet been established for triplebodies triggering through CD16, although it had been reported for other agents in related molecular formats, including the Fc-engineered CD19-antibody 4G7SDIE and the bispecific CD19-targeting fusion protein N19-C16 [39–41]. Therefore, we anticipated that a similar result may also be obtained for corresponding triplebodies, but experimental verification of this hypothesis was still needed. These agents have different sizes and space-filling properties, and may therefore differ in their steric access to CD16 epitopes on NK and γδ T cells. To test this hypothesis, the previously described triplebody ds(19-16-19) [26], with 2 binding sites for CD19 and one for CD16, was humanized and stabilized, and the new agent was named SPM-1. The protein was purified, characterized and compared here in NK cell-based ADCC assays to other CD19-specific agents in related molecular formats. In support of the hypothesis, SPM-1 was found capable indeed of mediating lysis of CD19-bearing target cells in combination with human γδ T cells as effectors in ADCC assays. In these studies we also observed that SPM-1 mediated a particularly rapid lysis of substrate-bound CD19-bearing

target cells in a time-resolved, impedance-based assay, the XCelligence® assay [41, 42]. This stimulating finding calls for additional future studies of the kinetics of the ADCC process mediated by antibody-derived agents with different molecular architecture, which will likely lead to a better understanding of the unusually high cytolytic potential of triplebodies compared to some of the related bi-specific agents [26].

RESULTS

Design and production of triplebody SPM-1

Triplebody SPM-1 was constructed based on the published parental triplebody ds(19-16-19) [26]. The scFv domains of the parental protein were derived from the murine monoclonal antibodies 4G7 and 3G8. To minimize immunogenicity, the CD16- and CD19-directed scFv sequences were humanized by CDR grafting [43, 44] plus subsequent adjustment of the framework. The humanized CD16 scFv was then disulfide-stabilized, whereas the 2 humanized CD19-binding domains were used without further stabilization, because this protein was sufficiently stable compared with disulfide-stabilized variants, which have also been studied (Figure 1A and additional data not shown). The cDNA coding sequences for the 2 CD19-specific scFvs were adjusted by mutations in the wobble bases to minimize homologous recombination in the producer cells, and thus to improve production yields of the desired protein. This procedure reduced the occurrence of truncated variants, which had been observed prior to this optimization.

SPM-1 was expressed in Freestyle™ 293-F cells (Life Technologies) and was purified in a 3-step procedure, which included capture from culture supernatants by zinc ion affinity chromatography followed by anion and cation exchange chromatography. This capture step and the ion exchange chromatography protocol followed industry standard procedures, and the downstream purification process is scalable and suitable for commercial production. Yields ranged from 1.7 - 5.5 mg of purified protein/L of culture supernatant in different production runs (Table 1). Purified SPM-1 eluted as a single monomeric peak in size exclusion chromatography profiles and was highly pure as evidenced by SDS-polyacrylamide gel electrophoresis (Figure 1B, 1C).

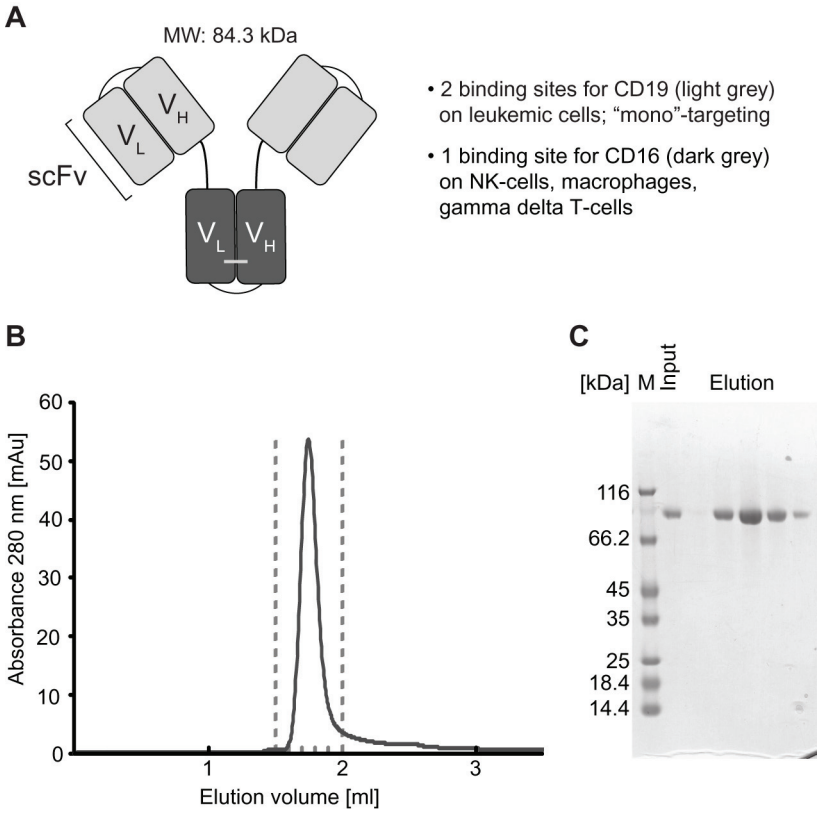

Figure 1: Structural characteristics and purification of triplebody SPM-1. A. CD19-specific scFv domains shown in light grey; CD16-specific scFv domain in dark grey. **B.** After purification with the 3-step chromatographic procedure described in Methods, SPM-1 eluted in size exclusion chromatography profiles (SEC) as a single monodisperse peak corresponding to the molecular mass of an SPM-1 monomer. Species of higher molecular mass (aggregates) were absent/below detection limit. **C.** Fractions from the SEC elution profile (eluting between the dashed lines in B) were analyzed by SDS-PAGE and stained with Coomassie blue. The preparation was of high purity; higher and lower molecular mass species were absent or only very minor contaminants.

Table 1: Biological activity and antigen affinity of triplebody SPM-1

Construct	Yield [mg/L cell culture]	Biol. Activity (SEM) EC50 [pM]	Affinity CD16 [nM]	Avidity CD19 [nM]
SPM-1	1.7 - 5.5	11 ± 3	12.0 ±1.5	17.5 ± 0.4

The affinity is the equilibrium binding constant K_D for monovalent binding to CD16 on stably transfected CHO-CD16 cells; the avidity is the K_D value of the molecule for bivalent binding to CD19-bearing SEM target cells.

Binding characteristics of SPM-1

Specificity of SPM-1 binding to CD19 and CD16 was established by cytofluorimetry with suitable control antibodies and control cells (unpublished data). The monovalent affinity of SPM-1 for CD16 and the bivalent avidity for CD19 were measured by determining the equilibrium binding constants (K_D) by flow cytometry with CD16- or CD19-bearing human cells as previously described [45, 46]. The K_D value of SPM-1 for CD16 was 12.0 ± 1.5 nM, which was lower than the value of 58.6 ± 4 nM reported for the parental triplebody ds(19-16-19). Therefore, the humanized plus disulfide-stabilized CD16 binding domain carried in SPM-1 displayed 4- to 5-fold stronger binding to human CD16 on living cells than the corresponding domain of the parental protein. The K_D value of SPM-1 for CD19 (17.5 ± 0.4 nM) was comparable to the value measured for the parental protein (13.0 ± 1.2 nM; Table 1) [26], and therefore, the humanization procedure has not significantly altered the binding avidity of the second-generation triplebody for CD19.

Cytolytic activity of SPM-1 in combination with human NK cells

The ability of SPM-1 to mediate cytolysis of human cancer cells by NK cells from unrelated healthy donors was tested in standardized redirected lysis (RDL) assays against malignant human B-lymphoid cell lines at an effector-to-target cell (E : T) ratio of 2 : 1. The target cell lines represented different classes of B-lymphoid neoplasias and carried different mean surface densities of CD19 (Table 2). All tested cell lines displayed a dose-dependent cytolytic response to treatment with SPM-1 plus NK cells (Figure 2). The potential of these cell lines for specific lysis was weakly correlated with their mean target antigen density: the SEM line with the highest CD19 density displayed the strongest cytolytic response, whereas the ARH-77 line with the lowest density displayed the weakest response. No specific lysis was observed, when the specificity control triplebody Her2-16-Her2 was used (Figure 2), as expected, because Her2 is not expressed on these target cells. The measured EC_{50}-values of 5.6 pM for the SEM line and 79.4 pM for ARH-77 cells (Table 1) were in the same range as the values previously reported for the non-humanized parental triplebody, which were 4.1 and 29 pM, respectively [26]. Therefore, in combination with NK cells from an unrelated healthy donor, SPM-1 displayed overall similar cytolytic potential for malignant B-lymphoid cell lines as the parental triplebody.

SPM-1 mediates stronger lysis of some primary cancer cell samples by NK cells than the therapeutic antibody Rituximab (MabThera®)

The ability of SPM-1 to mediate cytolysis of a panel of primary B-lymphoid cancer cell samples in conjunction with NK cells was compared with the corresponding ability of the clinically successful CD20 antibody Rituximab (MabThera®). Peripheral blood samples from 2 newly diagnosed B-CLL patients, from a relapsed B-CLL patient 4 years after treatment with Rituximab, from a Non-Hodgkin lymphoma patient with leukemic progression, and from an adolescent patient with a mixed phenotype acute leukemia (not otherwise specified) (MPAL (NOS)) were collected. Mean target antigen densities on the blast surfaces were determined by calibrated cytofluorimetry, and all blast populations with exception of the MPAL (NOS) sample were double-positive for CD19 and CD20 at varying mean densities (Table 3). The MPAL (NOS) sample was CD20-negative. The newly diagnosed B-CLL and NHL samples displayed dose-dependent responses to both SPM-1 and Rituximab, whereas the MPAL (NOS) sample responded only to treatment with SPM-1 (Figure 3). Blasts from the relapsed B-CLL patient did not respond to treatment with Rituximab under these conditions, although they expressed CD20 on their surface, and these cells were therefore not antigen-loss escape variants. They displayed a weak, but clearly measurable dose-dependent response to treatment with SPM-1. Therefore, they still were capable of responding to NK-mediated lysis, and thus their failure to respond to treatment with Rituximab must have been due to other causes. The EC_{50}-values for SPM-1 were 5- to 430-fold lower than those for Rituximab under these experimental conditions (Table 3).

SPM-1 mediates comparable cytotolytic activity by NK cells as related Fc-engineered antibody-derived agents

After having established that triplebody SPM-1 was capable of mediating effective lysis of cancer cells via the CD16-specific scFv domain in ADCC experiments with

Table 2: Surface expression of CD19 and EC_{50} values for RDL by SPM-1 with different malignant B lymphoid cell lines as targets

Cell Line	Subtype of malignancy	CD19 density [#]	EC_{50} (range) [pM]
SEM	Pro-B (mixed lineage)	42,600 ± 10,700	5.6 (2.5 – 10)
NALM-6	Pre-B	26,700 ± 11,400	6.1 (1.8 – 17.3)
RAJI	Burkitt's Lymphoma	31,900 ± 22,800	16.5 (5.4 – 38.5)
ARH-77	Mature B (myeloma)	2,400 ± 1,200	79.4 (38 – 645.3)

Antigen densities are given in copy numbers per cell.

human NK cells, we asked how strong this activity was compared with related molecular formats of antibody-derived proteins, which carry an Fc portion optimized for ADCC activity by suitable point mutations. To this effect we employed 2 CD19-specific minibodies, one with an engineered Fc-domain, mutated for optimized ADCC activity, the other with the non-mutated Fc-portion from the parental human IgG1 antibody. In addition, we had access to the Fc-engineered CD19-antibody 4G7SDIE [39, 41] for comparative cytotoxicity studies, which carried some of the same mutations in its Fc-portion as the optimized minibody (Figure 4A). Standardized 3 hr cytolysis assays were performed with NK cells from a healthy donor at an E : T ratio of 2 : 1 against SEM (pro-B ALL) and Namalwa (Burkitt lymphoma) target cells. No difference was observed between the dose-response of the target cells to treatment with SPM-1 or the Fc-engineered CD19 antibody 4G7SDIE and the Fc-engineered minibody, while treatment with the non-Fc-engineered minibody was ineffective (Figure 4B). Remarkably, SPM-1 and the Fc-engineered 4G7SDIE antibody produced a similar degree of maximum specific lysis in this endpoint assay, and both were active with similar EC_{50}-values, while clear differences in the kinetics of their action in ADCC experiments with γδ T cells as effectors were observed in the impedance-based, time-resolved assays described below (Figure 6; Supplementary Figure S1). Therefore, release assays measuring only the endpoint of cytotoxicity integrated over an entire measurement interval, typically of 3 - 4 hrs, fail to reveal kinetic details of the reaction, which however are likely to be important for an understanding of the *in vivo* activity of these agents in animal models and human recipients.

Activation of non-pre-stimulated γδ T cells from peripheral blood of healthy donors by SPM-1 plus target cells

Human γδ T cells express CD16 and are capable of mediating ADCC of malignant targets in combination with CD19-antibodies and the antibody-derived bispecific agent N19-C16 [39–41]. Therefore here we asked, whether primary human γδ T cells from healthy donors, not pre-stimulated by other means, can be activated for cytolysis by exposure to SPM-1 plus target cells. Peripheral blood mononuclear cells (PBMCs) were isolated from platelet-pheresis products from healthy donors and the fraction of γδ T cells in this population was (2.3 ± 1.2) % on average. These low frequencies necessitated an indirect detection method for the activation of primary untreated γδ T cells. To this effect, CD19-bearing pro-B (SEM) and pre-B ALL (NALM-6) cells were first incubated overnight with primary samples of γδ T cells, and subsequently SPM-1 or control agents were added and ADCC activity was indirectly monitored by measuring the appearance of the degranulation marker CD107a on the surface of the γδ T cells. In addition, intracellular concentrations of TNFα and IFN-γ were measured by cytofluorimetry as markers for activation towards cytolysis. In the absence of CD19-bearing targets, γδ T cells of only a few sensitive donors displayed a weak elevation of CD107a on their surface and a small increase in intracellular TNFα after addition of SPM-1. However, after overnight incubation with CD19-bearing target cells, γδ T cells from several donors showed a clear increase in cell surface CD107a and intracellular TNFα and IFN-γ after addition of SPM-1, and thus showed clear evidence for activation towards cytolysis by SPM-1 plus target cells (Figure 5).

SPM-1 mediates target cell lysis by both primary non-expanded and *ex vivo* expanded γδ T cells from healthy donors

To assess whether γδ T cells are capable of lysing CD19-bearing target cells by ADCC in combination with SPM-1 or control agents, and to observe the progress of this reaction in real time, viability of CD19-expressing, adherent MCF7-CD19 tm cells was monitored with the xCelligence assay system [41, 42]. This assay was initially used here with freshly isolated, non-expanded γδ T cells from 2 healthy donors. The γδ T cells were enriched in one case by positive selection with immunomagnetic (MACS) beads and reached a purity of 97 %, but the absolute number of cells collected in this manner was low. Specific lysis was obtained in combination with both SPM-1 and the CD19 antibody 4G7SDIE, in particular at

high E : T ratios of 10 : 1 and 20 : 1, but not with the control triplebody SPM-2 (data not shown). These results are consistent with earlier reports, in which specific lysis of MCF7-CD19 tm cells with similarly enriched non-expanded γδ T cells from healthy donors mediated by the 4G7SDIE antibody had been reported [41]. In conclusion, SPM-1 was capable of mediating ADCC of these adherent target cells by non-expanded γδ T cells from a healthy donor, but the available cell numbers were too low to permit a systematic study. Therefore, the experiments, which are described below (Figure 6; Supplementary Figure S1), were performed with *ex vivo* expanded γδ T cells.

For this purpose PBMCs from healthy volunteers obtained by leukapheresis were first expanded *ex vivo* in the presence of rhIL-2 and zolendronate as described previously [41]. After 12 -14 d in culture the total number of expanded cells was increased only marginally (by about 30 %), but the fraction of γδ T cells within the expanded population was increased by about 20 - 30-fold from typically 2 - 3 % to 35.9 – 60.6 %. The fraction of CD16-bearing γδ T cells in the expanded cell population was around 36 % for the sample from Donor 2. γδ T cells were then isolated from this population with immunomagnetic beads, which resulted in highly pure γδ T cells in sufficient numbers. The batch derived from Donor 2 was 98 % pure at this stage and was incubated once more overnight with IL-2 to remove contaminants resulting from the MACS enrichment procedure. This population was still heterogeneous with regard to CD16 antigen density on the cell surface. xCelligence assays were then performed with these cells using either SPM-1 or 4G7SDIE or control proteins as mediators of lysis. While the morphological and physiological properties of γδ T cells are likely to be affected by this *ex vivo* expansion, the use of this expanded population still permits us to conclude, whether γδ T cells as a defined T cell subset are capable in principle of achieving target cell lysis mediated by SPM-1.

Specific lysis values were calculated from the raw data and plotted for 3 different donors of γδ T cells at different E : T ratios as a function of time (Figure 6). Addition of SPM-1 caused a rapid increase in specific target cell lysis by γδ T cells from Donors 2 and 4 within the first 3 hrs. Close to 100 % of specific lysis was achieved within 12 hrs. By contrast, γδ T cells from Donor 3 did not produce a similarly rapid lysis during the first hours, but showed a steady slow increase in target cell lysis over the entire 12 hr measurement period. The

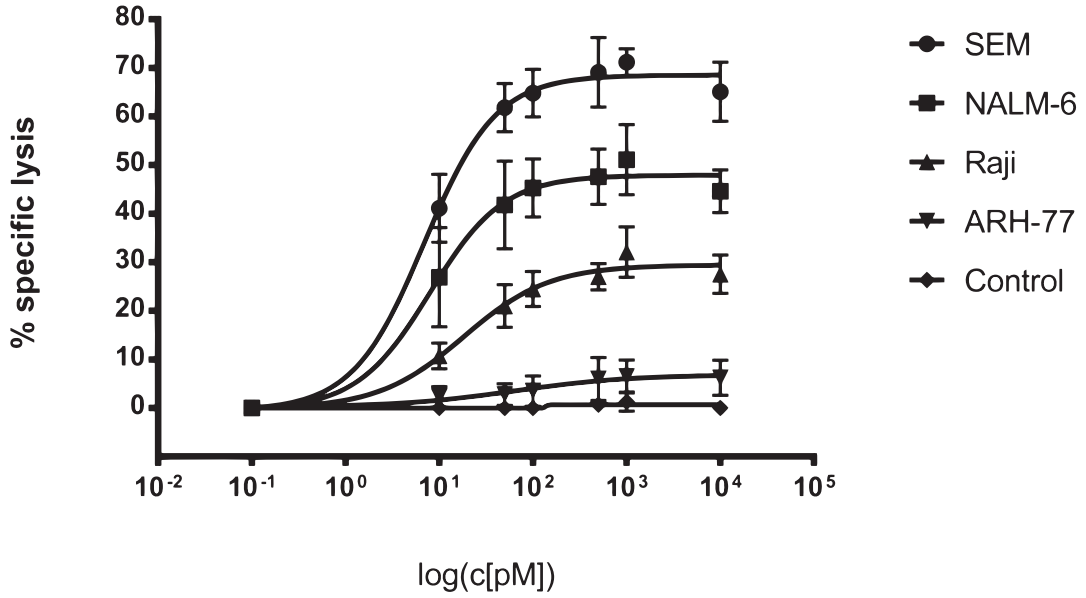

Figure 2: SPM-1 mediates lysis of a panel of CD19-bearing cell lines derived from various types of B cell malignancies. Dose response profiles from Redirected Lysis (RDL) assays performed with SPM-1 or control proteins plus *ex vivo* expanded MNCs from healthy donors. Calcein release assays as described in Methods. SEM cells were derived from a pro-B ALL, NALM-6 from a pre-B ALL, RAJI from a Burkitt's Lymphoma, and ARH-77 from a multiple myeloma. MNCs were used at an 8 : 1 effector-to-target cell (E : T) ratio, corresponding to a net NK : target cell ratio of 2 : 1, because NK cells accounted for approx. 25 % of the expanded MNC population. SPM-1 concentrations in the reaction mixtures in pM units. Specific lysis plotted on the vertical axis was computed as explained in Methods. The control triplebody targeting HER2 failed to induce specific lysis at comparable concentrations as SPM-1, because this antigen was undetectable on the target cells used here. In combination with HER2-bearing targets this triplebody was active in positive control experiments, performed separately. Data points plotted here are mean specific lysis percentages ± standard error of the mean (SEM) from n = 4 to 5 separate experiments.

Table 3: Target antigen densities and EC_{50} values for RDL / ADCC by SPM-1 or rituximab with primary lymphoma and leukemia blasts isolated from newly diagnosed patients

Patient	Antigen density [#]		EC_{50} [pM]	
	CD19	CD20	SPM1	Rituximab
B-CLL 1 (at diagnosis)	9,600 ± 500	4,000 ± 100	15.8	247.5
B-CLL 2 (at diagnosis)	7,600 ± 1,900	3,900 ± 1,200	3.0	1,300
Relapsed B-CLL	6,500 ± 1,700	1,800 ± 300	27.0	-
MPAL(NOS)	8,400 ± 2,800	0	86.0	-
NHL	14,600 ± 7,700	19,400 ± 2,200	35.7	185.7

Antigen densities are given in copy numbers per cell.

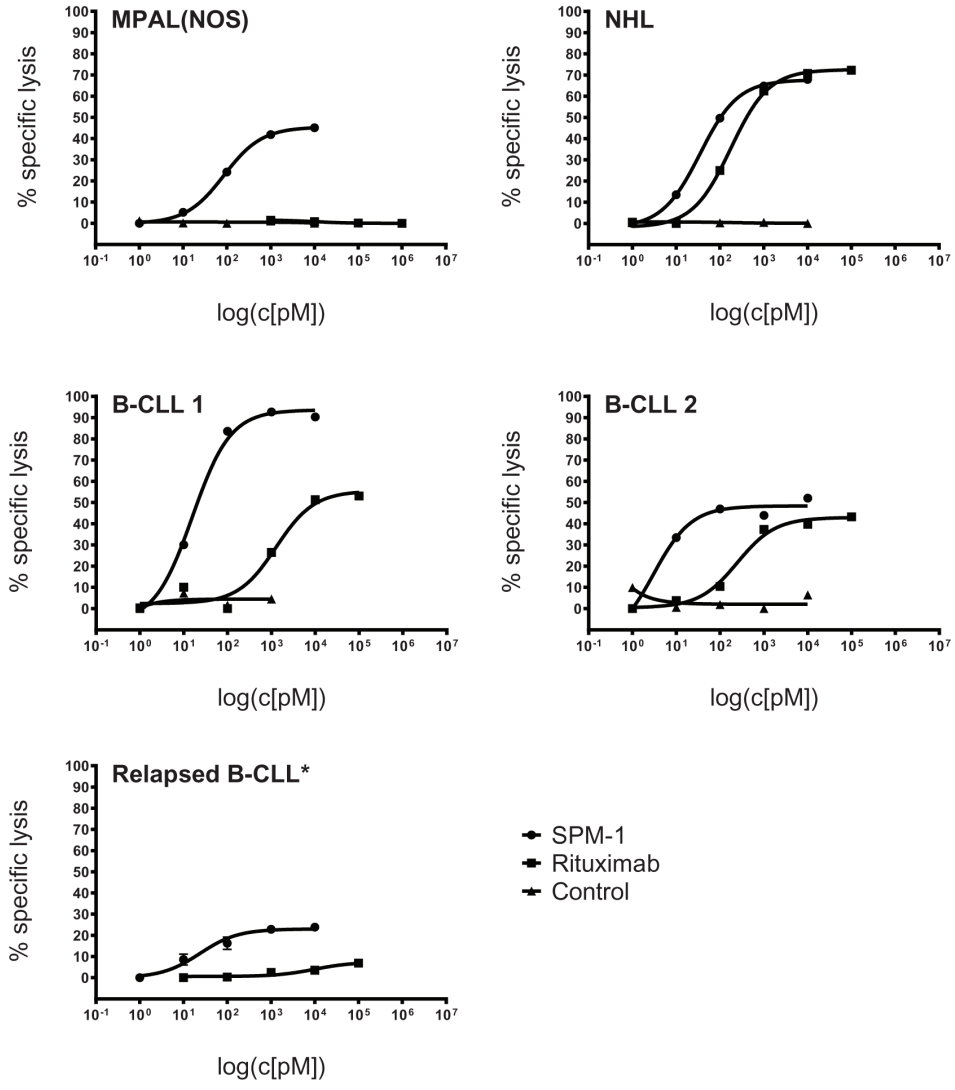

Figure 3: SPM-1 mediates stronger lysis of primary lymphoma- and leukemia blasts from newly diagnosed patients than the therapeutic antibody Rituximab (MabThera®). Malignant cells from peripheral blood of newly diagnosed patients were used as targets in RDL and ADCC assays with SPM-1 and Rituximab, respectively. SPM-1 and Rituximab were present in the reaction volumes in the concentrations shown in pM units. NK cells were used at a net E : T ratio of 2 : 1, as defined for Fig. 2. Samples were from 1 patient with a mixed phenotype acute leukemia (MPAL(NOS); $CD19^+$ $CD20^-$); 2 patients with B-CLL (CLL: chronic lymphocytic leukemia; $CD19^+$ $CD20^{LOW}$); 1 patient with a Non-Hogkin Lymphoma (NHL; $CD19^+$ $CD20^{HIGH}$) and 1 patient with newly relapsed B-CLL ($CD19^+$ $CD20^{DIM}$). This patient had undergone 6 previous treatments with Rituximab. Insufficient primary material from this patient was available to perform the HER2-16-HER2 control, which is indicated by an asterisk (*).

control triplebody SPM-2 with binding sites for antigens CD33 and CD123 [27, 34], which were not expressed on these targets, did not cause target cell lysis beyond the spontaneous antibody-independent lysis (AIC) of this batch of γδ T cells alone (Figure 6). Lysis mediated by SPM-1 showed a faster initial rise than lysis mediated by the Fc-optimized antibody 4G7SDIE, although towards the end of the measurement period the reaction rates mediated by both agents appear to have stabilized and to have reached close to constant values. The raw

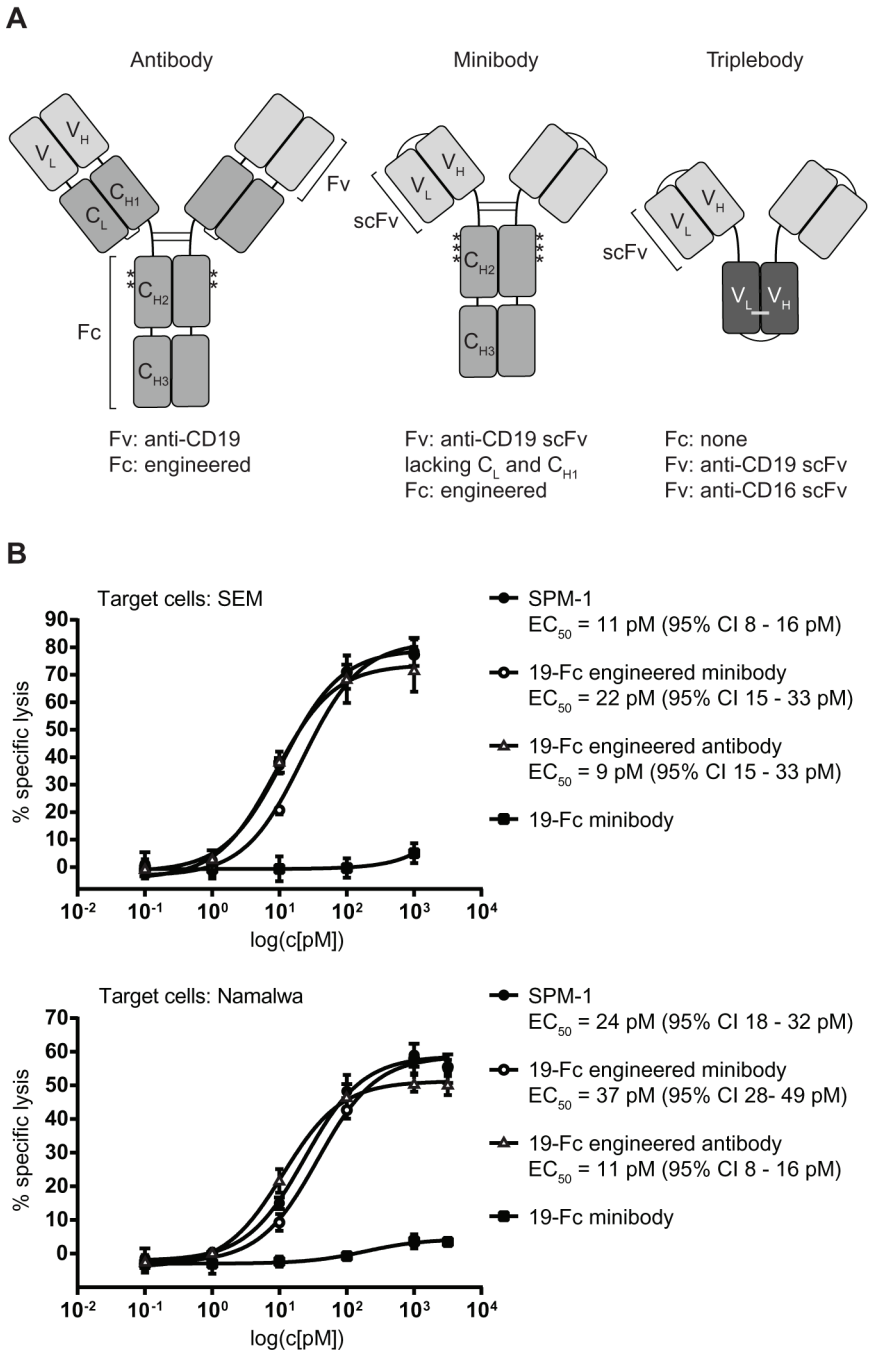

Figure 4: Triplebody SPM-1 performs equally well as other best-in-class CD19-specific agents in related molecular formats in comparative RDL/ADCC assays. A. Asterisks indicate positions of point mutations (substitutions S239D and I332E) in the Fc region of the Fc-engineered antibody 4G7SDIE. Single chain fragment variable (scFv) units used in the minibody and the triplebody are labeled. One minibody carried the non-engineered Fc-domain, the other the same 2 mutations S239D and I332E shown above for 4G7 SDIE plus a third substitution A330L (third asterisk). **B.** RDL analysis of SPM-1 (filled black circles) compared with the best-in-class antibody 4G7SDIE (open triangles), the Fc-engineered minibody (open circles) and the non-engineered minibody (black squares). Target cells: SEM (top) and Namalwa (bottom).

data for Donor 4 from this experiment are also shown in Supplementary Figure S1, because this representation visualizes in a particularly clear manner that the lytic process as followed by this assay did not proceed with a mono-phasic, but with an at least bi-phasic kinetics. This observation suggests that at least 2 different so far unknown molecular processes are at work at different stages of the overall reaction. In the Discussion section we attempt to relate these results to the different molecular architecture of these antibody-derived agents.

DISCUSSION

The key findings of this study are:

- The humanized and optimized triplebody SPM-1 can be produced in sufficient quantity and purity with an industry standard production and purification process, which can be scaled up for large-scale production.
- SPM-1 mediated efficient redirected lysis of CD19-bearing target cells in cell culture assays not only by NK cells but also by γδ T cells from healthy donors.
- In benchmark experiments with NK cells from healthy donors, SPM-1 was equally active as Fc-engineered antibody-derived proteins, including the CD19 antibody 4G7SDIE. It was active at similarly low EC_{50} concentrations in the picomolar range and mediated comparable maximum specific lysis as these best-in-class reference proteins.
- SPM-1 mediated efficient lysis of primary cells from patients with various B lineage malignancies and of cell lines derived from various B cell neoplasms by NK cells from healthy donors. The agent produced stronger ADCC lysis than Rituximab of primary cells from 3

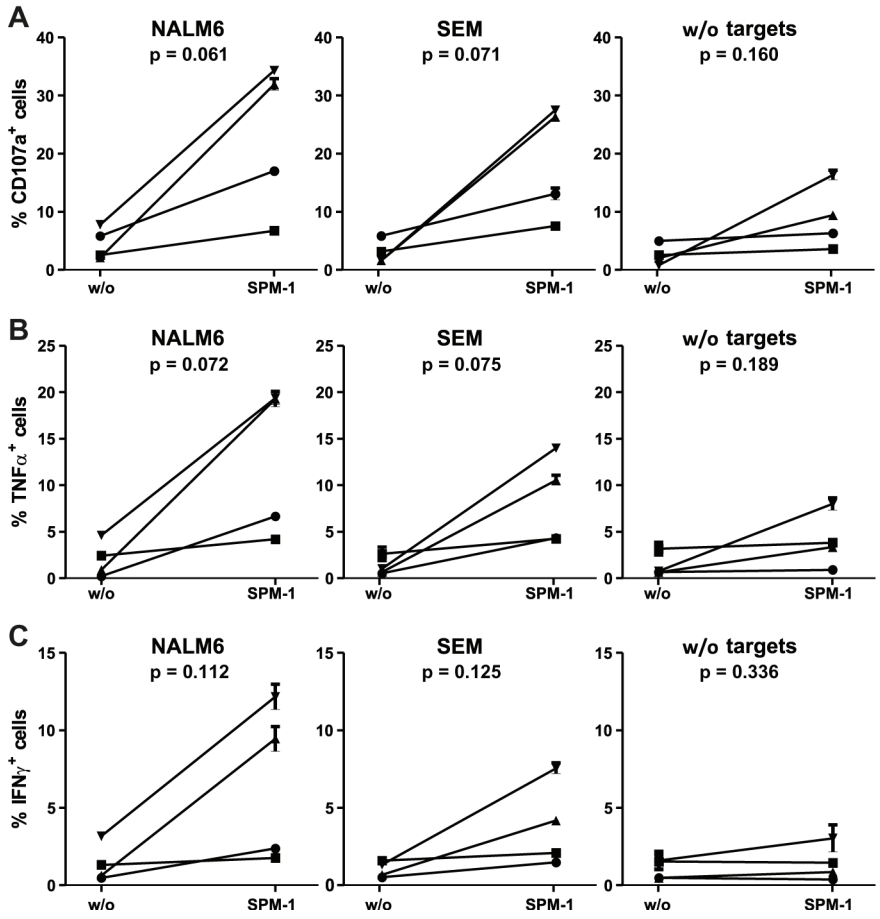

Figure 5: Primary γδ T cells are activated for cytolysis by exposure to SPM-1 plus target cells. A. Fresh γδ T cells were prepared from healthy donors as described in Methods and exposed to SPM-1 with or without NALM-6 or SEM target cells. Degranulation of γδ T cells was monitored indirectly by cytofluorimetric measurement of the surface antigen density of the degranulation marker CD107a. **B.** Changes in intracellular TNFα concentrations in primary γδ T cells following exposure to SPM-1 plus/minus target cells were measured cytofluorimetrically as described in Methods. **C.** Changes in intracellular IFN-γ concentrations in primary γδ T cells occurring after exposure to SPM-1 plus/minus target cells were measured cytofluorimetrically as described in Methods. Of the 6 samples from different donors that were analyzed, 4 had a γδ T cell content above 2 % in their PBMC compartments and each of these responded to exposure to SPM-1 plus target cells by increased cytokine production and increased surface exposure of the degranulation marker in comparison to treatment with the control triplebody SPM-2 or exposure to the target cells alone without mediator proteins.

B-CLL patients, one NHL patient and one MPAL (NOS) patient.

- Non-expanded γδ T cells from freshly drawn PBMC samples of healthy donors were activated for cytolysis by exposure to SPM-1 plus target cells, as evidenced by surface exposure of the degranulation marker CD107a and elevated intracellular concentrations of TNFα and IFN-γ.
- SPM-1 mediated lysis of surface-adherent target cells by both non-expanded and *ex vivo* expanded γδ T cells from healthy donors in the impedance-based xCelligence assay.
- In the xCelligence assay, SPM-1 mediated a rapid initial phase of lysis of surface-bound targets, faster than lysis mediated by the Fc-engineered reference antibody 4G7SDIE.

The humanized and optimized triplebody SPM-1 was equally potent in ADCC as the parental agent, and its production and purification by industry-standard procedures routinely used for commercial production of therapeutic antibodies was found to be possible. The ADCC assays presented here were performed with *ex vivo* expanded NK cells from healthy donors, which were pre-activated through long-term exposure to IL-2. We anticipate that SPM-1 will also be active in patients with B-lymphoid malignancies by directing autologous NK cells, provided it is administered at a time, when endogenous NK cells are present in sufficient numbers and are cytolytically active. This is the case for example for pediatric patients with acute lymphoblastic leukemia in a post-transplant setting a few weeks after transplantation, where donor-derived NK cells rapidly reconstitute the patient's blood and marrow and are active in mediating graft-versus-leukemia (GvL) effects [37].

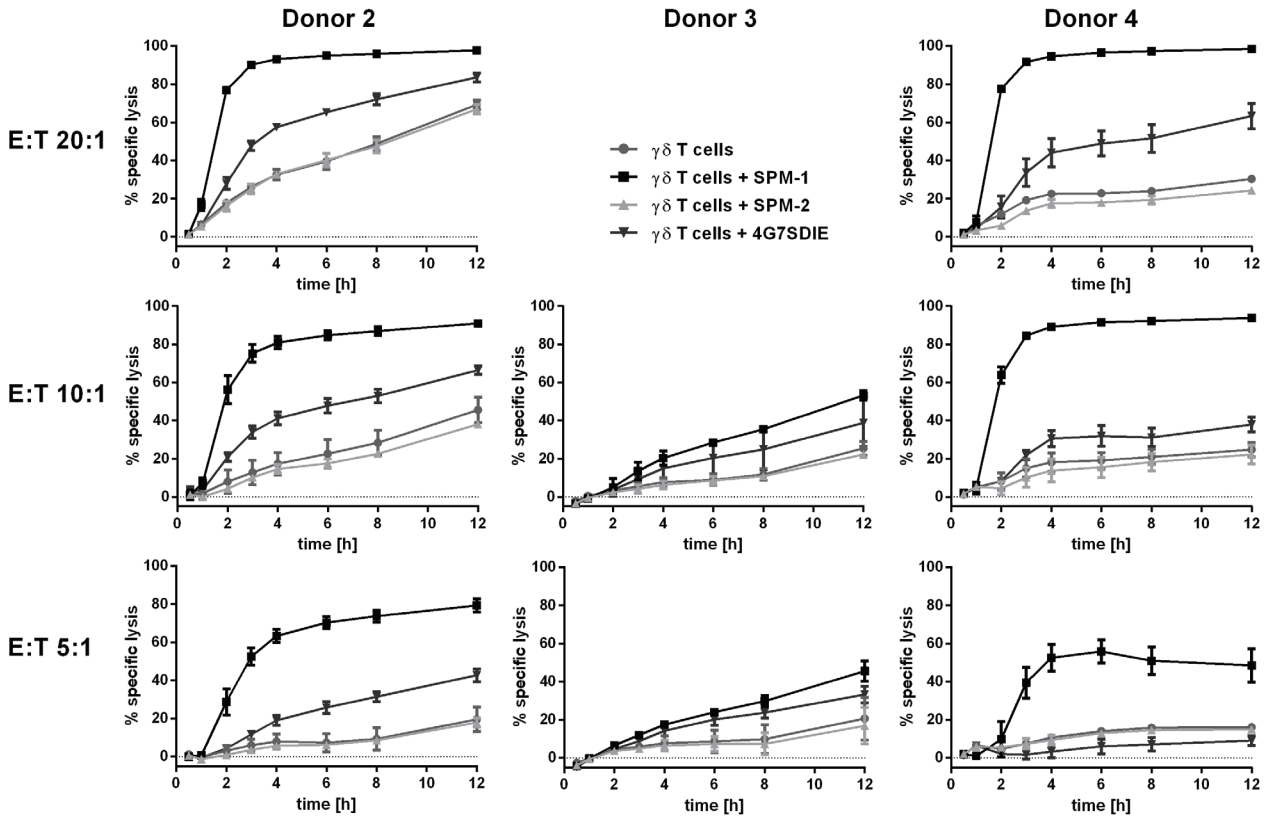

Figure 6: SPM-1 directs expanded γδ T cells from healthy donors for very rapid lysis of CD19-bearing MCF7-CD19 tm target cells, monitored in a real-time assay. For γδ T cell donors # 2, 3 and 4 specific lysis curves were calculated from the cell indices (CI) of MCF7-CD19 tm cells, measured over the time course of the reaction with 1 nM SPM-1 or control proteins. SPM-2: control triplebody 33-16-123 with scFv binding domains for the target antigens CD33 and CD123, which are not carried by the MCF7-CD19 tm cells. CI values measured after treatment with control triplebody SPM-2 were comparable to those obtained with γδ T cell controls alone. Measurements were performed with the help of the label-free impedance-based xCelligence assay as described in Methods. Decreasing CI values are a correlate of and indicative of target cell lysis. In the presence of triplebody SPM-1, CI values decreased to approximately 9-fold lower values than after treatment with γδ T cells alone (Patient 4: 0.1 versus 0.9). Furthermore, specific lysis upon treatment with SPM-1 was more rapid and efficient than after treatment with ADCC-optimized CD19-antibody 4G7SDIE.

It remains, however, to be demonstrated in experiments with autologous NK cells from patients not treated by a stem cell transplant, that these cells also achieve a sufficiently strong ADCC lysis of their cancer cells mediated by SPM-1. Corresponding studies have been performed for triplebody SPM-2, which mediated ADCC of a patient's AML cells by autologous NK cells, when these were drawn in first remission after a successful induction therapy [34]. The issue is still debated, because in AML autologous NK cells have been reported to be reduced in numbers and specific lytic potential in the tumor environment [19–22]. It is not clear, whether this reversible functional attenuation is equally important in B-lymphoid malignancies as in AML, because it is supposedly mediated at least in part by soluble mediators and the hypoxic milieu present in the marrow of AML patients. The tumor environment may be quite different for B-lymphoid malignancies, which evolve at different sites and in different cellular environments. We do not yet know, whether γδ T cells are present in sufficient numbers and in an active state for ADCC in patients with B cell malignancies at the sites of the cancer cells.

Triplebodies such as SPM-1 achieve similar cytotoxic effects as conventional therapeutic antibodies in cell culture ADCC assays in far lower concentrations. Rituximab for example is used in lymphoma therapy at concentrations in the range of 10 mg/kg, while Blinatumomab is used at concentrations in the range of 10 μg/kg, i.e. in approximately 1.000-fold lower doses [11]. In the results presented above with primary cells from patients with B cell malignancies (Figure 3), SPM-1 was active in ADCC assays in concert with NK cells with EC_{50}-values lower by 5- to 430-fold than those determined for Rituximab. This finding is consistent with the dose ranges of Rituximab and Blinatumomab used in clinical applications as quoted above. The primary cells from the relapsed B-CLL patient, which were not efficiently lysed by NK cells plus Rituximab (Figure 3), were not antigen-loss variants and still expressed surface CD20. More likely, they were resistant to ADCC by NK cells through a different mechanism. Such cases have been reported for other Rituximab-resistant patients. However, this resistance cannot have been a general resistance to all different pathways leading to death of target cells by ADCC, because the cells were still lysed by ADCC via NK cells plus SPM-1.

The Fc-engineered CD19 antibody 4G7SDIE, which is largely identical with the corresponding antibody XmAb5574 [9, 39, 41], has previously been shown to mediate potent ADCC by γδ T cells [41]. This T cell subset is particularly useful in combination with TCRαβ- and CD19-depleted allogeneic stem cell transplantation (allo-HSCT) [47]. In such cases, both γδ T cells and NK cells are available for graft-versus-leukemia activity and can maintain a certain level of immune protection of the host. The γδ T cell population is small but potent, and does not only provide a natural anti-cancer activity, but is also unlikely to elicit graft-versus-host-disease (GvHD), because of its independence from MHC-restriction. Furthermore these cells mediate significant anti-viral activity. Therefore, γδ T cells are a highly desirable population of immune effector cells for cancer immunotherapy [37, 38]. The results presented here establish that the CD16-binding module carried in SPM-1 is capable of engaging both NK and γδ T cells as effectors for lysis of leukemia cells. Efficient activation and engagement of γδ T cells by SPM-1 was demonstrated here, and the potential expansion of this leukocyte subset *in vivo* in response to activation holds promise for the treatment of leukemia patients with triplebodies triggering γδ T cells via CD16.

The most unexpected new finding of the present study was produced with the help of the xCelligence assay, which allowed us to follow a cytolytic reaction mediated by a triplebody in real time. The following unresolved problem has intrigued us for several years: the parental triplebody ds(19-16-19) of SPM-1 showed an approximately 3-fold stronger binding avidity to CD19 on leukemic target cells than the bispecific tandem diabody 19-16, but had an approximately 25-fold greater cytolytic potential than this diabody for a number of malignant B-lymphoid cell lines and primary cell samples from a number of patients with different B-lymphoid cancers [26]. It was hypothesized that the triplebody may have led to the formation of a tighter synapse between the cancer cells and the NK cells, and that this in turn may have led to a stronger activation of the NK cells for cytolysis. However, no direct evidence in support of this hypothesis has been produced, because structural methods for a comparative analysis of the fine structure of the synapses produced by both agents were not available. It came as a surprise that progress towards solving this problem may come from improving the resolution of measurement methods for kinetic aspects of synapse formation and the cytolytic reaction.

The key observation reported here (Figure 6; Supplementary Figure S1) is that the cytolytic reaction, as followed by the xCelligence assay, occurred with a biphasic kinetic or a kinetic of even greater complexity. A rapid initial change in the cell index (CI), a measure of viability of the cells (equated with a rapid first phase of cellular lysis [42]), was followed by at least one more phase of slower viability changes. We do not know the precise correlation between the changes in the CI-value and cellular death, and whether a change in CI is only achieved when a target cell is completely lysed, or whether it also occurs, when a target cell is not yet irreversibly dead, but has engaged in the first steps of a multi-step pathway to death. Cell death mediated by NK cells through the degranulation of granzymes is death by apoptosis, and occurs through a succession of steps, which can be individually monitored. An example in case is the time-resolved study of apoptosis by cytofluorimetry with staining of the target cells by annexin V and propidium iodide [48]. In this case an early

pre-apoptotic phase can be distinguished, characterized by annexin V staining but yet no influx of PI into the nucleus, which is still reversible. A subsequent late apoptotic state is characterized by more intense staining with both annexin V and PI, which is irreversible. It is not clear, whether the initial rapid change in the CI-value, which was observed here, reflects a truly irreversible step towards cellular death and complete lysis, mediated by γδ T cells, or only a change in impedance, which may be associated with reversible pre-apoptotic changes such as the rearrangements of the cellular membrane detected by binding of annexin V. Regardless of the precise correlation between events discovered by changes in CI in this assay and progressive stages on the path to cellular death as detected by other methods, the data shown here demonstrate the existence of more than one so far poorly understood reaction phases, which are likely to be highly informative about the mechanism of action of this triplebody.

A potential answer to the problem posed above, suggested by the results of the present study is that the strength of binding of a therapeutic protein to the target cell may not be the dominant determinant of its cytolytic potential. To build a productive cytolytic synapse, binding of the agent to the trigger on the effector cell is also important. Although the binding affinities of SPM-1 for CD16 on effector cells and of the CD16 receptor on effector cells for the Fc-domain of Fc-engineered antibodies such as 4G7SDIE are in the same order of magnitude, it is still possible that the triplebody has faster access to CD16 on the γδ T cell (and thus a faster "on"-rate) than the 4G7SDIE antibody. We suspect this to be the case, because the triplebody has only half the mass of the antibody and may have different space-filling properties and different flexibility, which may allow faster access to the CD16 epitope on the effector cell. This faster access may lead in turn to a faster formation of a synapse between the suface-adherent target cells and the triplebody-decorated γδ T cells. This could lead to the differences in the initial phase of changes in the CI index, which were detected by the xCelligence assay. This difference in the early stage of the kinetics may not affect the EC_{50}-values and the degree of maximum specific lysis, because both SPM-1 and the 4G7SDIE antibody mediated target cell lysis by NK cells with similar EC_{50}-values and similar maximum specific lysis (Figure 4B). It could however still have an impact on the pharmacokinetic properties of both agents, and thus on their anti-cancer activities *in vivo*. Therefore, the xCelligence assay offers a welcome enrichment of the set of tools available to study cytolytic processes in detail, even if it still does not allow for single cell resolution. Combining high throughput real-time assays with single-cell resolution assays is an important area for future improvements, which promises to be highly informative [49].

Taken together, the data presented here permit us to conclude that SPM-1 in combination with NK cells is highly active in ADCC reactions against primary cells from patients with a variety of B-lymphoid malignancies. It is capable of recruiting γδ T cells for cytolysis, and reveals unsuspected rapid reaction kinetics in time-resolved cytolysis assays. These properties make it both a valuable tool for further studies of the kinetics of the cytolytic process together with CD16-bearing effector cells, and a candidate for further clinical development as a highly potent alternative for the treatment of B-lymphoid malignancies with distinct advantages over available best-in-class agents.

MATERIALS AND METHODS

Generation of triplebodies and other antibodies and antibody-derived proteins

To produce triplebody SPM-1, the CD19-specific scFv domains contained in the parental triplebody ds(19-16-19) [26] were humanized with procedures developed in the laboratory of Dr. A. Honegger [43, 44]. The CD16-specific scFv was disulfide-stabilized according to published procedures [43]. SPM-1 contains a C-terminal hexa-histidine tag for purification purposes. Potentially immunogenic sequences that resulted from the standard cloning procedures used for the generation of the parental ds(19-16-19) were removed from the final protein. The coding sequence for SPM-1 was optimized to minimize homologous recombination between cDNA sequences coding for the CD19 binding domains by introducing variations in the wobble bases of the coding triplets. The cDNA was subcloned into a pSecTag2-HygroC expression vector (Life Technologies, Darmstadt, Germany). The Her2-16-Her2 triplebody was constructed by replacing the N- and C-terminal scFvs of a humanized successor molecule of the published triplebody ds(19-16-19) [26] with Her2-specific scFvs from the pSecTag2-HygroC-4D5-CD3 bispecific single chain Fv construct provided by Prof. M. Peipp [50] using standard molecular biology techniques.

The minibodies 4D5-IgG1-Fc and 4D5-IgG1-Fc engineered (provided by Prof. M. Peipp) contained a Her2 (clone 4D5)-specific scFv, a modified hinge region from an IgG, which allowed for disulfide-bridge formation, and a modified Fc-domain, harboring the substitutions S239D/I332E/A330L (SDIEAL) or no substitutions, respectively [50]. To generate the CD19-targeting minibodies, the 4D5-scFv was replaced by the CD19-targeting scFv from SPM-1.

For the expression of all proteins, human Freestyle™ 293-F cells (Life Technologies, Darmstadt, Germany) were transfected with the respective plasmid DNA using the 293fectin™ Transfection Reagent (Life Technologies, Darmstadt, Germany) according to the manufacturer´s instructions. Proteins were either expressed transiently or a pool of stably transfected cells was generated by continuous selection with 50 µg/ml hygromycin C.

Recombinant proteins were captured from cell culture supernatants via their C-terminal hexahistidine tags by metal-ion affinity chromatography. SPM-1 was further purified by anion- and cation-exchange chromatography. The scFv-minibodies and Her2-16-Her2 were further purified by size exclusion chromatography. Protein concentrations were determined by absorbance measurements at 280 nm and using the molar extinction coefficient derived from the amino acid sequence.

The quality of purified recombinant protein batches was analyzed by analytical size exclusion chromatography to monitor the presence of monomeric protein, aggregates, breakdown products, incompletely synthesized products, contaminants and products generated by homologous recombination. An Äkta liquid chromatography system was used, equipped with a Superdex S200 5/150 GL column (GE Healthcare Europe, Munich, Germany). Total amounts of 25 µg of protein in 50 µl volumes were loaded onto the column followed by isocratic elution with SEC buffer (20 mM Histidine-HCl pH 6.0, 150 mM NaCl). Eluted proteins were monitored by absorbance at 280 nm and by SDS-PAGE.

The CD19 antibody 4G7SDIE was provided by Prof. G. Jung and Dr. L. Grosse-Hovest from the University of Tübingen, Germany. This antibody harbors an engineered Fc-domain with the same substitutions S239D and I332E as the CD19 antibody XmAb 5574 [9, 39, 41]. The therapeutic CD20 antibody Rituximab (MabThera®) was obtained from Roche Pharma AG.

Target cells and culture conditions

The RAJI, NALM-6, SEM, NAMALWA, ARH-77 and MCF-7 cell lines were obtained from the German Collection of Microorganisms and Cell Cultures (DSMZ, Braunschweig, Germany). RAJI, NALM-6, NAMALWA and ARH-77 were cultured in RPMI 1640 medium (Invitrogen, Karlsruhe, Germany). MCF-7 and SEM cells were kept in EMEM and IMDM medium (Lonza, Basel, Switzerland), respectively. All media were supplemented with 10 % fetal calf serum or pooled human AB serum (Invitrogen, Karlsruhe, Germany), 100 U/ml penicillin, 100 µg/ml streptomycin, 1 mM sodium pyruvate and 2 mM L-glutamine (all reagents from Biochrome).

MCF-7-CD19 tm cells were generated as described [41]. Briefly, full-length cDNA coding for human CD19 (GenBank BC006338.2) was purchased from Source Bioscience (Berlin, Germany) and cloned into a suitable cDNA expression vector. MCF-7 cells were transfected with this plasmid by electroporation, and CD19-expressing clones were selected and sorted by flow cytometric analysis, respectively.

Preparation of primary cells from blood of human donors

Peripheral blood samples were drawn from subjects into EDTA solution at the Medical Center of the LMU Munich or isolated from platelet-pheresis products provided by the Institute for Transfusion Medicine of the University of Tübingen after receiving informed written consent. The project was approved by the Ethics Committee of the University of Munich Medical Center. Mononuclear cells (MNCs) from leukemia patients and healthy donors were enriched by density gradient centrifugation using the Lymphoflot reagent (Biotest, Dreieich, Germany) or Biocol Separating Solution (Biochrom, Berlin, Germany) according to manufacturer's instructions. PBMCs, also used as the source of leukemia cells from patient samples, were then either suspended in RPMI medium (Life Technologies) containing 10 % fetal bovine serum (FBS) with penicillin and streptomycin (PS) at 100 units/ml and 100 µg/ml, respectively, for immediate use, or stored frozen in a solution containing 90 % FBS and 10 % DMSO. Cell viability was assessed by Trypan blue exclusion before use.

Ex vivo expansion of MNCs as a source of NK cells from healthy donors

PBMCs were expanded *ex vivo* in RPMI medium containing Interleukin-2 (IL-2) plus 5 % human serum (Life Technologies) for 20 d after an initial period of culture in the presence of an OKT3 (CD3) antibody, and were then frozen in aliquots for subsequent use as described [30, 51]. Prior to use in cytolysis experiments, the cells were thawed and cultured overnight in RPMI medium containing 5 % human serum plus 50 units/ml and 50 µg/ml PS, respectively, but no additional IL-2.

Expansion of γδ T cells

PBMCs were seeded at 1.5 x 10^6 cells per well in 6-well plates and cultured in supplemented IMDM medium containing 100 IU/ml of recombinant human IL-2 (rhIL-2) (Novartis, Basel, Switzerland) and 400 nM zolendronate (Hexal, Holzkirchen, Germany). After 13 - 14 d of culture, expanded populations containing 35.9 - 60.6 % of γδ T cells were positively selected using a Hapten-modified TCR-γδ antibody and FITC-conjugated anti-Hapten MicroBeads with the autoMACS system (Miltenyi, Bergisch Gladbach, Germany). Purity of the isolated populations was (99.2 ± 0.8) % (n = 3) and isolated cells were incubated with 400 IU/ml rhIL-2 overnight prior to functional assays. Isolated γδ T cells had lost their FITC-labeling and had restored surface expression of TCR-γδ after 24 hrs (U Seidel, unpublished data).

Flow cytometric analysis

Flow cytometric analysis was performed with an Accuri C6 flow cytometer (BD Biosciences, Heidelberg, Germany). CD16- and CD56-specific monoclonal antibodies (mAbs) were used for the analysis of NK cell content in PBMC-preparations and measured against isotype control mAbs (Immunotech, Marseille, France). Unlabelled CD19- and CD20-specific and isotype control mAbs (BD Pharmingen) were used for the analysis of cell surface densities of the antigens on target cells. Surface expression was measured using a calibrated cytofluorimetric assay (QIFI KIT®; DAKO; Hamburg, Germany) as described [45, 52].

Determination of equilibrium binding constants (K_D) and serum stability measurements of SPM-1

Equilibrium binding constants (K_D values) were measured using a flow cytometry method as previously described [46]. The K_D values were calculated from the raw data by using a nonlinear regression curve fit with the help of GraphPad Prism 3 (Graph Pad Software, Inc, San Diego, CA). Measurement of *in vitro* stability of SPM-1 in human serum was performed as previously described [26].

Redirected lysis (RDL) assays using calcein release

Non-radioactive cytolysis assays based on the release of calcein from target cells were performed as previously described [30]. Calcein AM (Life Technologies)-labeled target cells were mixed with effector cells (*ex vivo* expanded MNCs) in RPMI 1640 GlutaMAX medium supplemented with 10 % FCS and 1 % Penicillin/Streptomycin at an E (NK cell) : T ratio of 2 : 1. After addition of different concentrations of SPM-1 or control antibodies and antibody derivates (minibodies), respectively, reactions were incubated at 37 °C with 5 % CO_2 for 3 - 4 hrs. Calcein release was then determined by measuring the fluorescence intensity (relative light units, RLU) in the supernatant with a Tecan Infinite M1000 microplate reader (Tecan Group Ltd, Männedorf) at 485/535 nm. Maximum lysis was achieved by addition 2.5 % Triton X-100. Specific lysis was calculated as follows:

$$\%\ Specific\ \ Lysis = 100 * \frac{[RLU\ (sample) - RLU\ \ (background\ \ release)]}{[RLU\ (\max lysis) - RLU\ (background)]}$$

EC_{50}-values (concentration of triplebody producing 50 % of maximum specific lysis) were determined using sigmoidal dose-response curve fits (GraphPadPrism, San Diego, CA).

γδ T cell degranulation assay using detection of cell surface CD107a

The fraction of γδ T cells ($CD3^+$, $TCR\gamma\delta^+$) was determined by flow cytometry. Samples with γδ T cell counts above 1.5 % were selected for CD107a assays. Equal numbers of PBMC and NALM-6 or SEM cells were incubated with 1 nM SPM-1 or control triplebody Her2-16-Her2, 2 µM GolgiStop reagent (BD Biosciences), 10 µg/ml Brefeldin A (Sigma, Steinheim, Germany) and the fluorescent labeled CD107a-APC antibody (Biolegend, San Diego, USA) overnight in supplemented IMDM medium at 37 °C in an incubator with a 5 % CO_2-atmosphere. PBMCs were then stained for surface and intracellular markers and analyzed by flow cytometry.

Intracellular cytokine staining (ICS) of γδ T cells for TNFα and IFN-γ

Intracellular cytokine staining of γδ T cells was performed with IFNγ-BV711, TNFα-PB, and isotype control antibodies supplied by Biolegend (San Diego, CA, USA). Briefly, after incubation of γδ T cells with SEM or NALM-6 cells and SPM-1 triplebody or controls, cells were washed and resuspended in 100 µl of PBS : 1 % albumin solution. Cells were then stained with γδ TCR mAb (BD Biosciences, Heidelberg, Germany) for 30 min on ice. To distinguish TNFα and IFN-γ producers within the γδ T cell populations, cells were washed, fixed and permeabilized by incubation with 250 µl of Cytofix/Cytoperm solution (BD Biosciences, Heidelberg, Germany) for 15 min. Cells were then stained with either PE conjugated TNFα or IFN-γ mAbs versus a control mAb for 30 min on ice. The cells were finally washed twice, resuspended in FACS buffer (PBS containing 2 % fetal calf serum (FCS) plus 0.05 % sodium azide) and analyzed by flow cytometry. The percentage of cytokine-positive cells within the given γδ T cell treatment group was then calculated and plotted.

Impedance-based cytotolysis assay with human γδ T cells as cytolytic effectors

The cytolytic potential of expanded γδ T cells was analyzed in a real-time cytotoxicty assay with an xCelligence RTCA SP instrument (ACEA Biosciences, San Diego, CA) as previously described [41, 42]. Briefly, $5x10^3$ MCF-7-CD19 tm cells were seeded into each well. Expanded γδ T cells and 1 nM SPM-1 or control triplebody Her2-16-Her2, respectively, were added 24 hrs later. Cell viability was monitored every 15 min for 48 hrs. Cell indexes (CI) were normalized to CI of the time-point, when γδ T cells were added, and specific lysis was calculated relative to control cells without any added γδ T cells.

ACKNOWLEDGMENTS

The authors thank Prof. M. Peipp, Kiel, for making cDNA coding for HER2-directed scFvs and for the SDIEAL mutated Fc-portions available; Prof. G. Jung and Dr. L. Grosse-Hovest, Tübingen, for the 4G7SDIE antibody; Prof. A. Plückthun, Zurich, for permission to use humanization procedures established in his institute; Prof. R. Slany, Erlangen for valuable advice; Prof. J. Rädler and E. Chatzopoulou, Munich; and Prof. M. Peterlin, San Francisco, for critical comments on the manuscript.

CONFLICTS OF INTEREST

The authors report no conflicts of interest.

GRANT SUPPORT

This study was supported by grants from the German Research Foundation (DFG) and from the association "Chimney Sweeps Help Children with Cancer" (Schornsteinfeger Helfen Krebskranken Kindern e.V.) to GHF; by support from the Bavarian Government (M4 excellence award) to KPH, GHF and FO; by grants from the DFG (SFB 685, Project C3), from the Deutsche Kinderkrebs-Stiftung (DKS) and from the Reinhold-Beitlich-Stiftung Tuebingen to PL and UJES; by funding from the Center for Integrated Protein Science Munich (CiPSM), Quantitative Biosciences Munich (QBM) and the doctoral program "i-Target: immunotargeting of cancer" (Elite Network of Bavaria) to KPH; and by a Ph.D. student research fellowship awarded to CCR by the German José Carreras-Leukemia Foundation (www.carreras-stiftung.de, Scholarship No. DJCLS F 13/05).

REFERENCES

1. Carter RH, Wang Y, Brooks S. Role of CD19 signal transduction in B cell biology. Immunologic research. 2002; 26:45-54.
2. Del Nagro CJ, Otero DC, Anzelon AN, Omori SA, Kolla RV, Rickert RC. CD19 function in central and peripheral B-cell development. Immunologic research. 2005; 31:119-131.
3. Ishiura N, Nakashima H, Watanabe R, Kuwano Y, Adachi T, Takahashi Y, Tsubata T, Okochi H, Tamaki K, Tedder TF, Fujimoto M. Differential phosphorylation of functional tyrosines in CD19 modulates B-lymphocyte activation. European journal of immunology. 2010; 40:1192-1204.
4. Tedder TF, Inaoki M, Sato S. The CD19-CD21 complex regulates signal transduction thresholds governing humoral immunity and autoimmunity. Immunity. 1997; 6:107-118.
5. Hammer O. CD19 as an attractive target for antibody-based therapy. mAbs. 2012; 4:571-577.
6. le Viseur C, Hotfilder M, Bomken S, Wilson K, Rottgers S, Schrauder A, Rosemann A, Irving J, Stam RW, Shultz LD, Harbott J, Jurgens H, Schrappe M, Pieters R, Vormoor J. In childhood acute lymphoblastic leukemia, blasts at different stages of immunophenotypic maturation have stem cell properties. Cancer cell. 2008; 14:47-58.
7. Weiland J, Elder A, Forster V, Heidenreich O, Koschmieder S, Vormoor J. CD19: A multifunctional immunological target molecule and its implications for Blineage acute lymphoblastic leukemia. Pediatric blood & cancer. 2015; 62:1144-1148.
8. Hekman A, Honselaar A, Vuist WM, Sein JJ, Rodenhuis S, ten Bokkel Huinink WW, Somers R, Rumke P, Melief CJ. Initial experience with treatment of human B cell lymphoma with anti-CD19 monoclonal antibody. Cancer immunology, immunotherapy. 1991; 32:364-372.
9. Kellner C, Zhukovsky EA, Potzke A, Bruggemann M, Schrauder A, Schrappe M, Kneba M, Repp R, Humpe A, Gramatzki M, Peipp M. The Fc-engineered CD19 antibody MOR208 (XmAb5574) induces natural killer cell-mediated lysis of acute lymphoblastic leukemia cells from pediatric and adult patients. Leukemia. 2013; 27:1595-1598.
10. Hamadani M, Forero A, Kipps TJ, Fanale MA, Cuneo A, Perez de Oteyza J, Gladstone D, Goswami T, Ibrahim RA, Liang M, Eck S, Elgeioushi N, Herbst R, Cheson BD. (2013). MEDI-551, an anti-CD19 antibody active in chronic lymphocytic leukemia (CLL) patients previously treated with rituximab. J Clin Immunol.
11. Bargou R, Leo E, Zugmaier G, Klinger M, Goebeler M, Knop S, Noppeney R, Viardot A, Hess G, Schuler M, Einsele H, Brandl C, Wolf A, et al. Tumor regression in cancer patients by very low doses of a T cell-engaging antibody. Science. 2008; 321:974-977.
12. Ribera JM, Ferrer A, Ribera J, Genesca E. Profile of blinatumomab and its potential in the treatment of relapsed/refractory acute lymphoblastic leukemia. OncoTargets and therapy. 2015; 8:1567-1574.
13. Kochenderfer JN, Rosenberg SA. Treating B-cell cancer with T cells expressing anti-CD19 chimeric antigen receptors. Nat Rev Clin Oncol. 2013; 10:267-276.
14. Maude SL, Frey N, Shaw PA, Aplenc R, Barrett DM, Bunin NJ, Chew A, Gonzalez VE, Zheng Z, Lacey SF, Mahnke YD, Melenhorst JJ, Rheingold SR, et al. Chimeric antigen receptor T cells for sustained remissions in leukemia. The New England journal of medicine. 2014; 371:1507-1517.
15. Lee DW, Kochenderfer JN, Stetler-Stevenson M, Cui YK, Delbrook C, Feldman SA, Fry TJ, Orentas R, Sabatino M, Shah NN, Steinberg SM, Stroncek D, Tschernia N, et al. T cells expressing CD19 chimeric antigen receptors for acute lymphoblastic leukaemia in children and young adults: a phase 1 dose-escalation trial. Lancet. 2015; 385:517-528.
16. Frey NV, Porter DL. CAR T-cells merge into the fast lane of cancer care. Am J Hematol. 2016; 91:146-150.

17. Barrett DM, Teachey DT, Grupp SA. Toxicity management for patients receiving novel T-cell engaging therapies. Current opinion in pediatrics. 2014; 26:43-49.

18. Rayes A, McMasters RL, O'Brien MM. Lineage Switch in MLL-Rearranged Infant Leukemia Following CD19-Directed Therapy. Pediatric blood & cancer. 2016.

19. Lichtenegger FS, Lorenz R, Gellhaus K, Hiddemann W, Beck B, Subklewe M. Impaired NK cells and increased T regulatory cell numbers during cytotoxic maintenance therapy in AML. Leukemia research. 2014; 38:964-969.

20. Sanchez-Correa B, Campos C, Pera A, Bergua JM, Arcos MJ, Banas H, Casado JG, Morgado S, Duran E, Solana R, Tarazona R. Natural killer cell immunosenescence in acute myeloid leukaemia patients: new targets for immunotherapeutic strategies? Cancer immunology, immunotherapy. 2016; 65:453-463.

21. Dulphy N, Chretien AS, Khaznadar Z, Fauriat C, Nanbakhsh A, Caignard A, Chouaib S, Olive D, Toubert A. Underground Adaptation to a Hostile Environment: Acute Myeloid Leukemia vs. Natural Killer Cells. Frontiers in immunology. 2016; 7:94.

22. Ullah MA, Hill GR, Tey SK. Functional Reconstitution of Natural Killer Cells in Allogeneic Hematopoietic Stem Cell Transplantation. Frontiers in immunology. 2016; 7:144.

23. Yokota T, Milenic DE, Whitlow M, Schlom J. Rapid tumor penetration of a single-chain Fv and comparison with other immunoglobulin forms. Cancer research. 1992; 52:3402-3408.

24. Thurber GM, Schmidt MM, Wittrup KD. Antibody tumor penetration: transport opposed by systemic and antigen-mediated clearance. Advanced drug delivery reviews. 2008; 60:1421-1434.

25. Thurber GM, Schmidt MM, Wittrup KD. Factors determining antibody distribution in tumors. Trends Pharmacol Sci. 2008; 29:57-61.

26. Kellner C, Bruenke J, Stieglmaier J, Schwemmlein M, Schwenkert M, Singer H, Mentz K, Peipp M, Lang P, Oduncu F, Stockmeyer B, Fey GH. A novel CD19-directed recombinant bispecific antibody derivative with enhanced immune effector functions for human leukemic cells. J Immunother. 2008; 31:871-884.

27. Kugler M, Stein C, Kellner C, Mentz K, Saul D, Schwenkert M, Schubert I, Singer H, Oduncu F, Stockmeyer B, Mackensen A, Fey GH. A recombinant trispecific single-chain Fv derivative directed against CD123 and CD33 mediates effective elimination of acute myeloid leukaemia cells by dual targeting. British journal of haematology. 2010; 150:574-586.

28. Roskopf CC, Schiller CB, Braciak TA, Kobold S, Schubert IA, Fey GH, Hopfner KP, Oduncu FS. T cell-recruiting triplebody 19-3-19 mediates serial lysis of malignant B-lymphoid cells by a single T cell. Oncotarget. 2014; 5:6466-6483. doi: 10.18632/oncotarget.2238.

29. Schubert I, Kellner C, Stein C, Kugler M, Schwenkert M, Saul D, Mentz K, Singer H, Stockmeyer B, Hillen W, Mackensen A, Fey GH. A single-chain triplebody with specificity for CD19 and CD33 mediates effective lysis of mixed lineage leukemia cells by dual targeting. mAbs. 2011; 3:21-30.

30. Schubert I, Kellner C, Stein C, Kugler M, Schwenkert M, Saul D, Stockmeyer B, Berens C, Oduncu FS, Mackensen A, Fey GH. A recombinant triplebody with specificity for CD19 and HLA-DR mediates preferential binding to antigen double-positive cells by dual-targeting. mAbs. 2012; 4:45-56.

31. Roskopf CC, Braciak TA, Fenn NC, Kobold S, Fey GH, Hopfner KP, Oduncu FS. Dual-targeting triplebody 33-3-19 mediates selective lysis of biphenotypic CD19+ CD33+ leukemia cells. Oncotarget. 2016;7:22579-22589. doi: 10.18632/oncotarget.8022.

32. Li L, Yazaki PJ, Anderson AL, Crow D, Colcher D, Wu AM, Williams LE, Wong JY, Raubitschek A, Shively JE. Improved biodistribution and radioimmunoimaging with poly(ethylene glycol)-DOTA-conjugated anti-CEA diabody. Bioconjug Chem. 2006; 17:68-76.

33. Schmidt MM, Wittrup KD. A modeling analysis of the effects of molecular size and binding affinity on tumor targeting. Molecular cancer therapeutics. 2009; 8:2861-2871.

34. Braciak TA, Wildenhain S, Roskopf CC, Schubert IA, Fey GH, Jacob U, Hopfner KP, Oduncu FS. NK cells from an AML patient have recovered in remission and reached comparable cytolytic activity to that of a healthy monozygotic twin mediated by the single-chain triplebody SPM-2. Journal of translational medicine. 2013; 11:289.

35. Gessner JE, Heiken H, Tamm A, Schmidt RE. The IgG Fc receptor family. Annals of hematology. 1998; 76:231-248.

36. Nimmerjahn F, Ravetch JV. Fcgamma receptors as regulators of immune responses. Nature reviews Immunology. 2008; 8:34-47.

37. Norell H, Moretta A, Silva-Santos B, Moretta L. At the Bench: Preclinical rationale for exploiting NK cells and gammadelta T lymphocytes for the treatment of high-risk leukemias. Journal of leukocyte biology. 2013; 94:1123-1139.

38. Wu YL, Ding YP, Tanaka Y, Shen LW, Wei CH, Minato N, Zhang W. gammadelta T cells and their potential for immunotherapy. International journal of biological sciences. 2014; 10:119-135.

39. Hofmann M, Grosse-Hovest L, Nubling T, Pyz E, Bamberg ML, Aulwurm S, Buhring HJ, Schwartz K, Haen SP, Schilbach K, Rammensee HG, Salih HR, Jung G. Generation, selection and preclinical characterization of an Fc-optimized FLT3 antibody for the treatment of myeloid leukemia. Leukemia. 2012; 26:1228-1237.

40. Durben M, Schmiedel D, Hofmann M, Vogt F, Nubling T, Pyz E, Buhring HJ, Rammensee HG, Salih HR,

Grosse-Hovest L, Jung G. Characterization of a bispecific FLT3 X CD3 antibody in an improved, recombinant format for the treatment of leukemia. Mol Ther. 2015; 23:648-655.

41. Seidel UJ, Vogt F, Grosse-Hovest L, Jung G, Handgretinger R, Lang P. gammadelta T Cell-Mediated Antibody-Dependent Cellular Cytotoxicity with CD19 Antibodies Assessed by an Impedance-Based Label-Free Real-Time Cytotoxicity Assay. Frontiers in immunology. 2014; 5:618.
42. Peper JK, Schuster H, Loffler MW, Schmid-Horch B, Rammensee HG, Stevanovic S. An impedance-based cytotoxicity assay for real-time and label-free assessment of T-cell-mediated killing of adherent cells. Journal of immunological methods. 2014; 405:192-198.
43. Ewert S, Honegger A, Pluckthun A. Stability improvement of antibodies for extracellular and intracellular applications: CDR grafting to stable frameworks and structure-based framework engineering. Methods. 2004; 34:184-199.
44. Kugler M, Stein C, Schwenkert M, Saul D, Vockentanz L, Huber T, Wetzel SK, Scholz O, Pluckthun A, Honegger A, Fey GH. Stabilization and humanization of a single-chain Fv antibody fragment specific for human lymphocyte antigen CD19 by designed point mutations and CDR-grafting onto a human framework. Protein Eng Des Sel. 2009; 22:135-147.
45. Bruenke J, Barbin K, Kunert S, Lang P, Pfeiffer M, Stieglmaier K, Niethammer D, Stockmeyer B, Peipp M, Repp R, Valerius T, Fey GH. Effective lysis of lymphoma cells with a stabilised bispecific single-chain Fv antibody against CD19 and FcgammaRIII (CD16). British journal of haematology. 2005; 130:218-228.
46. Benedict CA, MacKrell AJ, Anderson WF. Determination of the binding affinity of an anti-CD34 single-chain antibody using a novel, flow cytometry based assay. Journal of immunological methods. 1997; 201:223-231.
47. Handgretinger R. Negative depletion of CD3(+) and TcRalphabeta(+) T cells. Current opinion in hematology. 2012; 19:434-439.
48. Schwemmlein M, Stieglmaier J, Kellner C, Peipp M, Saul D, Oduncu F, Emmerich B, Stockmeyer B, Lang P, Beck JD, Fey GH. A CD19-specific single-chain immunotoxin mediates potent apoptosis of B-lineage leukemic cells. Leukemia. 2007; 21:1405-1412.
49. Chatzopoulou EI, Roskopf CC, Sekhavati F, Braciak TA, Fenn NC, Hopfner KP, Oduncu FS, Fey GH, Radler JO. Chip-based platform for dynamic analysis of NK cell cytolysis mediated by a triplebody. Analyst. 2016; 141:2284-2295.
50. Peipp M, Derer S, Lohse S, Staudinger M, Klausz K, Valerius T, Gramatzki M, Kellner C. HER2-specific immunoligands engaging NKp30 or NKp80 trigger NK-cell-mediated lysis of tumor cells and enhance antibody-dependent cell-mediated cytotoxicity. Oncotarget. 2015; 6:32075-32088. doi: 10.18632/oncotarget.5135.
51. Alici E, Sutlu T, Bjorkstrand B, Gilljam M, Stellan B, Nahi H, Quezada HC, Gahrton G, Ljunggren HG, Dilber MS. Autologous antitumor activity by NK cells expanded from myeloma patients using GMP-compliant components. Blood. 2008; 111:3155-3162.
52. Olejniczak SH, Stewart CC, Donohue K, Czuczman MS. A quantitative exploration of surface antigen expression in common B-cell malignancies using flow cytometry. Immunol Invest. 2006; 35:93-114.

CD19-specific triplebody SPM-1 engages NK and γδ T cells for rapid and efficient lysis of malignant B-lymphoid cells

SUPPLEMENTARY FIGURE

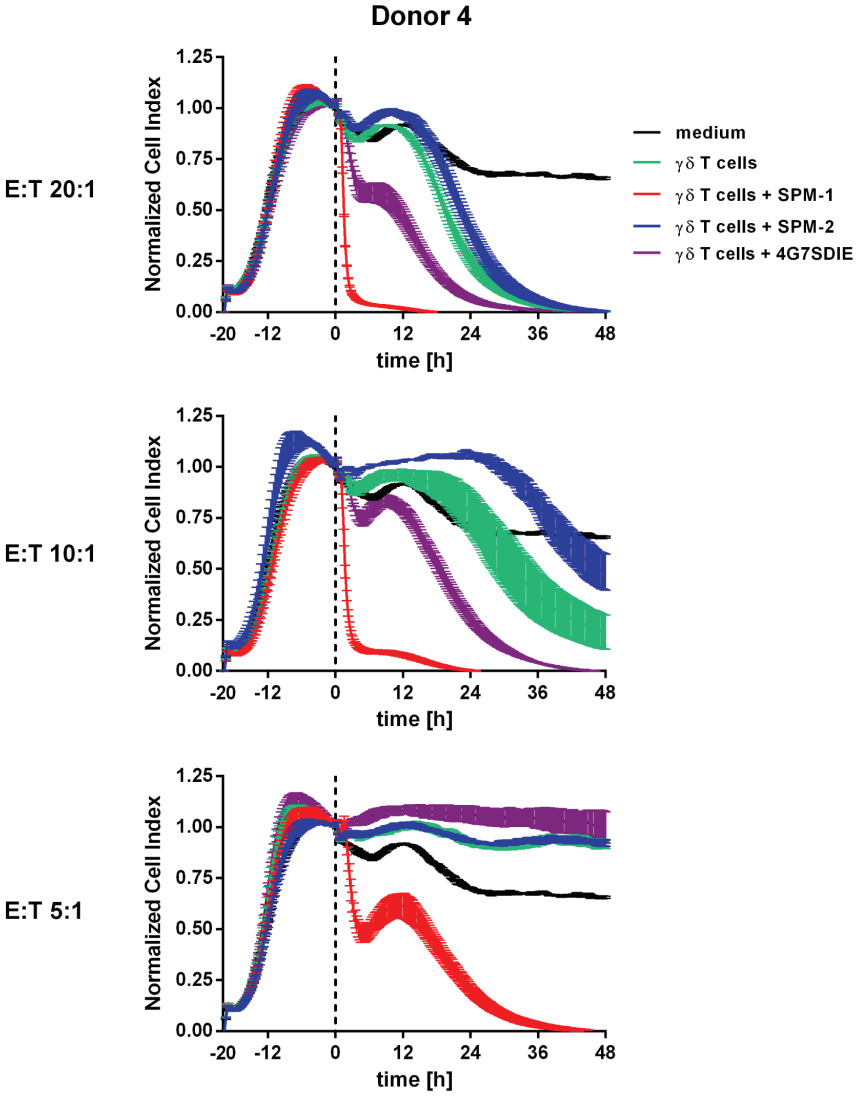

Supplementary Figure S1: SPM-1 directs expanded γδ T cells from healthy donors for very rapid lysis of CD19-bearing MCF7-CD19 tm target cells, monitored in a real-time assay. Raw data for the processed data of Donor 4 shown in Fig. 6. Cell indexes (CI) plotted here are a measure of the fraction of living cells contained in a population at the time of measurement. Adherent CD19-bearing MCF7-CD19 tm target cells were allowed to form a layer on the chip. Time of addition of the effector cells plus mediator protein (t_0) is indicated by a vertical dashed line. Normalized cell indices (CI) were measured as described in Methods and are a close correlate of life cells on the chip. SPM-1 caused a substantially more rapid loss in viability of the target cells than the best-in-class CD19-antibody 4G7SDIE, and the kinetics of loss of viability was not mono-phasic but showed clear evidence for at least 2 phases of the reaction, as evidenced by the shoulders and secondary peaks in the reaction profile.

3 Discussion

The vast heterogeneity among different cancer entities and within an individual cancer as well as its continuous evolution, which also allows a quick adaptation to environmental pressures such as therapeutic agents, render neoplastic diseases particularly difficult to cure. In order to defeat them, treatments need to be highly adaptable and versatile. Introducing this level of flexibility into surgical, chemo- or radiotherapeutic approaches is almost impossible and has only been achieved to some extent by developing different kinds of cytostatic agents that may be exchanged for one another and used at different intensities. Accordingly, modern chemotherapeutic regimens lead to long-term remission in 50 to 80% of acute leukemia patients.[3,4,7,8] Unfortunately the patients, who become therapy-refractory, have few options left: Immunotherapy offers a wider variety of mechanisms than conservative therapeutic approaches and achieves an unparalleled level of specificity, which reduces off-target side effects. The continuous improvement and development of new immunotherapeutic approaches thus remains an important task to help even more patients in the future. A particularly promising approach is the development of antibody derivatives that are capable of recognizing any desired tumor target antigen and that can activate any avenue of natural immune defense in order to exploit the extensive arsenal and versatility of leukocytes. The present work shows that triplebodies are capable of engaging $\alpha\beta$ and $\gamma\delta$ T cells as well as NK cells as effectors for the efficient and specific redirected lysis of cancer cells. Furthermore, dual-targeting of the lymphoid and myeloid differentiation antigens CD19 and CD33 was shown to lead to the selective and preferential lysis of biphenotypic leukemia blasts rather than single-positive cells *in vitro*. In addition, the author was involved in the preclinical development of NK cell-engaging triplebodies SPM-1 with specificity for CD19 and SPM-2 with specificity for CD33 and CD123. These developments provided convincing data that triplebodies can be produced in accordance with industry standard procedures for clinical use without any loss of activity.

3.1 Efficient T cell recruitment with single-chain triplebodies

T lymphocyte-dependent anti-cancer immunity is a particularly desirable immune response due to its high level of efficiency and the generation of immunologic memory. However, natural T cell responses are limited to cancer entities that display immunogenic TSA. In order to raise a T cell-mediated immune response against cancer cells that express “self” antigens only, it is therefore necessary to bypass the regular route of T cell activation. This can either be achieved by modifying the T cells themselves with TAA-recognizing receptors or by the administration of T cell-engaging

immunotherapeutics that target TAAs.[87,197] The cSMAC of the cytolytic T cell synapse, however, does not naturally contain soluble molecular mediators such as mAbs[244] and TCR engagement in the absence of co-stimulatory signals can lead to T cell anergy.[243,247] Nevertheless Anja Löffler and colleagues developed a CD19 and CD3ε bispecific scFv that induced lymphoma-directed cytotoxicity by non-stimulated T cells.[156] This agent underwent clinical development and became blinatumomab (Blincyto®), the first-in-class bispecific antibody derivative for the treatment of relapsed/refractory B-ALL.[251,252]

Single-chain triplebodies and previously developed bispecific formats from the research group of Prof. Fey (FAU Erlangen-Nuremberg) were capable of engaging different FcR-bearing innate immune effector cell populations such as NK cells and macrophages[211,214,253,254] as well as neutrophil granulocytes[148] for the elimination of cancer cells. The engagement of T lymphocytes with triplebodies, however, was attempted for the first time in the present work: Prototype triplebody 19-3-19 with bivalent monospecific targeting of CD19 and triplebody 33-3-19 with bivalent bispecific targeting of CD19 and CD33 were capable of efficient activation of healthy donor- and patient-derived T cells. This was shown by the elevation of activation markers CD69, CD49d (C. C. Roskopf, unpublished data) and CD25 on the T cell surface and the secretion of pro-inflammatory cytokines IL-2, IL-6, TNF-α and IFN-γ.[248,255] Importantly, polyclonal T cell activation was independent of the formation of an MHC : peptide-complex, but strictly required the presence of TAA and trigger antigen. Similar to BiTE®s[157,160], the molecules could neither induce cancer cell apoptosis in the absence of immune effectors, nor could they induce T cell activation in the absence of TAA-positive target cells. This property suggests that T cell-engaging triplebodies will not produce off-target toxicity *in vivo*. It was not further investigated, why anergy induction in T cells was circumvented by 19-3-19 and 33-3-19, but we hypothesize that it may involve TCR cross-linking after multiple specific binding events. *In vitro* the activated T cells eliminated more than 90% of target cells from B cell lines and primary patient samples within 24 hours.

Both 19-3-19 and 33-3-19 also induced T cell proliferation, in particular proliferation of the subset of $CD3^+$ $CD45RO^+$ cells, which contains memory effector T cells that no longer require priming by APC. The fate of naïve T cells upon stimulation by the triplebodies is unknown. It was also confirmed that not only $CD8^+$ effector T cells, but also the $CD4^+$ T cell population was relevant for the lysis efficiency mediated by T cell-engaging triplebodies (C. C. Roskopf, unpublished data).

While the difference in affinity for the target cell and the immune effector cell is not as pronounced in triplebodies as it is in the BiTE® blinatumomab (ΔK_D = 40 nM vs. 200 nM, respectively)[157,248], the target cells are still bound preferentially by the scTb. For BiTE® it has been suggested that the

T lymphocytes retain a high level of mobility as a consequence of this difference in affinity and the resultant preferential coating of target cells.[160] This may be one determining factor for maintaining the T lymphocytes' serial killing capacity. Importantly, bivalent cancer cell targeting by triplebodies implies that the combined affinities (i. e. avidity) of the two TAA-specific binding modules are stronger than the affinity of the single trigger antigen-specific binding module. By taking advantage of an avidity effect, it may therefore be possible to combine two low affinity TAA-specific binding moieties in a triplebody. This may further reduce the risk of killing single-positive healthy bystander cells. It remains to be determined, however, whether excessive triplebody concentrations can lead to an "oversaturation effect". This refers to a situation in which cytolytic synapses between cancer and T cells are formed less efficiently, because both the target cells and the immune effector cells are coated by the immunotherapeutic molecules rather than being connected by them.

As mentioned earlier, T cell activation by 19-3-19 and 33-3-19 led to the secretion of pro-inflammatory cytokines IFN-γ, TNF-α, IL-2 and IL-6, which was also reported for blinatumomab.[166,173,256] Therefore, it is probable that T cell-engaging triplebodies will also produce cytokine release syndrome in some subjects *in vivo*. CRS can be a very severe complication that may lead to multi-organ failure as in the case of the anti-CD28 superagonist TGN1412[188] or death as was recently reported in a patient receiving CD123-directed allogeneic CAR-T therapy.[208] However, clinical expertise regarding CRS and its management has been gained in the last couple of years as T cell-engaging cancer therapies have emerged.[42,185,187,190,257] The short half-life of BiTE® and scTb therapeutics may moreover limit the severity and duration of CRS upon cessation of therapy. Therefore, this concern should not prevent further development of T cell-engaging triplebodies.

The greatest shortcoming of the data presented on triplebodies 19-3-19 and 33-3-19 in the present work is the intrinsic instability and aggregation tendency of these molecules. These issues could not be resolved in spite of stabilization attempts by means of site-directed mutagenesis, introduction of an additional disulfide bond into the CD3ε scFv and different buffer formulations. Since the humanized CD19- and CD33-specific scFv that were used for the construction of 19-3-19 and 33-3-19 were also used for construction of the NK cell-engaging triplebodies SPM-1 and SPM-2, which display excellent biochemical properties[258,259], the OKT3-derived CD3ε–specific scFv appeared to introduce the molecular instability. However, this binding moiety is stable in the context of other trispecific molecules (M. Herrmann, unpublished data). Therefore the random combination of different scFv into a single polypeptide appears to be problematic, possibly due to intra- and interchain shuffling of the V domains that is dependent on the molecular context. The future construction of T cell-engaging triplebodies for use *in vivo* will therefore require more careful consideration and the individual

binding moieties may have to be stability-engineered (for example using the method by Xu *et al.* 2013[260]) for their respective molecular context. Initial concerns regarding poor accessibility of CD3ε on T cells to the CD3ε-binding moiety of T cell-engaging triplebodies in comparison to BiTE® due to partial sterical hindrance by the second TAA-targeting scFv did not come true.

Taken together, the present work has proven that triplebodies can engage T cells as well as NK cells for the efficient lysis of cancer cells. This establishes single-chain triplebodies as a molecular platform that allows for the flexible selection of an immune effector cell population. The choice of a suitable leukocyte population can thus be based on the immune state of individual patients, which adds a new layer to the personalization of cancer therapy.

3.2 Selective lysis of biphenotypic blasts by dual-targeting of CD19 and CD33

Multispecific targeting of more than one TAA is expected to hamper cancer immune escape by antigen loss, because the evolution of double- or multi-antigen-negative cancer cell clones is less probable than the evolution of single-negative clones.[152,155] Although this approach cannot protect cancer patients from relapse due to other mechanisms of immune escape, it is another step towards defeating neoplastic diseases. Moreover, the identification and thus targeting of specific cellular subpopulations is easier with more than one phenotypic surface marker. Healthy tissues may be single-positive for one of the targeted antigens or may express several targeted TAA to a lower extent or at a different ratio than the cancer cells. Therefore, selective lysis by multispecific antibody derivatives based on multiple targeting may reduce “on-target off-cancer” effects on healthy tissues. Based on these considerations, triplebody 33-3-19 was designed for the selective lysis of biphenotypic B/myeloid leukemia cells with concomitant expression of CD19 and CD33. This phenotype does not occur on healthy cells, but is frequently observed in the blasts of infant patients with mll-rearranged acute leukemia and has a very poor prognosis.[24,26,28]

The cytolytic potential of triplebody 33-3-19 against CD19 or CD33 single-positive as well as double-positive target cells in standard redirected lysis assays *in vitro* was as high as that of mono-targeting BiTE®-like molecules.[255] EC_{50}-values were in the picomolar range and the efficiency of lysis was weakly correlated with antigen surface density ($R^2 = 0.71$). However, CD19 and CD33 double-positive target cells were selectively lysed with a much higher efficiency than CD19 single-positive cells by 33-3-19 plus T cells, when both target cell populations were simultaneously present in the reaction. Under such experimental conditions, the double-positive target cells displayed a 145-fold higher sensitivity towards T cell-mediated lysis than the single-positive non-target cells. In the case of the

antigen combination CD19 and CD33, this selectivity effect was concentration-dependent, i. e. double-positive target cells were only preferentially lysed at subsaturating triplebody concentrations. When 33-3-19 was present in sufficient quantity to coat double- and single-positive target cells, the selectivity effect was lost, possibly due to an "oversaturation effect". This observation suggests that the concentration of multispecific agents for selective cancer cell lysis in a clinical setting would need to be adjusted depending on the antigen surface density and tumor burden of an individual patient. Nevertheless, there may be a concentration-dependent "selectivity window" for multispecifics that can potentially be maximized by affinity engineering[261] of the TAA-specific binding moieties. This would enable an even better distinction between cancer and non-cancer tissues and thus less "on-target off-tumor" side effects.

The data generated with 33-3-19 on the selective lysis of CD19 and CD33 double-positive target cells shows that this antigen pair is suitable for the distinction of biphenotypic B/myeloid leukemia blasts from single-positive bystander cells. In a similar manner, the antigen pairs CD19 and HLA-DR[213], ErbB2 and ErbB3[262], and EGFR and HER2[263] have been shown to mediate preferential lysis of double-positive target cells. Whether other target antigen pairs are also suitable for preferential lysis may not only depend on their combined density on the target cell surface, but also on their relative location to one another within the cell membrane: According to the "protein island"-model membrane proteins segregate into separate functional islands, some of which are anchored to the cytoskeleton while others can move fluidly across the membrane.[264-267] If target antigen pairs reside in separate immobile protein islands that are spaced far apart, the binding moieties of multispecific antibody derivatives may not be capable of binding them simultaneously as they have a limited span (mAb: 15 nm, scTb: 20 nm[254]). For the future design of multispecific antibodies that target novel antigen combinations it may therefore be reasonable to determine the relative location of the target antigens towards one another within the cell membrane, since this probably affects the cross-arm binding efficiency[268] of multispecific agents.

3.3 NK cells as immune effector cell population to combat MRD in AML patients

Although they have not received the same level of attention as CTL in recent years, NK cells are an immune effector cell population that also possesses a high cytotoxic potential and is therefore suitable for the redirected lysis of cancer cells.[269,270] Furthermore, NK cells are also capable of serial lysis and can proliferate and expand upon stimulation. These considerations as well as the fact that NK cells secrete a different range and concentration of cytokines compared to CTL, which may produce less pronounced CRS upon their therapeutic exploitation, formed the original rationale for choosing NK cells as the immune effector cell population engaged by triplebodies including SPM-1

and SPM-2. In addition, NK cell reconstitution following myelo- and lymphoablative treatments as well as HSCT is faster than the reconstitution of T lymphocytes.[270-272] These immune effectors may therefore be a better choice for eliminating MRD cells in acute leukemia patients by targeted therapy during maintenance treatment and in a post-transplant setting.

It has been reported, however, that the NK cell compartment is functionally impaired in AML patients.[273-276] Nevertheless, NK cell engaging-antibody derivatives that employ CD16-specific scFv rather than Fc-fragments for NK cell engagement were still capable of overcoming this functional impairment.[277,278] SPM-2 is a CD33 and CD123-specific NK cell-engaging triplebody that was designed for the specific lysis of LICs, which are likely contained among MRD cells. In an attempt to determine whether SPM-2 is also capable of overcoming the functional impairment of NK cells in AML patients, the autologous NK cells of an AML-M1 patient at different stages of treatment were compared to the NK cell compartment of her healthy monozygotic twin.[259] At initial diagnosis, the AML patient displayed a strongly reduced level of NK cells as well as of all other leukocyte populations, which was expected since the patient had 89.7% blasts in the bone marrow. The number of NK cells, however, normalized, when the patient achieved complete remission and was comparable to the healthy twin. Moreover, the expression level of activating natural cytotoxicity receptors (NCR) on the surface of the patient's NK cells was identical to that of her monozygotic twin and not affected by the disease. Accordingly, the patient's NK cells displayed the same cytotoxic potential in *in vitro* cytotoxicity tests with SPM-2 against autologous blasts from first diagnosis as the healthy twin's NK cells. If functional impairment was present due to different mechanisms (for example the stimulation of inhibitory receptors by soluble factors secreted by the AML cells), it did not have any disadvantageous effect on the functional efficiency of SPM-2. In fact SPM-2 was capable of specifically reducing the $CD34^+$ $CD38^{-/dim}$ $CD123^+$ AML-subpopulation, which is enriched for LIC, in primary samples from this patient. The clinical application of this dual-targeting agent in an MRD-setting may thus truly induce long-lasting remissions, because it can specifically eliminate a significant proportion of LIC. In additional experiments with primary samples from 29 AML patients and allogeneic NK effector cells, SPM-2 mediated effective redirected lysis of bulk cells in all samples but one regardless of the AML subtype and genetic risk group (T. A. Braciak *et al.*, manuscript submitted). Moreover, the $CD34^+$ $CD38^{-/dim}$ $CD123^+$ blast subpopulation in two of these patient samples displayed and even higher sensitivity towards NK cell killing mediated by SPM-2 than the bulk AML blasts, which also suggests that the LIC population can be efficiently targeted and eliminated by this agent. Therefore the antigen pair CD33 and CD123 and the engagement of NK cells as immune effectors appears to be suitable for targeted therapy of MRD in AML patients.

3.4 Engagement of γδ T cells by the CD16 binding moiety of SPM-1

The research group of Prof. Fey (FAU Erlangen-Nuremberg) previously reported that the CD16$^+$ mononuclear cell (MNC) compartment from the peripheral blood of healthy donors mediated cytotoxic activity against cancer cells together with antibody derivatives carrying the 3G8-derived CD16-binding moiety, which is also used in triplebodies SPM-1 and SPM-2, but has been humanized.[146] This MNC compartment does not only comprise FcγRIII-bearing NK cells, but also macrophages and γδ T cells.

γδ T cells usually account for 1 to 10% of the peripheral blood lymphocytes and they are a potentially valuable immune effector cell population for targeted immunotherapy of acute leukemias.[270,279] Their cytotoxic potential is as high as that of αβ T cells, but they do not cause GvHD and consequently they do not necessarily have to be depleted from hematopoietic stem cell transplants.[270,279] Instead, they can naturally enhance anti-viral immune responses in a post-transplant setting and contribute to the graft-versus-leukemia (GvL) effect, because they are not MHC-restricted and can recognize phosphoantigens (non-peptidic prenylpyrophosphate moieties), which are highly expressed by malignant B cells.[270]

Other immunotherapeutics have been described that successfully engaged γδ T cells via the activating receptor NKG2D for the lysis of lymphoma cells *in vitro*[280] and via Vγ9 for the lysis of pancreatic adenocarcinoma cells *in vitro* and *in vivo*[281,282], respectively. Furthermore, an Fc-engineered CD19-specific antibody – 4G7SDIE – was reported to engage γδ T cells effectively for ADCC of primary B-ALL cells.[250] During the preclinical development of SPM-1 in cooperation with the research group of Prof. Lang from the children's hospital Tübingen, we could show that triplebodies carrying a CD16-binding moiety are also capable of activating non-stimulated γδ T cells for the redirected lysis of cancer cells. This highlights the capacity of triplebodies to recruit different kinds of immune effector cells for the targeted immunotherapy of cancer and thus the platform character of the single-chain triplebody technology.

3.5 Difference in γδ T cell and NK cell response kinetics between mAbs and triplebodies

In the present work, triplebody SPM-1 induced the efficient redirected lysis of B lymphoma and leukemia cells at 5 to 430-fold lower concentrations than the CD20-specific mAb rituximab (MabThera®). The triplebody produced EC_{50}-values of 3 to 86 pM, when used against primary patient blasts, and was thus similarly potent as the BiTE® blinatumomab (Blincyto®) during its preclinical development: EC_{50}-values in the high femtomolar range were reported for this T cell-engaging

agent.[157] While this high cytotoxic potential may in part be explained by the higher antigen surface density of CD19 compared to CD20 on the majority of tested target cells, the lack of an Fc-region in SPM-1 and similar antibody derivatives is certainly another very important contributing factor. FcR-bearing immune cells throughout the body produce an "antigen sink" effect for mAb, but not for antibody derivatives that lack the Fc. Moreover, the direct ligation of the FcγRIII on NK and γδ T cells by the CD16-binding moiety of triplebodies appears to produce a highly efficient cytolytic synapse: As observed by Kellner *et al.* in 2008[211], the scTb displayed 3-fold stronger binding of target cells than bispecific scFv but 25-fold better lysis. One possible explanation is that triplebodies produce a tighter cytolytic synapse than bispecific scFv or mAb. This may result in prolonged activating receptor signaling and the exertion of physical forces that benefit NK cell-mediated cytolysis as it has been described for the cytolytic T cell synapse.[243,246,283] Evidence for this hypothesis was provided by the biphasic lysis kinetics of CD19-positive target cells that were observed during an impedance-based real-time cytotoxicity assay with SPM-1 and γδ T cells.[258] While both SPM-1 and the CD19-specific Fc-optimized mAb 4G7SDIE induced similar absolute target cell lysis within 24 hours, the triplebody caused a much more rapid elimination of CD19-positive target cells during the initial phase of the assay. Observations from cytotoxicity tests with CD123-positive target cells and SPM-2 plus pre-stimulated NK cells in single-cell cytometry assays[284] provided further evidence for the "tight synapse" hypothesis, as rapid killing of target cells by NK cells within the first hour after triplebody addition was observed. This killing behavior was attributed to the pre-stimulation of the NK cells, which results in a high intracellular concentration of lytic granules at the time of assay commencement. However, the presence of SPM-2 in the single-cell cytometry assay also appeared to have an influence on the speed of lytic granule replenishment or other metabolic processes during later stages of this assay. Thus triplebody involvement in cytolytic synapse-formation appears to influence intracellular signaling of the cytolytic machinery.

3.6 Perspective

The present work has established single-chain triplebodies as a highly versatile molecular platform for efficient targeted immunotherapy. Triplebodies can be used for the engagement of various desirable immune effector cell populations and for the highly selective lysis of cancer cells based on suitable antigen pairs for dual-targeting. The preclinical development of triplebodies SPM-1 and SPM-2 has further proven that such molecules can be produced in accordance with industry standard procedures, which may readily be scaled up. However, the problematic biochemical properties of the T cell-engaging triplebodies 19-3-19 and 33-3-19 also imply that individual molecular optimization will be necessary.

With dual-targeting triplebodies SPM-2 and 33-3-19 for the treatment of AML and MPAL, respectively, two immunotherapeutic agents have been developed that will potentially be useful for the selective and efficient treatment of AML and MPAL patients with high risk disease in the future. First it needs to be determined, however, whether the selectivity of lysis that these agents display *in vitro* for double-positive target cells translates into selective lysis *in vivo* and thus into reduced "on-target off-tumor" toxicity. Should this be the case, then these agents may induce deep remissions and prevent immune escape by antigen loss in some patients. However, since cancer can also exploit other avenues – including immunosuppression – to achieve immune escape, multispecific targeting of more than on TAA will probably be insufficient to cure advanced neoplastic disease by immunotherapy. Therefore a combination of multispecific agents that engage different immune effector cell populations for cancer cell lysis with other immunotherapeutic approaches such as checkpoint blockade seems to be a promising approach for the cure of cancer.

References

1. Hrusak O, Porwit-MacDonald A. Antigen expression patterns reflecting genotype of acute leukemias. *Leukemia* 2002; **16**: 1233-58.

2. Mejstrikova E, Kalina T, Trka J, Stary J, Hrusak O. Correlation of CD33 with poorer prognosis in childhood ALL implicates a potential of anti-CD33 frontline therapy. *Leukemia* 2005; **19**: 1092-4.

3. Ferlay J, Soerjomataram I, Ervik M, et al. GLOBOCAN 2012 v1.0, Cancer Incidence and Mortality Worldwide. Lyon, France: International Agency for Research on Cancer; 2013. (Accessed at http://globocan.iarc.fr.)

4. Kaatsch P, Spix C, Katalinic A, et al. Krebs in Deutschland 2011/2012. 10 ed. Berlin, Germany: Robert Koch-Institut/Gesellschaft der epidemiologischen Krebsregister in Deutschland e.V.; 2015.

5. Vardiman JW, Thiele J, Arber DA, et al. The 2008 revision of the World Health Organization (WHO) classification of myeloid neoplasms and acute leukemia: rationale and important changes. *Blood* 2009; **114**: 937-51.

6. Hiddemann W, Spiekermann K, Buske C, et al. Towards a pathogenesis-oriented therapy of acute myeloid leukemia. *Critical Reviews in Oncology/Hematology* 2005; **56**: 235-45.

7. Buske C, Spiekermann K, Braess J, Hiddemann W. Akute myeloische Leukämie. In: Hiddemann W, Bartram CR, eds. Die Onkologie - Teil 2. Heidelberg, Germany: Springer Medizin Verlag; 2010: 1637-71.

8. Hoelzer D, Schrappe M, Gökbuket N. Akute lymphatische Leukämie bei Erwachsenen und Kindern. In: Hiddemann W, Bartram CR, eds. Die Onkologie - Teil 2. Heidelberg: Springer Medizin Verlag; 2010: 1673-702.

9. Jaffe ES, Harris NL, Stein H, Isaacson PG. Classification of lymphoid neoplasms: the microscope as a tool for disease discovery. *Blood* 2008; **112**: 4384-99.

10. Herdegen T, Böhm R, Cimin-Bredée N, et al. Kurzlehrbuch Pharmakologie und Toxikologie. 2. Auflage ed. Stuttgart: Georg Thieme Verlag; 2010: 307-322.

11. Buchner T, Berdel WE, Haferlach C, et al. Age-related risk profile and chemotherapy dose response in acute myeloid leukemia: a study by the German Acute Myeloid Leukemia Cooperative Group. *Journal of Clinical Oncology* 2009; **27**: 61-9.

12. Ehninger A, Kramer M, Rollig C, et al. Distribution and levels of cell surface expression of CD33 and CD123 in acute myeloid leukemia. *Blood Cancer Journal* 2014; **4**: e218.

13. Cowan AJ, Laszlo GS, Estey EH, Walter RB. Antibody-based therapy of acute myeloid leukemia with gemtuzumab ozogamicin. *Frontiers in Bioscience (Landmark Edition)* 2013; **18**: 1311-34.

14. Thol F, Schlenk RF. Gemtuzumab ozogamicin in acute myeloid leukemia revisited. *Expert Opinion on Biological Therapy* 2014; **14**: 1185-95.

15. Stark A. FDA approves Mylotarg for treatment of acute myeloid leukemia. In: Release FN, ed. Silver Spring, Maryland (USA): U.S. Food & Drug Administration; 2017.

16. Jurcic JG. Ab therapy of AML: native anti-CD33 Ab and drug conjugates. *Cytotherapy* 2008; **10**: 7-12.

17. Lancet JE. New agents: great expectations not realized. *Best Practice & Research Clinical Haematology* 2013; **26**: 269-74.

18. Aigner M, Feulner J, Schaffer S, et al. T lymphocytes can be effectively recruited for ex vivo and in vivo lysis of AML blasts by a novel CD33/CD3-bispecific BiTE antibody construct. *Leukemia* 2013; **27**: 1107-15.

19. Krupka C, Kufer P, Kischel R, et al. CD33 target validation and sustained depletion of AML blasts in long-term cultures by the bispecific T-cell-engaging antibody AMG 330. *Blood* 2014; **123**: 356-65.

20. Rosenberg SA, Restifo NP. Adoptive cell transfer as personalized immunotherapy for human cancer. *Science* 2015; **348**: 62-8.

21. Porwit A, Bene MC. Acute Leukemias of Ambiguous Origin. *American Journal of Clinical Pathology* 2015; **144**: 361-76.

22. Weinberg OK, Arber DA. Mixed-phenotype acute leukemia: historical overview and a new definition. *Leukemia* 2010; **24**: 1844-51.

23. Matutes E, Pickl WF, Van't Veer M, et al. Mixed-phenotype acute leukemia: clinical and laboratory features and outcome in 100 patients defined according to the WHO 2008 classification. *Blood* 2011; **117**: 3163-71.

24. Rubnitz JE, Onciu M, Pounds S, et al. Acute mixed lineage leukemia in children: the experience of St Jude Children's Research Hospital. *Blood* 2009; **113**: 5083-9.

25. Yan L, Ping N, Zhu M, et al. Clinical, immunophenotypic, cytogenetic, and molecular genetic features in 117 adult patients with mixed-phenotype acute leukemia defined by WHO-2008 classification. *Haematologica* 2012; **97**: 1708-12.

26. Al-Seraihy AS, Owaidah TM, Ayas M, et al. Clinical characteristics and outcome of children with biphenotypic acute leukemia. *Haematologica* 2009; **94**: 1682-90.

27. Weinberg OK, Seetharam M, Ren L, Alizadeh A, Arber DA. Mixed phenotype acute leukemia: A study of 61 cases using World Health Organization and European Group for the Immunological Classification of Leukaemias criteria. *American Journal of Clinical Pathology* 2014; **142**: 803-8.

28. Mejstrikova E, Volejnikova J, Fronkova E, et al. Prognosis of children with mixed phenotype acute leukemia treated on the basis of consistent immunophenotypic criteria. *Haematologica* 2010; **95**: 928-35.

29. Shimizu H, Saitoh T, Machida S, et al. Allogeneic hematopoietic stem cell transplantation for adult patients with mixed phenotype acute leukemia: results of a matched-pair analysis. *European Journal of Haematology* 2015; **95**: 455-60.

30. Winter SS. Pediatric acute leukemia therapies informed by molecular analysis of high-risk disease. *Hematology American Society of Hematology Education Program* 2011; **2011**: 366-73.

31. Tallen G, Henze G, Von Stackelberg A. Treatment of children and adolescents with relapsed ALL: therapy target long-term healing. *Pharmazie in unserer Zeit* 2012; **41**: 214-21.

32. Downing JR, Shannon KM. Acute leukemia: a pediatric perspective. *Cancer Cell* 2002; **2**: 437-45.

33. Thomas X, Le Jeune C. Treating adults with acute lymphocytic leukemia: new pharmacotherapy options. *Expert Opinion on Pharmacotherapy* 2016; **17**: 2319-30.

34. Schrappe M, Hunger SP, Pui CH, et al. Outcomes after induction failure in childhood acute lymphoblastic leukemia. *The New England Journal of Medicine* 2012; **366**: 1371-81.

35. Zhang L, Wang SA. A focused review of hematopoietic neoplasms occurring in the therapy-related setting. *International Journal of Clinical and Experimental Pathology* 2014; **7**: 3512-23.

36. Huguet F, Tavitian S. Emerging biological therapies to treat acute lymphoblastic leukemia. *Expert Opinion on Emerging Drugs* 2016: 1-15.

37. Gudowius S, Recker K, Laws HJ, et al. Identification of candidate target antigens for antibody-based immunotherapy in childhood B-cell precursor ALL. *Klinische Pädiatrie* 2006; **218**: 327-33.

38. Olejniczak SH, Stewart CC, Donohue K, Czuczman MS. A quantitative exploration of surface antigen expression in common B-cell malignancies using flow cytometry. *Immunological Investigations* 2006; **35**: 93-114.

39. Hekman A, Honselaar A, Vuist WM, et al. Initial experience with treatment of human B cell lymphoma with anti-CD19 monoclonal antibody. *Cancer Immunology, Immunotherapy* 1991; **32**: 364-72.

40. Vlasveld LT, Hekman A, Vyth-Dreese FA, et al. Treatment of low-grade non-Hodgkin's lymphoma with continuous infusion of low-dose recombinant interleukin-2 in combination with the B-cell-specific monoclonal antibody CLB-CD19. *Cancer Immunology, Immunotherapy* 1995; **40**: 37-47.

41. Thomas X. Blinatumomab: a new era of treatment for adult ALL? *Lancet Oncology* 2015; **16**: 6-7.

42. Zugmaier G, Klinger M, Schmidt M, Subklewe M. Clinical overview of anti-CD19 BiTE((R)) and ex vivo data from anti-CD33 BiTE((R)) as examples for retargeting T cells in hematologic malignancies. *Molecular Immunology* 2015; **67**: 58-66.

43. Maude SL, Frey N, Shaw PA, et al. Chimeric antigen receptor T cells for sustained remissions in leukemia. *The New England Journal of Medicine* 2014; **371**: 1507-17.

44. Fischer A, Stark A. FDA approval brings first gene therapy to the United States: CAR T-cell therapy approved to treat certain children and young adults with B-cell acute lymphoblastic leukemia. Silver Spring, Maryland (USA): FDA News Release; 2017.

45. Jan M, Majeti R. Clonal evolution of acute leukemia genomes. *Oncogene* 2013; **32**: 135-40.

46. Lang F, Wojcik B, Rieger MA. Stem Cell Hierarchy and Clonal Evolution in Acute Lymphoblastic Leukemia. *Stem Cells International* 2015; **2015**: 137164.

47. van Niekerk G, Davids LM, Hattingh SM, Engelbrecht AM. Cancer stem cells: A product of clonal evolution? *International Journal of Cancer* 2017; **140**: 993-9.

48. Dick JE. Stem cell concepts renew cancer research. *Blood* 2008; **112**: 4793-807.

49. Greaves M. Cancer stem cells: back to Darwin? *Seminars in Cancer Biology* 2010; **20**: 65-70.

50. Bomken S, Fiser K, Heidenreich O, Vormoor J. Understanding the cancer stem cell. *British Journal of Cancer* 2010; **103**: 439-45.

51. Gupta R, Vyas P, Enver T. Molecular targeting of cancer stem cells. *Cell Stem Cell* 2009; **5**: 125-6.

52. Eppert K, Takenaka K, Lechman ER, et al. Stem cell gene expression programs influence clinical outcome in human leukemia. *Nature Medicine* 2011; **17**: 1086-93.

53. Hanekamp D, Cloos J, Schuurhuis GJ. Leukemic stem cells: identification and clinical application. *International Journal of Hematology* 2017; **105**: 549-57.

54. Wang X, Huang S, Chen JL. Understanding of leukemic stem cells and their clinical implications. *Molecular Cancer* 2017; **16**: 2.

55. Anderson K, Lutz C, van Delft FW, et al. Genetic variegation of clonal architecture and propagating cells in leukaemia. *Nature* 2011; **469**: 356-61.

56. Ma X, Edmonson M, Yergeau D, et al. Rise and fall of subclones from diagnosis to relapse in pediatric B-acute lymphoblastic leukaemia. *Nature Communications* 2015; **6**: 6604.

57. Scheel C, Weinberg RA. Phenotypic plasticity and epithelial-mesenchymal transitions in cancer and normal stem cells? *International Journal of Cancer* 2011; **129**: 2310-4.

58. Bonnet D, Dick JE. Human acute myeloid leukemia is organized as a hierarchy that originates from a primitive hematopoietic cell. *Nature Medicine* 1997; **3**: 730-7.

59. Lapidot T, Sirard C, Vormoor J, et al. A cell initiating human acute myeloid leukaemia after transplantation into SCID mice. *Nature* 1994; **367**: 645-8.

60. Jordan CT, Upchurch D, Szilvassy SJ, et al. The interleukin-3 receptor alpha chain is a unique marker for human acute myelogenous leukemia stem cells. *Leukemia* 2000; **14**: 1777-84.

61. Vergez F, Green AS, Tamburini J, et al. High levels of CD34+CD38low/-CD123+ blasts are predictive of an adverse outcome in acute myeloid leukemia: a Groupe Ouest-Est des Leucemies Aigues et Maladies du Sang (GOELAMS) study. *Haematologica* 2011; **96**: 1792-8.

62. Jin L, Lee EM, Ramshaw HS, et al. Monoclonal antibody-mediated targeting of CD123, IL-3 receptor alpha chain, eliminates human acute myeloid leukemic stem cells. *Cell Stem Cell* 2009; **5**: 31-42.

63. Hombach AA, Abken H. Shared target antigens on cancer cells and tissue stem cells: go or no-go for CAR T cells? *Expert Review of Clinical Immunology* 2017; **13**: 151-5.

64. Felipe Rico J, Hassane DC, Guzman ML. Acute myelogenous leukemia stem cells: from Bench to Bedside. *Cancer Letters* 2013; **338**: 4-9.

65. Thomas D, Majeti R. Biology and relevance of human acute myeloid leukemia stem cells. *Blood* 2017; **129**: 1577-85.

66. Valent P. Targeting of leukemia-initiating cells to develop curative drug therapies: straightforward but nontrivial concept. *Current Cancer Drug Targets* 2011; **11**: 56-71.

67. Pollyea DA, Jordan CT. Therapeutic targeting of acute myeloid leukemia stem cells. *Blood* 2017; **129**: 1627-35.

68. Horton SJ, Huntly BJ. Recent advances in acute myeloid leukemia stem cell biology. *Haematologica* 2012; **97**: 966-74.

69. Taussig DC, Miraki-Moud F, Anjos-Afonso F, et al. Anti-CD38 antibody-mediated clearance of human repopulating cells masks the heterogeneity of leukemia-initiating cells. *Blood* 2008; **112**: 568-75.

70. Farrar JE, Schuback HL, Ries RE, et al. Genomic Profiling of Pediatric Acute Myeloid Leukemia Reveals a Changing Mutational Landscape from Disease Diagnosis to Relapse. *Cancer Research* 2016; **76**: 2197-205.

71. Hong D, Gupta R, Ancliff P, et al. Initiating and cancer-propagating cells in TEL-AML1-associated childhood leukemia. *Science* 2008; **319**: 336-9.

72. Wilson K, Case M, Minto L, et al. Flow minimal residual disease monitoring of candidate leukemic stem cells defined by the immunophenotype, CD34+CD38lowCD19+ in B-lineage childhood acute lymphoblastic leukemia. *Haematologica* 2010; **95**: 679-83.

73. Kong Y, Yoshida S, Saito Y, et al. CD34+CD38+CD19+ as well as CD34+CD38-CD19+ cells are leukemia-initiating cells with self-renewal capacity in human B-precursor ALL. *Leukemia* 2008; **22**: 1207-13.

74. Aoki Y, Watanabe T, Saito Y, et al. Identification of CD34+ and CD34- leukemia-initiating cells in MLL-rearranged human acute lymphoblastic leukemia. *Blood* 2015; **125**: 967-80.

75. le Viseur C, Hotfilder M, Bomken S, et al. In childhood acute lymphoblastic leukemia, blasts at different stages of immunophenotypic maturation have stem cell properties. *Cancer Cell* 2008; **14**: 47-58.

76. Gawad C, Koh W, Quake SR. Dissecting the clonal origins of childhood acute lymphoblastic leukemia by single-cell genomics. *Proceedings of the National Academy of Sciences USA* 2014; **111**: 17947-52.

77. Bateman CM, Colman SM, Chaplin T, et al. Acquisition of genome-wide copy number alterations in monozygotic twins with acute lymphoblastic leukemia. *Blood* 2010; **115**: 3553-8.

78. Greaves MF, Maia AT, Wiemels JL, Ford AM. Leukemia in twins: lessons in natural history. *Blood* 2003; **102**: 2321-33.

79. Maia AT, van der Velden VH, Harrison CJ, et al. Prenatal origin of hyperdiploid acute lymphoblastic leukemia in identical twins. *Leukemia* 2003; **17**: 2202-6.

80. D'Errico G, Machado HL, Sainz B, Jr. A current perspective on cancer immune therapy: step-by-step approach to constructing the magic bullet. *Clinical and Translational Medicine* 2017; **6**: 3.

81. Restifo NP, Dudley ME, Rosenberg SA. Adoptive immunotherapy for cancer: harnessing the T cell response. *Nature Reviews Immunology* 2012; **12**: 269-81.

82. Rutkowski MR, Stephen TL, Conejo-Garcia JR. Anti-tumor immunity: myeloid leukocytes control the immune landscape. *Cellular Immunology* 2012; **278**: 21-6.

83. Chen DS, Mellman I. Oncology meets immunology: the cancer-immunity cycle. *Immunity* 2013; **39**: 1-10.

84. Hess C, Venetz D, Neri D. Emerging classes of armed antibody therapeutics against cancer. *Medicinal Chemical Communications* 2014; **5**: 408-31.

85. Coley WB. The Treatment of Inoperable Sarcoma by Bacterial Toxins (the Mixed Toxins of the Streptococcus erysipelas and the Bacillus prodigiosus). *Proceedings of the Royal Society of Medicine* 1910; **3**: 1-48.

86. McCarthy EF. The toxins of William B. Coley and the treatment of bone and soft-tissue sarcomas. *The Iowa Orthopaedic Journal* 2006; **26**: 154-8.

87. Stein C, Schubert I, Fey GH. Natural Killer (NK)- and T-Cell Engaging Antibody-Derived Therapeutics. *Antibodies* 2012; **1**: 88-123.

88. Mellman I, Coukos G, Dranoff G. Cancer immunotherapy comes of age. *Nature* 2011; **480**: 480-9.

89. Davis ID. An overview of cancer immunotherapy. *Immunology and Cell Biology* 2000; **78**: 179-95.

90. Lawrence MS, Stojanov P, Polak P, et al. Mutational heterogeneity in cancer and the search for new cancer-associated genes. *Nature* 2013; **499**: 214-8.

91. Weide B, Garbe C, Rammensee HG, Pascolo S. Plasmid DNA- and messenger RNA-based anti-cancer vaccination. *Immunology Letters* 2008; **115**: 33-42.

92. Cintolo JA, Datta J, Mathew SJ, Czerniecki BJ. Dendritic cell-based vaccines: barriers and opportunities. *Future Oncology* 2012; **8**: 1273-99.

93. Brunet JF, Denizot F, Luciani MF, et al. A new member of the immunoglobulin superfamily--CTLA-4. *Nature* 1987; **328**: 267-70.

94. Leach DR, Krummel MF, Allison JP. Enhancement of antitumor immunity by CTLA-4 blockade. *Science* 1996; **271**: 1734-6.

95. van der Merwe PA, Bodian DL, Daenke S, Linsley P, Davis SJ. CD80 (B7-1) binds both CD28 and CTLA-4 with a low affinity and very fast kinetics. *The Journal of Experimental Medicine* 1997; **185**: 393-403.

96. Lipson EJ, Drake CG. Ipilimumab: an anti-CTLA-4 antibody for metastatic melanoma. *Clinical Cancer Research* 2011; **17**: 6958-62.

97. Robert C, Thomas L, Bondarenko I, et al. Ipilimumab plus dacarbazine for previously untreated metastatic melanoma. *The New England Journal of Medicine* 2011; **364**: 2517-26.

98. Ansell SM, Lesokhin AM, Borrello I, et al. PD-1 blockade with nivolumab in relapsed or refractory Hodgkin's lymphoma. *The New England Journal of Medicine* 2015; **372**: 311-9.

99. Fehrenbacher L, Spira A, Ballinger M, et al. Atezolizumab versus docetaxel for patients with previously treated non-small-cell lung cancer (POPLAR): a multicentre, open-label, phase 2 randomised controlled trial. *Lancet* 2016; **387**: 1837-46.

100. Larkin J, Chiarion-Sileni V, Gonzalez R, et al. Combined Nivolumab and Ipilimumab or Monotherapy in Untreated Melanoma. *The New England Journal of Medicine* 2015; **373**: 23-34.

101. Topalian SL, Sznol M, McDermott DF, et al. Survival, durable tumor remission, and long-term safety in patients with advanced melanoma receiving nivolumab. *Journal of Clinical Oncology* 2014; **32**: 1020-30.

102. Keating GM. Nivolumab: A Review in Advanced Nonsquamous Non-Small Cell Lung Cancer. *Drugs* 2016; **76**: 969-78.

103. Pianko MJ, Liu Y, Bagchi S, Lesokhin AM. Immune checkpoint blockade for hematologic malignancies: a review. *Stem Cell Investigation* 2017; **4**: 32.

104. Ok CY, Young KH. Checkpoint inhibitors in hematological malignancies. *Journal of Hematology & Oncology* 2017; **10**: 103.

105. Knaus HA, Kanakry CG, Luznik L, Gojo I. Immunomodulatory Drugs: Immune Checkpoint Agents in Acute Leukemia. *Current Drug Targets* 2017; **18**: 315-31.

106. Krupka C, Kufer P, Kischel R, et al. Blockade of the PD-1/PD-L1 axis augments lysis of AML cells by the CD33/CD3 BiTE antibody construct AMG 330: reversing a T-cell-induced immune escape mechanism. *Leukemia* 2015.

107. Feucht J, Kayser S, Gorodezki D, et al. T-cell responses against CD19+ pediatric acute lymphoblastic leukemia mediated by bispecific T-cell engager (BiTE) are regulated contrarily by PD-L1 and CD80/CD86 on leukemic blasts. *Oncotarget* 2016; **7**: 76902-19.

108. Couzin-Frankel J. Breakthrough of the year 2013. Cancer immunotherapy. *Science* 2013; **342**: 1432-3.

109. McNutt M. Cancer immunotherapy. *Science* 2013; **342**: 1417.

110. Behring Ev. Ueber das Zustandekommen der Diphtherie-Immunität und der Tetanus-Immunität bei Thieren. 1890.

111. Ehrlich P. Croonian Lecture: On Immunity with Special Reference to Cell Life. *Proceedings of the Royal Society of London* 1899; **66**: 424-48.

112. Ehrlich P. Experimental Researches on Specific Therapy: On Immunity with special Reference to the Relationship between Distribution and Action of Antigens*: FIRST HARBEN LECTURE† A2 - HIMMELWEIT, F. The Collected Papers of Paul Ehrlich: Pergamon; 1960: 106-17.

113. Nossal GJ, Lederberg J. Antibody production by single cells. *Nature* 1958; **181**: 1419-20.

114. Janeway CA, Travers P, Walport M, Shlomchik MJ. Immunobiology: the immune system in health and disease. 6th ed. ed: Garland Science; 2005: 103-197 and 319-405.

115. Elgert KD. Ch. 4: Antibody Structure and Function. Immunology: Understanding The Immune System: John Wiley & Sons; 1998: 58-78.

116. Harris LJ, Larson SB, Hasel KW, McPherson A. Refined Structure of an Intact IgG2a Monoclonal Antibody. *Biochemistry* 1997; **36**: 1581-97.

117. Maynard J, Georgiou G. Antibody engineering. *Annual Review of Biomedical Engineering* 2000; **2**: 339-76.

118. Weiner LM, Surana R, Wang S. Monoclonal antibodies: versatile platforms for cancer immunotherapy. *Nature Reviews Immunology* 2010; **10**: 317-27.

119. Cotton RG, Milstein C. Letter: Fusion of two immunoglobulin-producing myeloma cells. *Nature* 1973; **244**: 42-3.

120. Kohler G, Milstein C. Continuous cultures of fused cells secreting antibody of predefined specificity. *Nature* 1975; **256**: 495-7.

121. Schroff RW, Foon KA, Beatty SM, Oldham RK, Morgan AC, Jr. Human anti-murine immunoglobulin responses in patients receiving monoclonal antibody therapy. *Cancer Research* 1985; **45**: 879-85.

122. Shawler DL, Bartholomew RM, Smith LM, Dillman RO. Human immune response to multiple injections of murine monoclonal IgG. *The Journal of Immunology* 1985; **135**: 1530-5.

123. Chames P, Van Regenmortel M, Weiss E, Baty D. Therapeutic antibodies: successes, limitations and hopes for the future. *British Journal of Pharmacology* 2009; **157**: 220-33.

124. Winter G, Milstein C. Man-made antibodies. *Nature* 1991; **349**: 293-9.

125. Morrison SL, Johnson MJ, Herzenberg LA, Oi VT. Chimeric human antibody molecules: mouse antigen-binding domains with human constant region domains. *Proceedings of the National Academy of Sciences USA* 1984; **81**: 6851-5.

126. Neuberger MS, Williams GT, Mitchell EB, Jouhal SS, Flanagan JG, Rabbitts TH. A hapten-specific chimaeric IgE antibody with human physiological effector function. *Nature* 1985; **314**: 268-70.

127. Jones PT, Dear PH, Foote J, Neuberger MS, Winter G. Replacing the complementarity-determining regions in a human antibody with those from a mouse. *Nature* 1986; **321**: 522-5.

128. Clark M. Antibody humanization: a case of the 'Emperor's new clothes'? *Immunology Today* 2000; **21**: 397-402.

129. Chames P, Baty D. Antibody engineering and its applications in tumor targeting and intracellular immunization. *FEMS Microbiology Letters* 2000; **189**: 1-8.

130. Lazar GA, Dang W, Karki S, et al. Engineered antibody Fc variants with enhanced effector function. *Proceedings of the National Academy of Sciences USA* 2006; **103**: 4005-10.

131. Mimura Y, Katoh T, Saldova R, et al. Glycosylation engineering of therapeutic IgG antibodies: challenges for the safety, functionality and efficacy. *Protein & Cell* 2017.

132. Sinclair AM, Elliott S. Glycoengineering: the effect of glycosylation on the properties of therapeutic proteins. *Journal of Pharmaceutical Sciences* 2005; **94**: 1626-35.

133. Abramowicz D, Schandene L, Goldman M, et al. Release of tumor necrosis factor, interleukin-2, and gamma-interferon in serum after injection of OKT3 monoclonal antibody in kidney transplant recipients. *Transplantation* 1989; **47**: 606-8.

134. Van Wauwe JP, De Mey JR, Goossens JG. OKT3: a monoclonal anti-human T lymphocyte antibody with potent mitogenic properties. *The Journal of Immunology* 1980; **124**: 2708-13.

135. Smith MR. Rituximab (monoclonal anti-CD20 antibody): mechanisms of action and resistance. *Oncogene* 2003; **22**: 7359-68.

136. Ecker DM, Jones SD, Levine HL. The therapeutic monoclonal antibody market. *mAbs* 2015; **7**: 9-14.

137. Reichert JM. Antibodies to watch in 2017. *mAbs* 2017; **9**: 167-81.

138. Müller D, Kontermann R. Recombinant bispecific antibodies for cellular cancer immunotherapy. *Current Opinion in Molecular Therapeutics* 2007; **9**: 319-26.

139. Kontermann R. Dual targeting strategies with bispecific antibodies. *mAbs* 2012; **4**.

140. Al-Hussaini M, Rettig MP, Ritchey JK, et al. Targeting CD123 in acute myeloid leukemia using a T-cell–directed dual-affinity retargeting platform. *Blood* 2016; **127**: 122-31.

141. Chichili GR, Huang L, Li H, et al. A CD3xCD123 bispecific DART for redirecting host T cells to myelogenous leukemia: preclinical activity and safety in nonhuman primates. *Science Translational Medicine* 2015; **7**: 289ra82.

142. Kuo S-R, Wong L, Liu J-S. Engineering a CD123xCD3 bispecific scFv immunofusion for the treatment of leukemia and elimination of leukemia stem cells. *Protein Engineering, Design and Selection* 2012; **25**: 561-70.

143. Luo D, Mah N, Krantz M, et al. Vl-Linker-Vh Orientation-Dependent Expression of Single Chain Fv Containing an Engineered Disulfide-Stabilized Bond in the Framework Regions. *The Journal of Biochemistry* 1995; **118**: 825-31.

144. Wolf E, Hofmeister R, Kufer P, Schlereth B, Baeuerle PA. BiTEs: bispecific antibody constructs with unique anti-tumor activity. *Drug Discovery Today* 2005; **10**: 1237-44.

145. Moore PA, Zhang W, Rainey GJ, et al. Application of dual affinity retargeting molecules to achieve optimal redirected T-cell killing of B-cell lymphoma. *Blood* 2011; **117**: 4542-51.

146. Bruenke J, Barbin K, Kunert S, et al. Effective lysis of lymphoma cells with a stabilised bispecific single-chain Fv antibody against CD19 and FcgammaRIII (CD16). *British Journal of Haematology* 2005; **130**: 218-28.

147. Peipp M, Saul D, Barbin K, et al. Efficient eukaryotic expression of fluorescent scFv fusion proteins directed against CD antigens for FACS applications. *Journal of Immunological Methods* 2004; **285**: 265-80.

148. Guettinger Y, Barbin K, Peipp M, et al. A recombinant bispecific single-chain fragment variable specific for HLA class II and Fc alpha RI (CD89) recruits polymorphonuclear neutrophils for efficient lysis of malignant B lymphoid cells. *The Journal of Immunology* 2010; **184**: 1210-7.

149. Schmidt MM, Wittrup KD. A modeling analysis of the effects of molecular size and binding affinity on tumor targeting. *Molecular Cancer Therapeutics* 2009; **8**: 2861-71.

150. Thurber GM, Schmidt MM, Wittrup KD. Antibody tumor penetration: transport opposed by systemic and antigen-mediated clearance. *Advanced Drug Delivery Reviews* 2008; **60**: 1421-34.

151. Yokota T, Milenic DE, Whitlow M, Schlom J. Rapid tumor penetration of a single-chain Fv and comparison with other immunoglobulin forms. *Cancer Research* 1992; **52**: 3402-8.

152. Cuesta AM, Sainz-Pastor N, Bonet J, Oliva B, Alvarez-Vallina L. Multivalent antibodies: when design surpasses evolution. *Trends in Biotechnology* 2010; **28**: 355-62.

153. Nunez-Prado N, Compte M, Harwood S, et al. The coming of age of engineered multivalent antibodies. *Drug Discovery Today* 2015; **20**: 588-94.

154. Spiess C, Zhai Q, Carter PJ. Alternative molecular formats and therapeutic applications for bispecific antibodies. *Molecular Immunology* 2015; **67**: 95-106.

155. Wortzel RD, Philipps C, Schreiber H. Multiple tumour-specific antigens expressed on a single tumour cell. *Nature* 1983; **304**: 165-7.

156. Loffler A, Kufer P, Lutterbuse R, et al. A recombinant bispecific single-chain antibody, CD19 x CD3, induces rapid and high lymphoma-directed cytotoxicity by unstimulated T lymphocytes. *Blood* 2000; **95**: 2098-103.

157. Dreier T, Lorenczewski G, Brandl C, et al. Extremely potent, rapid and costimulation-independent cytotoxic T-cell response against lymphoma cells catalyzed by a single-chain bispecific antibody. *International Journal of Cancer* 2002; **100**: 690-7.

158. Dreier T, Baeuerle PA, Fichtner I, et al. T cell costimulus-independent and very efficacious inhibition of tumor growth in mice bearing subcutaneous or leukemic human B cell lymphoma xenografts by a CD19-/CD3- bispecific single-chain antibody construct. *The Journal of Immunology* 2003; **170**: 4397-402.

159. Loffler A, Gruen M, Wuchter C, et al. Efficient elimination of chronic lymphocytic leukaemia B cells by autologous T cells with a bispecific anti-CD19/anti-CD3 single-chain antibody construct. *Leukemia* 2003; **17**: 900-9.

160. Hoffmann P, Hofmeister R, Brischwein K, et al. Serial killing of tumor cells by cytotoxic T cells redirected with a CD19-/CD3-bispecific single-chain antibody construct. *International Journal of Cancer* 2005; **115**: 98-104.

161. Schlereth B, Quadt C, Dreier T, et al. T-cell activation and B-cell depletion in chimpanzees treated with a bispecific anti-CD19/anti-CD3 single-chain antibody construct. *Cancer Immunology, Immunotherapy* 2006; **55**: 503-14.

162. Bargou R, Leo E, Zugmaier G, et al. Tumor regression in cancer patients by very low doses of a T cell-engaging antibody. *Science* 2008; **321**: 974-7.

163. Nagorsen D, Bargou R, Ruttinger D, Kufer P, Baeuerle PA, Zugmaier G. Immunotherapy of lymphoma and leukemia with T-cell engaging BiTE antibody blinatumomab. *Leukemia & Lymphoma* 2009; **50**: 886-91.

164. Handgretinger R, Zugmaier G, Henze G, Kreyenberg H, Lang P, von Stackelberg A. Complete remission after blinatumomab-induced donor T-cell activation in three pediatric patients with post-transplant relapsed acute lymphoblastic leukemia. *Leukemia* 2011; **25**: 181-4.

165. Topp MS, Kufer P, Gokbuget N, et al. Targeted therapy with the T-cell-engaging antibody blinatumomab of chemotherapy-refractory minimal residual disease in B-lineage acute lymphoblastic leukemia patients results in high response rate and prolonged leukemia-free survival. *Journal of Clinical Oncology* 2011; **29**: 2493-8.

166. Klinger M, Brandl C, Zugmaier G, et al. Immunopharmacologic response of patients with B-lineage acute lymphoblastic leukemia to continuous infusion of T cell-engaging CD19/CD3-bispecific BiTE antibody blinatumomab. *Blood* 2012; **119**: 6226-33.

167. Topp MS, Gokbuget N, Zugmaier G, et al. Long-term follow-up of hematologic relapse-free survival in a phase 2 study of blinatumomab in patients with MRD in B-lineage ALL. *Blood* 2012; **120**: 5185-7.

168. Alcharakh M, Yun S, Dong Y, et al. Blinatumomab-induced donor T-cell activation for post-stem cell transplant-relapsed acute CD19-positive biphenotypic leukemia. *Immunotherapy* 2016; **8**: 847-52.

169. Brower V. Phase 1/2 study of blinatumomab in relapsed paediatric ALL. *Lancet Oncology* 2016; **17**: e525.

170. Gokbuget N, Kelsh M, Chia V, et al. Blinatumomab vs historical standard therapy of adult relapsed/refractory acute lymphoblastic leukemia. *Blood Cancer Journal* 2016; **6**: e473.

171. von Stackelberg A, Locatelli F, Zugmaier G, et al. Phase I/Phase II Study of Blinatumomab in Pediatric Patients With Relapsed/Refractory Acute Lymphoblastic Leukemia. *Journal of Clinical Oncology* 2016; **34**: 4381-9.

172. Gokbuget N, Zugmaier G, Klinger M, et al. Long-term relapse-free survival in a phase 2 study of blinatumomab for the treatment of patients with minimal residual disease in B-lineage acute lymphoblastic leukemia. *Haematologica* 2017.

173. Nagele V, Kratzer A, Zugmaier G, et al. Changes in clinical laboratory parameters and pharmacodynamic markers in response to blinatumomab treatment of patients with relapsed/refractory ALL. *Experimental Hematology & Oncology* 2017; **6**: 14.

174. Topp MS, Gokbuget N, Stein AS, et al. Safety and activity of blinatumomab for adult patients with relapsed or refractory B-precursor acute lymphoblastic leukaemia: a multicentre, single-arm, phase 2 study. *Lancet Oncology* 2015; **16**: 57-66.

175. Khan MW, Gul Z. Blinatumomab may induce graft versus host leukemia in patients with pre-B ALL relapsing after hematopoietic stem cell transplant. *Clinical Case Reports* 2016; **4**: 743-6.

176. Marini BL, Sun Y, Burke PW, Perissinotti AJ. Successful reintroduction of blinatumomab in a patient with relapsed/refractory acute lymphoblastic leukemia following grade 4 cytokine release syndrome. *Journal of Oncology Pharmacy Practice* 2016.

177. Brischwein K, Schlereth B, Guller B, et al. MT110: a novel bispecific single-chain antibody construct with high efficacy in eradicating established tumors. *Molecular Immunology* 2006; **43**: 1129-43.

178. Offner S, Hofmeister R, Romaniuk A, Kufer P, Baeuerle PA. Induction of regular cytolytic T cell synapses by bispecific single-chain antibody constructs on MHC class I-negative tumor cells. *Molecular Immunology* 2006; **43**: 763-71.

179. Haas C, Krinner E, Brischwein K, et al. Mode of cytotoxic action of T cell-engaging BiTE antibody MT110. *Immunobiology* 2009; **214**: 441-53.

180. Herrmann I, Baeuerle PA, Friedrich M, et al. Highly efficient elimination of colorectal tumor-initiating cells by an EpCAM/CD3-bispecific antibody engaging human T cells. *PLoS One* 2010; **5**: e13474.

181. Cioffi M, Dorado J, Baeuerle PA, Heeschen C. EpCAM/CD3-Bispecific T-cell engaging antibody MT110 eliminates primary human pancreatic cancer stem cells. *Clinical Cancer Research* 2012; **18**: 465-74.

182. Osada T, Hsu D, Hammond S, et al. Metastatic colorectal cancer cells from patients previously treated with chemotherapy are sensitive to T-cell killing mediated by CEA/CD3-bispecific T-cell-engaging BiTE antibody. *British Journal of Cancer* 2010; **102**: 124-33.

183. Peng L, Oberst MD, Huang J, et al. The CEA/CD3-bispecific antibody MEDI-565 (MT111) binds a nonlinear epitope in the full-length but not a short splice variant of CEA. *PLoS One* 2012; **7**: e36412.

184. Ross SL, Sherman M, McElroy PL, et al. Bispecific T cell engager (BiTE(R)) antibody constructs can mediate bystander tumor cell killing. *PLoS One* 2017; **12**: e0183390.

185. Ribera JM, Ferrer A, Ribera J, Genesca E. Profile of blinatumomab and its potential in the treatment of relapsed/refractory acute lymphoblastic leukemia. *OncoTargets and Therapy* 2015; **8**: 1567-74.

186. Teachey DT, Rheingold SR, Maude SL, et al. Cytokine release syndrome after blinatumomab treatment related to abnormal macrophage activation and ameliorated with cytokine-directed therapy. *Blood* 2013; **121**: 5154-7.

187. Frey NV, Porter DL. Cytokine release syndrome with novel therapeutics for acute lymphoblastic leukemia. *Hematology American Society of Hematology Education Program* 2016; **2016**: 567-72.

188. Suntharalingam G, Perry MR, Ward S, et al. Cytokine storm in a phase 1 trial of the anti-CD28 monoclonal antibody TGN1412. *The New England Journal of Medicine* 2006; **355**: 1018-28.

189. Vogt N, Hess K, Bialek R, et al. Epileptic seizures and rhinocerebral mucormycosis during blinatumomab treatment in a patient with biphenotypic acute leukemia. *Annals of Hematology* 2017; **96**: 151-3.

190. Barrett DM, Teachey DT, Grupp SA. Toxicity management for patients receiving novel T-cell engaging therapies. *Current Opinion in Pediatrics* 2014; **26**: 43-9.

191. Rayes A, McMasters RL, O'Brien MM. Lineage Switch in MLL-Rearranged Infant Leukemia Following CD19-Directed Therapy. *Pediatric Blood & Cancer* 2016.

192. Ruella M, Maus MV. Catch me if you can: Leukemia Escape after CD19-Directed T Cell Immunotherapies. *Computational and Structural Biotechnology Journal* 2016; **14**: 357-62.

193. Braig F, Brandt A, Goebeler M, et al. Resistance to anti-CD19/CD3 BiTE in acute lymphoblastic leukemia may be mediated by disrupted CD19 membrane trafficking. *Blood* 2017; **129**: 100-4.

194. De Benedittis C, Papayannidis C, Venturi C, et al. The clonal evolution of two distinct T315I-positive BCR-ABL1 subclones in a Philadelphia-positive acute lymphoblastic leukemia failing multiple lines of therapy: a case report. *BMC Cancer* 2017; **17**: 523.

195. Nagel I, Bartels M, Duell J, et al. Hematopoietic stem cell involvement in BCR-ABL1-positive ALL as potential mechanism of resistance to blinatumomab therapy. *Blood* 2017.

196. Lichtenegger FS, Krupka C, Kohnke T, Subklewe M. Immunotherapy for Acute Myeloid Leukemia. *Seminars in Hematology* 2015; **52**: 207-14.

197. Aldoss I, Bargou RC, Nagorsen D, Friberg GR, Baeuerle PA, Forman SJ. Redirecting T cells to eradicate B-cell acute lymphoblastic leukemia: bispecific T-cell engagers and chimeric antigen receptors. *Leukemia* 2017; **31**: 777-87.

198. Sadelain M, Brentjens R, Riviere I. The basic principles of chimeric antigen receptor design. *Cancer Discovery* 2013; **3**: 388-98.

199. Stone JD, Aggen DH, Schietinger A, Schreiber H, Kranz DM. A sensitivity scale for targeting T cells with chimeric antigen receptors (CARs) and bispecific T-cell Engagers (BiTEs). *Oncoimmunology* 2012; **1**: 863-73.

200. Frey NV, Porter DL. CAR T-cells merge into the fast lane of cancer care. *American Journal of Hematology* 2016; **91**: 146-50.

201. Kochenderfer JN, Dudley ME, Feldman SA, et al. B-cell depletion and remissions of malignancy along with cytokine-associated toxicity in a clinical trial of anti-CD19 chimeric-antigen-receptor-transduced T cells. *Blood* 2012; **119**: 2709-20.

202. Kochenderfer JN, Rosenberg SA. Treating B-cell cancer with T cells expressing anti-CD19 chimeric antigen receptors. *Nature Reviews Clinical Oncology* 2013; **10**: 267-76.

203. Lee DW, Kochenderfer JN, Stetler-Stevenson M, et al. T cells expressing CD19 chimeric antigen receptors for acute lymphoblastic leukaemia in children and young adults: a phase 1 dose-escalation trial. *Lancet* 2015; **385**: 517-28.

204. Wei G, Ding L, Wang J, Hu Y, Huang H. Advances of CD19-directed chimeric antigen receptor-modified T cells in refractory/relapsed acute lymphoblastic leukemia. *Experimental Hematology & Oncology* 2017; **6**: 10.

205. Gill S, June CH. Going viral: chimeric antigen receptor T-cell therapy for hematological malignancies. *Immunology Reviews* 2015; **263**: 68-89.

206. Mardiros A, Dos Santos C, McDonald T, et al. T cells expressing CD123-specific chimeric antigen receptors exhibit specific cytolytic effector functions and antitumor effects against human acute myeloid leukemia. *Blood* 2013; **122**: 3138-48.

207. Arcangeli S, Rotiroti MC, Bardelli M, et al. Balance of Anti-CD123 Chimeric Antigen Receptor Binding Affinity and Density for the Targeting of Acute Myeloid Leukemia. *Molecular Therapy* 2017.

208. Moore J, Harnest S. Cellectics Reports Clinical Hold of UCART123 Studies. In: SA C, ed. New York (USA)2017.

209. Hanada K, Restifo NP. Double or nothing on cancer immunotherapy. *Nature Biotechnology* 2013; **31**: 33-4.

210. Kloss CC, Condomines M, Cartellieri M, Bachmann M, Sadelain M. Combinatorial antigen recognition with balanced signaling promotes selective tumor eradication by engineered T cells. *Nature Biotechnology* 2013; **31**: 71-5.

211. Kellner C, Bruenke J, Stieglmaier J, et al. A novel CD19-directed recombinant bispecific antibody derivative with enhanced immune effector functions for human leukemic cells. *Journal of Immunotherapy* 2008; **31**: 871-84.

212. Schubert I, Kellner C, Stein C, et al. A recombinant triplebody with specificity for CD19 and HLA-DR mediates preferential binding to antigen double-positive cells by dual-targeting. *mAbs* 2012; **4**: 45-56.

213. Schubert I, Saul D, Nowecki S, Mackensen A, Fey GH, Oduncu FS. A dual-targeting triplebody mediates preferential redirected lysis of antigen double-positive over single-positive leukemic cells. *mAbs* 2014; **6**: 286-96.

214. Kugler M, Stein C, Kellner C, et al. A recombinant trispecific single-chain Fv derivative directed against CD123 and CD33 mediates effective elimination of acute myeloid leukaemia cells by dual targeting. *British Journal of Haematology* 2010; **150**: 574-86.

215. Schubert I, Kellner C, Stein C, et al. A single-chain triplebody with specificity for CD19 and CD33 mediates effective lysis of mixed lineage leukemia cells by dual targeting. *mAbs* 2011; **3**: 21-30.

216. Wang K, Wei G, Liu D. CD19: a biomarker for B cell development, lymphoma diagnosis and therapy. *Experimental Hematology & Oncology* 2012; **1**: 36.

217. Weiland J, Elder A, Forster V, Heidenreich O, Koschmieder S, Vormoor J. CD19: A multifunctional immunological target molecule and its implications for Blineage acute lymphoblastic leukemia. *Pediatric Blood & Cancer* 2015; **62**: 1144-8.

218. Tedder TF. CD19: a promising B cell target for rheumatoid arthritis. *Nature Reviews Rheumatology* 2009; **5**: 572-7.

219. Hammer O. CD19 as an attractive target for antibody-based therapy. *mAbs* 2012; **4**: 571-7.

220. Carter RH, Wang Y, Brooks S. Role of CD19 signal transduction in B cell biology. *Immunologic Research* 2002; **26**: 45-54.

221. Ishiura N, Nakashima H, Watanabe R, et al. Differential phosphorylation of functional tyrosines in CD19 modulates B-lymphocyte activation. *European Journal of Immunology* 2010; **40**: 1192-204.

222. Del Nagro CJ, Otero DC, Anzelon AN, Omori SA, Kolla RV, Rickert RC. CD19 function in central and peripheral B-cell development. *Immunologic Research* 2005; **31**: 119-31.

223. Tedder TF, Inaoki M, Sato S. The CD19-CD21 complex regulates signal transduction thresholds governing humoral immunity and autoimmunity. *Immunity* 1997; **6**: 107-18.

224. Uckun FM, Sun L, Qazi S, Ma H, Ozer Z. Recombinant human CD19-ligand protein as a potent anti-leukaemic agent. *British Journal of Haematology* 2011; **153**: 15-23.

225. Chung EY, Psathas JN, Yu D, Li Y, Weiss MJ, Thomas-Tikhonenko A. CD19 is a major B cell receptor-independent activator of MYC-driven B-lymphomagenesis. *Journal of Clinical Investigation* 2012; **122**: 2257-66.

226. Freeman SD, Kelm S, Barber EK, Crocker PR. Characterization of CD33 as a new member of the sialoadhesin family of cellular interaction molecules. *Blood* 1995; **85**: 2005-12.

227. Laszlo GS, Estey EH, Walter RB. The past and future of CD33 as therapeutic target in acute myeloid leukemia. *Blood Reviews* 2014; **28**: 143-53.

228. Crocker PR, Paulson JC, Varki A. Siglecs and their roles in the immune system. *Nature Reviews Immunology* 2007; **7**: 255-66.

229. Paul SP, Taylor LS, Stansbury EK, McVicar DW. Myeloid specific human CD33 is an inhibitory receptor with differential ITIM function in recruiting the phosphatases SHP-1 and SHP-2. *Blood* 2000; **96**: 483-90.

230. Lajaunias F, Dayer JM, Chizzolini C. Constitutive repressor activity of CD33 on human monocytes requires sialic acid recognition and phosphoinositide 3-kinase-mediated intracellular signaling. *European Journal of Immunology* 2005; **35**: 243-51.

231. Vitale C, Romagnani C, Falco M, et al. Engagement of p75/AIRM1 or CD33 inhibits the proliferation of normal or leukemic myeloid cells. *Proceedings of the National Academy of Sciences USA* 1999; **96**: 15091-6.

232. Vitale C, Romagnani C, Puccetti A, et al. Surface expression and function of p75/AIRM-1 or CD33 in acute myeloid leukemias: engagement of CD33 induces apoptosis of leukemic cells. *Proceedings of the National Academy of Sciences USA* 2001; **98**: 5764-9.

233. Chen J, Olsen J, Ford S, et al. A new isoform of interleukin-3 receptor {alpha} with novel differentiation activity and high affinity binding mode. *Journal of Biological Chemistry* 2009; **284**: 5763-73.

234. Testa U, Riccioni R, Diverio D, Rossini A, Lo Coco F, Peschle C. Interleukin-3 receptor in acute leukemia. *Leukemia* 2004; **18**: 219-26.

235. Broughton SE, Hercus TR, Nero TL, et al. Crystallization and preliminary X-ray diffraction analysis of the interleukin-3 alpha receptor bound to the Fab fragment of antibody CSL362. *Acta Crystallographica Section F Structural Biology Communications* 2014; **70**: 358-61.

236. Broughton SE, Hercus TR, Hardy MP, et al. Dual mechanism of interleukin-3 receptor blockade by an anti-cancer antibody. *Cell Reports* 2014; **8**: 410-9.

237. Blalock WL, Weinstein-Oppenheimer C, Chang F, et al. Signal transduction, cell cycle regulatory, and anti-apoptotic pathways regulated by IL-3 in hematopoietic cells: possible sites for intervention with anti-neoplastic drugs. *Leukemia* 1999; **13**: 1109-66.

238. Liu K, Zhu M, Huang Y, Wei S, Xie J, Xiao Y. CD123 and its potential clinical application in leukemias. *Life Sciences* 2015; **122**: 59-64.

239. Testa U, Riccioni R, Militi S, et al. Elevated expression of IL-3Ralpha in acute myelogenous leukemia is associated with enhanced blast proliferation, increased cellularity, and poor prognosis. *Blood* 2002; **100**: 2980-8.

240. Nievergall E, Ramshaw HS, Yong AS, et al. Monoclonal antibody targeting of IL-3 receptor alpha with CSL362 effectively depletes CML progenitor and stem cells. *Blood* 2014; **123**: 1218-28.

241. Steelman LS, Algate PA, Blalock WL, et al. Oncogenic effects of overexpression of the interleukin-3 receptor on hematopoietic cells. *Leukemia* 1996; **10**: 528-42.

242. Griffiths GM, Tsun A, Stinchcombe JC. The immunological synapse: a focal point for endocytosis and exocytosis. *The Journal of Cell Biology* 2010; **189**: 399-406.

243. Katzman SD, O'Gorman WE, Villarino AV, et al. Duration of antigen receptor signaling determines T-cell tolerance or activation. *Proceedings of the National Academy of Sciences USA* 2010; **107**: 18085-90.

244. Galandrini R, Capuano C, Santoni A. Activation of Lymphocyte Cytolytic Machinery: Where are We? *Frontiers in Immunology* 2013; **4**: 390.

245. Le Floc'h A, Huse M. Molecular mechanisms and functional implications of polarized actin remodeling at the T cell immunological synapse. *Cellular and Molecular Life Sciences* 2015; **72**: 537-56.

246. Basu R, Whitlock BM, Husson J, et al. Cytotoxic T Cells Use Mechanical Force to Potentiate Target Cell Killing. *Cell* 2016; **165**: 100-10.

247. Chappert P, Schwartz RH. Induction of T cell anergy: integration of environmental cues and infectious tolerance. *Current Opinion in Immunology* 2010; **22**: 552-9.

248. Roskopf CC, Schiller CB, Braciak TA, et al. T cell-recruiting triplebody 19-3-19 mediates serial lysis of malignant B-lymphoid cells by a single T cell. *Oncotarget* 2014; **5**: 6466-83.

249. Kugler M, Stein C, Schwenkert M, et al. Stabilization and humanization of a single-chain Fv antibody fragment specific for human lymphocyte antigen CD19 by designed point mutations and CDR-grafting onto a human framework. *Protein Engineering, Design and Selection* 2009; **22**: 135-47.

250. Seidel UJ, Vogt F, Grosse-Hovest L, Jung G, Handgretinger R, Lang P. gammadelta T Cell-Mediated Antibody-Dependent Cellular Cytotoxicity with CD19 Antibodies Assessed by an Impedance-Based Label-Free Real-Time Cytotoxicity Assay. *Frontiers in Immunology* 2014; **5**: 618.

251. Advani AS. Blinatumomab: a novel agent to treat minimal residual disease in patients with acute lymphoblastic leukemia. *Clinical Advances in Hematology & Oncology* 2011; **9**: 776-7.

252. Folan SA, Rexwinkle A, Autry J, Bryan JC. Blinatumomab: Bridging the Gap in Adult Relapsed/Refractory B-Cell Acute Lymphoblastic Leukemia. *Clinical Lymphoma, Myeloma & Leukemia* 2016; **16 Suppl**: S2-5.

253. Bruenke J, Fischer B, Barbin K, et al. A recombinant bispecific single-chain Fv antibody against HLA class II and FcgammaRIII (CD16) triggers effective lysis of lymphoma cells. *British Journal of Haematology* 2004; **125**: 167-79.

254. Singer H, Kellner C, Lanig H, et al. Effective elimination of acute myeloid leukemic cells by recombinant bispecific antibody derivatives directed against CD33 and CD16. *Journal of Immunotherapy* 2010; **33**: 599-608.

255. Roskopf CC, Braciak TA, Fenn NC, et al. Dual-targeting triplebody 33-3-19 mediates selective lysis of biphenotypic CD19+ CD33+ leukemia cells. *Oncotarget* 2016.

256. Brandl C, Haas C, d'Argouges S, et al. The effect of dexamethasone on polyclonal T cell activation and redirected target cell lysis as induced by a CD19/CD3-bispecific single-chain antibody construct. *Cancer Immunology, Immunotherapy* 2007; **56**: 1551-63.

257. Wilke AC, Gokbuget N. Clinical applications and safety evaluation of the new CD19 specific T-cell engager antibody construct blinatumomab. *Expert Opinion on Drug Safety* 2017: 1-12.

258. Schiller CB, Braciak TA, Fenn NC, et al. CD19-specific triplebody SPM-1 engages NK and gammadelta T cells for rapid and efficient lysis of malignant B-lymphoid cells. *Oncotarget* 2016; **7**: 83392-408.

259. Braciak TA, Wildenhain S, Roskopf CC, et al. NK cells from an AML patient have recovered in remission and reached comparable cytolytic activity to that of a healthy monozygotic twin mediated by the single-chain triplebody SPM-2. *Journal of Translational Medicine* 2013; **11**: 289.

260. Xu L, Kohli N, Rennard R, et al. Rapid optimization and prototyping for therapeutic antibody-like molecules. *mAbs* 2013; **5**: 237-54.

261. Mazor Y, Hansen A, Yang C, et al. Insights into the molecular basis of a bispecific antibody's target selectivity. *mAbs* 2015; **7**: 461-9.

262. McDonagh CF, Huhalov A, Harms BD, et al. Antitumor activity of a novel bispecific antibody that targets the ErbB2/ErbB3 oncogenic unit and inhibits heregulin-induced activation of ErbB3. *Molecular Cancer Therapeutics* 2012; **11**: 582-93.

263. Mazor Y, Oganesyan V, Yang C, et al. Improving target cell specificity using a novel monovalent bispecific IgG design. *mAbs* 2015; **7**: 377-89.

264. Lillemeier BF, Mortelmaier MA, Forstner MB, Huppa JB, Groves JT, Davis MM. TCR and Lat are expressed on separate protein islands on T cell membranes and concatenate during activation. *Nature Immunology* 2010; **11**: 90-6.

265. Lillemeier BF, Pfeiffer JR, Surviladze Z, Wilson BS, Davis MM. Plasma membrane-associated proteins are clustered into islands attached to the cytoskeleton. *Proceedings of the National Academy of Sciences USA* 2006; **103**: 18992-7.

266. Klammt C, Lillemeier BF. How membrane structures control T cell signaling. *Frontiers in Immunology* 2012; **3**: 291.

267. Roh KH, Lillemeier BF, Wang F, Davis MM. The coreceptor CD4 is expressed in distinct nanoclusters and does not colocalize with T-cell receptor and active protein tyrosine kinase p56lck. *Proceedings of the National Academy of Sciences USA* 2015; **112**: E1604-13.

268. Harms BD, Kearns JD, Iadevaia S, Lugovskoy AA. Understanding the role of cross-arm binding efficiency in the activity of monoclonal and multispecific therapeutic antibodies. *Methods* 2014; **65**: 95-104.

269. Sanchez-Correa B, Campos C, Pera A, et al. Natural killer cell immunosenescence in acute myeloid leukaemia patients: new targets for immunotherapeutic strategies? *Cancer Immunology, Immunotherapy* 2016; **65**: 453-63.

270. Norell H, Moretta A, Silva-Santos B, Moretta L. At the Bench: Preclinical rationale for exploiting NK cells and gammadelta T lymphocytes for the treatment of high-risk leukemias. *Journal of Leukocyte Biology* 2013; **94**: 1123-39.

271. Dunbar EM, Buzzeo MP, Levine JB, Schold JD, Meier-Kriesche HU, Reddy V. The relationship between circulating natural killer cells after reduced intensity conditioning hematopoietic stem cell transplantation and relapse-free survival and graft-versus-host disease. *Haematologica* 2008; **93**: 1852-8.

272. Ullah MA, Hill GR, Tey SK. Functional Reconstitution of Natural Killer Cells in Allogeneic Hematopoietic Stem Cell Transplantation. *Frontiers in Immunology* 2016; **7**: 144.

273. Khaznadar Z, Henry G, Setterblad N, et al. Acute myeloid leukemia impairs natural killer cells through the formation of a deficient cytotoxic immunological synapse. *European Journal of Immunology* 2014; **44**: 3068-80.

274. Lichtenegger FS, Lorenz R, Gellhaus K, Hiddemann W, Beck B, Subklewe M. Impaired NK cells and increased T regulatory cell numbers during cytotoxic maintenance therapy in AML. *Leukemia Research* 2014; **38**: 964-9.

275. Stringaris K, Sekine T, Khoder A, et al. Leukemia-induced phenotypic and functional defects in natural killer cells predict failure to achieve remission in acute myeloid leukemia. *Haematologica* 2014; **99**: 836-47.

276. Dulphy N, Chretien AS, Khaznadar Z, et al. Underground Adaptation to a Hostile Environment: Acute Myeloid Leukemia vs. Natural Killer Cells. *Frontiers in Immunology* 2016; **7**: 94.

277. Reiners KS, Kessler J, Sauer M, et al. Rescue of impaired NK cell activity in hodgkin lymphoma with bispecific antibodies in vitro and in patients. *Molecular Therapy* 2013; **21**: 895-903.

278. Vyas M, Schneider A-C, Shatnyeva O, et al. Mono- and dual-targeting triplebodies activate natural killer cells and have anti-tumor activity in vitro and in vivo against chronic lymphocytic leukemia. *OncoImmunology* 2016: e1211220.

279. Wu YL, Ding YP, Tanaka Y, et al. gammadelta T cells and their potential for immunotherapy. *International Journal of Biological Sciences* 2014; **10**: 119-35.

280. Peipp M, Wesch D, Oberg HH, et al. CD20-Specific Immunoligands Engaging NKG2D Enhance gammadelta T Cell-Mediated Lysis of Lymphoma Cells. *Scandinavian Journal of Immunology* 2017.

281. Oberg HH, Peipp M, Kellner C, et al. Novel bispecific antibodies increase gammadelta T-cell cytotoxicity against pancreatic cancer cells. *Cancer Research* 2014; **74**: 1349-60.

282. Oberg HH, Kellner C, Gonnermann D, et al. gammadelta T cell activation by bispecific antibodies. *Cellular Immunology* 2015; **296**: 41-9.

283. Tkach K, Altan-Bonnet G. T cell responses to antigen: hasty proposals resolved through long engagements. *Current Opinion in Immunology* 2013; **25**: 120-5.

284. Chatzopoulou EI, Roskopf CC, Sekhavati F, et al. Chip-based platform for dynamic analysis of NK cell cytolysis mediated by a triplebody. *Analyst* 2016; **141**: 2284-95.

285. Kipriyanov SM, Moldenhauer G, Martin AC, Kupriyanova OA, Little M. Two amino acid mutations in an anti-human CD3 single chain Fv antibody fragment that affect the yield on bacterial secretion but not the affinity. *Protein Engineering* 1997; **10**: 445-53.

286. Schwemmlein M, Peipp M, Barbin K, et al. A CD33-specific single-chain immunotoxin mediates potent apoptosis of cultured human myeloid leukaemia cells. *British Journal of Haematology* 2006; **133**: 141-51.

287. Stein C, Kellner C, Kugler M, et al. Novel conjugates of single-chain Fv antibody fragments specific for stem cell antigen CD123 mediate potent death of acute myeloid leukaemia cells. *British Journal of Haematology* 2010; **148**: 879-89.

288. Carter P, Presta L, Gorman CM, et al. Humanization of an anti-p185HER2 antibody for human cancer therapy. *Proceedings of the National Academy of Sciences USA* 1992; **89**: 4285-9.

289. Kurrle R, Shearman CW, Moore GP, Seiler F, (inventors); Genzyme Corporation and Behringwerke Aktiengesellschaft, (assignees). Improved monoclonal antibodies against the human alpha/beta t-cell receptor, their production and use. European patent EP0403156. 1997.

Figures

Figure 1: Models of tumor heterogeneity. Tumors are composed of phenotypically and functionally heterogeneous cells. There are two theories as to how this heterogeneity arises, which are particularly relevant in acute leukemia. The clonal evolution model and the cancer stem cell model [based on John E. Dick, 2008][48] 17

Figure 2: Schematic representation of IgG domains and 3D structure of IgG based on x-ray crystallography studies. (a) IgG is composed of 2 heavy and 2 light chains. V domains (V_L/V_H) at the N-terminal end of the polypeptide chains, which form the antigen-binding clefts, are followed by one (C_L) or three (C_{H1-3}) constant domains, respectively. Each domain has one internal disulfide bond. The two heavy chains are linked via two cystines in the highly flexible hinge region. The light and heavy chains are also connected via a disulfide bond between the C_L and C_{H1} domains. The C_{H2} and C_{H3} domains form the fragment crystallizable (Fc), while the V domains plus the C_L and C_{H1} domains in the two identical arms with antigen binding activity form the antigen-binding fragments (Fab). (b) Three-dimensional structure of mouse IgG2a antibody Mab231 based on x-ray diffraction data (blue shades: constant domains; orange shades: variable domains). The distinct barrel-shaped structure that is constructed from two β sheets in each Ig domain is clearly discernible. The junction between the V domains and the C_L/C_{H1} domains (elbow region) confers additional flexibility [adapted from Harris *et al.*, 1997].[116] 22

Figure 3: Anti-tumor mechanisms mediated by IgGs. (a) IgGs bind to pro-tumorigenic chemokines and cytokines and thereby neutralize them. (b) Antibodies opsonize (i.e. coat) the tumor cell and block pro-tumorigenic receptors and/or interactions with the tumor microenvironment. (c) Tumor-specific antibodies recruit complement to the tumor cell surface, thereby labeling the cell for destruction. (d) Antibody-dependent cellular cytotoxicity (ADCC) is initiated by the recognition of IgG-coated tumors by FcR, which are expressed on immune effector cells such as NK cells, macrophages and neutrophils. These interactions lead to ADCC and tumor cell apoptosis through the delivery of perforin and granzymes. (e) The IgG-coated apoptotic tumor cells can bind FcR on phagocytes and initiate Fc-dependent phagocytosis, leading to the lysosomal degradation of the tumor cell. (f) Peptides derived from lysosomal degradation of tumor cells can be loaded onto MHC class II molecules, leading to the activation of $CD4^+$ T helper cells. In addition to $CD4^+$ T cell activation, DCs can cross-present tumor antigen-derived peptides and prime cytotoxic $CD8^+$ T cells [based on Weiner *et al*., 2010].[118] 24

Figure 4: Schematic representation of bispecific antibody and antibody-derived formats that are investigated in clinical trials. Left panel: Bispecific full-length IgGs. Right panel: Bispecific antibody fragments [based on Hess *et al.*, 2013].[84] 26

Figure 5: Domain arrangement and putative 3D shape of a single-chain triplebody based on small angle x-ray scattering (SAXS) data. (a) Block-structure of the gene cassette for a scTb is shown [based on Kellner *et al.*, 2008].[211] (b) Schematic representation of a scTb. (c) An overlay of the shape of triplebody [19x16x19] predicted from SAXS data [Nadja C. Fenn, unpublished] and the three-dimensional structure of 3 scFvs based on x-ray crystallography is shown. The two distal scFvs have a putative spread of 20 nm [adapted from Georg H. Fey, 8th Fabisch-Symposium, March 21st 2012]. 30

Figure 6: Schematic representation of the molecular structure of CD19. The extracellular region of CD19 with its two C2-type Ig-like domains forms a co-receptor complex together with CD21/CD35, CD225 and CD81. Signaling through CD19 can either be triggered upon cell autonomous aggregation or upon ligand-binding to the mature BCR. This results in sequential phosphorylation of the indicated tyrosine residues in the cytoplasmic tail of CD19 and subsequent activation of multiple signaling cascades that induce B cell proliferation and differentiation [based on Wang *et al.*, 2012 and Carter *et al.*, 2002].[216,220] 32

Figure 7: Schematic representation of the molecular structure of CD33. The extracellular region of CD33 is composed of two Ig-like domains of the V- and C2-set with intra-domain disulfide-links. CD33 recognizes specific sialylated glycans and thereby mediates cell-cell interactions. Intracellular signaling is modulated by CD33 upon phosphorylation of specific tyrosine residues within the ITIM and ITIM-like motifs in its cytoplasmic tail and upon ubiquitination [based on Laszlo et al., 2012].[227] 34

Figure 8: Schematic representation of the molecular structure of CD123, the alpha-chain of the IL-3 receptor. Two isoforms of CD123 exist with three (SP1) and two (SP2) extracellular domains, respectively. Both isoforms have a transmembrane domain and identical short cytoplasmic domains with a membrane-proximal proline-rich region. CD123 is involved in activation of the STAT signaling pathway and in cell survival. The N-terminal Ig-like D1 of the SP1 isoform of CD123 is flexible and can adopt an open and a closed conformation, whose biological function is unclear [based on Blalock et al., 1999].[237] 36

Tables

Table 1: Currently used classification systems of Acute Myeloid Leukemia (AML). 11

Table 2: Requirements for assigning more than one lineage to a single blast population in mixed phenotype acute leukemia according to the WHO 2008 classification. 13

Table 3: Classification systems used for B precursor lymphoid neoplasms. 14

Acknowledgements

First of all I would like to thank my supervisors Prof. Hopfner and Prof. Oduncu. Thank you for entrusting me with this project, for your valuable insight, advice, supervision and for your continuous support. Thank you also for being willing to chat, whenever I showed up at your doors, and for the enjoyable working atmosphere in your respective laboratories. Furthermore, I would also like to express my sincere gratitude to Prof. Fey for recruiting and training me. His enthusiasm for antibody derivatives and cancer immunotherapy revived my fascination for science and I thoroughly enjoyed our conversations.

I am also truly grateful to PD Kobold, who always had an open ear and helpful advice, when I was in a pinch. His constructive criticism improved my project approach and my publications immensely. Prof. Endres has also been an invaluable supporter during my doctoral studies. His trust and faith in my abilities have often given me the confidence to keep going.

Special thanks are due to my colleagues at the hospital Dr. Braciak and Kerstin Lämmermann, to my colleagues at the Gene Center Dr. Fenn, Dr. Wildenhain, Dr. Schiller and Alexandra Schele, and to my colleagues in Erlangen Dr. Schubert and Stefanie Nowecki. Thank you for teaching, advising and supporting me.

Not only my triplebody colleagues, but the entire antibody team in the Hopfner group has been awesome. Thank you to Nadine Moritz, Monika Herrmann and Laia Pascual Ponce for our lively scientific and not so scientific discussions and the nice working environment. I always enjoyed stopping by. I am also truly grateful to the rest of the Hopfner research group, especially Charlotte Lässig, for welcoming me, whenever I came to the Gene Center. Finally, it was an equally great pleasure to work with Elisavet Chatzopoulou from Prof. Rädler's research group on NK cell-mediated cytolysis. I always looked forward to her visits.

During the Spectramab meetings the discussion of my project with Prof. Jacob and Prof. Petterlin was also really helpful. I want to thank them for their attentiveness during my presentations and for their constructive criticism and suggestions.

I am also very grateful for the generous financial support from the foundation "Kaminkehrer helfen krebskranken Kindern", the DFG-graduate school 1202 and especially from the German José Carreras Leukemia-Foundation (DJCLS F 13/05, www.carreras-stiftung.de).

Last - but certainly not least - I want to thank the people that I love and that have accompanied me all the way and especially through the last two years. In many respects it has been a very difficult time, but you stuck with me and kept my head above water, whenever I felt like drowning. Thank you Nicky, André and Sonja, Mum, Dad, Markus and Oliver and thank you “harter Kern”.

Jeder von uns ist in der Lage
die Welt ein kleines Stück zu verbessern,
dabei ist jedoch auch jeder einzelne in der Pflicht,
seinen eigenen Beitrag zu leisten.
Zen-Weisheit

Appendix A: Sequence Data

Name of scFv	Amino acid sequence Details from bioinformatic analysis
muCD3ε (OKT3-derived)[134] **245 aa, 26.6 kDa, $V_H \rightarrow V_L$**	DIKLQQSGAELARPGASVKMSCKTSGYTFTRYTMHWVKQRPGQGLEWIGY INPSRGYTNYNQKFKDKATLTTDKSSSTAYMQLSSLTSEDSAVYYCARYYDD HYCLDYWGQGTTLTVSSVEGGSGGSGGSGGSGGVDDIQLTQSPAIMSASP GEKVTMTCRASSSVSYMNWYQQKSGTSPKRWIYDTSKVASGVPYRFSGSG SGTSYSLTISSMEAEDAATYYCQQWSSNPLTFGAGTKLELK Isoelectric point (pI) 8.67, molar extinction coefficient (ext. coeff.) 61,560 M^{-1} cm^{-1}, grand average of hydropathicity (GRAVY) -0.592
Mutants of muCD3ε scFv	
muCD3ε C105S[285]	DIKLQQSGAELARPGASVKMSCKTSGYTFTRYTMHWVKQRPGQGLEWIGY INPSRGYTNYNQKFKDKATLTTDKSSSTAYMQLSSLTSEDSAVYYCARYYDD HYSLDYWGQGTTLTVSSVEGGSGGSGGSGGSGGVDDIQLTQSPAIMSASP GEKVTMTCRASSSVSYMNWYQQKSGTSPKRWIYDTSKVASGVPYRFSGSG SGTSYSLTISSMEAEDAATYYCQQWSSNPLTFGAGTKLELK
dsmuCD3ε	DIKLQQSGAELARPGASVKMSCKTSGYTFTRYTMHWVKQRPGQCLEWIGY INPSRGYTNYNQKFKDKATLTTDKSSSTAYMQLSSLTSEDSAVYYCARYYDD HYCLDYWGQGTTLTVSSVEGGSGGSGGSGGSGGVDDIQLTQSPAIMSASP GEKVTMTCRASSSVSYMNWYQQKSGTSPKRWIYDTSKVASGVPYRFSGSG SGTSYSLTISSMEAEDAATYYCQQWSSNPLTFGCGTKLELK
dsmuCD3ε C105S	DIKLQQSGAELARPGASVKMSCKTSGYTFTRYTMHWVKQRPGQCLEWIGY INPSRGYTNYNQKFKDKATLTTDKSSSTAYMQLSSLTSEDSAVYYCARYYDD HYSLDYWGQGTTLTVSSVEGGSGGSGGSGGSGGVDDIQLTQSPAIMSASP GEKVTMTCRASSSVSYMNWYQQKSGTSPKRWIYDTSKVASGVPYRFSGSG SGTSYSLTISSMEAEDAATYYCQQWSSNPLTFGCGTKLELK
dshuCD16 (3G8-derived)[253] **250 aa, 26.5 kDa, $V_L \rightarrow V_H$**	DIVLTQSPSSLSASVGDRVTITCKASQSVDFDGDSFMNWYQQKPGKAPKLLI YTTSNLESGVPSRFSASGSGTDFTLTISSLQPEDFATYYCQQSNEDPYTFGCG TKVEIKRGGGGSGGGGSGGGGSGGGGSEVQLVESGGGDVQPGGSLRLSC AFSGFSLRTSGMGVGWIRQAPGKCLEWVAHIWWDDDKRYNPSVKGRFTI SKDTSSNTVYLQMNSLRAEDTAVYYCAQINPAWFAYWGQGTLVTVSS pI 5.20, ext. coeff. 53,775 M^{-1} cm^{-1}, GRAVY -0.331
huCD19 (4G7-derived)[249] **254 aa, 27.1 kDa, $V_L \rightarrow V_H$**	DIVMTQSPATLSLSPGERATLSCRSSKSLLNSNGNTYLYWFQQKPGQAPRLL IYRMSNLASGVPARFSGSGSGTDFTLTISSLEPEDFAVYYCMQHLEYPLTFGQ GTKVEIKRGGGGSGGGGSGGGGSGGGGSEVQLVESGGGDVQPGGSLRLS CKASGYTFTSYVMHWVRQAPGKGLEWVGYINPYNDGTKYNESVKGRFTLS SDKSSSTAYLQMNSLRAEDTAVYYCARGTYYYGSRVFDYWGQGTLVTVSS pI 8.58, ext. coeff. 49,070 M^{-1} cm^{-1}, GRAVY -0.374

huCD33 (AG Fey)[286] **243 aa, 25.9 kDa, $V_H \rightarrow V_L$**	EVQLVESGGGLIQPGGSLRLSCAASGFPLTSYGVSWVRQPPGKGLEWLGVI WGDGSTNYHSALISRFTISRDNSKNTLYLQMNSLRAEDTAVYYCARDTYYPY YAMDYWGQGTTVTVSSGGGGSGGGGSGGGGSDIQMTQSPSSLSASVGD RVTITCKASQDVSTAVAWYQQKPGKAPKLLIYSASYRYTGVPSRFSGSGSGT DFTLTISSLQPEDFATYYCQQHYSTPLTFGQGTKLEIKRS pI 8.32, ext. coeff. 53,080 M^{-1} cm^{-1}, GRAVY -0.330
dshuCD123 (AG Fey)[287] **250 aa, 26.7 kDa, $V_H \rightarrow V_L$**	EVQLVESGGGLVQPGGSLRLSCAASGFTFTDYYMSWVRQAPGKCLEWLALI RSKADGYTTEYSASVKGRFTISRDDSKNSLYLQMNSLKTEDTAVYYCARDAA YYSYYSPEGAMDYWGQGTSVTVSSGGGGSGGGGSGGGGSDIQMTQSPSS LSASVGDRVTITCKASQNVDSAVAWYQQKPGKAPKALIYSASYRYSGVPSRF SGSGSGTDFTLTISSLQPEDFATYYCQQYYSTPWTFGCGTKVEIKR pI 7.74, ext. coeff. 57,675 M^{-1} cm^{-1}, GRAVY -0.378
huHer2 (4D5-8-derived)[288] **248 aa, 26.3 kDa, $V_L \rightarrow V_H$**	DIQMTQSPSSLSASVGDRVTITCRASQDVNTAVAWYQQKPGKAPKLLIYSA SFLYSGVPSRFSGSRSGTDFTLTISSLQPEDFATYYCQQHYTTPPTFGQGTKV EIKRGGGGSGGGGSGGGGSGGGGSEVQLVESGGGLVQPGGSLRLSCAASG FNIKDTYIHWVRQAPGKGLEWVARIYPTNGYTRYADSVKGRFTISADTSKNT AYLQMNSLRAEDTAVYYCSRWGGDGFYAMDYWGQGTLVTVSS pI 8.81, ext. coeff. 50,100 M^{-1} cm^{-1}, GRAVY -0.363
muTCR (BMA031-derived)[289] **243 aa, 25.9 kDa, $V_H \rightarrow V_L$**	EVQLQQSGPELVKPGASVKMSCKASGYKFTSYVMHWVKQKPGQGLEWIG YINPYNDVTKYNEKFKGKATLTSDKSSSTAYMELSSLTSEDSAVHYCARGSYY DYDGFVYWGQGTLVTVSAGGGGSGGGGSGGGGSAQQIVLTQSPAIMSAS PGEKVTMTCSATSSVSYMHWYQQKSGTSPKRWIYDTSKLASGVPARFSGS GSGTSYSLTISSMEAEDAATYYCQQWSSNPLTFGAGTKLELK pI 8.53, ext. coeff. 58,580 M^{-1} cm^{-1}, GRAVY -0.425

BLACK - framework residues, BLUE – complementarity determining regions (CDR), GREEN – residues for potential disulfide-stabilization